JYU DISSERTATIONS 678

Ra'ad M. Khair

Biomechanical Recovery Factors in Non-Surgically Treated Ruptured Achilles Tendons

UNIVERSITY OF JYVÄSKYLÄ
FACULTY OF SPORT AND
HEALTH SCIENCES

JYU DISSERTATIONS 678

Ra'ad M. Khair

Biomechanical Recovery Factors in Non-Surgically Treated Ruptured Achilles Tendons

Esitetään Jyväskylän yliopiston liikuntatieteellisen tiedekunnan suostumuksella
julkisesti tarkastettavaksi yliopiston Liikunta-rakennuksen auditoriossa L303
elokuun 25. päivänä 2023 kello 12.

Academic dissertation to be publicly discussed, by permission of
the Faculty of Sport and Health Sciences of the University of Jyväskylä,
in building Liikunta, auditorium L303, on August 25, 2023, at 12 o'clock noon.

JYVÄSKYLÄN YLIOPISTO
UNIVERSITY OF JYVÄSKYLÄ

JYVÄSKYLÄ 2023

Editors
Simon Walker
Faculty of Sport and Health Sciences, University of Jyväskylä
Timo Hautala
Open Science Centre, University of Jyväskylä

ISBN 978-951-39-9693-2 (PDF)
URN:ISBN:978-951-39-9693-2
ISSN 2489-9003

Permanent link this publication: http://urn.fi/URN:ISBN:978-951-39-9693-2

ABSTRACT

Khair, Ra'ad
Biomechanical recovery factors in non-surgically treated ruptured Achilles tendons
Jyväskylä: University of Jyväskylä, 2023, 100 p.
(JYU Dissertations
ISSN 2489-9003; 678)
ISBN 978-951-39-9693-2

Achilles tendon rupture (ATR) is a frequent and disabling injury. In the last decade the incidence of ATR has been increasing especially in middle aged men participating in recreational sports. Plantar flexion strength decrements and endurance impairments are observed in patients with ATR whether treated surgically or non-surgically. Factors associated with good recovery are yet to be determined, particularly in non-surgically treated patients. Therefore, the aim of this thesis was to examine Achilles tendon (AT) and triceps surae (TS) muscle-tendon unit biomechanics in non-surgically treated patients 1-year after ATR. The results show that after rupture, non-surgically treated tendons heal to an elongated length, accompanied by remodeling of the TS muscles to shorter fascicles, and a reduced muscle cross-sectional area. However, stiffness in the injured AT was not different compared to the contralateral limb 1-year after rupture, in contrast with previous studies done on surgically treated tendons around the same time point. The relative contribution of flexor hallucis longus (FHL) during submaximal plantarflexion was higher in the injured limb, and this appeared to compensate for the decreased medial gastrocnemius activity. The lengthening of the injured tendon was associated with greater relative FHL activity, lower stiffness, and worse patient-reported outcomes. It seems that the increased length of the tendon after rupture is responsible for the observed objectively measured and self-reported functional deficits. Non-surgical treatment after ATR seems to allow the conservation of the displacement pattern in the ruptured tendon, suggesting that non-surgical treatment may preserve normal subtendon organization. However, displacement amplitude and non-uniformity were altered after rupture. Using selective electrical stimulation to scan for the representative areas of the TS subtendons within the cross section of the AT, the data indicates that lateral gastrocnemius subtendon was located in the most anterior region adjacent to medial gastrocnemius both in the healthy and ruptured, non-surgically treated tendon. The novel method developed in this thesis enables individual assessment of the TS subtendon organization within the AT and may enable patient-specific rehabilitation protocols in the future.

Keywords: Achilles tendon; rupture; flexor hallucis longus muscle; non-uniformity; stiffness; ultrasonography.

TIIVISTELMÄ (ABSTRACT IN FINNISH)

Khair, Ra'ad
Biomekaaniset toipumistekijät ei-operatiivisesti hoidetuissa akillesjänne-repeämissä
Jyväskylä: University of Jyväskylä, 2023, 100 p.
(JYU Dissertations
ISSN 2489-9003; 678)
ISBN 978-951-39-9693-2

Akillesjänteen repeämä on yleinen ja invalidisoiva vamma. Viime vuosikymmenten aikana repeämien esiintyvyys on lisääntynyt erityisesti urheilua harrastavilla keski-ikäisillä miehillä. Vammasta aiheutuu anatomisia ja toiminnallisia puutteita, jotka voivat jatkua useita vuosia. Hoitolinjasta riippumatta repeämäpotilailla on havaittu nilkan ojennusvoiman ja kestävyyden heikkenemistä. Hyvään toipumiseen liittyviä tekijöitä ei tunneta kovin hyvin varsinkaan ei-operatiivisesti hoidetuilla potilailla. Tämän väitöskirjan tavoitteena oli tutkia akillesjänteen ja kaksipäisen kantalihaksen lihas-jänneyksikön biomekaniikkaa ei-operatiivisesti hoidetuilla potilailla 1 vuosi repeämän jälkeen. Tulokset osoittavat loukkaantuneiden jänteiden olevan tervettä jännettä pidempiä. Pidentyneeseen jänteeseen liittyy kaksipäisen kantalihaksen lihassolujen mukautuminen lyhyemmiksi suuremmalla pennaatiokulmalla ja pienempi poikki-pinta-ala. Loukkaantuneen jänteen jäykkyys ei kuitenkaan eronnut terveeseen jänteeseen verrattuna vuoden kuluttua repeämästä, toisin kuin aiemmissa tutkimuksissa, joissa jännettä on hoidettu operatiivisesti. Ison varpaan koukistajalihaksen (FHL) suhteellinen osuus pohjelihasten tuottamasta voimasta submaksimaalisen plantaarifleksion aikana oli suurempi loukkaantuneessa jalassa, ja tämä näytti kompensoivan kaksoiskantalihaksen pienempää lihasaktiivisuutta. Loukkaantuneen jänteen pidentyminen oli yhteydessä suurempaan suhteelliseen FHL-aktiivisuuteen, pienempään jäykkyyteen ja heikompaan itseraportoituun toimintakykyyn. Jänteen pidentyminen repeämän jälkeen vaikuttaa olevan tärkeä seikka kuntoutumisessa. Jänteen sisäisessä liikkeessä havaittiin muutoksia, mutta osalla potilaista hoito mahdollisti terveen jänteen merkkinä pidetyn epähomogeenisen liikkeen. Jänteen sisäisen liikkeen avulla tutkimuksessa pystyttiin tunnistamaan sisemmän ja uloimman kaksoiskantalihaksen jänteiden sijainti osana akillesjännettä. Tähän käytettiin projektissa kehitettyä uutta menetelmää, joka voi tulevaisuudessa mahdollistaa kuntoutuksen yksilöllistämisen.

Avainsanat: Akillesjänne; repeämä; flexor hallucis longus lihas; geometria; epätasaisuus; jäykkyys; ultraäänitutkimus.

Author

Ra'ad Khair
Faculty of Sport and Health Sciences
Neuromuscular Research Center
P.O. Box 35
FI-40014 University of Jyväskylä
Finland
Raedkhair92@gmail.com

Supervisors

Professor Taija Finni, PhD
Faculty of Sport and Health Sciences
Neuromuscular Research Center
P.O. Box 35
FI-40014 University of Jyväskylä
Finland

Professor Neil Cronin, PhD
Faculty of Sport and Health Sciences
Neuromuscular Research Center
P.O. Box 35
FI-40014 University of Jyväskylä
Finland

Reviewers

Associate professor Katarina Nilsson Helander, MD
Sahlgrenska Universitetssjukhuset
Område 3 Ortopedi
43180 Mölndal
Sweden

Professor Jens Bojsen-Møller, PhD
University of Southern Denmark
J. B. Winsløws Vej 19, 3
5000 Odense C
Denmark

Opponent

Professor Stig Peter Magnusson
University of Copenhagen
Bispebjerg Bakke 23,
2400 København NV
Denmark

ACKNOWLEDGEMENTS

I am immensely grateful to my supervisors Professors Taija Finni and Neil Cronin. Their vast expertise in muscle-tendon biomechanics in combination with their enthusiasm for research is a source of inspiration. Their insightful feedback, guidance, and mentorship have been invaluable in shaping my growth from a student to a researcher. Neil, thank you for being present at my first post-COVID conference presentation and for the constructive feedback. Taija, I will always remember that smoked salmon and the boat trip at your summer cottage.

I would like to acknowledge and extend my sincere gratitude to all my co-authors. Lauri Stenroth, your knowledge, and insight were instrumental in ensuring the accuracy and the quality of this work. Without Juha Paloneva contributions our participation in NoARK project and the successful collaboration with KSSHP would not have been possible. Aleksi Reito, thank you for your valuable contribution in the field of statistics and clinical insight. Ville Ponkilainen thank you for being responsive and open for discussion.

I express my gratitude to the technical staff of the department, with special thanks for Jouni Tukiainen and Sirpa Roivas. You always were there to save us from a device malfunction. Your technical expertise is invaluable to the successful completion of this research work and for the faculty of sport and health sciences.

Special thanks to all participants for spending time on evaluations, and for the Academy of Finland for supporting this work.

I also want to thank my friend and colleague Dr. Francesco Cenni for all the good discussions and fruitful exchange of ideas. Nothing competes with a good biomechanics discussion over an authentic Italian pizza.

I truly appreciate Maria Sukanen for the daily support through writing this thesis and making the data collection smooth and enjoyable. I am grateful.

I would like to express my outmost gratitude for my parents for providing me a good platform in life. My brother Ali for his support through the journey of higher education. The love of my family was and is a constant source of motivation and inspiration, and I am forever grateful.

Jyväskylä 24.04.2023
Ra'ad Khair

ORIGINAL PUBLICATIONS AND AUTHOR CONTRIBUTION

The thesis is based on the following original papers, which will be referred to in the text by their Roman numerals:

I Khair, R.M., Stenroth, L., Péter, A., Cronin, N.J., Reito, A., Paloneva, J., & Finni, T. (2021). Non-uniform displacement within ruptured Achilles tendon during iso-metric contraction. *Scandinavian Journal of Medicine and Science in Sports,* 31(5), 1069–1077.

II Khair, R.M., Stenroth, L., Cronin, N.J., Reito, A., Paloneva, J., & Finni, T. (2022). Muscle-tendon morphomechanical properties of non-surgically treated Achilles tendon 1-year post-rupture. *Journal of Clinical Biomechanics,* 92, 105568.

III Khair, R.M., Stenroth, L., Cronin, N.J., Reito, A., Paloneva, J., & Finni, T. (2022). In vivo localised gastrocnemius subtendon representation within the healthy and ruptured human Achilles tendon. *Journal of Applied Physiology*, 133(1), 11–19.

IV Khair, R.M., Stenroth, L., Cronin, N.J., Reito, A., Ponkilainen, V., & Finni, T. (2023). Exploration of muscle-tendon biomechanics one year after Achilles tendon rupture and the compensatory role of flexor hallucis longus. *Journal of Biomechanics*, 111586.

The author of the current thesis was responsible for all the measurements starting from 2019 until the present date. The author analyzed all the data and was the first and corresponding author of the original papers, reflecting a major role in drafting and editing the manuscripts.

CONTENTS

1 INTRODUCTION

The Achilles tendon is a crucial component for everyday locomotion. Tendons transmit force that is produced by the muscular tissue to propel movement. Despite the considerable strength of the Achilles tendon, chronic and acute injuries are very common and result in significant long-term deficits regarding function and physical activity. Achilles tendinopathy occurs in 6% of the general population during their lifetime, and with a higher incidence in long distance runners with a cumulative lifetime incidence of 52% (Kujala et al., 2005). The pathogenesis of tendinopathy is poorly understood and can be regarded as a failure of the adaptation or healing process of the tendon. It is not clear if chronic tendinopathy would result in acute Achilles tendon rupture.

Achilles tendon rupture is a severe injury with long term deficits that persist for several years and may be even permanent. The incidence of Achilles tendon rupture has been increasing in recent decades to an annual incidence of ~20-31/100 000 individuals (Ganestam et al., 2016), typically occurring in middle aged men participating in recreational sports. An important factor contributing to the persisting deficits in plantarflexion strength and endurance is the increased length of the tendon after rupture. After rupture the length of the tendon starts to increase in the first weeks and has have been reported to continue up to 6 months (Eliasson et al., 2018; Kangas et al., 2007). Lengthening of the tendon after rupture is an important cause of morbidity (Silbernagel et al., 2012a). Better understanding of detailed anatomical and biomechanical factors is key to providing better treatment and rehabilitation protocols.

Regardless of whether treated surgically or non-surgically, patients with Achilles tendon rupture have disabling long-term anatomical and functional impairments. Different types of treatments have been studied; however, there is no consensus regarding the optimal treatment option. Although non-surgical treatment is considered safe (Deng et al., 2017; Reda et al., 2020; Reito et al., 2018), most studies and follow-ups have been done on surgically treated patients. There is limited long-term biomechanical information about tissue recovery post-rupture in humans, especially in non-surgically treated tendons.

The Achilles tendon comprises both the gastrocnemius and the soleus muscles, distinct bundles of fascicles that arise from each muscle head called subtendons, and that rotate with varying degrees during the course to insert on the posterior aspect of the calcaneal tuberosity. Due to this complex hierarchical structure, the tendon is subjected to complex non-uniform loading that can cause heterogeneity of strain within the tendon. Recent advancement in ultrasonic imaging methods such as speckle tracking have shown non-uniformities within the AT during various tasks (Slane & Thelen, 2014c). *In vivo* studies show that non-uniform motion within the AT is a function of a healthy tendon and might play an important role in the ability of the TS muscles to perform their differing functional roles (Clark & Franz, 2021; Franz & Thelen, 2016). Yet, very little attention is paid to the restoration of the regional distribution within the Achilles tendon cross-sectional area and its effect on the recovery process and function after Achilles tendon rupture.

Biomechanics may hold the key for understanding movement and muscle-tendon function in health and disease. Thus, the purpose of the current thesis was to conduct a comprehensive study of muscle-tendon unit biomechanics 1-year after Achilles tendon rupture in non-surgically treated patients. Additionally, this thesis aimed to investigate the non-uniformity and anatomical organization of the Achilles tendon in healthy and ruptured tendons. These novel assessments can provide new information about the mechanistic behavior of the Achilles tendon and advance our understanding of how patients recover after acute Achilles tendon rupture.

2 REVIEW OF THE LITERATURE

2.1 Achilles tendon-triceps surae complex

2.1.1 Anatomy

The calf muscle is located in the posterior aspect of the lower leg. The most superficial muscle, the gastrocnemius, has 2 origins. The larger medial head arises from the medial femur condyle and extends more distally compared to the lateral. While the lateral head arises from the lateral surface of the lateral femoral condyle. The soleus (SOL) muscle lies under the gastrocnemius and originates entirely from below the knee, extending more distally compared to the gastrocnemius muscles. The soleus originates from the posterior aspect of the head and superior fourth of the fibula, the soleal line and the middle third of the medial border of the tibia. The gastrocnemius and the SOL muscles together are called the triceps surae (TS) muscle. The main function of the TS muscle complex is ankle plantarflexion. However, the gastrocnemius muscle also acts on the knee by assisting in knee flexion, as the muscles cross the knee joint. Each one of the TS muscles descend down without interfering or interlapping (Szaro et al., 2009) in the form of distinct bundles of fascicles, called subtendons (Finni et al., 2018; Handsfield et al., 2016), to form the Achilles tendon(AT).

The AT is formed by joining of the subtendons of the triceps surae muscles. Proximally, the tendon starts relatively flat and becomes progressively rounder in shape until it reaches the superior calcaneal tuberosity and then flatten again centimeters away from its insertion on the middle lower part of the posterior surface of the calcaneus (O'Brien, 2005). The AT twist to the counterclockwise direction on the right side and to the clockwise direction on the left. Mainly three types of twisting is described depending on the degree of torsion: type I, least torsion; type II, moderate; and type III, extreme (Edama et al., 2015; Pękala et al., 2017).

Anatomical studies of the AT showed inconsistency in describing the twisting and the representative location of the TS subtendons within the cross-section of the AT. Szaro *et al.* (2009) assumed that medial gastrocnemius (MG) occupy the lateral superficial area of the tendon, while lateral gastrocnemius (LG) and SOL were assumed to occupy the lateral and medial deep area of the tendon. Pękala *et al.* (2017) described the differences between the three twisting groups at the pre-insertional level of the tendon. If the superficial layer was found to be mostly occupied by MG, it was classified as type I; the presence of MG and SOL was classified as type II, and when dominantly occupied by SOL it was classified as type III. Accordingly, if the deep area is occupied by a combination of LG and SOL type I dominantly LG type II and a combination of the gastrocnemius muscles type III.

At the insertion level of the calcaneal tuberosity Edama *et al.* (2015) also classified the twisting to three groups. When the SOL attached the deep layer of the calcaneal tuberosity was classified as type I, both LG and SOL were classified as type II, and LG was classified as extreme twist type III. This could be due to the wide individual anatomical variation in twisting and contribution of the TS muscles to the AT (O'Brien, 2005).

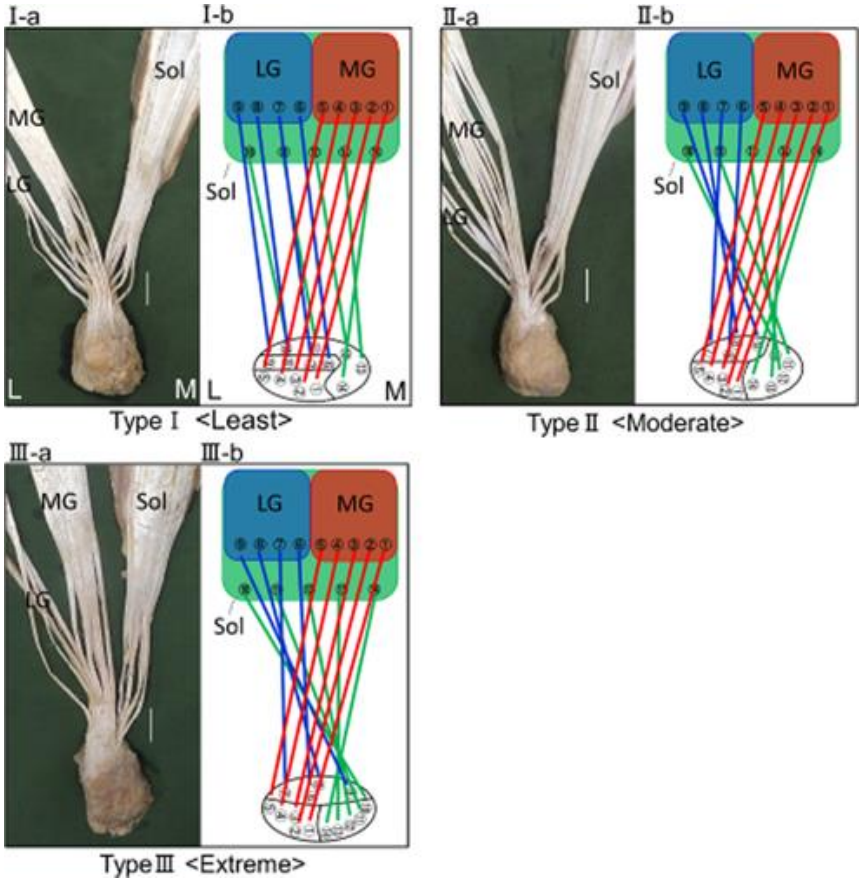

FIGURE 1 The structure of the AT includes individual subtendon twist in addition to the overall twist. The figure shows the three individual patterns, adapted with permission from (Edama et al., 2015).

2.1.2 Composition and structure

2.1.2.1 Achilles tendon

Tendons are mechanically responsible for transmitting forces between muscles and bones, and in doing so, permit locomotion. Tendons are dense multi-unit hierarchical structure composed of collagen molecules, fibrils, fiber bundles, and fascicles that run parallel to the tendon's long axis.

Like all tendons, 50–70% of the AT weight is water. Collagen account for 60–85% of the tendon dry weight of which 95% is type I collagen (Kjær, 2004), followed by proteoglycans, glycoproteins, and elastic fibers (Thorpe & Screen, 2016). Small amounts of collagen types III, V, XI, XII and XIV are also found (Thorpe, Birch, et al., 2013). The components within the tendon is produced by tenoblasts and tenocytes, which are elongated variants of fibroblasts and fibrocytes arranged in a complex hierarchical manner to form the tendon proper (Hess et al., 1989). Through cross-linking soluble tropocollagen molecules create insoluble collagen molecules, which then aggregate into microfibrils and form collagen fibrils that are visible under electron microscope (Kannus, 2000).

The diameter of collagen fibrils in the Achilles tendon varies from 30–150 nm. The basic unit of the tendon, the collagen fiber, is created by the grouping of multiple fibrils, which then are grouped together to form fascicles (Fig. 2). Collagen fibers and fascicles are surrounded by a connective tissue sheet called endotenon, which allow the fiber groups to glide and provide access channels for blood vessels, nerves, and lymphatics to the deep portions of the tendon. On the outer surface, the tendon is surrounded by a fine connective tissue called the epitenon (Galloway et al., 2013; Kastelic et al., 1978). The epitenon is a dense fibrillar network that contains collagen fibers 8-10 nm thick with multiple orientations (Jozsa et al., 1991). The epitenon is connected with the paratenon on its outer surface and the endotenon on its inner surface (Kannus, 2000). Paratenon function as an elastic outer sleeve permitting the tendon to slide relative to the surrounding tissue (Hess et al., 1989). The AT is characterized with a distinct paratenon with thin gliding membranes that facilitate smooth movement of the tendon against surrounding tissues (Kannus, 2000).

The extracellular matrix surrounding the collagen fibers include a wide variety of small molecules in addition to proteoglycans, glycosaminoglycans (GAGs), and structural glycoproteins. These molecules provide stability of the collagenous system and maintain homeostasis and collagen fibrillogenesis. Proteoglycans and GAGs have considerable water-binding capacity and plays a role in improving the elasticity of the tendon tissue against shear and compressive forces. Proteoglycans have a protein core where one or more CAGs are attached. They are large negatively charged hydrophilic molecules that are able to entrain water 50 times their weight. Proteoglycans are usually stiffly extended between the collagen fibers and fibrils, providing the collagen fibrils with a high capacity to resist high compressive and tensile forces.

In addition to collagen, other non-collagenous proteins might be present in the tendons. For example, adhesive glycoproteins like fibronectin, thrombos-

pondin, tenascin-C, and undulin have been the ability to bind to either other macromolecules or cellular surfaces (Kannus et al., 1998). However, there are still numerous proteins present in tendons whose functions and identities remain to be established (Kannus, 2000). Presently, there is a lack of specific compositional data available on the human Achilles tendon (Freedman et al., 2014a)

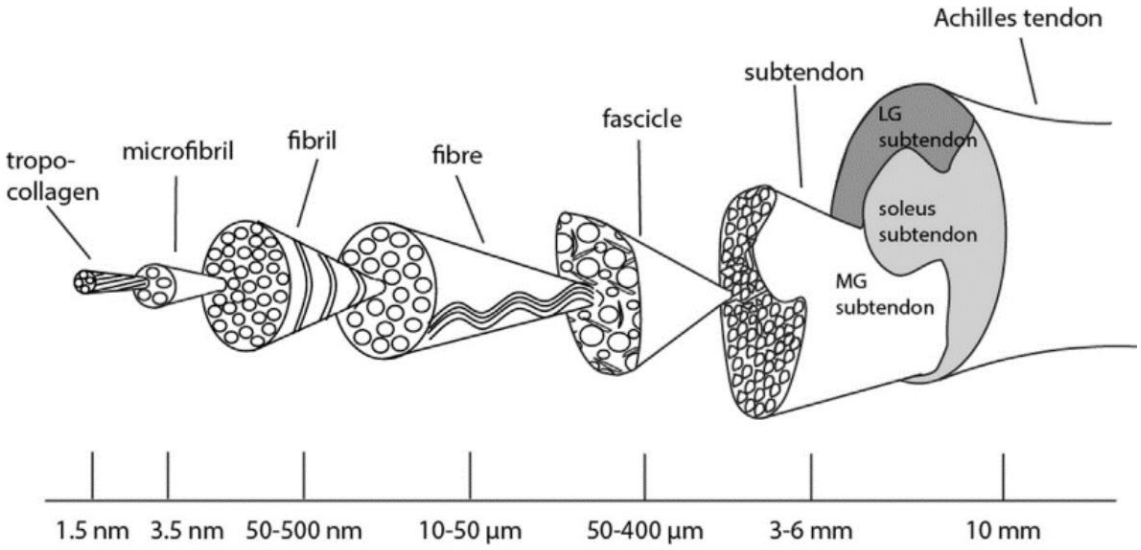

FIGURE 2 Achilles tendon hierarchy adapted with permission from (Handsfield et al., 2016).

2.1.2.2 Triceps surae

The geometrical arrangement of fibers within a muscle is referred to as muscle architecture. Muscle length, fascicle length and pennation angle, anatomical and physiological cross-sectional area (PCSA) are variables used to define the architecture of a muscle. The triceps surae muscles have relatively short fascicles compared to the muscle length because of the pennated configuration. On average, fascicle length to muscle belly length have been reported to be 19% for MG, 27% for LG and 11% for SOL (Ward et al., 2009). In terms of design, the TS muscle is suited to generate large forces as opposed to large muscle excursion, due to their high pennation angle and short fascicles configuration (Lieber & Bodine-Fowler, 1993).

The gastrocnemius muscle is unipennate where muscle fibers align relatively uniform with a large number of type II fibers, the gastrocnemius muscle is involved in fast force excursion that is important during activities like running. The soleus structure is more complex with 2 compartments: a bipennate anterior compartment and a unipennate posterior compartment (Chow et al., 2000) that might vary among individuals (Hodgson et al., 2006). The SOL is important in walking and maintaining posture and is composed mostly of slow, red type I fibers (Maffulli & Almekinders, 2007).

Muscle mass and fiber length is an important indicator of muscle force generating capacity. As muscle mass increase, PSCA increase (Ward et al.,

2009). The largest PCSA among the triceps surae muscle is the soleus. The SOL PCSA is almost 5 times greater than the LG and 3 times greater than that of the MG (Ward et al., 2009). Thus, SOL is the strongest and is capable of generating the biggest amount of force among the TS muscles.

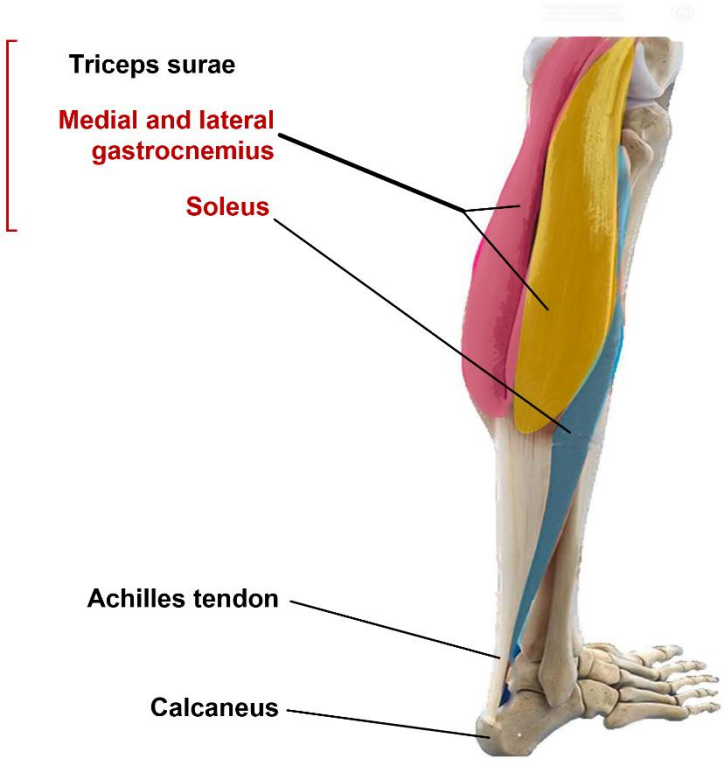

FIGURE 3 Posterior view of the lower limb showing triceps surae muscle group and Achilles tendon. The soleus muscle can be seen under the medial and lateral heads of the gastrocnemius. Achilles tendon extends from the muscle-tendon junction to its insertion on the calcaneus, adapted with permission from (Finni & Vanwanseele, 2023).

2.2 Mechanical behavior of the triceps surae Achilles tendon complex

2.2.1 Mechanics of the Achilles tendon

The Achilles tendon transmits force generated by the TS muscles to the calcaneus, enabling locomotion. Its complex structure allows the tendon to withstand high loads, 12.5 times body weight during activities such as running, or as high as 9 kN (Komi et al., 1992). The Achilles tendon possesses high capacity of elastic energy storage, that play a significant role in efficiency of force production and energy saving (Komi et al., 1992).

The tendon's mechanical properties are usually measured with tensile tests, the deformation of the tendon structure under certain amount of force (and the subsequent resisting force) is measured and used to provide a mechanical characterization of the tendon. Several parameters can be determined from tensile tests, including stress and strain, stiffness, and Young's modulus. Previously, the tensile properties of the tendon used to be performed on dissected tendon from humans or animals using testing devices to load the tendon (Maganaris et al., 2008). Latterly, imaging methods like ultrasonography have made it possible to obtain tensile characteristics of the tendon in a physiological environment without invasive procedures (Fukashiro et al., 1995).

Usually, in biomechanical studies, the tendon and aponeurosis are connected together in series with muscle fascicles (Fukashiro et al., 1995; Fukunaga et al., 1996). This model is useful for *in vivo* studies as it allows estimations of length changes in passive series elastic components; however it is important to distinguish aponeurosis from the tendon to avoid erroneous estimations of tissue loading, mechanics and energetics (Epstein et al., 2006). Finni *et al.* (2022) found that adding 1-3 cm above the location of the MG MTJ increase the displacement and strain of the AT. Thus, methodological considerations and fine-tuning of the assessment tools are needed for accurate estimation of the tendon properties.

Tendons, as well as other connective tissues, have viscoelastic properties, meaning they display spring like elastic properties and fluid like viscous properties (Butler et al., 1978). Hysteresis for instance is the difference between the loading and unloading curve in the stress-strain cycle and is a manifestation of the viscous characteristics of the tendon. The stiffness and Young's modulus are parameters describing the elastic properties of the tendon. Evidence suggest that the elastic properties dominate in the human tendon (Peltonen et al., 2013). Thus, in this thesis, the elastic properties of the tendon are discussed in more detail.

During tensile testing, the tendon is gradually elongated, and when combined with the force a force-elongation curve is created. Stress is quantified as the force applied to the tendon divided by its cross-sectional area (CSA), while strain is determined as the percentage change in the tendon length due to the applied force. Usually in literature the stress-strain curve is used to describe the mechanical properties of the tendon and can be divided into 4 regions (Fig. 4). The initial part of the curve characterized by a lower slope called the toe-region. The lower slope is caused by the straightening of collagen fiber crimp and is dependent on the type and the sample site within the tendon (Miller et al., 2012; Wilmink et al., 1992). Then in region II, as the collagen fibers get aligned and straightened by the increased elongation, a relatively straight line is formed that approximates the collagen response to elongation, accordingly this region is called the linear region. Until the end of the linear region, sliding between collagen molecules is reversible with no or minimal damage to the structure (Depalle et al., 2015; Svensson et al., 2012). In region III, when the collagen fibers within the tendon is stretched to a strain more than 4-5% microscopic failure start to occur. Finally, in region IV, further elongation beyond 8-10% strain

will cause a complete tendon rupture in an unpredictable manner and the load-supporting ability of the tendon is lost (J. H.-C. Wang, 2006). Tendon strain values varies between studies and might be under-estimated with some studies reporting strain values up to 14% (Devkota & Weinhold, 2003).

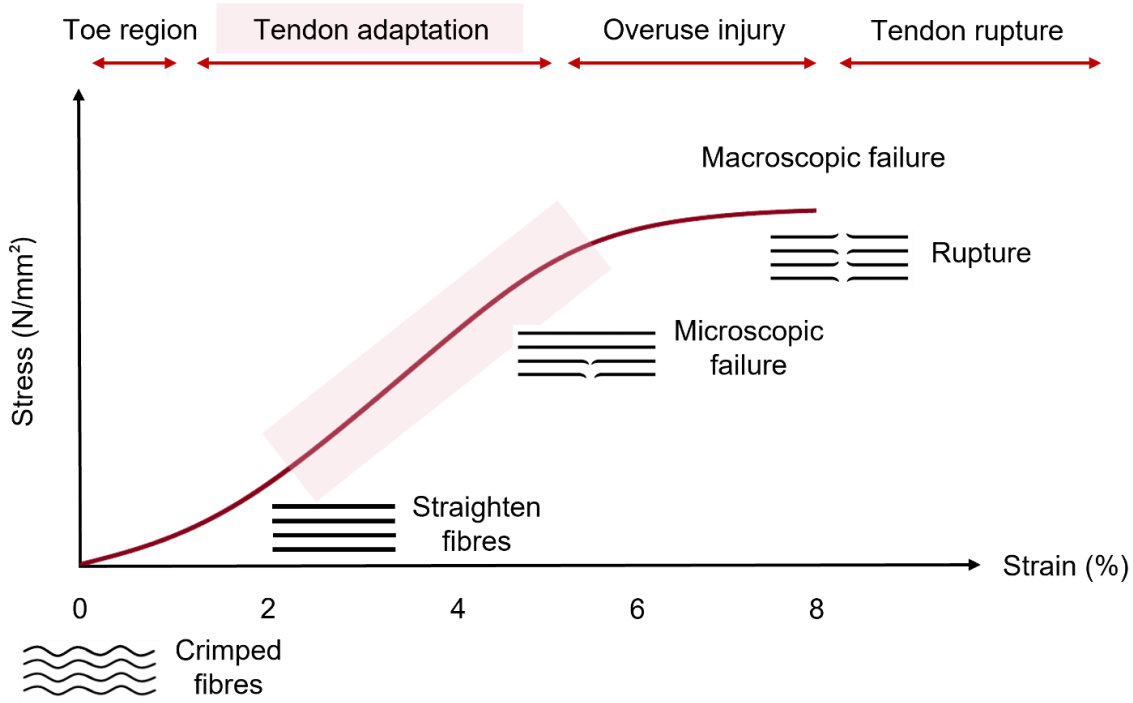

FIGURE 4 Tendon stress-strain curve.

2.2.1.1 Stiffness

The stiffness of the tendon determines the storage and release of potential elastic energy, and have an influence on force production (Lichtwark & Wilson, 2007; Reeves, 2006), within this context the stiffness of tendons have been frequently studied. Tendon stiffness is the ratio between the estimated tendon force divided by tendon's elongation ($\Delta F/\Delta L$) (Kubo et al., 2002). The stiffness is measured from the linear part of the force-elongation curve (Fig. 5).

Tendon dimensions including length and CSA, and material properties govern the stiffness of the tendon. For example, if we compare two tendons with the same mechanical properties, a longer tendon would elongate more under the same load, and the change in the force-elongation slope would be directly proportional to the extra length of the tendon (Proske & Morgan, 1987). Likewise, an increase in tendon CSA will lead to a higher tendon stiffness (Butler et al., 1978).

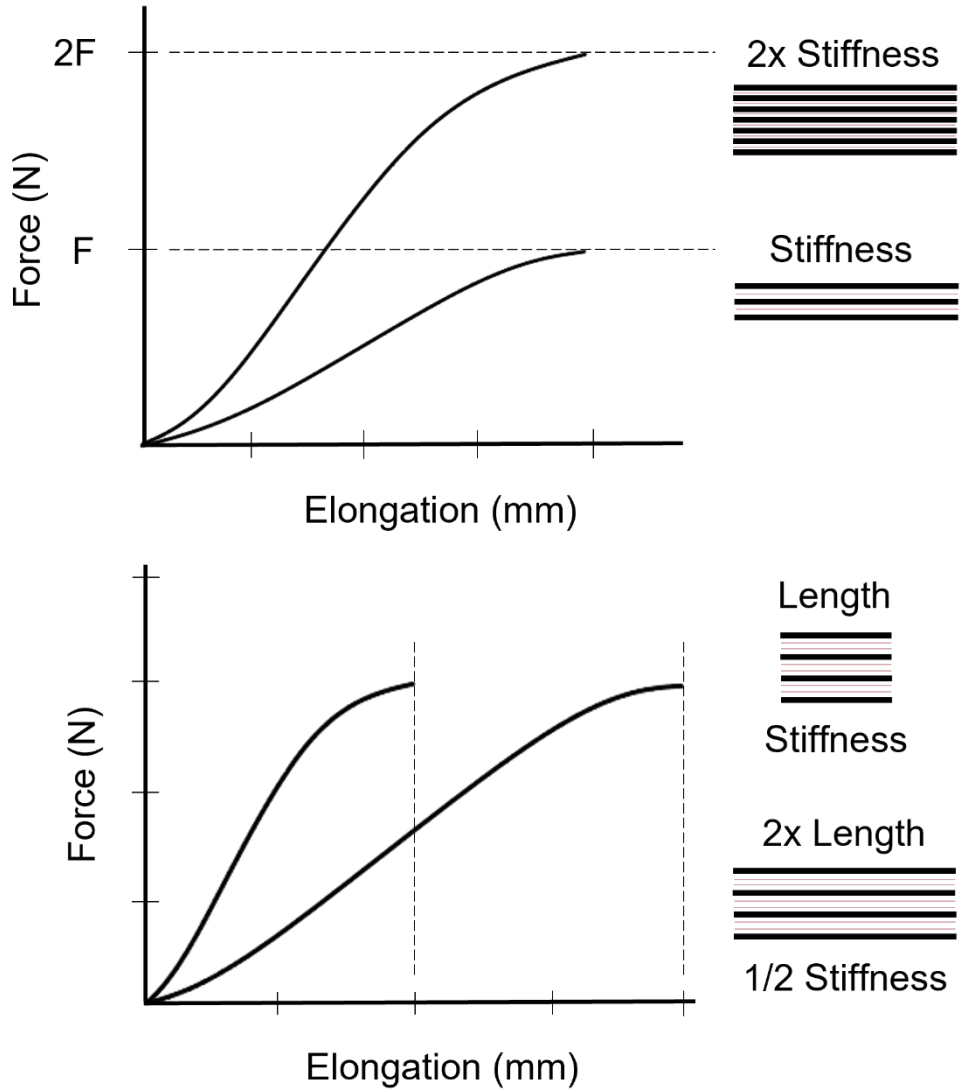

FIGURE 5 The effects of change in the length or the cross sectional area on the load - deformation curve adapted from (Butler et al., 1978).

2.2.1.2 Young's modulus

To provide a quantitative measure about the mechanical behavior of the tendon material. The tensile properties are normalized to the dimensions of the tendon to describe the mechanical behavior factoring the geometrical dimensions. Young's modulus in literature is described as the stress-strain curve. Stress is measured as the force divided by the cross-sectional area of the tendon, and strain as the change in the percentage of tendon length caused by loading. Both stress and strain are independent of dimensions of the tested material, thus making Young's modulus a useful parameter to compare between different materials and tendons (Butler et al., 1978).

2.2.2 Mechanics of the muscle

The properties of the muscle fibers determine the speed and the magnitude of the force that can be generated by the muscle. The mechanical behavior of the muscle is determined fundamental properties that are highly conservative irrespective of the muscle fiber type. Force-length, and force-velocity relationships, and the contractile history the muscle determine the muscle force generation and mechanical behavior (Hodgson et al., 2005; Rassier & Herzog, 2004). This thesis will focus on the force-length relationship as the other properties are beyond the scope of the thesis.

One of the most important functional characteristics of skeletal muscles is the dependence of the force generation potential on the muscle length. The force-length dependency was first described on a large Hungarian frog medial gastrocnemius muscle (Blix, 1894). The authors concluded that the muscle force decreases with muscle length. Later, Gordon et al. was able to overcome serious technical obstacles and managed to show that muscle fiber force correspond to the sarcomere length (Gordon et al., 1966). This observation aligns with the crossbridge theory of muscle contraction suggested by (Huxley, 1957). According to this theory, the length-dependence of muscle force is a result of the extent of the overlap between the actin and myosin filaments at various sarcomere lengths (Fig. 6).

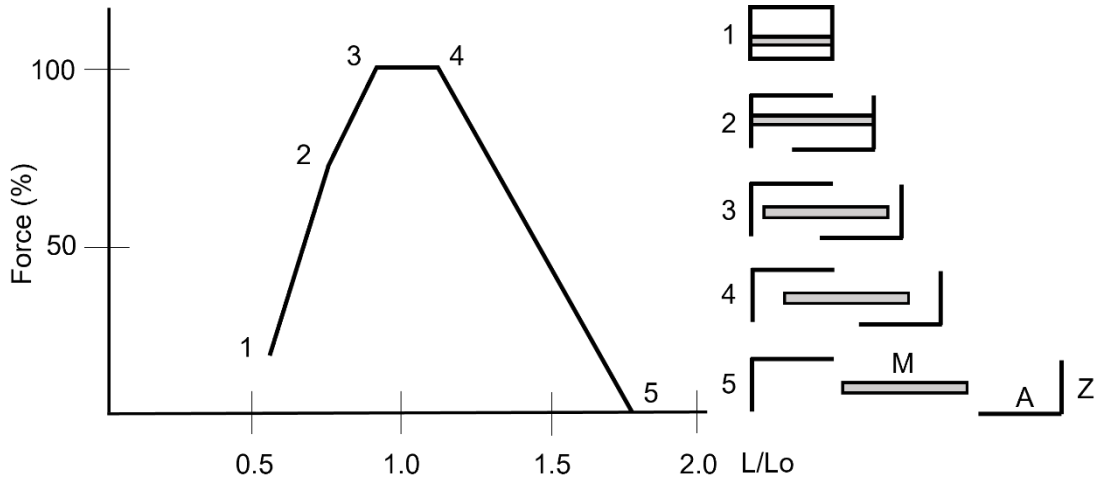

FIGURE 6 Representation of the dependence of the force produced by a sarcomere on its length (left) and the overlap between actin (A) and myosin (M) filaments at 5 different sarcomere lengths (right). Force is presented as percentage of the maximal force at the optimal length L0. At length 3 and 4 the maximal force can be produced by the sarcomere because of the actin and myosin filaments overlap. At length 5 there is no overlap thus no force no force can be produced adapted from (Huxley, 1957).

The total force of the muscle is a result of active and passive forces of the muscle. The active force-length relationship is computed by subtracting the passive

from the total force of the muscle. The passive force of the muscle arises from the connective tissue acting in parallel to the force generating contractile tissue.

The active force-length relationship curve is a smooth curve with a plateau region around the medium range of attainable muscle length (Fig. 6). The muscle force increases in the ascending limb of the curve and decrease in the descending limb. The sarcomere length that produces the greatest force is called the optimal length. In human muscles, force can be generated by sarcomeres within lengths ranging from 0.5 to 1.5 times the optimal length (Hill, 1953; Zajac, 1989). Estimations of the optimal length was computed to be between the sarcomere lengths of 2.64–2.81 μm (Rassier et al., 1999). Later, this was supported with experimental studies where optimal length was reported to be between 2.54–2.78 μm with a mean optimal length of 2.66 μm (Gollapudi & Lin, 2009).

The available data on human sarcomere lengths are limited. In vivo sarcomere length can be measured using laser diffraction (Lieber et al., 1994) or micro-endoscopy (Llewellyn et al., 2008) methods. Although, both of the aforementioned methods are invasive, it can be concluded that sarcomeres length in humans are around 3–4 μm (Zatsiorsky & Prilutsky, 2012). Despite lack of data on the TS muscle operating range on the force-length relations, estimations have been made using joint torque, ultrasonography, and muscle architecture data (Cutts, 1988; Fukunaga et al., 2001; Herzog et al., 1991; Maganaris, 2003). These studies all suggest that the TS muscles operate around the plateau and ascending limb regions of the force length relationship.

The muscles are required to meet versatile functional demands. Some muscles are required to produce high forces while others undergo large excursion. Different arrangement of the muscle building block sarcomeres, allow the muscle to achieve the functional requirements considering constraints set by the skeleton and the force-length and force-velocity relationships. Furthermore, the muscular system is configured to minimize energy loss by using the minimum amount of muscle mass able to cope with functional requirements.

The muscle contractile tissue arrangement in series or in parallel are notably able to define the function of the muscle. If we lay out the two extremes of muscle architecture, muscle (A) sarcomeres are aligned in series along the length of the muscle in the direction of force transmission. Muscle (B) sarcomeres are primarily aligned in parallel with shorter fibers compared to muscle A. Assuming similar volumes, hence same number of cross bridges and similar stress-strain properties of both muscles' sarcomeres. The capacity of shortening velocity and range is directly related to the number of sarcomeres in series. Muscle A are able to contract more rapidly and have a greater excursion range compared to muscle B. Force generation capacity is directly related to the number of fibers in parallel, which approximates to the PCSA of the muscle (Wilson & Lichtwark, 2011). Hence, the muscle with shorter and more fibers in parallel, muscle B, would have larger force generation capacity. Both muscle forms will have the same peak power generating capability, because power is defined as force multiplied by velocity. Therefore, muscle A can shorten quickly due to higher fiber length, while muscle B is able to generate more force as a result of higher PCSA.

Pennation angle of the muscle is the angle of the muscle fibers relative the muscle axis of force generation and is measured as the angle between the aponeurosis of the muscle and the fascicles. The angulation of the fibers have an effect on the force applied to the tendon by the muscle contraction (Fukunaga et al., 1997). From a mechanical view the contraction force of the muscle is reduced by a factor of cosine of the pennation angle, the larger the pennation angle, the greater the reduction in force development. Despite losing some force generation capacity in terms of mechanics, pennation is a space saving strategy that allows for more fibers to be arranged within a given volume allowing for a higher PCSA (Reeves et al., 2006). This is a representation of how the body has evolved to pack muscles in the minimum amount of mass that can cope with functional requirements.

It is generally recognized that one of the trade-offs in pennated muscles, is the lower shortening velocity and excursion range compared to longer fibered muscles. This is a result of the shorter distance between the distal and proximal muscle-tendon junction (MTJ) of the muscle and is proportional to the cosine of the pennation angle. If a pennate muscle is to shorten to a given degree greater fascicle shortening is needed. This reduction in velocity is offset partly by the rotation of the fascicles while shortening (Maganaris et al., 1998). When fibers shorten, they rotate to a greater pennation angle. This is called muscle gear ratio and is calculated as the ratio of muscle belly shortening to muscle fascicle shortening (Azizi & Roberts 2014). The augmentation effect of the fibers on the pennation angle while shortening result in greater shortening in the muscle of that in the fascicles, the outcome is muscle gearing ratio greater than one.

In the case of the TS muscle and other muscles operating on the ascending limb of the force-length relationship, muscle belly gearing allows for a greater force generation at a particular joint rotation (Gordon et al., 1966). Furthermore, muscle belly gearing enable the muscle to contract with slower velocity, increasing the force generation capacity, since muscle force generation is dependent on muscle velocity (Hill, 1938). Muscle belly gearing is thought to equal 1/cosine of the muscle pennation angle, however the change in muscle thickness due to bulging is not taken in consideration (Zajac, 1989). The change in muscle shape and thickness can amplify the muscle gearing, even in muscles with a pennation angle less than 20 (Azizi et al., 2008; Zajac, 1989). Furthermore, high gear ratio during eccentric contraction may compensate for the shorter fascicles in pennate muscles and protect the muscle from damage while actively lengthening (Azizi & Roberts, 2014). Muscle belly gearing have been reported to be around 1.05 for MG and 1.1 for LG in shortening contractions. It should be noted that muscle gear ratio depends on the level of force generation (Randhawa et al., 2013).

2.2.3 Intra-tendinous mechanics

The idea that a certain mechanical independence exists between the sub-tendon of the TS muscles, and even within the same muscle have been tested before *in vi*vo and in rats (Arndt et al., 1999, 1999; Arndt et al., 1998; Finni et al., 2018).

Previously, Arndt and colleagues have found asymmetry in forces transmitted through the AT, and showed that forces through the AT can be changed with changing knee angles (Arndt et al., 1999; Arndt et al., 1998).

Later, the advancements in the field of ultrasonography in combination with speckle tracking algorithms created the possibility to perform in vivo measurements of local non-uniform deformation within the AT (Arndt et al., 2012). Their findings demonstrated that the anterior region of the tendon displaced more than the posterior region with an average of 2.1 mm during passive ankle movements (Fig. 7). Later, Slane and Thelen (2014a) confirmed the finding and validated the tracking algorithm (Slane & Thelen, 2014a, 2015). They further demonstrated that non-uniformity within the tendon was less in middle aged adults during passive stretches and eccentric contractions (Slane & Thelen, 2014a, 2015). The anterior region consistently showed larger displacement compared to the posterior region of the tendon, but the displacement was more uniform in the older adults. Decreased ankle torque output was found to be associated with more uniform displacement within the Achilles tendon in older adults (Franz & Thelen, 2015).

The non-uniform motion within the Achilles tendon is a function of healthy tendon (Slane & Thelen, 2014c). The different structures of the triceps surae muscles and force generating capacities (Ward et al., 2009), generate complex non-uniform loading within the Achilles tendon. The ability of the subtendons to displace relative to each other is important to facilitate the optimal triceps surae muscles function, in order to perform their differing tasks (Clark & Franz, 2021; Franz & Thelen, 2016).

In studies to date, participant data have been presented as mean values, not taking in consideration the individual anatomical variations (Edama et al., 2015). It may be expected that AT displacement pattern is influenced with individual-specific geometrical and anatomical properties.

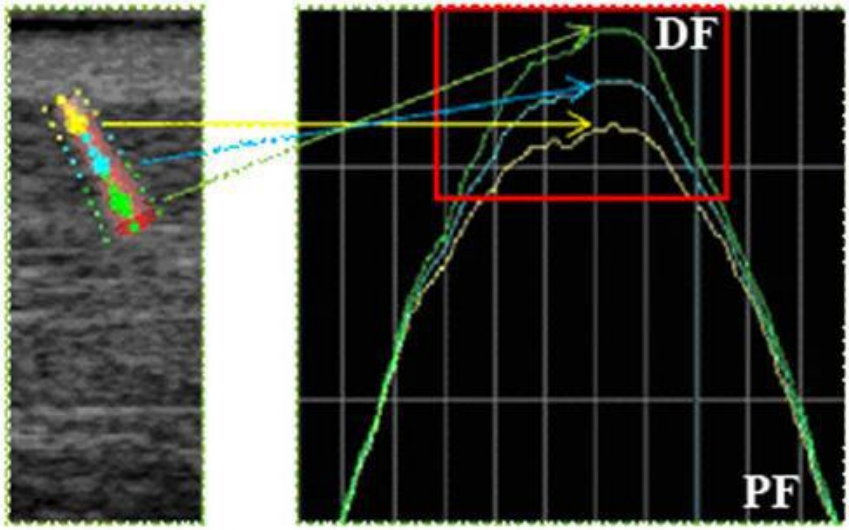

FIGURE 7 Non-uniformity within the Achilles tendon between the anterior and posterior regions of the tendon during passive dorsiflexion, with permission from (Arndt et al., 2012).

2.2.4 Muscle-tendon interaction during movement

Combined, the muscle and the connective tissue between two bone-tendon junctions is called the muscle tendon unit (MTU) and are responsible for the generation of movement. Muscles produce force that is transmitted via the connective tendinous tissue to allow joint movement. The muscle belly is situated between the distal and proximal MTJ, that connect the MTU to bones. Aponeurosis around and inside the muscle is also an extension of the outer tendon, that serve as an attachment surface for muscle fascicles. The tendon and the aponeurosis are the passive element component in the MTU and are referred to as tendinous tissue (TT). The tendinous tissue plays three important different roles in the MTU, energy conservation, power amplification and power attenuation (Roberts & Azizi, 2011). The interaction between the active muscle fibers and the passive series elastic components of the TT enhances the work output and expand the functional versatility of the muscles.

Some elastic energy can be stored in muscles, however most of the elastic energy is stored and returned by the passive series elastic elements of the TT. Tendons have almost 10 times the capacity of muscular tissue to store elastic energy. Biewener *et al.* (1998) showed that wallabies are able achieve a saving of as much as 50% of the total energy expenditure utilizing the energy return from the gastrocnemius, plantaris and flexor digitorum longus tendons while hopping. Furthermore, tendons can reduce the amount of shortening needed form the muscle reducing the energy expenditure of muscle contraction (Alexander, 1974; Alexander & Vernon, 1975). Earlier, Goslow *et al.* (1973) showed in cats that during a step the elastic recoil of the AT reduce the amount work needed to be done by the soleus. Later, in a paramount study on the gastrocnemius tendon of the turkey Roberts *et al.* (1997) showed that, while running, the turkey tendon was stretched and recoiled as the ankle flexed and extended while the fascicles of the gastrocnemius muscle remained constant and mainly did isometric contraction. Tendons are remarkably energy dense spring structures, that play an important role in cycling the elastic energy within the MTU, minimizing the energy cost of movement.

The aponeurosis behaves like variable stiffness springs during active contractions (Azizi & Roberts, 2009a). During active force production the stiffness of the aponeurosis increase, increasing the capacity of energy storage and recovery in the TT (Azizi & Roberts, 2009a). This variable stiffness within the TT may alter the fascicle length behavior that occur in the muscle, altering the fascicle strain for a given MTU strain (Azizi et al., 2008). This allows the optimization of the TT stiffness to improve the performance and economy of the MTU in active force production. The TT enables the muscle to overcome the constraints of force-length and force-velocity relationships, and is associated with the performance, efficiency, and economy of the locomotion with the human body.

Tendons can function as power amplifiers, when energy stored in the tendon is recoiled rapidly, like a catapult. This mechanism can result in MTU shortening velocity that exceed the optimal velocity of muscle power generation (Sawicki et al., 2015b). For instance, during squat jump MTU length stay con-

stant while the MG fascicles shorten almost isometrically, storing energy in the AT (Kurokawa et al., 2001). Within this frame the tendon is responsible for most of the energy generated by the MTU. A similar mechanism is used in walking and counter-movement jump (Biewener et al., 1998). Additionally, compliant tendons allow uncoupling behavior of the muscle fascicle from the MTU which assist the muscle with power amplification to function at different velocities and lengths in the cycle with maximal power output during acceleration tasks (Roberts & Azizi, 2010). The uncoupling of the muscle fascicles from the MTU, also assists the muscle with power attenuation in rapid deceleration tasks (Roberts & Azizi, 2010). The tendon can attenuate power by reducing peak forces and muscle lengthening velocity when dealing with a rapid decline in the body inertia. The tendon act as a mechanical buffer protecting the muscular tissue by reducing the amount of energy the muscle needs to dissipate in a short amount of time (Thelen et al., 2005).

The function of the TT is regulated by the timing and intensity of the muscle contractions. Changes in muscle contraction can alter the MTU function and change the function of the TT from power attenuation to power amplification (Sawicki et al., 2015a). Furthermore, an appropriate amount of stiffness in the TT is crucial for efficient power generation in the MTU (Lichtwark & Barclay, 2010; Lichtwark & Wilson, 2005). Different tasks require different stiffness in the tendinous tissue to be optimized, for instance simulation studies estimated that AT stiffness around 150 N/mm optimizes the efficiency of walking, and running is optimized with a stiffer tendon around 250N/mm (Lichtwark & Wilson, 2008).

Humans are unique among mammals in their ability to stand upright on two legs. The maintenance of balance during bipedal standing was considered to be a simple and a static task. However, recent evidence suggests the process is far more intricate than previously believed. The Achilles tendon-triceps surae MTU have to constantly produce the right amount of force to balance the body at a given ankle joint. Using ultrasound in combination with tracking algorithms that are able to track small length changes in contractile components as small as 1 µm. Loram *et al.* (2005) showed that during voluntary sway and quite standing (Loram et al., 2004) the TS muscles anticipate and dynamically balance the body. Changes in the contractile component length occur in a paradoxical manner in the TS (Loram et al., 2004). The behavior of the contractile component is attributed to the compliance of the TT. Individuals with low series elastic stiffness require larger adjustments in the contractile component, whereas individuals with high series elastic stiffness have less or no paradoxical muscle movements.

2.3 Achilles tendon rupture

2.3.1 Epidemiology

The Achilles tendon is among the strongest tendons in the human body. Despite its remarkable strength, the AT is susceptible to both overuse injuries and sudden, acute injuries such as complete ruptures. The incidence of Achilles tendon rupture (ATR) has been on the rise (Houshian et al., 1998; Leppilahti & Orava, 1998). In Oulu Finland the average incidence increased from 2 to 12 ruptures per 100,000 in a decade from 1986 to 1994. Similar trend was reported in Denmark with an increase from 18 to 37 rupture per 100,000 from 1984 to 1996 (Houshian et al., 1998). Most of the ruptures reported by Houshian *et al.* (1998) were during sport related activities, 89% of the ruptures occurred in sport and racket games, with the highest incidence observed in the 30–39 years old age group. Ruptures that are not related to sports peak at a mean age of 52. In patients who have previously suffered an ATR there is almost 200–fold increase in the risk of tendon rupture in the contralateral limb (Årøen et al., 2004). Men are more susceptible to ATR than women, with a male-to female ratio ranging from 2:1 to 18:1, on average 6:1 (Čretnik & Frank, 2004; Houshian et al., 1998; Leppilahti & Orava, 1998). Pardes *et al.* (2016) found that male rats tendons have inferior mechanical properties and superior muscle mass size compared to female rats. There is a possibility that poorer tendon properties in combination with superior muscle mass lead to more degenerative changes over time and are responsible for the increased rates of acute ATR in middle-aged men (Pardes et al., 2016).

2.3.2 Etiology and mechanism of rupture

The etiology of the Achilles tendon rupture is considered to have multiple contributing factors, but the exact cause of the rupture is still a subject of debate (Leppilahti & Orava, 1998; Waterston et al., 1997). The most discussed theories are the chronic degeneration theory and the mechanical theory.

It is unclear whether AT rupture is preceded by chronic degeneration of the tendon or not, but the degeneration theory might explain the high incidence in the middle and older-aged population (Leppilahti & Orava, 1998). With ageing the blood flow and vascular supply decrease in the tendon (Hastad et al., 1959; Leppilahti & Orava, 1998). The low vascularity impairs the regeneration process in the tendon. Repetitive microtraumas with impaired regeneration may cause permanent tendon weakening and eventually rupture (Davidsson & Salo, 1969; Fox et al., 1975; Hattrup & Johnson, 1985). This theory is supported by angiographic and histological findings pointing to a decreased vascularity in the zone from 2–6 cm above the insertion of the tendon (Curt, 1958), that seem to increase with ageing (Hastad et al., 1959). In addition, there are age-related changes in collagen cross-linking and diameter (Sargon et al., 2005; Tuite et al., 1997). Kannus and Józsa (1991) used advanced histological techniques to study

tendons that suffered spontaneous rupture and found that almost all tendons exhibit pre-existing histopathological changes, such as hypoxic degeneration, mucoid degeneration, tendolipomatosis, or calcifying tendinopathy (Kannus & Józsa, 1991). There is limited evidence that local and systemic corticosteroids injections increase the risk of ATR (Mahler & Fritschy, 1992; Newnham et al., 1991). Systemic diseases such as gout, lupus erythematosus and rheumatoid arthritis can be associated with Achilles tendon rupture.

The mechanical theory suggests that a failure in the normal mechanism that inhibits uncoordinated excessive muscle contraction in the MTU, might play a primary role in the sudden rupture of the AT (Inglis & Sculco, 1981). In this theory, even a healthy tendon in a young patient might rupture as a result of the violent sudden strain. Rats experiments support the mechanical theory, where oblique stress with tendon loading was found to lead the healthy tendon to rupture in anesthetized rats (Barfred, 1973).

The mechanisms of AT rupture can be classified to three distinct categories. The first involves pushing off with the weight-bearing forefoot while the knee is extended, this mechanism occur in the start of a sprint, jumping and running and is reported by the majority of patients. The second mechanism involves a sudden and unexpected ankle dorse flexion, which occurs when the patient trips into a hole or stumbles downstairs. The third mechanism involves a forceful dorsiflexion of a foot that is in a plantar-flexed position, which may result from a fall from a height (Arner, 1959).

2.3.3 Healing of the tendinous tissue

Tendon healing goes through three main sequential and overlapping phases: Starting with inflammatory, then proliferative phase and lastly remodeling phase (Fig. 8) (Aspenberg, 2007). The inflammatory phase starts immediately after rupture and is marked with hematoma, the release of interleukins and TNF produced by pro-inflammatory M1 macrophages, whereas the secondary inflammatory response is marked with growth factors involved in neovascularization, such as vascular endothelial growth factor (VEGF), fibroblast growth factors (FGF) and platelet-derived growth factor (PDGF), and profibrotic factors, such as transforming growth factor (TGF)-β and connective tissue growth factor (CTGF) (Durgam & Stewart, 2017). As a result, vascularity is increased, cells are recruited and a tendon granuloma is produced (Aspenberg, 2007). Angiogenesis occurs in the proliferative phase and the tendon granuloma start to produce primarily collagen type III. In this stage the tendon granuloma mechanical strength starts to gradually increase. A tendon callus is produced 10–14 days after rupture connecting the torn tendon ends together. Late in the proliferation phase the production of collagen type I gradually take over, and the callus reaches its largest size. The tissue weakness is compensated by the large transverse area. In the remodeling stage the collagen fibers are re-absorbed and rearranged to enhance architecture and cross-linking. This stage starts a month after injury and can last for more than a year. The tissue mechanical properties gradually increase and the transverse area decrease (Hope & Saxby, 2007). The

healing results in altered Achilles tendon compositional properties, and the mechanical quality does not recover completely.

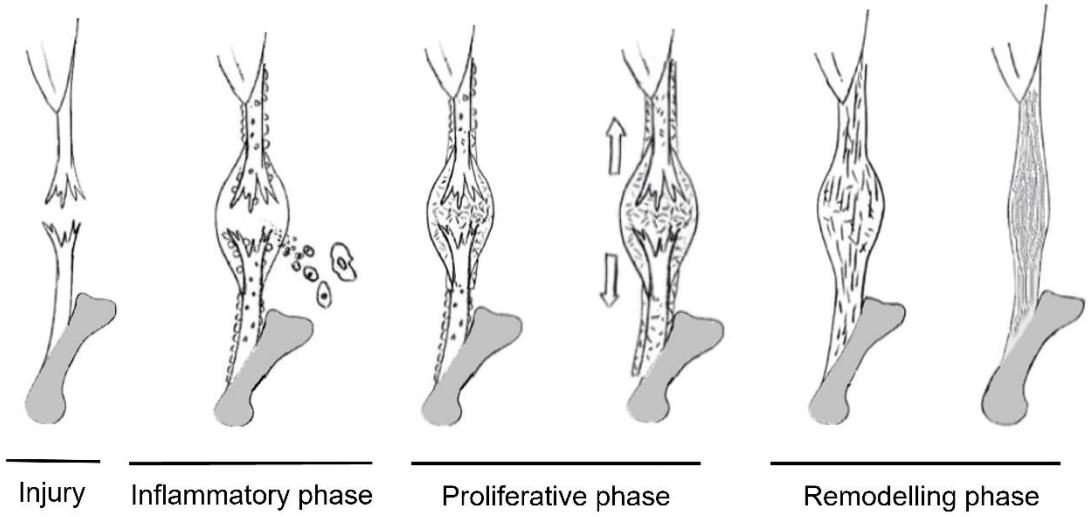

FIGURE 8 Representation of the healing phases after Achilles tendon rupture adapted with permission from (Aspenberg, 2007).

Early loading has been shown to be beneficial to the tendon material properties in animal and surgically treated tendons (Andersson et al., 2012; Eliasson et al., 2012; Schepull & Aspenberg, 2013a). Mechanical tension over the rupture area can stimulate the expression of growth factors and pro-inflammatory substances that can prompt collagen protein synthesis (Aspenberg, 2007; Heinemeier & Kjaer, 2011). Even short episodes of tendon loading can improve the expression of CDMP-2, and regulate more than 150 genes (Aspenberg, 2007; Eliasson et al., 2013). Harnessing the therapeutic effects of mechanical tension during the remodeling stage is necessary to enhance the re-alignment of the collagen fibers (Bring et al., 2007), improving the ability of the tendon tissue to withstand dynamic and static stress (Nagasawa et al., 2008).

Nutrition and diet may also have a role in the healing of the tendon after rupture. There are few studies addressing proper nutrition or supplementation following tendon injury (Curtis, 2016). Vitamin C is a promoter of collagen synthesis, and is necessary for the enzymatic synthesis of both collagen proteins and tendons proteoglycans (Berg & Kerr, 1992; Curtis, 2016). High dose of vitamin C supplementation in rats was found to promote early angiogenesis and increase the activity for procollagen-secreting fibroblasts and overall type I collagen production (Ömeroğlu et al., 2009). Another rat study observed greater tendon strength and less adhesion formations following Taurine injections in the tendon repair site (Akdemir et al., 2015). These studies provide some evidence that nutritional interventions might promote collagen synthesis in vivo, potentially improving and speeding up recovery.

In tendons, collagen forms the major extracellular protein. Interventions that increase collagen synthesis, may be helpful in rebuilding tendons. Collagen peptides might positively influence the anabolic process to synthesis elastin and

collagen type I and III in the extra cellular matrix (Schunck & Oesser, 2013). The research on collagen peptides is still scarce. However, there is a several reports of athletes and patients with tendinopathy that benefited from the intake of collagen peptides in combination with rehabilitation programs (Baar, 2019; Praet et al., 2019). Jerger and colleagues (2022) reported that supplementation of collagen peptides combined with resistance training led to greater hypertrophy in tendinous structure and tendon stiffness in healthy active men (Jerger et al., 2022). The ideal treatment following Achilles tendon rupture should be a multifactorial program including good nutrition, supplements, properly timed rehabilitation program and surgery if needed.

2.3.4 Treatment and Management protocols

Achilles tendon rupture treatment options can be divided into two main options: surgical and non-surgical. Despite many randomized control trials and systemic reviews comparing between the two treatments (Deng et al., 2017; Erickson et al., 2015; Jones et al., 2012; Khan et al., 2005; Khan & Smith, 2010), the best treatment option is still debatable (Lantto et al., 2016; Olsson et al., 2011, 2013). Surgical treatment has 2–4 times lower risk of re-rupture (Bergkvist et al., 2012; Wallace et al., 2011; Wilkins & Bisson, 2012) compared to non-surgical treatment but has 4–6 higher risk of other complications such as scar problems, nerve injury and wound infection (Bhandari et al., 2002; Erickson et al., 2015; Holm et al., 2015). Surgery might lead to faster return to work (Erickson et al., 2015), but there is no clear evidence favoring one treatment over the other, there seem to be no difference in the long-term functional outcomes.

Immediately, after rupture the ankle is immobilized in equinus position approximately 30 degrees of plantar flexion whether treated surgically or non-surgically. This is done to approximate the two ends of the tendon, prompt healing, and prevent elongation of the tendon (Ellison et al., 2017). Previous protocols used a cast for 8 weeks to immobilize the ankle, but since early mobilization have been gaining popularity in the last decade (Mortensen et al., 1999; Suchak et al., 2006; Twaddle & Poon, 2007). In some protocols the cast is removed 2–4 weeks after rupture and weightbearing is encouraged with an orthosis (Brumann et al., 2014; Saxena et al., 2022). Heel wedges are usually used in the period between 4–12 weeks after rupture to maintain a sufficient degree of plantar flexion in the early weeks of recovery to reduce strain on the tendon while walking (Akizuki et al., 2001; Sandberg et al., 2015). Early mehcanoloading could enhance the healing potential of the tendon and was found to be associated with lower re-rupture rate (Holm et al., 2015; Nilsson-Helander et al., 2010; Twaddle & Poon, 2007; van der Eng et al., 2013). However, there is some evidence that early weight bearing might lead to more elongation of the ruptured tendon in surgically treated patients especially in the early recovery period (Eliasson et al., 2018). Recently, Rendek *et al.* (2022) found that early loading 3 weeks after rupture in patients treated non-surgically led to lower elastic modulus and slightly longer tendon length in the loaded group compared to the control group, where patients performed unloaded ankle range of motion

exercises ranging from maximum plantar flexion to neutral ankle position. In surgically treated patients the same protocol did not show differences between the groups (Schepull & Aspenberg, 2013b). The baseline and the healing process may differ between the surgically and non-surgically treated tendons, as may the response to different rehabilitation protocols. Thus, it could be beneficial to investigate the two treatments separately.

Controlled early motion of the ankle might lead to quicker regain of the ankle range of motion and faster functional recovery resulting in higher patient satisfaction compared to immobilization (Huang et al., 2015; Maffulli et al., 2003; McCormack & Bovard, 2015). Controlled early motion is usually combined with early weight bearing under the umbrella of early functional mobilization. Although long term strength deficits and altered functional capacity in the ruptured limb persist in both early and delayed mobilization protocols (Maffulli et al., 2003; Mortensen et al., 1999). Early functional mobilization can increase blood flow and collagen synthesis in the in the peritendinous tissue of the AT (Kjaer et al., 2005; Magnusson & Kjaer, 2019), resulting in rapid healing in the early recovery period. There is little consensus of the definition of early functional mobilization between studies (Saxena et al., 2022). Different studies use different combinations of ankle motion, weight bearing and heel wedges, a specific evidence-based protocol is not yet available. Controlled early ankle mobilization need to be distinguished from early weight bearing, as the evidence in not clear how the two variables interact and effect the recovery after rupture.

Recently the "GAIT" (German, American, and Italian Tendon) study group suggested a rehabilitation protocol advising no weight bearing for the first 2–3 weeks. Furthermore, it was advised to avoid any exercise beyond the neutral range of the ankle, and to delay stretching and eccentric exercise for later than the first 12 weeks (Saxena et al., 2022). This was suggested to mitigate the lengthening of the tendon in the injured limb. The recovery after ATR seems to be time sensitive and more studies are needed to develop a treatment protocol where the tendon is loaded and mobilized adequately at the right time, to optimize the healing process and minimize the lengthening of the tendon.

2.4 Outcomes following Achilles tendon rupture

2.4.1 Structural outcomes

After Achilles tendon rupture there are several structural changes that occur in the injured limb (Kangas et al., 2007; Silbernagel et al., 2012b). The most notable change in the tendon structure is the increase in the tendon length, that occurs regardless of the treatment approach (Rosso et al., 2013). Studies have shown that tendon length increase in the early recovery stages, with most of the lengthening taking place in the first 6 weeks (Kangas et al., 2007; Silbernagel et al., 2012b). The tendon length continue to increase up to 6 month, then can un-

dergo slight shortening from 6 to 12 months (Kangas et al., 2007). Moreover, the tendon thickness and CSA have been shown to increase up to 2 times or more the contralateral limb AT size (Wang et al., 2013; Zellers et al., 2020). The increase in tendon thickness is thought to be a compensation for the degradation of the compositional material (Freedman et al., 2014b). Zellers *et al.* (2020) found that asymmetry in tendon CSA at 12 weeks can function as biomarkers for tendon healing prognosis and functional recovery 1-year after rupture (Zellers et al., 2020). Larger tendons at 12 weeks indicate a good response to rehabilitation and lead to better long term functional outcomes.

The structure and function of the calf muscles are also affected by ATR. Studies have shown that immobilizing the calf muscle in a shortened position during the early stages of recovery can stimulate the remodeling of the TS muscles (Brorsson et al., 2017; Mullaney et al., 2006). Hullfish et al. (2019) found that the MG muscle had shorter and more pennate fascicles compared to the contralateral limb in the first 4 weeks after rupture, but there was no change in muscle thickness (Hullfish et al., 2019a). Similar structural differences were reported in the MG muscle at 1-year (Peng et al., 2019), and 2-years after rupture (Svensson et al., 2019), with both studies reporting a loss of muscle mass and shorter fascicles in the gastrocnemius muscle, but no difference in the pennation angle. Nicholson and colleagues investigated structural changes 4.5 years after rupture and found that the MG muscle had less thickness and more pennated shorter fascicles, SOL muscle with shorter fascicles and less thickness. In contrast, LG was not affected to the same degree as the rest of the TS muscle, as only fascicle length was found to be shorter in the ruptured limb (Nicholson et al., 2020). Muscles are sensitive to changes in mechanical tension (de Boer et al., 2008), and therefore the sudden change in muscle-tendon tension can elicit changes in the MG and the TS muscles, which persist to a chronic nature as a result of the increased length of the tendon.

2.4.2 Mechanical outcomes

The Achilles tendon rupture damages the fibrous structure and the organization of the tendon altering the elastic properties of the tendon. Chen *et al*., (2013) measured the elasticity of freshly ruptured tendons within 24 hours after rupture and found lower more heterogeneous elasticity compared to the contralateral limb (Chen et al., 2013). The fresh ruptured area was mesh like and filled with fluids, which shear wave elastography did not retrieve any reading from signifying a loss of the AT material properties acutely after rupture. Multiple studies reported lower stiffness in the ruptured limb up to 2 years post rupture (Chen et al., 2013; Geremia et al., 2015; McNair et al., 2013; Wang et al., 2013). However, when Agres *et al.* (2015) investigated stiffness 2–6 years after rupture, higher stiffness was found in the injured tendons compared to the contralateral limb (Agres et al., 2015). Post rupture, the stiffness of the tendon initially drops, then gradually increase towards in the remodeling stage, to match or even exceed the stiffness in the contralateral limb (Agres et al., 2015; Karamanidis &

Epro, 2020). Higher stiffness may help mitigate the impairments in force production caused by the extra length of the tendon. Since the TS muscle operate mostly on the ascending limb of the force-length relationship (Holzer et al., 2020), higher stiffness help the muscle muscles to preserve favorable sarcomeres length during force generation by reducing the operating range.

Recent in vivo studies have found a more uniform internal displacement within surgical treated tendons 1-year after rupture (Fröberg et al., 2017). This aspect is usually overlooked in the management of ATR, despite studies suggesting that non-uniformity within the AT is important for the TS to perform their differing functional roles (Clark & Franz, 2021; Franz & Thelen, 2016). Non-uniformity within the tendon might be associated with TS fascicle length and the maximal amount that fascicles can shorten while exerting force. More uniform within-tendon displacement after rupture may stem from changes in TS structure and dynamics. Thus, shortening of fascicles in the ruptured limb could result in a smaller operating range, translating to more uniform displacement within the AT.

2.4.3 Neuromuscular outcomes

In addition to the well-documented structural and mechanical changes, there are also neuromuscular alterations that contribute to persistent performance deficits after ATR (Wenning et al., 2021). Studies have found increased TS muscle activity (Suydam et al., 2015; Wenning et al., 2021) and higher mean frequency of surface electromyography (EMG) (McHugh et al., 2019). These findings have been reported in various tasks including eccentric and concentric contractions, indicating alterations in TS motor unit coordination and potentially a preferential activation of fast-twitch muscle fibers.

Furthermore, flexor hallucis longus (FHL) has been found to have a 5% bigger cross-sectional area (CSA) in patients with ATR. This increase in the CSA of FHL muscle is a result of increased use of the muscle after ATR. Motor strategies used during the early recovery phase to produce plantar flexion force might avert or decrease tensile force transmitted through the AT, by recruiting deep flexors such as FHL (Finni et al., 2006), and persist due to the shortened position of the TS. This leads to a higher relative contribution of the FHL to the plantar flexion torque produced in the ruptured limb (Finni et al., 2006; Heikkinen et al., 2017), and could potentially serve as a marker of neuromuscular recovery.

2.4.4 Functional outcomes

Persisting functional deficits and decreased plantar flexion strength are common after ATR (Bressel & McNair, 2001; Brorsson et al., 2017; Ellison et al., 2017; Heikkinen et al., 2017; Lantto et al., 2016; Olsson et al., 2011). Multiple studies have reported strength deficits ranging from 20 to 25% at 1-year, and 10% at least 2-years after rupture (Keating & Will, 2011; Möller et al., 2001, 2002). These strength deficits manifest especially when the ankle is in the end-range of plan-

tar flexion (Mullaney et al., 2006). Mullaney *et al.* (2006) found an average of 27% plantar flexion strength deficits in plantar flexed position but did not observe any weakness when the ankle was in dorsiflexed position.

In addition to decreased strength, deficits in physical activities like jumping, running, and endurance of calf muscles have been shown in both long- and short-term periods after ATR. Nilsson-Helander *et al.* (2010) found that the ruptured leg had lower jump and endurance test scores compared to the contralateral leg at 6 and 12 months after rupture (Nilsson-Helander et al., 2010). Despite a good patient-reported outcome score in the same study, many patients did not return to the same pre-injury physical activity level.

Moreover, Karamanidis and Epro (2020) found that even engaging in high-volume, high-load training, two elite athletes had significant deficits in plantar flexion force in the injured limb 2.5 years after the injury (Karamanidis & Epro, 2020). Furthermore, Trofa *et al.* (2017) reported that approximately 30% of professional athletes who experience an Achilles tendon rupture are unable to continue their careers (Trofa et al., 2017). Therefore, ATR can result in irreversible deficits that may prevent participation in certain activities that were possible before the injury.

3 PURPOSE OF THE STUDY

Achilles tendon plays an important role in locomotion. Impairments after Achilles tendon rupture affect a range of daily activities and, in the long term, the overall quality of life. Whether treated surgically or non-surgically, patients suffer from long-term or even permanent anatomical and functional deficits. Particularly, plantar flexor strength and endurance impairments can persist for several years and likely impact participation in demanding activities.

The Achilles tendon is subjected to complex loading that can cause heterogeneity of strain within the tendon (Bojsen-Møller & Magnusson, 2015). Differential forces produced by the different TS muscles lead to non-uniform internal displacement within the Achilles tendon. Non-uniformity within the AT plays an important role in allowing the TS to perform their differing functions (Clark & Franz, 2021; Franz & Thelen, 2016). This is an important characteristic of the Achilles tendon, yet usually overlooked following Achilles tendon rupture.

Biomechanics may hold the key for understanding human movement and muscle-tendon interactions in health and disease including Achilles tendon rupture patients. Given the force and endurance deficits in plantar flexors after Achilles tendon rupture (Silbernagel et al., 2012b), and the clinical importance of regaining capacity and functionality in the ruptured limb, it would be useful to understand biomechanical factors associated with good recovery. While many studies are done on surgically treated patients, this study will further our understanding of the biomechanics and anatomy of the Achilles tendon, and how non-surgically treated patients recover 1-year after Achilles tendon rupture.

Thus, the primary purpose of this thesis was to investigate biomechanical changes 1-year after Achilles tendon rupture. A secondary aim was to examine the interactions and association between structural, mechanical, and neuromuscular factors, and ultimately identify biomechanical factors that could explain good recovery from Achilles tendon rupture.

The specific aims and hypotheses of the current thesis were:

1. To investigate internal tendon displacement patterns in non-surgically treated patients and attempt to classify patients into groups based on their displacement patterns (I).

   Hypothesis: The ruptured tendon would show a more uniform displacement pattern compared to the contralateral AT. Also, it was expected to find different cluster groups based on different displacement patterns.

2. To evaluate alterations in mechanical and structural properties of non-surgically treated muscle-tendon units 1-year after rupture, and to examine their associations with force production capacity and functional outcomes (II).

   Hypothesis: The injured Achilles tendon would be more compliant, thicker and have a longer resting length, and MG would have smaller CSA, and shorter more pennate fascicles. Inter-limb differences in MTU morphomechanical parameters were expected to be associated with MVC, walking speed and patient-reported clinical outcomes.

3. To compare internal Achilles tendon displacement patterns during voluntary and selective isolated contraction of medial and lateral gastrocnemius muscles between injured and un-injured limbs. This was done using a novel method combining speckle tracking with selective electrical stimulation (III).

   Hypothesis*:* Voluntary and electrically-induced contractions would lead to different displacement patterns. Furthermore, the injured tendon would show less, and more uniform displacement compared to the un-injured tendon.

4. To explore interconnections between structural, mechanical, and neuromuscular parameters and their associations with markers of good recovery (IV).

   Hypothesis: Tendon stiffness would be associated with the lengthening of the tendon after rupture. MG fascicle length and higher voluntary maximal torque would be related to non-uniformity within the Achilles tendon. Lastly, EMG activity of the plantar flexors and the relative contribution of FHL during isometric contraction would be higher in the injured limb- to counteract the structural deficits- and be proportional to the increased length of the tendon after rupture.

4 METHODS

4.1 Study design and subjects

4.1.1 Study design

This was a cross-sectional study embedded in a clinical cohort study "Non-operative treatment of Achilles tendon Rupture in Central Finland: a prospective cohort study – NoARC" (trial registration: NCT03704532). This thesis presents data from patients 1-year after unilateral Achilles tendon rupture that were treated non-surgically.

4.1.2 Participants

A total of 35 patients volunteered to participate in the biomechanical study that made up the 4 original papers included in this thesis. Data collection was simultaneous with writing of the papers, thus the sample number increased from 20 participants (I) to 35 (IV).

Participants were recruited through Central Finland Hospital. All patients within Central Finland health care district that suffered unilateral Achilles tendon rupture were offered the information to volunteer in the biomechanical study. Participants were diagnosed within 14 days of the rupture using guidelines of the American Academy of Orthopaedic Surgeons (AAOS): a positive Thompson test, decreased plantarflexion strength, presence of a palpable gap, and increased passive ankle dorsiflexion with gentle manipulation (Surgeons, 2009). Inclusion criteria were 2 of the 4 AAOS criteria with clear onset of symptoms, closed rupture, residence in the catchment area of the hospital district, minimum of 18 years old, ability to understand and speak Finnish and normal walking ability (>100m without aid before rupture). Patients that were treated surgically, suffered a re-rupture, or an avulsion fracture in the calcaneus were excluded from the sample.

4.1.3 Non-surgical treatment protocol

Participants were treated non-surgically in combination with early mobilization. Immediately after ATR, the ankle was cast in full equinus for 2 weeks. After 2 weeks, the physician clinically assessed tendon uniformity. If uniformity was confirmed, the foot was moved into plantarflexion using a 20° equinus open sole cast allowing toe movement. Patients were encouraged to bear full weight by treatment week 4, if possible, with a custom-made functional walking orthosis with 1 cm thick heel wedge. At week 8, the orthosis was removed, and progressive physiotherapy began. Walking, swimming, underwater running, and cycling were recommended after 8 weeks. The aim was to gradually increase loading to enable pain-free walking, after which more intense activities could be included. Light jogging was permitted when the patient exhibited ankle mobility close to that of the un-injured limb, was able to walk and could perform heel raises without pain (Reito et al., 2018).

4.1.4 Coronavirus pandemic 2019

Worldwide implementation of unprecedented public restrictions and protection measures was introduced because of coronavirus 2019 (COVID-19). The Finnish government announced restrictions on March 16, 2020. Citizens were asked to minimize social interaction, and to avoid non-essential contact in public places. Schools and universities were closed, and face-to-face teaching was suspended; remote working and teaching was recommended where possible. The elderly aged 70 years and older were told to quarantine at home and leave only when necessary. Multiple studies reported that the restriction measures had an effect on various types of traumas and injuries (Christey et al., 2020; Myer et al., 2011; Park et al., 2020). However, no change in the incidence of severe injuries was detected in Finland (Riuttanen et al., 2021).

During the pandemic period, the median age of the participants in the biomechanical study decreased. However, there was no such decrease in the median age of patients who suffered Achilles tendon ruptures in the Central Finland Hospital healthcare district area, as shown in Fig. 9. This discrepancy may be due to the elderly population's avoidance of unnecessary social participation in fear of contracting the infectious disease. It is worth noting that the median age of the study participants returned to normal once the government relaxed quarantine measures.

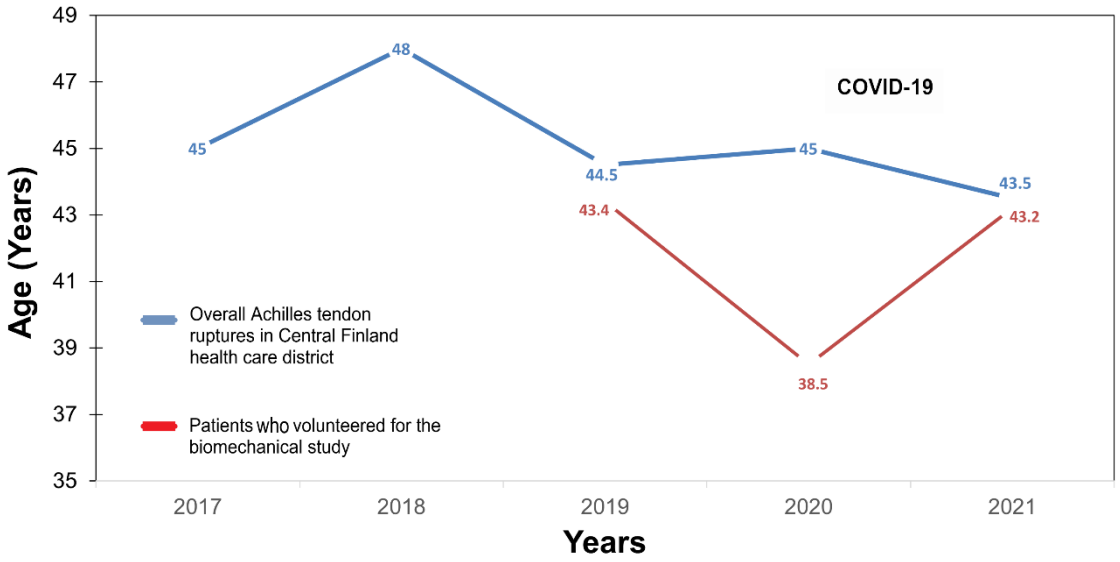

FIGURE 9 Median age of patients who suffered Achilles tendon rupture in Central Finland health care district in blue, and patients who volunteered for the biomechanical study in red.

4.1.5 Ethical considerations

The study was approved by the Research Ethics Committee of Central Finland Health Care District (Approval number: 2U/2018) and amended in March 2021. All methods conformed to the standards set by the latest revision of the Declaration of Helsinki. An informed consent explaining the details of the study and possible risks was signed by the patients. Participants authorized the use of data for research purposes and were able to withdraw at any time. Each participant was assigned an identification number that was used to pseudonymize the data.

4.2 Study protocol data collection and analysis

Upon arrival to the laboratory participants were prepared for the measurements, whereby both malleoli and first and fifth metatarsal heads were marked with a pen. Photos of the foot were taken with a ruler beneath them as a reference. First, Achilles tendon resting angle (ATRA) was measured in prone position with knee flexed at 90° and a relaxed ankle. The reference points were the head of the fibula, distal tip of the malleolus and the tip of the fifth metatarsal head. A goniometer was placed over the lateral malleolus mark with the two arms pointing towards the other two reference marks (Carmont et al., 2015). Then, the origins and insertions of the three TS subtendon length were identified using a 3.6-cm linear probe (UST-5411, Aloka alpha10, Japan). Images of Achilles tendon thickness and MG fascicle length were acquired when relaxed in prone position with the foot resting over the edge of the bed. Extended field

of view function was used to acquire CSA images of MG and LG at 50% of MG muscle length with the knee flexed to 90º and the ankle in neutral position.

Then, participants were prepared for measuring muscle activity using EMG. The skin of each participant was shaved, cleaned, and abraded with alcohol pads to reduce skin impedance. Disposable dual surface silver-silver electrode Ambu BlueSensor N electrodes (Ambu A/S, Ballerup, Denmark) were placed on the triceps surae muscles of each leg with an interelectrode distance of 22 mm in accordance with SENIAM (Surface Electromyography for the Non-Invasive Assessment of Muscles) recommendations (Stegeman & Hermens, 2007). FHL electrode was placed between the SOL insertion and the FHL muscle-tendon junction where only the FHL muscle belly lies (Péter et al., 2015), with an interelectrode distance of 16 mm. Location of the electrode placement was confirmed during isolated big toe plantar flexion using ultrasound imaging.

After checking the quality of EMG signals, participants were seated in a custom-made ankle dynamometer (University of Jyväskylä, Finland) with hip, knee, ankle, and first metatarsophalangeal joints fixed at 120°, 0°, 90°, and 0° respectively. The seat was locked in position with foot and thigh strapped to avoid any heel lift or postural changes during isometric contractions. A monitor was positioned in front of the participant to enable them to follow the torque signal in real time. After a series of submaximal contractions to warm up, participants performed unilateral maximal voluntary contractions (MVCs) starting with the un-injured limb. Participants tried to reach maximum torque in 2-3 seconds and decrease back to zero resulting in a 6 second pyramid-shaped torque curve. Participants received verbal encouragement to ensure maximal effort. They performed at least 2 MVC trials and the trial with the highest torque was used for further analysis. During the MVCs, MG MTJ length changes were tracked using a 6-cm linear probe (Aloka alpha10, Japan).

Then, participants stepped out of the chair and EMG electrodes were removed. Participants were asked to walk at their preferred speed with the instruction "walk at the speed you normally walk freely down the street" for 6 meters with photocells at both ends. Preferred walking speed was defined as the average of 3 trials.

Lastly, the thickest part of both the gastrocnemius muscles was located using ultrasound imaging. The skin was cleaned, and a pair of 32 mm diameter electrodes (Niva Medical Oy) was attached over each muscle with ~ 1 cm between the electrodes (Fig. 10). Participants returned to the ankle dynamometer and were strapped in with the aforementioned settings. The 3.6-cm probe was attached longitudinally with the distal edge ~ 2 cm above the calcaneus to image the tendon displacement at 50 Hz. Unilateral contractions corresponding to 30% of un-injured MVC were performed. Then, with the participant relaxed, single stimulation pulses were elicited with increasing intensity using a constant current electrical stimulator (DS7AH; Digitimer, Hertfordshire, UK) until the motor threshold was exceeded, confirmed by a visible muscle twitch (Bojsen-Møller et al., 2010; Finni et al., 2017). If a corresponding displacement was not observed clearly in the ultrasound image of the AT, higher stimulation intensity was used. AT displacement was imaged 1 second before and through-

out the tetanic pulse of 1000 µs at 100 Hz at the pre-determined stimulation intensity. MG and LG were stimulated in random order. The entire protocol was then repeated for the un-injured limb.

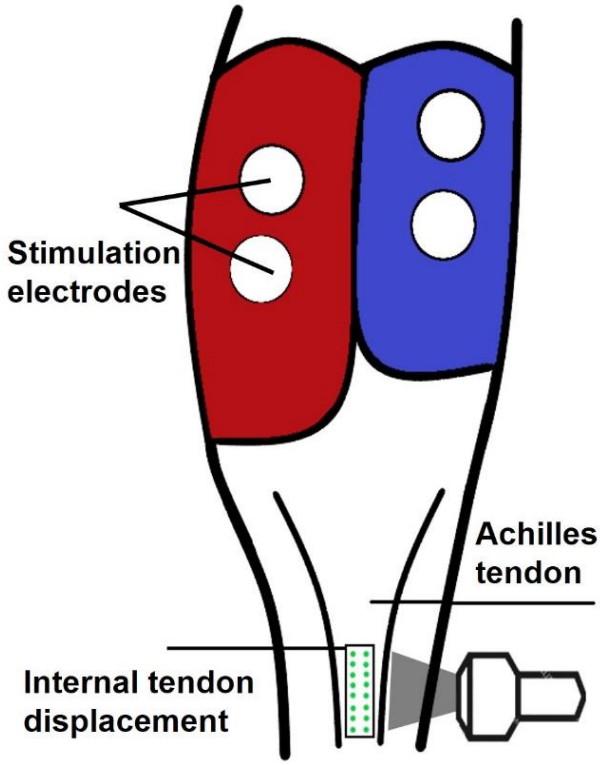

FIGURE 10 Schematic representation of the stimulation experimental setup, illustrating a participant's right limb. The resulting displacement from electrically-evoked and voluntary contractions was recorded at 50 Hz using a 3.6-cm linear probe.

4.2.1 Data collection

Analog data were sampled at a minimum of 1 kHz via a 16-bit A/D board (Power 1401, Cambridge Electronic Design, Cambridge, UK) connected to the lab computer, and signals were recorded using Spike2 software (Cambridge Electronic Design, Cambridge, UK). To synchronize data, a TTL-pulse was sent manually via Spike2 to trigger the recording of the US device for 8 seconds and to deliver the 0.7 second tetanic pulse.

4.2.2 Tendon and muscle structure (II, III, IV)

The most distal MTJ point of MG, LG and SOL and most proximal point of the calcaneus were scanned using the 3.6 probe and marked on the skin. Then, the distance between the calcaneal mark and the MTJ of each TS muscle was measured with a measuring tape following the curvature of the leg (Barfod et al., 2015). The reliability of this method was tested, whereby four healthy limbs

were measured on two separate days. The subtendon lengths of the triceps surae muscles were measured and the intraclass correlation coefficient ($ICC_{3.1}$) was calculated (Hopkins, 2000). $ICC_{3.1}$ was 0.99 (90% CI 0.97–0.99) with a coefficient of variation (CV) of 6.6%.

Achilles tendon thickness was analyzed 1 cm above the calcaneus. Two images were taken per limb per subject, and the mean values were calculated and used for further analysis. The repeatability of this method was measured using the two images acquired per limb. Typical repeated measures error for tendon thickness was 4.1%.

MG fascicle length and pennation angle (PA) were acquired in prone position as described above using the 6-cm linear probe (UST-5712; 7.5 MHz). Images were taken from the central portion of the muscle belly halfway between the MTJ and the crease of the knee where the deep and superficial aponeuroses of the muscle were parallel (Bolsterlee et al., 2016). Average values from two images were used for further analysis. Repeated measures typical error was 6.2% for MG fascicle length and 6.5% for pennation angle.

CSA images of MG and LG were taken at 50% of MG muscle length in prone position with the knee flexed to 90°. A guiding frame was attached to the skin to ensure that the image was taken in the transverse plane. The extended field of view function was used to visualize CSA. All structural image analysis was done using ImageJ (1.44b, National Institutes of Health).

4.2.3 Mechanical properties of the Achilles tendon (II, IV)

4.2.3.1 Achilles tendon moment arm and force

Force data were collected via a transducer in the foot pedal of the ankle dynamometer. A potentiometer placed under the heel was used to detect heel lift during contractions. Data were sampled at 1 kHz.

AT moment arm length was calculated from photos taken in the sagittal plane from both medial and lateral sides of the foot with pen marks on the malleoli as a reference. The moment arm was measured as the horizontal distance from the estimated center of rotation (axis through the tip of the medial and lateral malleoli) to the midpoint of the AT (Arampatzis et al., 2005). First, the horizontal distance from the ankle joint center to the posterior aspect of the AT skin (M1) was measured with a custom MATLAB (R2018a) script. Then, the distance from the skin to the midpoint of the tendon (M2) was measured from a sagittal plane ultrasound image taken from the AT (see below), and subtracted from the ankle center of rotation to AT distance:

AT moment arm: $MA = M1 - M2$ (Kongsgaard et al., 2011).

AT force was calculated as the plantar flexion torque measured by the dynamometer divided by the respective AT moment arm (MA) of each subject. A small joint rotation (heel lift) usually occurs during isometric plantarflexion tasks, resulting in an overestimation of MTJ displacement. This displacement

was recorded and corrected using the potentiometer under the heel (Ackermans et al., 2016). The mean (SD) magnitude of heel lift during MVC was 2.0 mm (4.3) and 0.5 mm (0.08) during 30% submaximal contractions.

4.2.3.2 Tracking of the Achilles tendon

Evaluating mechanical properties, especially strain and stiffness, requires high measurement precision. Including the aponeurosis in estimates of tendon length change can artificially increase measured elongation (Arampatzis et al., 2007; Arellano et al., 2019; Azizi & Roberts, 2009b; Finni et al., 2022). Accordingly, the exact MG MTJ location was tracked (Fig. 11) rather than a more proximal point on the aponeurosis to avoid the effects of increased elongation, which could overestimate displacement and strain (Finni et al., 2022).

During maximal isometric contractions, MG MTJ displacement was imaged with the 6 cm linear probe in B mode. The ultrasound probe was strapped over the most distal part of MG, as elongation measured at MTJ represents tendon elongation with the possible heel lift accounted for. Ultrasound videos were sampled at 70 Hz for 8 seconds per contraction using the same Aloka device as for the resting measurements. MTJ displacement was tracked manually with Tracker 5.1.3 Software (https://physlets.org/tracker/) using a 4 cm calibration bar and an oval-shaped feature template (length: 0.3–1 cm, height: 0.25–0.50 cm). Accuracy was visually confirmed for each trial. Displacement data were smoothed using a 0.14 s moving average. Maximum displacement was then extracted for each participant's highest torque of each respective limb to represent AT elongation.

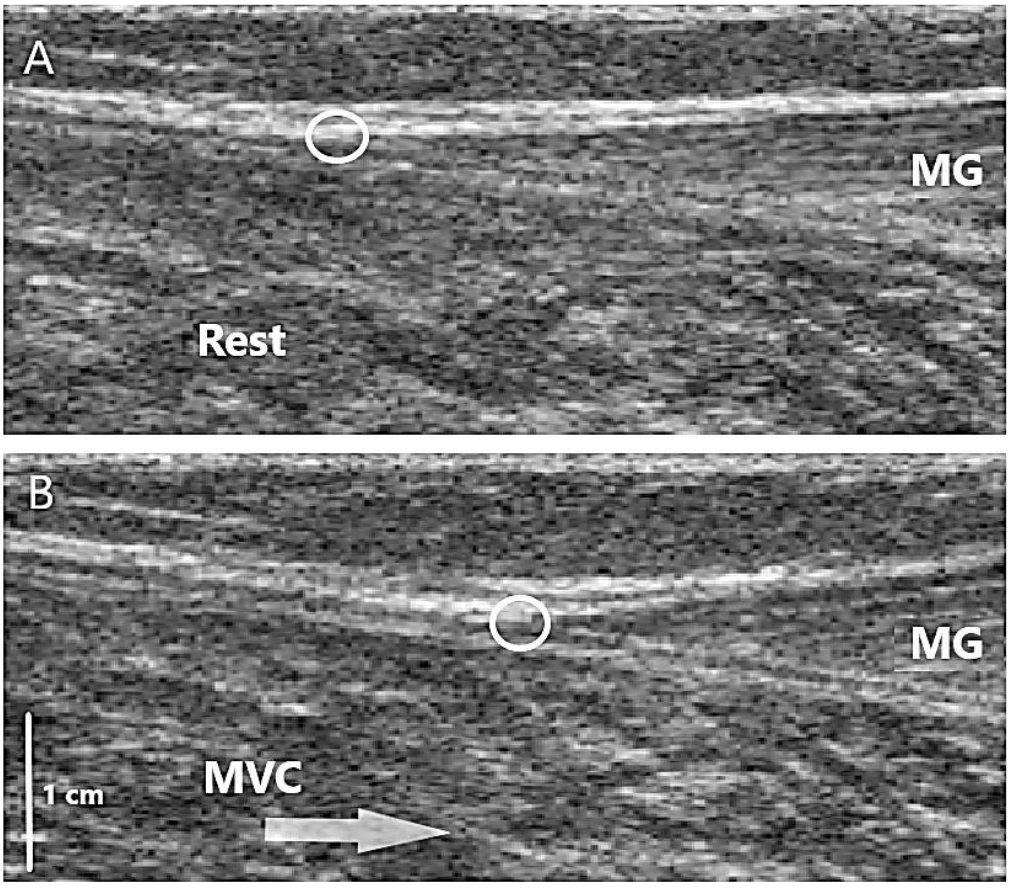

FIGURE 11 B-mode ultrasound images of the MG MTJ (A) at rest and (B) during MVC. Circles indicate the position of the tracked MTJ.

4.2.3.3 Achilles tendon stiffness

Tendon elongation and force recordings were synchronized, allowing AT force-elongation relations to be constructed for each subject and fitted to a second order polynomial forced through zero (Magnusson et al., 2001). In some cases, mostly injured limbs, a second order polynomial fit was applied only up to 80% of MVC or below (Fig. 12). This was done because AT length reached a plateau while plantarflexion force was still increasing, resulting in poorly fitting polynomials when using data up to 100% of MVC (Fig. 12).

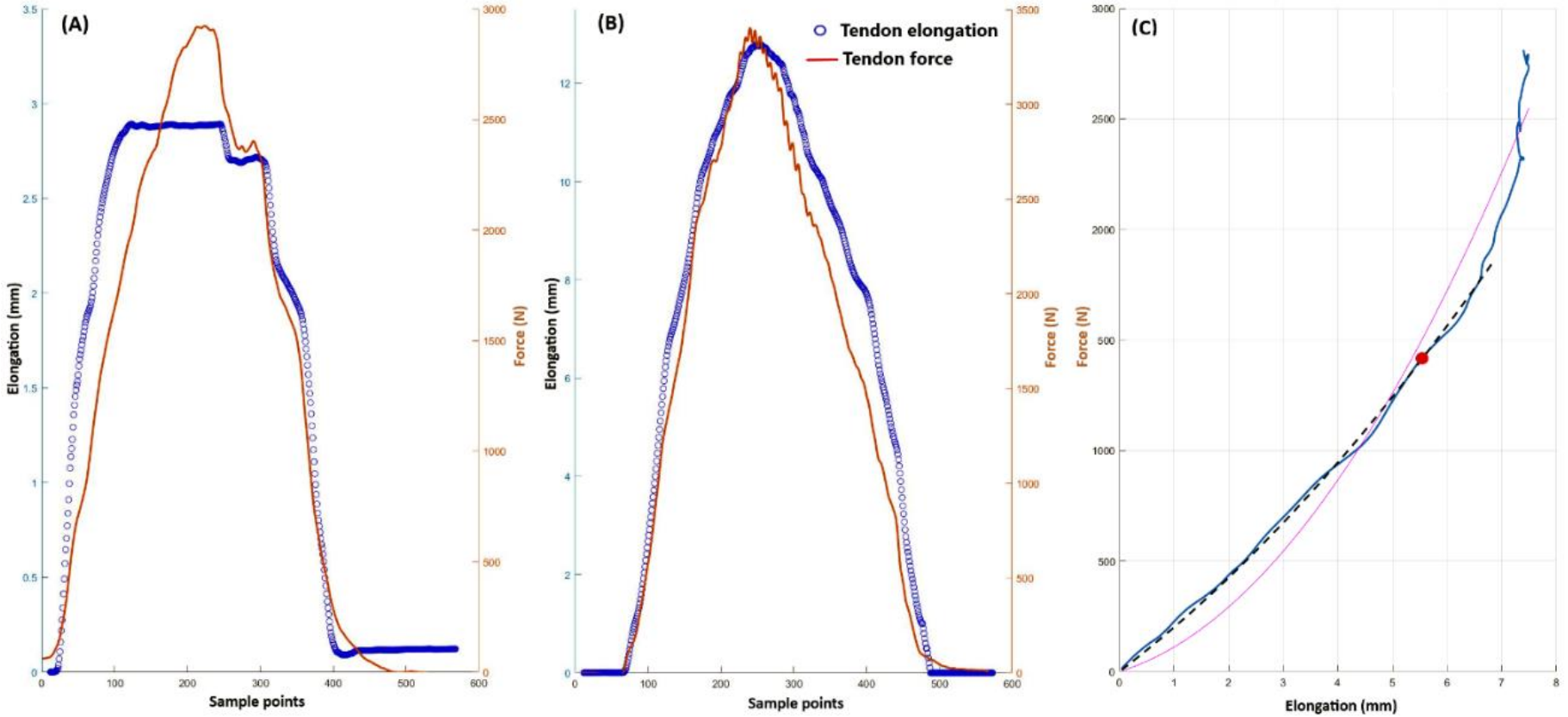

FIGURE 12 Example of synchronized raw tendon force and elongation data for both limbs of one subject. (A) Injured limb, where AT elongation reached a plateau while force was still increasing. (B) Data from the same subject's un-injured limb. (C) The elongation plateau in some subjects (as seen in A) causes the force-elongation curve to rise vertically at high forces, resulting in a poor 0-100% polynomial fit (solid pink line). In this case, a polynomial fit to 80% of MVC (black dashed line) yielded a better curve fit. Stiffness was defined as the slope of the fitted curve at 50% MVC of the injured limb (red dot).

The second order polynomial described the force-elongation behavior of the tendon well, as evidenced by R^2 values that always exceeded 0.90. From the polynomial, tendon stiffness was taken as a tangent at 50% MVC of the injured limb (Fig. 12C). In this way, the stiffness of both limbs was calculated at the same absolute force level. Normalized stiffness was also calculated because AT elongation at a given force depends on the resting length of the tendon (Arampatzis et al., 2007). Normalized stiffness was defined as the slope of the tendon force-AT strain relationship.

4.2.4 Internal Achilles tendon displacement (I, III, IV)

Recently, ultrasonic speckle tracking has been validated to allow quantification of AT internal movement (Beyer et al., 2018; Slane & Thelen, 2014b). The speckle tracking algorithm was implemented in MATLAB (R2018a & R2020a, MathWorks Inc, Natick, MA, USA) and followed the configuration of Slane and Thelen (2014c, b). The region of interest (ROI) was manually positioned over the distal part of the tendon. The size of the ROI was adjusted individually to ensure that only the tendon tissue was included. Inside the ROI, a grid of 6 locations across the thickness of the tendon and eleven across the length of the tendon was generated (Fig. 13B). The 6 locations across the tendon are referred to starting from superficial (location 1), to deep (location 6) respectively. All tracking was visually monitored to ensure that the ROI remained within the tendon throughout the movement. Although the configuration of Slane and Thelen (2014c, b) was utilized, the median filter was not used in the data processing (Slane & Thelen, 2014b, 2014c). Only a low-order polynomial was utilized to reduce noise in the tracked nodal displacements (Slane & Thelen, 2014c).

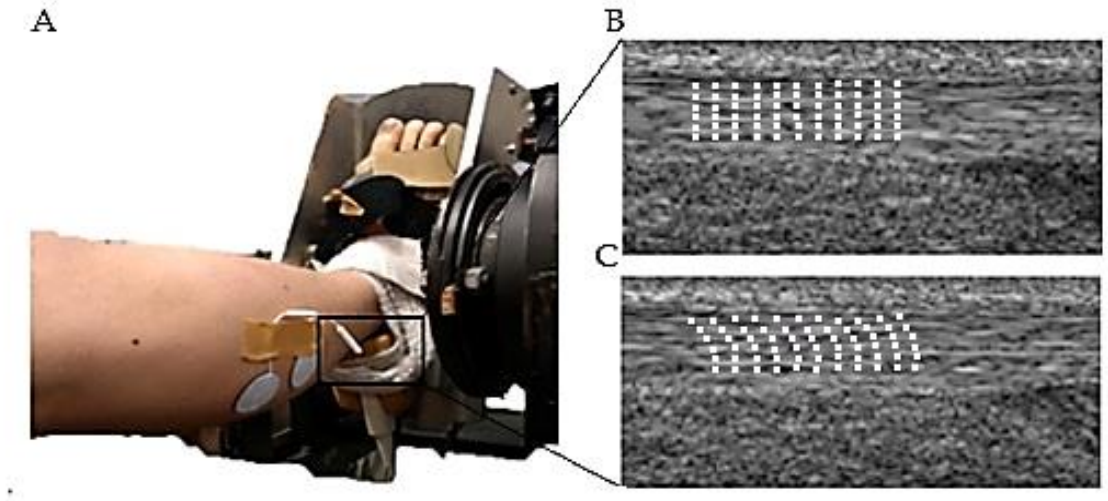

FIGURE 13 An overview of the torque measurement setup (A) and an example of ultrasound image analysis (B, C). The probe was fixed with an elastic bandage over the distal AT. B: The tendon at rest with the grid of 66 nodes generated across the AT (11 across the length and 6 across the width) overlaid on the image. C: The same grid of nodes during 30% MVC ramp contraction.

The reliability of the same video tracking was evaluated by analyzing ten videos twice since the algorithm might be sensitive to the initial placement of the nodes. This revealed excellent repeatability with a correlation of $r_p = 0.94$, $p < 0.01$ and 0.2% change in mean. Furthermore, the effect of polynomial fitting on the tracked internal tendon displacement was investigated by repeating the analysis for 3 ultrasound videos with and without the polynomial fitting. The videos included two voluntary contraction videos corresponding to 10 and 30% of the un-injured MVC and one electrically-evoked contraction video. The displacement amplitude and pattern were very similar with and without the fitting polynomial (Fig. 14).

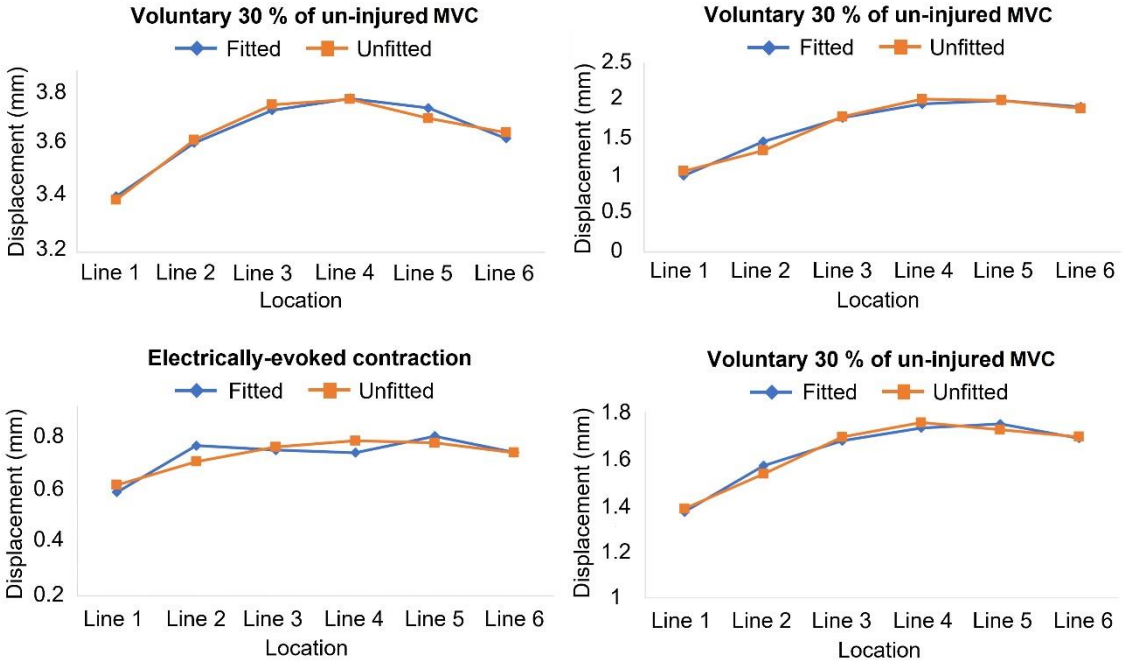

FIGURE 14 Comparison of tracked internal tendon displacement between analyses using polynomial fitting (orange) and without (blue), in both voluntary (above) and electrically-evoked (below) contractions.

Displacements of nodes along each of the 6 antero-posterior rows were averaged and peak displacements of the average data were extracted for analysis. The values and locations of maximal and minimal displacement across the tendon were extracted. Tendon non-uniformity was calculated as the difference between maximum and minimum displacement across the 6 locations. Furthermore, displacement was normalized by dividing non-uniformity by the average peak displacement across all regions.

To facilitate the comparison of displacement patterns between electrically induced contractions and volitional activation, the displacement data were normalized to the maximum displacement value. Displacement ratio was calculated in the range 0–1, where 0 is minimum displacement location and 1 is maximum displacement location. The relative displacement relation between 6 locations across the tendon is hereafter referred to as the displacement pattern. This

was done because voluntary contraction produced higher torque and overall AT displacement than electrically-induced contractions.

4.2.5 Neuromuscular activation during isometric plantar flexion (IV)

EMG signals of the triceps surae muscles and FHL were collected at 1500 Hz using a Noraxon wireless EMG system (Noraxon Inc., Scottsdale, AZ, USA). The data were filtered using a fourth order Butterworth filter between 20–450 Hz with a custom-made MATLAB script. Root mean square (RMS) envelopes were then computed using a moving 50 ms window and normalized to the RMS from a 1 second window during MVC. The mean EMG amplitude of each muscle was calculated in a 1 second window around the peak torque of the 30% MVC contraction condition and used for further analysis. Total EMG activity of all plantar flexor muscles was also computed by summing SOL, MG, LG and FHL activity. This cumulative value denoted 100% and was used to evaluate the relative contribution of each muscle to total plantarflexion activity (Masood et al., 2014).

4.2.6 Patient-reported outcome (II)

The Achilles tendon rupture score (ATRS) survey consists of 10 questions that assess self-reported limitations in different aspects of AT function. The survey was developed and validated by Nilsson-Helander *et al.* (2007) and has been translated to multiple languages since then. The original survey items are assessed with a Likert scale where 10 is the best possible score. The Finnish ATRS score is not validated, where the scores are flipped and 0 is best possible score, indicating a normal functioning AT. The score system was flipped to approximate the patients experience with other assessment scales used in clinical practice. Patients filled out the ATRS surveys in the hospital at the 1-year follow up, 24 patients were asked to fill the survey, 5 were non responders.

4.3 Statistical analysis

All statistical analysis except (I) was performed using JASP (JASP, Amsterdam, Netherlands). The descriptive data are reported as mean (SD), unless otherwise stated. Skewness and kurtosis were checked to ensure the normality of the data. If outliers were detected, the test was done with (i.e. the entire sample) and without the outlier. Pairwise t-tests were used to explore differences between limbs (injured vs. un-injured) in structural, neuromechanical, and mechanical properties. The level of significance was set at $p < 0.05$. Inter-limb differences (Δ) were calculated for all variables as percentage (%):

difference between limbs: (*Injured – un-injured*)/(*un-injured*) * 100 (Carabello et al., 2010).

Tendon non-uniformity during submaximal isometric contraction (I). Statistical analyses were performed using SPSS (IBM SPSS Statistics for Windows, Release 24.0, Chicago, Illinois). Two-way repeated measures ANOVA was performed for peak tendon displacement (6 locations) and limb condition (un-injured vs injured). When the assumption of sphericity- determined by Mauchly's test- was violated, Greenhouse-Geisser adjustment was applied. Bonferroni adjusted post hoc test was used to compare displacement values between locations for each group separately.

K-means clustering (I) (JASP version 0.11.1) was used to classify patients according to AT displacement patterns. Cluster numbers (i.e. the value of K) were chosen using the elbow method with respect to the Bayesian information criterion (BIC) value. Clustering was repeated 5 times for each group and confirmed that each data point was consistently assigned to the same cluster group. Furthermore, to explore the validity of clustering, two-way repeated measures ANOVA for peak tendon displacement (6 locations) and clustered groups as a factor was performed for the injured and un-injured limbs separately.

Two-sided paired t-tests were used to compare MVC torque values between limbs, and to compare maximal and minimal displacement values at the limb and cluster level. Non-parametric Wilcoxon signed rank test and two-sided paired t-tests were used to compare peak relative displacement between limbs due to the skewness of the data. Preferred walking speed, tendon peak relative displacement, locations of maximum and minimum displacement between un-injured clustered groups, and MVC torque were compared between cluster groups for each limb separately using Independent Samples t-test for the injured limb and one-way ANOVA for the un-injured limb.

Adjusted linear mixed models (II). Mechanical and structural differences between limbs of 24 patients were compared using linear mixed models. A linear mixed model with random intercepts was built using limb condition (injured vs un-injured) and age as fixed factors, and patient ID as a random factor. Model terms were tested using the Satterthwaite method for each variable independently. Restricted maximum likelihood with Satterthwaite approximation was used since it produces acceptable type 1 error for small sample sizes (Luke, 2017). Descriptive data are presented as fixed effect estimates 95% CI and adjusted p values.

Displacement patterns during electrically-induced and voluntary contractions (III). The main interest of this analysis was in the three- and two-way interaction effects, indicating how the displacements were distributed between the tendon locations in the different conditions and limbs. Three-way repeated-measures ANOVA was performed to investigate the effects of contraction type (Voluntary, MG, and LG stimulations), limb condition (injured vs un-injured) and tendon location (across 6 locations) on the normalized displacement of the tendon. If significant three-way interactions were detected, two-way analysis was performed, followed by simple pairwise comparisons with Bonferroni-adjustment when a significant main effect was found. Greenhouse-Geisser adjustment was applied when the assumption of sphericity was violated.

Relationships and inter-connections between measured biomechanical inter-limb differences (II, IV). Relationships between measured factors were examined using bivariate Pearson's correlation (II) and partial correlations controlled for age and sex (IV). Correlations were interpreted as 0.1 (weak), 0.4 (moderate), and 0.70 (strong) (Schober et al., 2018).

Multivariable linear regression (I, II, IV). To examine the associations of measured variables with patient-reported outcomes, functional outcomes (MVC, preferred walking speed) and factors that are likely associated with good recovery, multivariable linear regression models were built with age and gender as confounding factors. Correlations within predictors were examined using Pearson's correlation. If a strong correlation (> 0.7) was found, one of the correlated variables was removed to ensure collinearity. The inclusion of covariates in models was based on previous knowledge (Agres et al., 2015; Clark & Franz, 2018; Heikkinen et al., 2017; Hullfish et al., 2019b; McHugh et al., 2019; W. C. Peng et al., 2019; Stäudle et al., 2020; Wenning et al., 2021), considering the associations detected in the aforementioned correlations.

5 RESULTS

In this chapter the main results of this thesis are presented. For more details, please refer to the original papers (I-IV). This thesis presents data for 35 patients (6 females; means ± SD age: 41.1 ± 9.8 years, height: 175.9 ± 7.1 cm, mass: 83.1 ± 13.9 kg) 1-year after unilateral non-surgically treated ATR.

5.1 Structural properties (II, III, IV)

The lengths of all the TS muscle subtendons were longer in the injured limb compared to the un-injured with a mean difference (95% CI) of 2.0 cm (1.5–2.6 cm) for MG, 1.9 cm (1.3–2.4 cm) for LG and 1.8 cm (0.9–2.7 cm) for SOL. The ruptured tendons were also thicker by 0.46 cm (0.4–0.5 cm). ATRA was smaller in the ruptured limb with a mean difference (95% CI) of 5.9 ° (3.9–7.6 °).

At rest the MG of ruptured limb had 1.0 cm (0.8–1.2 cm) shorter fascicles, but no difference was detected for the pennation angle (1.5 °, 0.3–3.3 °). MG CSA was smaller in the injured limb (2.0 cm^2, 1.3–2.7 cm^2), but no difference was detected for LG CSA (0.6 cm^2, -0.1–1.3 cm^2). Mean values and inter-limb differences are summarized in Table 1. For adjusted analysis readers are referred to (II).

TABLE 1 Descriptive data of measured variables and their inter-limb differences.

	Un-injured	Injured	Inter-limb difference (Δ)	p value
SOL subtendon length (cm)	8.79 ± 3.47	10.36 ± 3.71	29.1%	p < 0.001
MG subtendon length (cm)	18.90 ± 1.92	20.99 ± 2.20	11.4%	p < 0.001
LG subtendon length (cm)	21.59 ± 1.60	23.51 ± 1.99	9.1%	p < 0.001
AT Thickness (cm)	0.48 ± 0.10	0.95 ± 0.22	99.8%	p < 0.001
ATRA	0.48 ± 0.10	0.95 ± 0.22	–4.5%	p < 0.001
MG fascicle length (cm)	4.75 ± 0.76	3.75 ± 0.67	20.3%	p < 0.001
MG CSA (cm^2)	14.64 ± 3.91	12.59 ± 3.61	–13.5%	p < 0.001
LG CSA (cm^2)	7.79 ± 2.12	7.19 ± 2.74	– 5.9%	p = 0.091
Non-uniformity (mm)	1.47 ± 1.02	0.91 ± 0.76	–11.6%	p = 0.017
Normalized non-uniformity (mm)	0.43 ± 0.29	0.26 ± 0.18	–11.4%	p = 0.005
Stiffness (N/m)	639.2 ± 305.5	594.6 ± 337.5	–2.9%	p = 0.328
Normalized stiffness (kN/strain)	115.9 ± 54.8	121.1 ± 70.2	8.9%	p = 0.548
AT elongation (mm)	11.13 ± 6.18	7.00 ± 4.85	–28.3%	p < 0.001
MVC (Nm)	199.0 ± 65.7	158.9 ± 68.0	–19.7%	p < 0.001
SOL EMG (%)	21.4 ± 7.1	32.8 ± 17.8	67.3%	p = 0.003
MG EMG (%)	35.5 ± 11.9	45.0 ± 16.4	35.8%	p < 0.001
LG EMG (%)	22.4 ± 12.2	31.7 ± 20.7	65.5%	p = 0.027
FHL EMG (%)	19.5 ± 20.0	35.7 ± 21.4	176.3%	p = 0.005

Electromyography (EMG) activities are mean values of a 1-second window during the submaximal ramp contraction expressed as % of EMG recorded during maximal voluntary contraction. The submaximal plantarflexion torque level was the same in both limbs (30% of the maximum of un-injured limbs). AT elongation was tracked during maximum contraction. P values refer to pair-wise T-test comparing the limbs with bolded values indicating a significant difference between limbs ($p < 0.05$).

5.2 Mechanical properties (II, IV)

There was no statistical difference in AT stiffness between limbs 1-year after rupture, with a mean difference (95% CI) of 44.8 N/m (-47.1–136.4 N/m). Similarly, there was no difference in normalized stiffness (5.2 kN/strain, -12.2–22.6 kN/strain). The ruptured tendons displayed lower AT elongation during MVC with a mean difference (95% CI) of 4.2 mm (2.1–6.3 mm). Plantar flexion MVC torque was lower in the injured limb, with an inter-limb difference of 40.0 Nm (27.3–52.8 Nm).

5.3 Internal Achilles tendon displacement (I, III, IV)

5.3.1 Non-uniform displacement within non-surgically treated rupture AT

The same absolute torque level was reached during submaximal contraction for the un-injured (mean ± SD 61.48 ± 20.82 Nm) and injured limb (61.41 ± 20.75

Nm). Furthermore, there was no statistically significant difference in stimulation-evoked torque levels between limbs in response to stimulation of either muscle.

During submaximal contractions the ruptured limb internal displacement was more uniform with a mean difference (95% CI) of 0.56 mm (0.11–1.02 mm) compared to the contralateral limb. Normalized non-uniformity was also larger in the un-injured limb with a mean difference (95% CI) of 0.17 (0.05–0.29).

The same phenomena were observed during isolated electrically-stimulated contractions (III). The un-injured limb non-uniformity was higher compared to the injured limb with a mean difference (95% CI) of 0.11 mm (0.04–0.18 mm) during the stimulation of MG (MG_{stim}), and 0.09 mm (0.03–1.42 mm) during LG stimulation (LG_{stim}). When non-uniformity was compared between stimulated muscles in the same limb, there was no statistically significant difference in either limb, with a mean difference (95% CI) of 0.016 mm (-0.06–0.09 mm) for un-injured and 0.003 mm (-0.05–0.05 mm) for the injured limb.

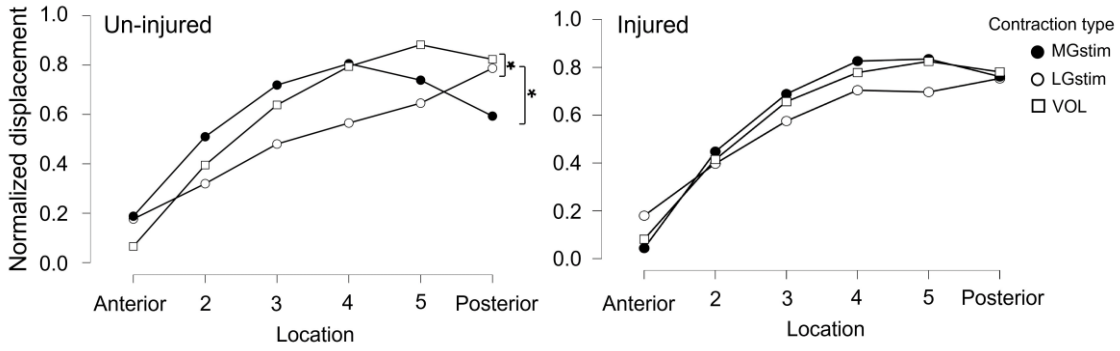

FIGURE 15 Mean ± SD normalized displacement patterns during voluntary and selective electrically-induced contractions of the medial (MG) and lateral (LG) gastrocnemius muscles in the un-injured (left) and injured limb (right). Graphs represent group means. Individual patterns for the un-injured limb are shown in Fig 16. * = difference between contraction types ($p < 0.05$).

5.3.2 Voluntary and electrically-induced displacement patterns

The absolute values of the 6 tendon locations were normalized to enable comparison of displacement patterns between voluntary and stimulation conditions (Fig. 15). There was a significant two-way interaction of contraction type*location on tendon displacement (F (10–978) = 3.7, $p < 0.001$). Initial three-way analysis was followed by a two-way repeated-measures ANOVA for the effect on tendon displacement at the levels of limb condition and contraction type.

There was no significant location*limb condition interaction effect on tendon displacement at each contraction type level (Fig. 15). There was a significant contraction type*location interaction effect on tendon displacement (F (10–492) = 3.8, $p < 0.001$) in the un-injured limb, while the interaction effect was not significant for the injured limb (F (10–486) = 1.11, $p = 0.353$). Simple pairwise

comparisons were done between the contraction types for the un-injured limb with a Bonferroni adjustment applied. The analysis showed that the LGstim displacement pattern was significantly different to MGstim ($p = 0.007$), and voluntary contraction ($p = 0.003$). Individual displacement patterns are shown in Fig. 16.

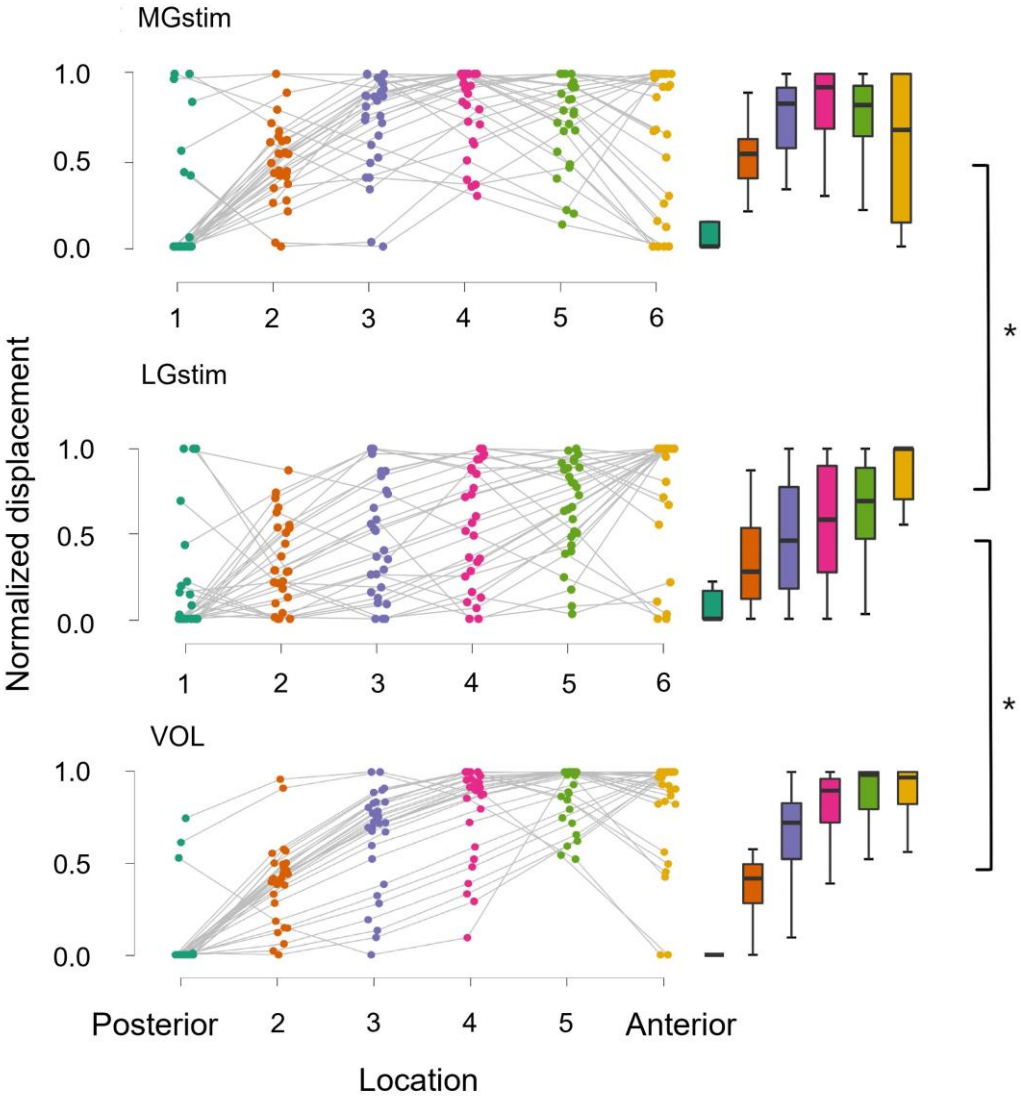

FIGURE 16 Normalized displacement patterns in the un-injured limb. Left: Raw data points for each participant during (VOL) voluntary and selective electrical stimulation across the 6 locations of the Achilles tendon. Right: Box plots of means and SD for each location (1–6 respectively). * = difference between contraction types ($p < 0.05$).

5.3.3 Clustering participants according to internal Achilles tendon displacement (I)

The analysis classified participants into three groups (n = 7, within-cluster sum of squares: 8.40; n = 8, 5.03; n = 5, 5.14; $p < 0.001$), according to the internal AT displacement in the un-injured limb, while only two groups were formed in the injured limb (n = 5, 11.58; n = 15, 25.44; $p < 0.001$) (Fig. 17).

There was a significant difference in tendon non-uniformity ($p = 0.040$) between injured limb clusters, but not between un-injured limb clusters. Two-tailed paired t-test showed significant differences between maximum and minimum displacement for all the un-injured clusters, with mean differences (95% CI) of 1.3 mm (0.29–2.5 mm) in group 1, 1.1 mm (0.61–1.6 mm) in group 2, and 1.5 mm (0.18–2.8 mm) in group 3. For the injured limb clusters, there was a significant difference between maximum and minimum displacement in group 1, with a mean difference (95% CI) of 0.48 mm (0.29–0.67 mm), but no significant difference in group 2, mean difference (95% CI) 1.3 mm (0.02–2.6 mm).

For more detailed analysis between clustered groups readers are referred to (I).

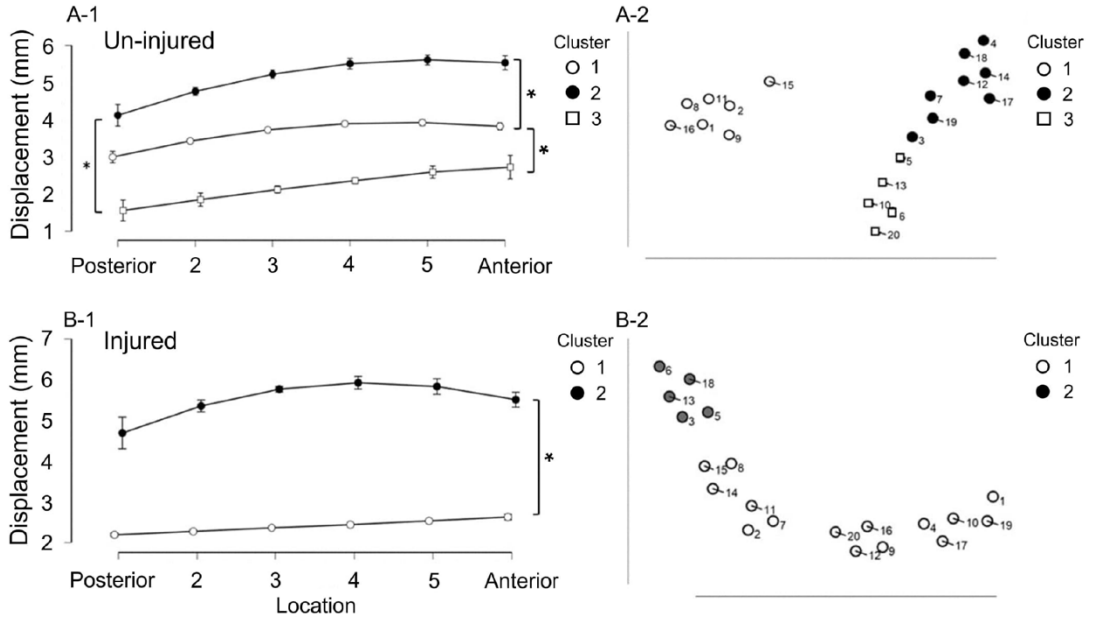

FIGURE 17 Cluster plots based on peak tendon displacements. A-1: mean displacement patterns for the three clusters formed for the healthy limb. A-2: 2D representation of the clusters, whereby each circle represents one patient's data; similar displacement patterns appear close to each other, and dissimilar displacement patterns are further apart in the space. B-1: the displacement patterns for the two clusters found for the injured limb. B-2: Each data point separated into clusters. * = difference between groups ($p < 0.001$).

5.3.4 Neuromuscular properties

During submaximal isometric contraction at the same torque level, the normalized EMG amplitude was higher for all the TS muscles and the FHL in the injured limb compared to the un-injured with a mean difference (95% CI) of 9.54 (4.51–14.57) for MG, 12.79 (3.82–21.74) for LG, 10.71 (3.66–17.75) for SOL, and 16.33 (5.31–27.36) for FHL.

The combined cumulative RMS of the three TS muscles accounted for 81.9% of the EMG activity in the un-injured limb compared to 75.8% in the injured limb with no significant difference between limbs (Fig. 18). The relative MG contribution was lower in the injured limb with a mean difference of 0.061 (95% CI 0.02–1.0). This was accompanied by an increased FHL contribution to total EMG in the injured limb, with a mean inter-limb difference of –0.061 (95% CI -1.06–-0.016).

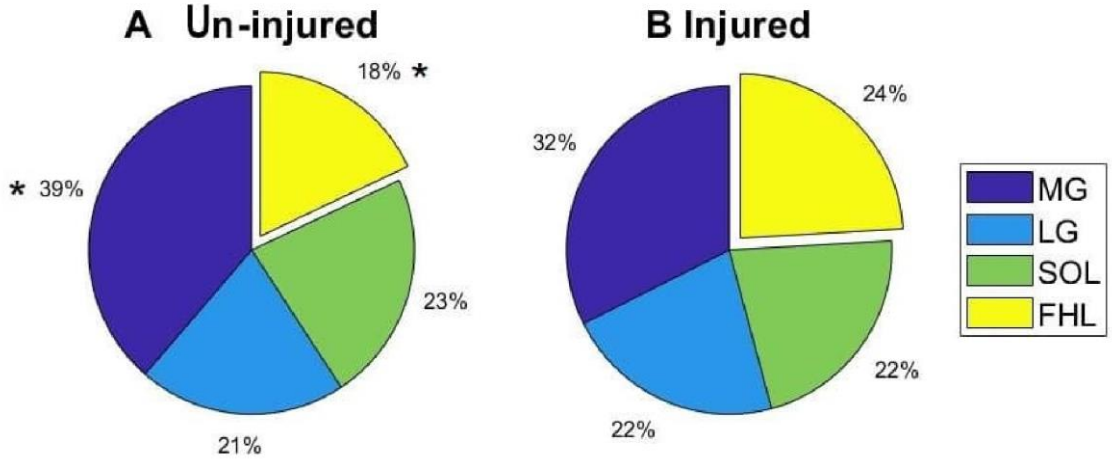

FIGURE 18 Relative contribution of medial gastrocnemius (MG), lateral gastrocnemius (LG), soleus (SOL) and flexor hallucis longus (FHL) to total cumulative EMG activity during submaximal ramp isometric contraction in the un-injured (A) and injured limbs (B). * = difference between limbs within a given muscle ($p < 0.05$).

5.3.5 Interactions and associations between the measured variables (I, II, III, IV)

5.3.5.1 Exploratory interconnections (II, IV)

When correlations were controlled for age and sex (IV), Δ stiffness was negatively correlated with MG and LG Δ subtendon lengths. Inter-limb length differences of MG, SOL, and LG subtendons were positively associated with higher Δ FHL normalized EMG% amplitude. All other associations between structural and neuromuscular inter-limb differences are presented in Fig. 19. Using Pearson's correlation (II), inter-limb difference of MG CSA was positively correlated with normalized stiffness ($r = –0.46$, 95% CI [0.1–0.7], $p = 0.26$).

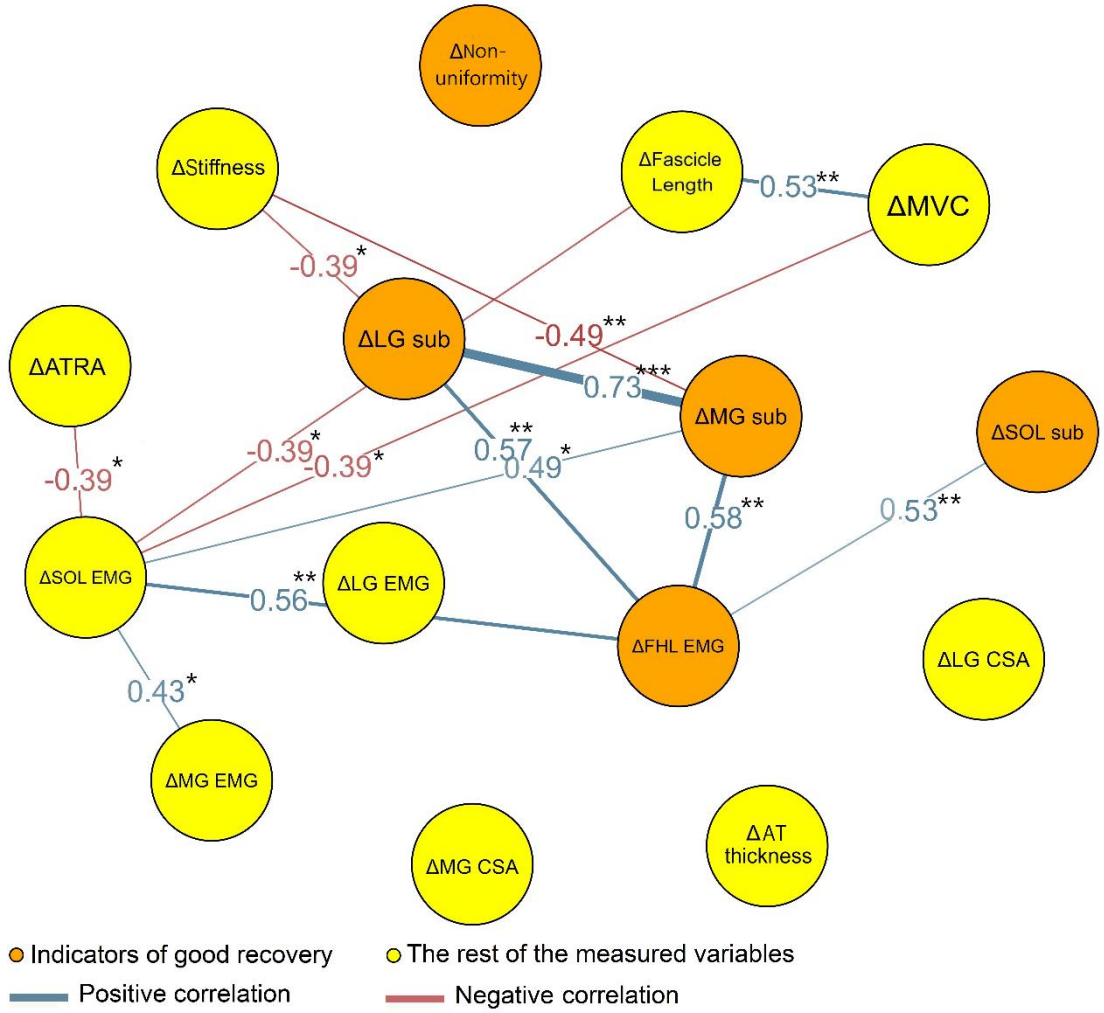

FIGURE 19 Network plot exploring the connections between interlimb (Δ) differences in structural and neuromechanical variables. The nodes are positioned using Fruchterman-Reingold algorithm which organizes the network based on the strength of the connections between nodes. Edges between nodes indicate significant interactions with the correlation coefficient outlined on the edge between any two nodes. Blue edges indicate a positive correlation, and red indicates a negative correlation. Orange nodes represent factors that were chosen to explore as indicators of good recovery, and yellow nodes represent the other measured variables. * = $p < 0.05$, ** = $p < 0.01$, *** = $p < 0.001$.

5.3.5.2 Associations between functional and morphological outcomes after ATR (II)

Multivariable regression models with age and sex as covariates were built to investigate the associations between morphological and functional outcomes including MVC inter-limb difference, walking speed, and patient-reported outcomes (ATRS). The ATRS model explained 69% of the variance ($F(8,9) = 2.51$, $p = 0.096$) with a root mean square error (RMSE) of 9.02. Δ MG subtendon was associated with ATRS ($\beta = 0.61$ (0.22–1.00), $r(9) = 3.548$, $p = 0.006$). As for Δ

MVC, the model explained 46% of the variance (F (8,13) = 1.38, p = 0.292) with RMSE of 15.83. Inter-limb difference of MG fascicle length was positively associated with Δ MVC (β = 1.22 (0.24–2.20), r (13) = 2.688, p = 0.019). The preferred walking speed model explained 41% of the variance (F (8, 12) = 1.052, p = 0.452) with RMSE of 0.11. None of the parameters were related to preferred walking speed.

5.3.5.3 Markers of good recovery (IV)

Considering the sample size (IV), only 4 covariates were included in each model to avoid model overfitting. Age and sex were included in all models and complemented with two other variables. Models were built based on previous knowledge, considering the previous exploratory correlations.

The MG subtendon length model explained 26% of the variance (F (4,27) = 2.63, p = 0.056) with RMSE of 9.06. Δ Stiffness was associated with Δ MG subtendon length (β = -0.12, [95% CI - 0.20–-0.03]) (Fig. 20). In the LG subtendon model, where 19% of the variance was explained (F (4,26) = 1.52, p = 0.225) with RMSE of 8.26, Δ stiffness was associated with Δ LG subtendon length (β = -0.086, [95% CI -0.16–-0.006]). SOL subtendon length model explained 20% of the variance (F (4,31) = 1.72, p = 0.174) with RMSE of 37.09. There were no detectable associations between Δ ATRA (β = 0.38, [95% CI -2.14–2.91]), or Δ stiffness (β = 0.05, [95% CI -0.30–0.40]) and Δ SOL subtendon length.

The non-uniformity model explained 11% of the variance (F (4,30) = 0.96, p = 0.44) with RMSE of 149.58. Δ MG fascicle length (β = 5.08, [95% CI -0.64–10.80]) and Δ MVC (β = -2.49, [95% CI -6.36–1.40]) were not associated with the inter-limb difference in AT non-uniformity.

The FHL normalized EMG% amplitude model explained 48% of the variance (F (5,21) = 3.83, p = 0.0127) with RMSE of 150.5. MG (β = 11.56, [95% CI 4.22–18.90]) and SOL Δ subtendon lengths (β = 2.18, [95% CI 0.10–4.05]) were both significantly associated with FHL Δ EMG activity.

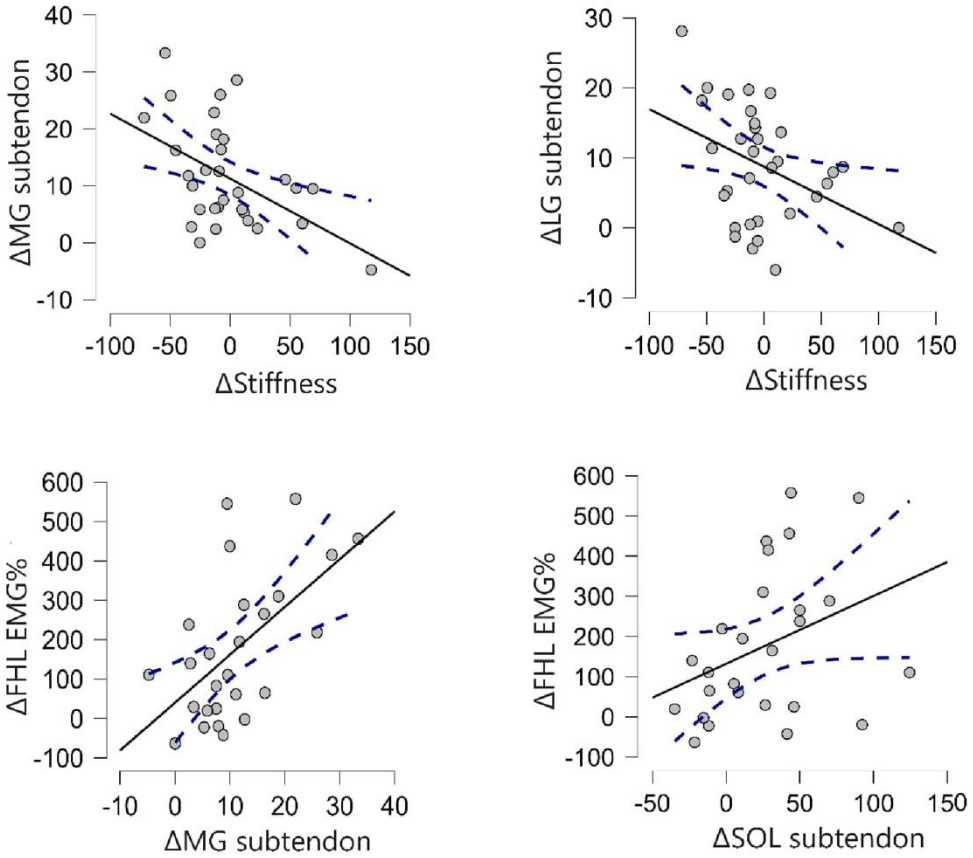

FIGURE 20 Scatterplots and regression lines of the significant associations from the multivariable regression models. The upper row shows the relationship between Δ gastrocnemii subtendon lengths and Δ stiffness, and in the lower row Δ FHL normalized EMG% amplitude with the independent variables from the Δ FHL multivariate regression model. The blue dashed lines represent 95% CI.

6 DISCUSSION

The main findings of the current thesis were:

1. Non-surgically treated tendons seem to heal to an elongated length, accompanied with MG muscle remodeling to shorter fascicles along with a decrease in muscle mass. The lengthening of the tendon after rupture was associated with clinical outcome scores and seems to be responsible for the observed objectively measured and self-reported functional deficits (II, IV).

2. One year after rupture, non-surgically treated tendons exhibited more uniform displacement than in the contralateral limb, indicating impaired sliding between the tendon fascicles. Unsupervised cluster analysis was able to classify displacement behavior within the AT into three groups in the un-injured limb and two groups in the injured limb. Distinct displacement patterns may arise from individual anatomical variations and could play a vital role in stress distribution across the tendon (I).

3. Stiffness of non-surgically treated tendons did not differ when compared to the contralateral limb 1-year after rupture. However, plantar flexion strength deficit in the ruptured limb was present. In addition to tendon lengthening after rupture, MG muscle remodeling seems to be one of the main causes of lower force production capacity in the ruptured limb (II, IV).

4. Achilles tendon displacement patterns were different in response to selective stimulation of LG compared to MG stimulation or voluntary contraction in both the injured and un-injured limbs. Non-surgical treatment after ATR does not seem to alter the displacement pattern within the ruptured tendon suggesting that non-surgical treatment may preserve the normal subtendon organization. However, displacement amplitude and non-uniformity were altered after rupture (III).

5. Selective electrical stimulation in combination with speckle tracking can be used to identify the distributions of medial and lateral gastrocnemius subtendon representations within the distal Achilles tendon. In the majority of this thesis sample, lateral gastrocnemius subtendon was found in the most anterior region adjacent to medial gastrocnemius both in the un-injured and non-surgically treated tendons (III).

6. Flexor hallucis longus was relatively more active during submaximal plantar flexion in the ruptured limb compared to the contralateral limb. This increase in activity was positively correlated with the degree of tendon lengthening after rupture. Moreover, greater lengthening of the tendon after rupture was associated with lower stiffness, worsening the ramifications of the rupture (IV).

6.1 Structural properties in non-surgically treated tendons

The present thesis examined the Achilles tendon-triceps surae MTU structural properties of non-surgically treated patients 1-year after rupture. In the ruptured limb tendons were thicker and all of the TS muscle subtendons were longer compared to the contralateral limb. MG was smaller with shorter and more pennate fascicles (Fig. 21). The lengthening of the tendon is probably a contributing factor to the observed changes in the MG and the rest of the TS muscles.

Tendons in the injured limb were almost two times thicker compared to the un-injured. Increases in the CSA and thickness of ruptured tendons have been reported after both surgical and non-surgical treatment of ATR (Rendek et al., 2022; Wang et al., 2013; Zellers et al., 2018). Previously, rat studies have reported a relationship between increased CSA of the tendon and lower elastic modulus following ATR (Andersson et al., 2012). Thus, the increase in thickness may be a compensation for impaired material properties in the ruptured tendon resulting from compositional changes or changes in the internal organization of the material (Freedman et al., 2014b). Animal models have shown that non-surgical treatment leads to higher grade organization of collagen fibers, and a more healthy tendon-like appearance compared with a greater proportion of scar tissue in the operative group (Krapf et al., 2012). Given that non-surgical treatment may be associated with less scar tissue formation than surgical treatment, non-surgically treated tendons might regain biomechanical properties with a smaller increase in thickness compared to a tendon with scar tissue.

The length of gastrocnemii subtendons in the injured limb were on average 10.3% longer than in the contralateral limb. Previous studies have shown that lengthening of the tendon occurs mostly in the first 6 weeks after rupture (Kangas et al., 2007; Silbernagel et al., 2012b), and has been reported to persist for long periods after rupture (Agres et al., 2015). The increase in the ruptured

tendon length has been shown to be associated with impaired walking performance and heel raise performance in the injured limb (Agres et al., 2015; Baxter et al., 2019; Silbernagel et al., 2012a). Since MTU length stays constant, the increase in tendon length is presumably associated with decreased MG fascicle length. Indeed, we detected an inverse correlation between the shortening of the MG fascicles and the difference in MG subtendon length between limbs (II). This association was not detected when controlling for age and sex (IV). The functional consequences of tendon elongation and the associated muscle shortening depend on sarcomere level adaptations. If there was no change in serial sarcomere number, the sarcomeres would be shorter for a given joint angle post-rupture, which would negatively affect force production capacity as TS muscles operate mostly on the ascending limb of the force-length relationship (Holzer et al., 2020). On the other hand, reduced sarcomere number could restore the sarcomere operating length at a specific joint angle. However, force production capacity would still be compromised as the sarcomeres would be forced to operate over a larger operating range for a given joint angle.

The subtendon length of the SOL muscle was on average 1.56 cm longer in the injured compared to the contralateral limb. Although this increase was less than observed in the gastrocnemii, it resulted in a 29% longer SOL subtendon than on the contralateral side, suggesting that SOL structure and force production capacity could be affected the most by tendon lengthening.

In this thesis we only examined the morphological changes of the MG muscle. We believe that all muscles of the TS would likely follow a similar recovery trend, and the recovery trend might differ slightly depending on the degree of the respective lengthening of the adjacent subtendon of each muscle head. In the injured limb MG had a smaller CSA, with shorter fascicles at rest. Interestingly, LG was less atrophied and did not demonstrate the same magnitude of difference in CSA as seen in MG. Accordingly, the LG subtendon showed the smallest difference in length between limbs; 9% compared to 11% for MG. Additionally, Hirata *et al.* (2015) reported that MG has a more plantarflexed slack position than LG. Thus, it is reasonable to assume that MG is more sensitive to the increased length of the tendon after rupture resulting in more atrophy than in LG. Previous studies have also observed less atrophy in LG compared to the rest of the TS muscles (Aufwerber et al., 2020; Nicholson et al., 2020). In Future studies, it may be necessary to conduct a more comprehensive analysis of functional and structural recovery of each TS muscle.

Muscles are able to sense changes in mechanical tension and regulate their architectural configuration (de Boer et al., 2008) by adding or removing sarcomeres, as shown in animal studies (Williams & Goldspink, 1973). Post-rupture, a sudden loss of muscle-tendon tension due to the increase in AT length probably elicits plantar flexor muscle remodeling and a removal of serial sarcomeres. Hullfish et al. (2019) showed higher pennation angle in the injured limb and shorter fascicle length in the first 4 weeks of conservative treatment (Hullfish et al., 2019b), but no change in muscle thickness. In the present study performed 1-year post rupture (II), higher pennation angle and shorter fascicles were accompanied with smaller CSA in the injured versus the contralateral limb (Fig.

21). Therefore, the acute alterations in MG muscle architecture seem to persist after one-year post-rupture, with an additional loss of muscle mass. We also observed that a greater difference in MG CSA between limbs was associated with a greater inter-limb difference in normalized AT stiffness. This may indicate that increased AT length leads to remodeling in MG structure. Changes in MG structure would alter the muscle force production capacity, thereby also affecting tendon stiffness and influencing the mechanical loading environment of the tendon.

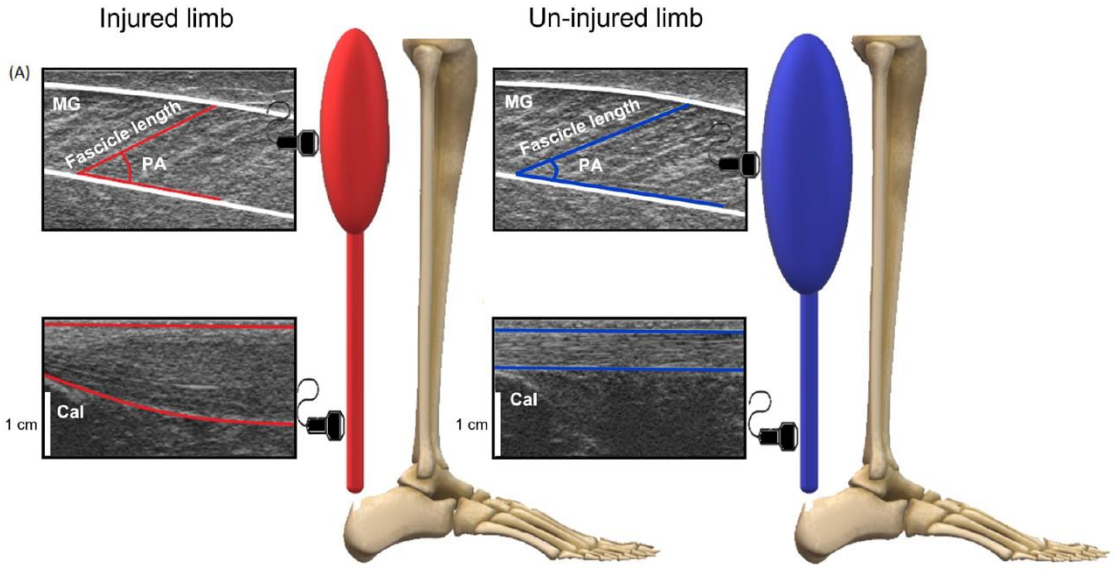

FIGURE 21 Ultrasonographic images of muscle-tendon unit structural properties 1-year post-rupture in both limbs. (A) images of MG muscle where pennation angle and fascicle length were analyzed. (B) Images where AT thickness was measured 1 cm away from the calcaneal insertion. Injured limb AT was longer and thicker than the un-injured AT. At rest, MG had a smaller CSA with longer and more pennate fascicles.

After rupture, the TS muscles probably adapt by resetting fascicle length (dictated by serial sarcomere number) and pennation angle to a new optimum for force production at a joint angle at which the force requirement during normal locomotion is largest. This still leads to reductions in the range of motion at which force can be produced (Stäudle et al., 2020) and the ability of the plantar flexors to perform work (Baxter et al., 2019). We found that the reduction in MG fascicle length was inversely correlated with increased pennation angle (II), as shown previously (Hullfish et al., 2019b). This morphological adaptation has functional consequences, as the increase in pennation angle increases muscle belly gearing (Lichtwark & Wilson, 2007). Muscle belly gearing reduces muscle fiber shortening for a given muscle belly shortening, so the increase in pennation angle helps to preserve force production due to the force-velocity and force-length relationships. The downside of increased pennation angle is that a

lower proportion of the fiber force is transmitted in the direction of the tendon and thus to the skeleton. Therefore, the increase in pennation angle likely preserves the muscle's force production and work generation capability in concentric muscle actions but negatively affects force production in isometric conditions.

6.2 Mechanical properties in non-surgically treated tendons

There was no difference in stiffness between the ruptured and contralateral tendons. This contrasts with previous studies where AT stiffness was lower in the injured limb 3–12 months after surgery (Chen et al., 2013; Geremia et al., 2015; McNair et al., 2013; Wang et al., 2013), but higher when investigated 2–6 years post-rupture (Agres et al., 2015; Stäudle et al., 2020). Initially, in the healing phase, tendon stiffness is lower, which gradually increases towards normal values in the remodeling stage, at least in mice (Palmes et al., 2002). Similarly, in humans, after an initial drop post-rupture, stiffness increases to eventually match or even exceed that of the un-injured tendon (Agres et al., 2015; Karamanidis & Epro, 2020; Stäudle et al., 2020). Non-surgical treatment prompt a superior organization of collagen fibers compared to greater scar tissue in operated rats tendons (Krapf et al., 2012). The higher-grade organization of collagen may have facilitated the recovery of the tendon mechanical properties 1-year after rupture.

These changes in tendon stiffness have functional consequences via their effects on the muscle's force-length and force-velocity relationships. As TS muscles operate mostly on the ascending limb of the force-length relationship (Holzer et al., 2020), a higher AT stiffness helps to preserve favorable sarcomere lengths during force generation by reducing muscle shortening. In the long-term, higher tendon stiffness may help to ameliorate the impairments in force production caused by the lengthening of the tendon, albeit incompletely (Stäudle et al., 2020). AT stiffness is also positively correlated with TS rate of force development (Monte & Zignoli, 2021; Muraoka et al., 2005; Peng et al., 2019). Hence, from the viewpoint of isometric force production, it may be beneficial if the injured tendon remodels to have higher stiffness than the contralateral tendon (Fig 22). However, this could negatively affect locomotion efficiency and performance as there seems to be an optimal stiffness for cyclically generating force and power (Lichtwark & Wilson, 2007; Orselli et al., 2017).

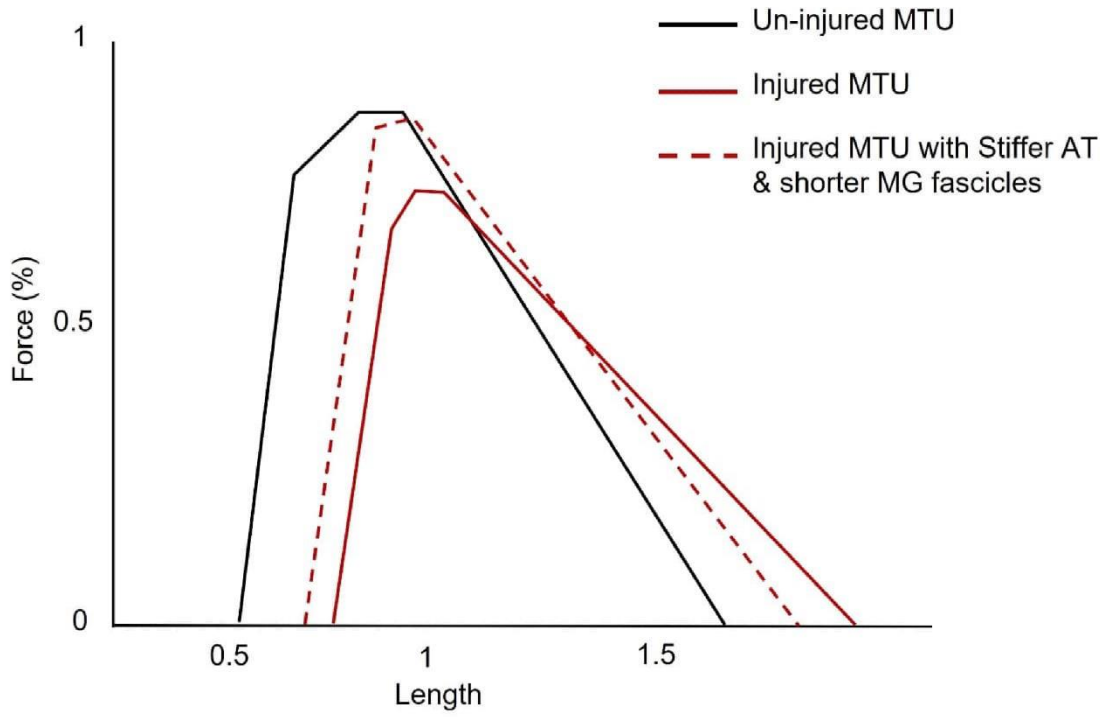

FIGURE 22 Schematic example of force-length relationships in the injured MTU (red solid line), un-injured MTU (black solid line) and injured MTU with a stiffer tendon and shorter MG fascicles. Adapted from (Stäudle et al., 2020).

In the present sample, the observed increase in AT thickness may have contributed to the restoration of AT stiffness. We also observed a negative association between Δ stiffness and subtendon length difference in the gastrocnemii muscles (II, IV), indicating that more AT lengthening is associated with lower stiffness, which negatively affects isometric force production capacity. For example, if we compare two tendons with the same mechanical properties, a longer tendon would elongate more under the same load, and the change in the force-elongation slope would be directly proportional to the extra length of the tendon (Proske & Morgan, 1987). Thus, excessive tendon lengthening after rupture would result in lower stiffness.

During stiffness assessments we observed a plateau in the displacement of medial gastrocnemius MTJ while plantarflexion force continued to increase at the end of an isometric contraction. This phenomenon was more pronounced in the injured limb (Fig. 12) and may have been due to changes in MTU structure post-rupture. The shortened MG fascicles may have led to a relatively quick saturation of MG force generation due to the muscle's force-length properties. Furthermore, deep flexors such as FHL may make a larger contribution to plantar flexion torque in the ruptured limb (Finni et al., 2006). Along with the potential contribution of the soleus muscle, these factors may result in increased plantar flexion torque that would not be detectable when tracking the MG MTJ. This novel observation highlights the role of synergistic muscles in compensating plantarflexion torque deficits after AT rupture (Heikkinen et al., 2017), and warrants careful examination of data and decision making in relation to stiffness

assessments. We decided to compare stiffness at 50% of MVC of the injured limb to allow comparisons to be made for all participants. Therefore, direct comparisons to previous studies with different methodologies are not advisable.

The fact that we calculated stiffness based on MG MTJ displacement may explain why we did not detect any associations between the interlimb difference in SOL subtendon length and stiffness difference between limbs (IV); local stiffness values probably differ at the SOL insertion. Furthermore, when displacement during electrically-evoked contractions was tracked at the distal free AT (III), we observed higher mean displacement in the injured limb compared to the contralateral at the same absolute torque values, indicating lower stiffness. This differs from (II, IV) where we found that stiffness between limbs was not different when measured at the MG MTJ during isometric voluntary contractions (Fig. 23). These observations suggest that in the distal free AT, stiffness may be altered and manifest lower values in injured limb at low force levels (III), while globally, based on the entire MG subtendon, stiffness seems to be similar between limbs 1 year after rupture (II, IV). The discrepancy observed in stiffness could indicate an extension of the toe region, or slackness of the tendon in the injured limb at low forces, while the linear region of the force-displacement curve may be similar between limbs. A similar phenomenon of an extended range of tendon strain at low stresses has been reported previously after 4 weeks of limb unloading by suspension (Shin et al., 2008).

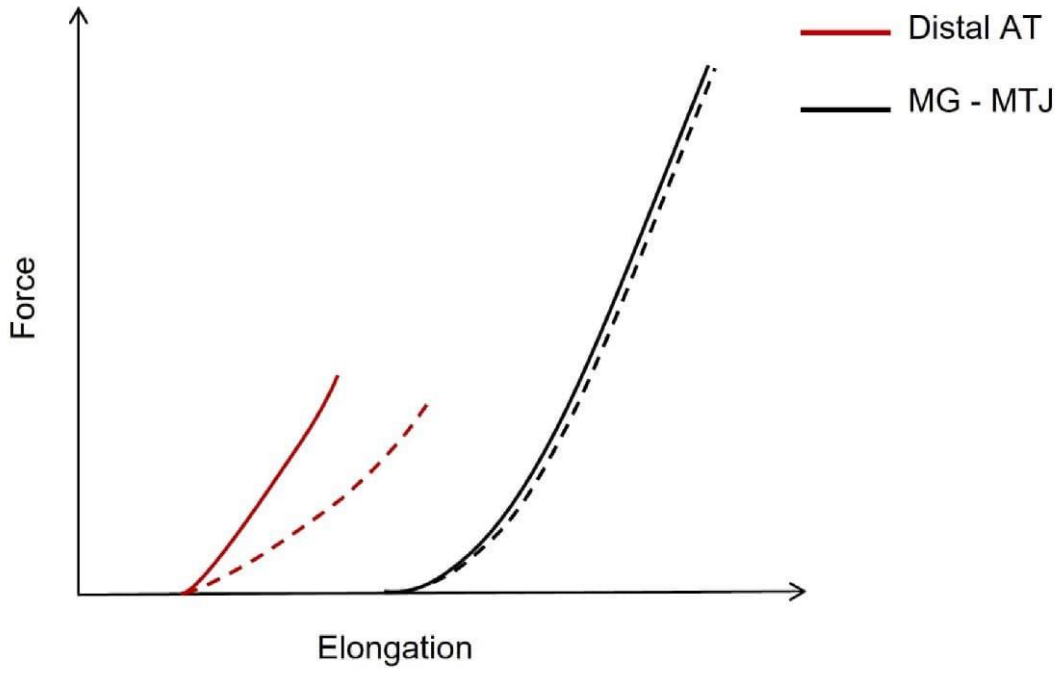

FIGURE 23 Representation of the AT stiffness calculated from the displacement at the MG MTJ and the observed stiffness at the distal free AT. Dashed lines represent the injured limb and solid lines represent the un-injured limb.

The combination of a ~ 20% plantar flexion strength deficit in the injured limb with no difference in AT stiffness led to the reduction in maximal tendon elon-

gation. Reduced maximal elongation may negatively affect movement economy due to a reduced capacity to store elastic potential energy in the tendon. This may also predispose the muscle to eccentrically-induced muscle damage or strain as the tendon cannot work as efficiently to dissipate energy and reduce the power of the negative work done by the muscle (Roberts & Azizi, 2010). However, there may be benefits associated with the reduced maximal tendon elongation related to tendon injury risk. Lower maximal elongation coupled with an increase in tendon length greatly reduces tendon strain, which has been speculated to be important for reducing the risk of tendon injury (Karamanidis & Epro, 2020) and fatigue damage (Wren et al., 2003).

6.3 Internal Achilles tendon displacement

6.3.1 AT non-uniformity in non-surgically treated tendons

To the best of our knowledge this body of work (I, III, IV) is the first to show a more uniform within-tendon displacement in non-surgically treated patients after ATR, as previous studies were done on surgically treated patients (Fröberg et al., 2017). Displacement within the ruptured tendons was more uniform during voluntary and electrically-evoked contractions at the same plantar flexion torque.

The observed impairments in non-uniformity of the ruptured tendons could be explained by several factors. First, changes in TS muscle structure, including shorter fascicles, may lead to a decrease in the displacement of individual subtendons. We found a reduction in displacement of MG MTJ (II), as was reported in ATR patients previously (De la Fuente et al., 2016; Finni et al., 2003). Shorter fascicles could result in a shorter operating range and quick saturation of TS muscle length changes, reducing displacement and non-uniformity within the tendon. This phenomenon was also present even when non-uniformity was normalized, indicating that mechanical sliding within the tendon fascicles was impaired after ATR. This could be caused by interfascicular matrix adhesion, limiting relative displacement between different parts of the AT (Thorpe et al., 2013).

Alterations in TS motor coordination and compensatory adaptation of the motor strategy used to produce plantar flexion torque might lead to a more uniform displacement within the AT. Motor control adapts to make greater use of FHL in plantarflexion due to altered force production capabilities in the TS muscles. This leads to a higher relative contribution of FHL to the plantarflexion torque produced in the ruptured limb, as we observed (IV) in accordance with several studies of ATR patients (Finni et al., 2006; Heikkinen et al., 2017). A higher contribution of FHL muscle at a given plantar flexion torque would elicit less tensile force that is transmitted through the AT. This in turn would result in less overall displacement and gliding within the AT.

Gastrocnemius and soleus have different functional roles, despite having a common distal tendon and working synergistically as ankle plantar flexors (Francis et al., 2013; Lenhart et al., 2014). It has been suggested that in order to perform their differing functional roles, these muscles rely on the ability of the subtendons to displace relative to each other (Clark & Franz, 2021; Franz & Thelen, 2016). Thus, the impaired displacement observed in the injured limb may have an adverse effect on the ability of TS muscles to function in an optimal way (Clark & Franz, 2021; Franz & Thelen, 2015; Fröberg et al., 2017).

6.3.2 Voluntary and electrically-induced displacement patterns in ruptured and healthy tendons

Tendon displacement during voluntary and electrically-induced contractions was normalized to the ratio of maximum displacement to facilitate the comparison between different contraction conditions. There was no difference in the normalized displacement patterns between the ruptured and contralateral limb (Fig. 24), implying that the anatomical subtendon organization was not altered after ATR in non-surgically treated patients.

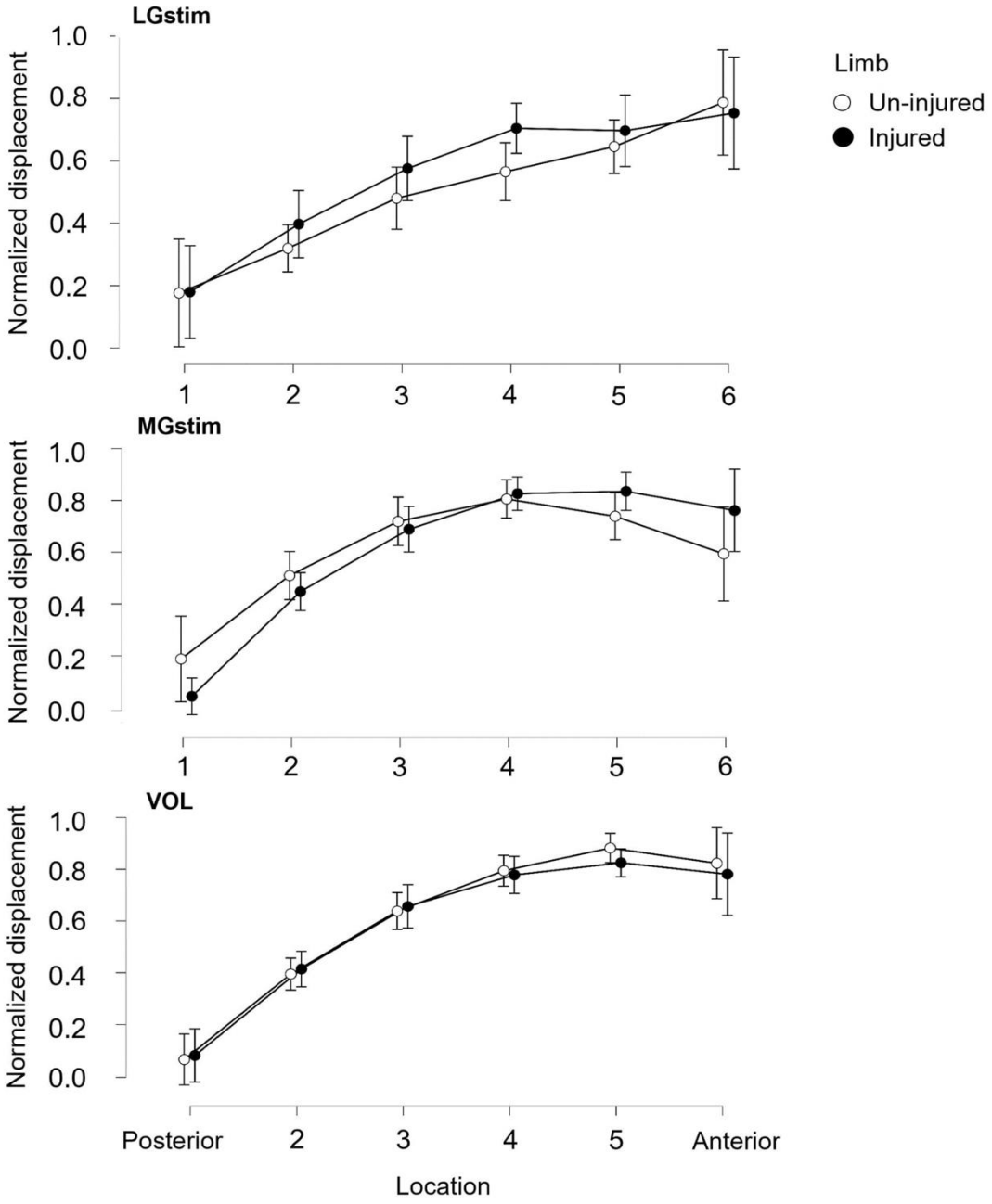

FIGURE 24 Normalized displacement patterns during voluntary (VOL) and selective electrically-induced contractions of medial (MG) and lateral (LG) gastrocnemius muscles in the un-injured and injured limbs.

Displacement patterns within the AT were different during LG_{stim} compared to voluntary and MG_{stim} in the un-injured limb (Fig. 15). In voluntary contractions, peak displacement was typically found in the two most anterior locations. Voluntary contraction typically activates all synergistic muscles and leads to disproportionate tissue displacement within the tendon due to mechanical and structural differences between TS muscles (Albracht et al., 2008). On the other hand, the low, stimulation-induced force can be assumed to be mainly transmit-

ted serially to the targeted muscle's subtendon (Tian et al., 2012). Although lateral force transmission may occur (Finni et al., 2017), the main pathway of force is the stiffest structure. Hence, the location of peak displacement in response to stimulation can be considered to reveal the location of tendon fascicles within the cross-section of the AT.

Displacement during LG_{stim} peaked in the anterior tendon (III, Fig. 3), implying that the most anterior area could be occupied by tendon fascicles arising from LG subtendon. In anatomical studies, Pękala *et al*. (2017) and Edama *et al*. (2015) found that SOL occupied the anterior portion and LG the lateral portion of the tendon at the level of the SOL MTJ. However, due to high torsion within AT, LG tendon fascicles are likely located anteriorly in the more distal tendon (Edama et al., 2015; Pękala et al., 2017). Furthermore, in a recent study, three tendons were dissected, and 3D computer-aided models were constructed based on these tendons. In the model that twisted the most, LG subtendon was found to completely occupy the anterior portion of the distal AT (Yin et al., 2021). Therefore, anatomical studies are consistent with the present observations regarding the location of the LG subtendon.

There was no difference in displacement patterns between voluntary and MG_{stim} (Fig. 15). However, during MG_{stim} displacement peaked around the 4th and 5th locations in un-injured tendons, indicating that fascicles originating from MG could be present in the mid-to-anterior part of the tendon. Unlike in LG_{stim}, there was more individual variation in the location of peak displacement in MG_{stim}. Due to individual differences in free tendon length, the superior-inferior field of view may not have been consistent across subjects relative to tendon length. When comparing these observations to the anatomical maps provided by previous cadaver studies, natural anatomical variation may explain the observed heterogeneity in peak displacement in response to MG_{stim} (Edama et al., 2015; Pękala et al., 2017; Yin et al., 2021).

In all contraction types the minimum displacement always occurred in the posterior tendon and maximum displacement in the mid-to-anterior tendon. This is consistent with the findings of Lehr *et al.* (2021) in which SOL and MG were electrically stimulated (Lehr et al., 2021), and the tendon was split into two halves in accordance with the function-structure relationship (Clark & Franz, 2018; Lehr et al., 2021; Stenroth et al., 2019). The anterior half always displaced the most in response to MG and SOL stimulations in different ankle positions. The difference between (III) and Lehr *et al.* (2021) is in the interpretation of the data regarding which subtendon is represented in the deep part of the tendon. Lehr *et al.* (2021) interpreted greater non-uniformity and displacement in the representative part of the stimulated muscle-tendon when SOL was stimulated compared to MG as evidence of consistency with the anatomical function-structure consideration (Lehr et al., 2021). In paper (III), we relied on the principle that the main pathway of force is the stiffest structure. Thus, with selective electrical stimulation, the observed regional displacement can inform us about regions within the tendon cross-section corresponding to fascicles arising from the stimulated TS muscle. Based on this principle we found that the mid-to-deep part of the tendon displaced most when MG was stimulated and the deep

part when LG was stimulated. A similar approach was used by Klaiber *et al*. (2023) with the ultrasound probe in an axial position, to obtain the localized displacement of MG and LG within the cross-section of the tendon (Klaiber et al., 2023). The authors found that isolated contraction of the MG led to displacement in the medial part of the tendon while LG contraction resulted in displacement in the posterior-lateral part of the tendon. The discrepancy between the studies can likely be explained by the different probe placements between the studies. The organization of the subtendon within the cross-section of the AT between two different probe placements might differ as a result of subtendon twisting. In study (III), we placed the probe at the most distal part of the AT, while in the two aforementioned studies the probe placement was more proximal.

The displacement data (I, III) show that there are considerable individual variations (Fig. 16) in subtendon organization in both ruptured and un-injured tendons. This clearly indicates the need to consider individual variations in subtendon organization and within-tendon displacement among the population. Usually participants' data are presented as means and high standard deviations, as in Klaiber *et al.* (2023). It may instead be preferable to present individual data or to stratify participants according to their displacement patterns.

6.3.3 Clustered groups

Using unsupervised cluster analysis (I), we were able to classify AT displacement behavior into 3 clusters in the un-injured limb whereas only 2 were identified in the injured limb (Fig. 17), which may arise from subject-specific anatomical variations in AT subtendons (Edama et al., 2015). Subject-specific tendon characteristics are a vital determinant of stress distribution across the tendon (Hansen et al., 2017; Shim et al., 2014), which may lead to variation in the location and magnitude of peak displacement within the free AT. Participants in different clusters showed different patterns and locations of maximal displacement across the tendon. However, in spite of any individual differences, the phenomenon of non-uniform displacement between independent tendon fascicles across the AT was evident in all of the un-injured clusters, further supporting the idea that this is a sign of healthy tendon function (Slane & Thelen, 2014b; Thorpe et al., 2013). Such individual differences further highlight the need for personalized diagnostic and treatment approaches. For further details on the clustered groups in ruptured and un-injured tendons readers are referred to (I).

6.4 Neuromuscular properties in non-surgically treated tendons

In the injured limb, there was a higher relative contribution of FHL to the summed normalized EMG activity compared to the un-injured limb at the same submaximal isometric torque level. The relative contribution of FHL was 8% higher in the injured limb, whereas in MG the contribution was 7% lower com-

pared to the un-injured limb (Fig. 18). Compensatory strategies likely start shortly after rupture, where force is averted away from the freshly ruptured AT by increasing the contribution of FHL to plantarflexion torque. This motor strategy may become a persistent feature in ATR patients. Altered motor control may be driven by the potentially disadvantageous position of the TS muscles on the force-length curve. The shift in the TS operating range on the force-length curve (Suydam et al., 2015), and changes in the MG fascicles length (II), correspond to the degree of increase in tendon length after rupture, which seems to be the primary cause of structural and neuromechanical changes. Indeed, we found that patients whose FHL EMG activity was higher in the injured limb also exhibited greater inter-limb differences in tendon length.

The mean relative amplitudes of all the TS muscles were higher in the injured limb during submaximal isometric contractions. This could be a result of the TS muscles functioning outside the optimum region on the force-length curve, where greater activation level is needed to achieve the same amount of absolute torque as in the contralateral limb (Suydam et al., 2015). McHugh and colleagues found that the increase in activation was more pronounced in patients with plantar flexion weakness. In patients without weakness in plantar flexion between the limbs there was no difference in the TS muscle median frequencies (McHugh et al., 2019). The authors interpreted this as a sign of excessive tendon lengthening in patients with marked plantar flexion weakness (McHugh et al., 2019). In addition to potential changes in the sarcomere level operating length of the TS muscles, the decreased PCSA of the muscles necessitates increased muscle activation to reach a given joint moment output in the injured limb.

It should be noted that strength deficits after ATR manifest especially when the ankle is in the end-range of plantar flexion. Mullaney and colleagues found an average of 27% plantar flexion strength deficits when the ankle was in a plantar flexed position but did not observe weakness when the ankle was in dorsi flexion (Mullaney et al., 2006). Thus, it may be that the current sample would have shown larger neuromuscular and strength impairments in a plantar flexed ankle position.

6.5 Factors associated with function and good recovery after Achilles tendon rupture

In the current thesis we observed that the inter-limb difference in MG tendon length was associated with patient-reported outcomes 1-year after rupture, in accordance with previous ATR studies (Kangas et al., 2007; Pajala et al., 2009; Silbernagel et al., 2012a). The sample in the present thesis (II) had a relatively good ATRS (mean 14.7). The patient with the worst outcome (47/100) also had the most elongated tendon when compared to the contralateral limb. Furthermore, the inter-limb length difference between limbs was negatively associated

with stiffness difference between limbs. Differences in tendon length were also associated with greater FHL mean amplitude difference between limbs; the more elongated the injured tendon, the greater the relative FHL activity corresponding to the degree of change in the TS muscle. It seems that lengthening of the tendon after rupture might be the primary cause of the observed objectively measured neuromuscular and structural alterations in the injured limb and could be responsible for the self-reported functional deficits.

Initially we hypothesized that gastrocnemii and SOL muscle activity might mirror the differences in non-uniformity (Clark & Franz, 2018), but we did not find such associations. As stated earlier, shorter fascicles likely result in a shorter operating range and quick saturation of TS force production (II) (De la Fuente et al., 2016), reducing displacement and non-uniformity within the tendon. However, non-uniformity within the ruptured and healthy tendons might be more complex than anticipated.

Preferred walking speed 1-year after ATR was close to values reported in healthy individuals, suggesting a recovery of daily functions where the MTU operates sub-maximally. Stäudle *et al.* (2022) reported comparable kinematics and contractile behavior of the MG muscle during walking in ATR patients 2 years after rupture (Stäudle et al., 2022). The authors concluded that despite atrophy in MG, the muscle was capable of generating sufficient force during walking in ATR patients. However, during maximal effort tasks, deficits were present, and the size of the deficit was positively associated with inter-limb differences in MG fascicle length. The present results indicate that the atrophy and structural changes in MG are among the main causes of lower force production capacity in the injured limb. The impairments after rupture can be long-lasting, even after returning to pre-injury activities, and can persist even with high training volumes and high loads (Karamanidis & Epro, 2020). Thus, while patients with ATR might recover their daily function, irreversible changes in the MTU might limit their ability to resume high intensity activities.

6.6 Limitations

The main limitation of the current thesis is the cross-sectional study design. In cross-sectional designs it is not possible to establish a true cause and effect relationship. The results provided by the current thesis can be interpreted to represent muscle-tendon properties 1-year after ATR in non-surgically treated patients. However, for factors that we associated with good recovery, the results should be interpreted carefully. Longitudinal studies should be conducted to reveal the effect of biomechanical properties on recovery and physical function.

Also, in this thesis we only examined the morphological changes of the gastrocnemius muscles. Although, we can speculate that the SOL muscle would likely follow a similar recovery trend as the gastrocnemius muscles. The SOL subtendon was 30% longer in the injured limb compared to the contralateral

limb and this might warrant further investigations to better understand the magnitude of changes in the SOL muscle structure subsequent to ATR.

Another limitation is the small sample of patients recruited in this study, especially in (I, II). Despite the small sample size, changes in the ruptured limb were so evident that a small sample should be sufficient to identify inter-limb differences in patients with ATR. Previously, Silbernagel *et al.* (2010) reported that 8 patients with unilateral ATR was sufficient to identify inter-limb differences with 90% power. Furthermore, Fröberg *et al.* (2017) found statistical differences in a sample of 11 patients when investigating displacement within the AT, similar to study (I) of this thesis.

In this study, there are some limitations associated with biomechanical measurements. For stiffness calculations we assumed that the axes of the ankle joint rotation and dynamometer were aligned. This assumption is not always valid and might have affected stiffness values. However, the error was likely similar in both limbs within an individual, and thus should not affect the integrity of the stiffness comparison between limbs.

Another limitation is the nature of two-dimensional imaging that might not fully capture the complex three-dimensional behavior of the TS subtendons. This could lead to errors when estimating AT tissue displacement (I, III). The speckle tracking algorithm uses a low order polynomial fit to regularize displacement (Slane & Thelen, 2014c). This may reduce variation in displacement between the 6 locations across the tendon. However, filtering has been deemed necessary to reduce noise and erroneous estimates (Svensson et al., 2021), and was applied here in the same manner as in previous studies (Lehr et al., 2021).

Ultrasonographic imaging is sensitive to the probe orientation and pressure applied on the skin. The applied pressure may influence the measures of fascicle length and pennation angle. We evaluated the typical error from two sequential images that were acquired during the measurements and found a relatively low error of ~ 6%. Thus, the systematic error is not likely to invalidate group comparisons (II).

Regarding the isolated evoked electrical stimulations, it should be noted that LG muscle has different compartments that are innervated by two main nerves and numerous sub-branches (Segal et al., 1991), so stimulation might activate different branches of the muscle causing more variability in the displacement pattern. Furthermore, selective activation of LG might stiffen the connective tissue between SOL and LG, facilitating force transmission (Finni et al., 2018). Thus, the representation of LG or MG subtendon that we observed within the AT may have been influenced by lateral force transmission at the level of the muscle or tendon. However, this effect was likely minimal since it has been shown that lateral force sharing within the human Achilles tendon is small at low forces (Haraldsson et al., 2008).

EMG values were normalized to the RMS during MVCs, and therefore represent the activity of the muscles during submaximal contraction relative to the maximal plantar flexion effort (III). The EMG normalization method may be prone to errors, including the possibility that that the ankle flexors were not fully activated during maximal contractions. Thus, caution should be taken

when making inferences based on the findings, although they are consistent with the results of previous studies (McHugh et al., 2019; Suydam et al., 2015; Wenning et al., 2021).

6.7 Practical implications

The results of the present study conform and strengthen the prevailing concept that rehabilitation protocols should prioritize minimizing the lengthening of the tendon after rupture, since it seems to be the cause of structural changes and functional deficits. Early loading has been shown to be beneficial to the tendon material properties in animal and surgically treated tendons (Andersson et al., 2012; Eliasson et al., 2012; Schepull & Aspenberg, 2013a). However, early ankle mobilization with excessive dorsi flexion could increase the risk of tendon lengthening (Hillin et al., 2019), so patients should be cautious when loading not to stretch the tendon beyond neutral ankle range of motion especially in the early recovery phase.

Promoting muscle activation of the TS and especially MG may have positive effects on muscle fascicle adaptation, leading to preservation of force producing capacity. Considering the association between muscle force and tendon stiffness (Arampatzis et al., 2007), it may be deduced that improving muscle strength improves tendon stiffness, mitigating the effects of tendon lengthening in patients with ATR.

Blood flow restriction training has been shown to increase tendon stiffness with low mechanical loading (Centner et al., 2019). This could be important, particularly in the early stages of rehabilitation, where loss of muscle strength may hinder the ability to load the tendon enough to prompt a stimulus with traditional strength training. Additionally, it may also prove beneficial later on, if excessive tendon lengthening makes it challenging to load the tendon sufficiently. Thus, blood flow restricted training may be a useful tool to increase tendon stiffness, and prompt mechanical stimuli in the TS muscles, especially in the early rehabilitation phase.

The results suggest that TS muscle weakness is partially compensated by FHL, but FHL's capacity to compensate for the loss of strength in the injured limb is limited due to a relatively short plantarflexion moment arm. Thus, treatment and rehabilitation protocols should not emphasize the role of FHL in order to allow recovery of the TS.

7 MAIN FINDINGS AND CONCLUSIONS

The results of the present thesis indicate that non-surgically treated tendons heal to an elongated length, accompanied by remodeling of the TS muscles to shorter, more pennate fascicles, and a reduced muscle mass. The lengthening of the tendon after rupture seems to be the primary cause of the observed objectively measured and self-reported functional deficits. The lengthening of the injured tendon was also associated with greater relative FHL activity, potentially the main driver of neuromuscular changes. Furthermore, lengthening of the tendon after rupture was associated with lower stiffness, worsening the ramifications of the rupture.

Quantifying internal tendon displacement might provide new insight for evaluating recovery following ATR. We observed more uniform within-tendon displacement in voluntary and electrically-evoked contractions after rupture, highlighting the long-term effects of ATR, which might be a combination of changes in plantar flexor muscle structure and impaired relative displacement between the different parts of the Achilles tendon.

The present data suggest considerable individual variations in subtendon organization and displacement patterns within the AT. We were able to classify displacement patterns into different clusters, which may arise from subject-specific anatomical variations in the subtendons of the AT. Subject-specific tendon characteristics are a vital determinant of stress distribution across the tendon, which may in turn lead to variations in the location and magnitude of peak displacement within the AT.

Selective transcutaneous stimulation in combination with speckle tracking can be used to scan for the representative areas of the TS subtendons within the cross-section of the AT. In the majority of the sample, lateral gastrocnemius subtendon was found in the most anterior region adjacent to medial gastrocnemius both in the healthy and ruptured, non-surgically treated tendon.

Finally, despite higher EMG activity in all the TS and FHL muscles, plantarflexion maximum torque was still lower in the injured limb. The relative FHL muscle activity during submaximal plantarflexion was higher in the injured limb, and this appeared to compensate for a decrease in MG activity.

YHTEENVETO (SUMMARY IN FINNISH)

Biomekaaniset toipumistekijät ei-operatiivisesti hoidetuissa akillesjänne-repeämissä

Akillesjänne on tärkeä osa jokapäiväistä liikkumista. Jänteet välittävät lihaskudoksen tuottamaa voimaa liikkeen aikaansaamiseksi. Akillesjänteen huomattavasta lujuudesta huolimatta krooniset ja akuutit vammat ovat hyvin yleisiä, ja ne aiheuttavat pitkällä aikavälillä merkittäviä toimintakyvyn ja fyysisen aktiivisuuden puutteita. Akillesjänteen tendinopatiaa esiintyy 6 prosentilla väestöstä koko elämänsä aikana, ja sitä esiintyy enemmän pitkän matkan juoksijoilla, joilla kumulatiivinen esiintyvyys koko elämän aikana on 52 prosenttia. Tendinopatian patogeneesi tunnetaan huonosti, ja sitä voidaan pitää jänteen sopeutumis- tai paranemisprosessin epäonnistumisena. Ei ole selvää, johtaako krooninen tendinopatia akuuttiin akillesjänteen repeämään.

Akillesjänteen repeämä on vakava vamma, johon liittyy pitkäaikaista toimintavajetta, joka voi jatkua useita vuosia. Akillesjänteen repeämän esiintyvyys on lisääntynyt viime vuosikymmeninä. Vuosittainen esiintyvyys on ~20-31/100 000 henkilöä, repeämän ollessa tyypillinen vapaa-ajan urheilua harrastavilla keski-ikäisillä miehillä. Tärkeä tekijä, joka vaikuttaa nilkan ojennusvoiman ja kestävyyden pysyviin puutteisiin, on jänteen pituuden kasvu repeämän jälkeen. Jänteen pituus alkaa kasvaa repeämän jälkeen ensimmäisten viikkojen aikana, ja sen on raportoitu jatkuvan jopa 6 kuukauden ajan. Jänteen pidentyminen repeämän jälkeen on merkittävä toimintakykyyn vaikuttava tekijä. Yksityiskohtaisten anatomisten ja biomekaanisten tekijöiden parempi ymmärtäminen on avainasemassa parempien hoito- ja kuntoutusprotokollien laatimisessa.

Riippumatta siitä, hoidetaanko akillesjänteen repeämää operatiivisesti vai ei, akillesjänteen repeämästä kärsivillä potilailla on pitkällä aikavälillä anatomisia muutoksia ja toiminnallista vajetta. Erilaisia hoitomuotoja on tutkittu, mutta optimaalisesta hoitovaihtoehdosta ei ole päästy yksimielisyyteen. Vaikka ei-operatiivista hoitoa pidetään turvallisena, useimmat tutkimukset ja seurantatutkimukset on tehty operatiivisesti hoidetuilla potilailla. On olemassa vain vähän pitkän aikavälin biomekaanista tietoa repeämän jälkeisestä kudoksen palautumisesta, erityisesti ei-operatiivisesti hoidetuista jänteistä.

Akillesjänne käsittää sekä kaksoiskantalihaksista että leveästä kantalihaksesta lähtevät kolme erillistä osajännettä (subtendons), jotka kiertyvät kulkiessaan kohti kiinnityskohtaansa kantaluussa. Tämän monimutkaisen rakenteen vuoksi jänne altistuu epätasaiselle kuormitukselle, joka voi aiheuttaa heterogeenistä rasitusta jänteessä. Viimeaikainen kehitys ultraäänikuvantamismenetelmissä, kuten täpläseuranta (speckle tracking) -menetelmässä, on paljastanut akillesjänteen sisäisen liikkeen olevan epäyhtenäistä eri tehtävien aikana. *In vivo* -tutkimukset osoittavat, että epäyhtenäinen liike akillesjänteessä on terveen jänteen ominaisuus, ja sillä saattaa olla tärkeä rooli kolmipäisen pohjelihaksen kyvyssä suorittaa erilaisia toiminnallisia tehtäviä. Kuitenkin on hyvin vähän kiinnitetty huomiota siihen, miten osajänteet jakautuvat akillesjänteen

poikkipinta-alalle yksilötasolla, ja miten yksilölliset erot akillesjänteen sisäisessä liikkeessä voivat vaikuttaa repeämästä palauttamiseen ja jänteen toimintaan akillesjänteen repeämän jälkeen.

Biomekaniikka voi olla avain jänteen ja lihas-jänneyksikön toiminnan ymmärtämiseen terveillä ja erilaisissa patologioissa. Niinpä tämän opinnäytetyön tarkoituksena oli tehdä kattava tutkimus lihas-jänneyksikön biomekaniikasta 1 vuosi akillesjänteen repeämän jälkeen ei-operatiivisesti hoidetuilla potilailla. Lisäksi pyrimme tutkimaan akillesjänteen liikkeen epäyhtenäisyyttä ja anatomista rakennetta terveissä ja revenneissä jänteissä. Käytetyt uudet arviointimenetelmät voivat antaa uutta tietoa akillesjänteen mekaanisesta käyttäytymisestä ja edistää ymmärrystämme siitä, miten potilaat toipuvat akuutin akillesjänteen repeämän jälkeen. Tässä väitöskirjassa tutkittiin akillesjänteen lihas-jänneyksikön biomekaniikkaa ei-operatiivisesti hoidetuilla potilailla vuosi repeämän jälkeen.

Tulokset osoittavat, että repeämän jälkeen ei-operatiivisesti hoidetut jänteet paranevat pitkänomaisiksi, mihin liittyy kaksipäisen kantalihaksen lihassolujen mukautuminen lyhyemmiksi suuremmalla pennaatiokulmalla ja poikkipinta-alalla (II, IV). Loukkaantuneen jänteen jäykkyys ei eronnut terveeseen jänteeseen verrattuna vuoden kuluttua repeämästä, toisin kuin aiemmissa tutkimuksissa, jotka on tehty operatiivisesti hoidetuilla jänteillä (II). Ei-operatiivinen hoito sai aikaan paremman kollageenisäikeiden järjestäytymisen, kun operatiivisesti hoidetuissa rottien jänteissä oli enemmän arpikudosta. Kollageenin korkeatasoisempi järjestäytyminen on saattanut helpottaa jänteen mekaanisten ominaisuuksien palautumista vuoden kuluttua repeämästä.

Ison varpaan koukistajalihaksen (FHL) suhteellinen osuus pohjelihasten tuottamasta voimasta submaksimaalisen plantaariflesion aikana oli suurempi loukkaantuneessa raajassa, ja tämä näytti kompensoivan kaksoiskantalihaksen pienempää aktiivisuutta. On totta, että FHL kompensoi osittain kolmipäisen pohjelihaksen heikkoutta, mutta FHL:n kyky kompensoida voiman menetystä loukkaantuneessa raajassa on rajallinen lyhyen vipuvarren vuoksi. Näin ollen hoidoissa ja kuntoutuksessa ei pitäisi korostaa FHL:n roolia kolmipäisen kantalihaksen toipumisen mahdollistamiseksi, vaan pyrkiä minimoimaan akillesjänteen pidentyminen repeämän jälkeen.

Loukkaantuneen jänteen pidentyminen liittyi suurempaan suhteelliseen FHL-aktiivisuuteen, pienempään jäykkyyteen ja heikompaan itseraportoituun toimintakykyyn. Näyttää siltä, että jänteen pitenemä repeämän jälkeen on vastuussa havaituista objektiivisesti mitatuista ja itseraportoiduista toiminnallisista puutteista. Repeämän jälkeinen ei-operatiivinen hoito näyttää mahdollistavan jänteen sisäisen liikkeen palautumisen. Osalla potilaista hoito mahdollisti terveen jänteen merkkinä pidetyn epähomogeenisen liikkeen. Liikkeen amplitudi ja epätasaisuus kuitenkin muuttuivat repeämän jälkeen (I, III). Käyttämällä selektiivistä sähköstimulaatiota pohjelihaksiin pyrimme selvittämään akillesjänteen osajänteiden anatomisten alueiden sijaintia yksilötasolla. Jänteen sisäisen liikkeen avulla pystyimme tunnistamaan uloimman kaksoiskantalihaksen sijaitsevan jänteen etummaisella alueella sisemmän kaksoiskantalihaksen osajänteen vieressä sekä terveessä että repeytyneessä, ei-operatiivisesti hoidetuissa jäntees-

sä (III). Loukkaantuneen jänteen pidentyminen näyttää olevan syynä rakenteellisiin muutoksiin ja toiminnallisiin puutteisiin. Loukkaantuneen jänteen kuormittaminen edistäisi kolmipäisen kantalihasten aktivoitumista ja parantaisi jänteen jäykkyyttä, mikä auttaisi lieventämään jänteen pidentymisen vaikutuksia.

REFERENCES

Ackermans, T. M. A., Epro, G., McCrum, C., Oberländer, K. D., Suhr, F., Drost, M. R., Meijer, K., & Karamanidis, K. (2016). Aging and the effects of a half marathon on Achilles tendon force–elongation relationship. *European Journal of Applied Physiology*, *116*(11–12), 2281–2292.

Agres, A. N., Duda, G. N., Gehlen, T. J., Arampatzis, A., Taylor, W. R., & Manegold, S. (2015). Increased unilateral tendon stiffness and its effect on gait 2–6 years after Achilles tendon rupture. *Scandinavian Journal of Medicine & Science in Sports*, *25*(6), 860–867. https://doi.org/10.1111/sms.12456

Akdemir, O., Lineaweaver, W. C., Cavusoglu, T., Binboga, E., Uyanikgil, Y., Zhang, F., Pekedis, M., & Yagci, T. (2015). Effect of taurine on rat Achilles tendon healing. *Connective Tissue Research*, *56*(4), 300–306. https://doi.org/10.3109/03008207.2015.1026437

Akizuki, K. H., Gartman, E. J., Nisonson, B., Ben-Avi, S., & McHugh, M. P. (2001). The relative stress on the Achilles tendon during ambulation in an ankle immobiliser: Implications for rehabilitation after Achilles tendon repair. *British Journal of Sports Medicine*, *35*(5), 329–333.

Albracht, K., Arampatzis, A., & Baltzopoulos, V. (2008). Assessment of muscle volume and physiological cross-sectional area of the human triceps surae muscle in vivo. *Journal of Biomechanics*, *41*(10), 2211–2218. https://doi.org/10.1016/j.jbiomech.2008.04.020

Alexander, R. M. (1974). The mechanics of jumping by a dog (Canis familiaris). *Journal of Zoology*, *173*(4), 549–573.

Alexander, R. M., & Vernon, A. (1975). The mechanics of hopping by kangaroos (Macropodidae). *Journal of Zoology*, *177*(2), 265–303.

Andersson, T., Eliasson, P., Hammerman, M., Sandberg, O., & Aspenberg, P. (2012). Low-level mechanical stimulation is sufficient to improve tendon healing in rats. *Journal of Applied Physiology*, *113*(9), 1398–1402. https://doi.org/10.1152/japplphysiol.00491.2012

Arampatzis, A., Karamanidis, K., Morey-Klapsing, G., De Monte, G., & Stafilidis, S. (2007). Mechanical properties of the triceps surae tendon and aponeurosis in relation to intensity of sport activity. *Journal of Biomechanics*, *40*(9), 1946–1952. https://doi.org/10.1016/j.jbiomech.2006.09.005

Arampatzis, A., Morey-Klapsing, G., Karamanidis, K., DeMonte, G., Stafilidis, S., & Brüggemann, G.-P. (2005). Differences between measured and resultant joint moments during isometric contractions at the ankle joint. *Journal of Biomechanics*, *38*(4), 885–892. https://doi.org/10.1016/j.jbiomech.2004.04.027

Arellano, C. J., Konow, N., Gidmark, N. J., & Roberts, T. J. (2019). Evidence of a tunable biological spring: Elastic energy storage in aponeuroses varies with transverse strain in vivo. *Proceedings of the Royal Society B: Biological Sciences*, *286*(1900). https://doi.org/10.1098/rspb.2018.2764

Arndt, A., Bengtsson, A.-S., Peolsson, M., Thorstensson, A., & Movin, T. (2012). Non-uniform displacement within the Achilles tendon during passive ankle joint motion. *Knee Surgery, Sports Traumatology, Arthroscopy*, *20*(9), 1868–1874.

Arndt, A., Brüggemann, G.-P., Koebke, J., & Segesser, B. (1999). Asymmetrical loading of the human triceps surae: I. Mediolateral force differences in the Achilles tendon. *Foot & Ankle International*, *20*(7), Article 7.

Arndt, A. N., Komi, P. V., Brüggemann, G.-P., & Lukkariniemi, J. (1998). Individual muscle contributions to the in vivo achilles tendon force. *Clinical Biomechanics*, *13*(7), 532–541. https://doi.org/10.1016/S0268-0033(98)00032-1

Arner, O. (1959). Subcutaneous rupture of the Achilles tendon. A study of 92 cases. *Acta. Chir. Scandinavica Supplementum.*, *239*.

Årøen, A., Helgø, D., Granlund, O. G., & Bahr, R. (2004). Contralateral tendon rupture risk is increased in individuals with a previous Achilles tendon rupture. *Scandinavian Journal of Medicine & Science in Sports*, *14*(1), 30–33. https://doi.org/10.1111/j.1600-0838.2004.00344.x

Aspenberg, P. (2007). Stimulation of tendon repair: Mechanical loading, GDFs and platelets. A mini-review. *International Orthopaedics*, *31*(6), 783–789. https://doi.org/10.1007/s00264-007-0398-6

Aufwerber, S., Edman, G., Grävare Silbernagel, K., & Ackermann, P. W. (2020). Changes in Tendon Elongation and Muscle Atrophy Over Time After Achilles Tendon Rupture Repair: A Prospective Cohort Study on the Effects of Early Functional Mobilization. *The American Journal of Sports Medicine*, *48*(13), 3296–3305. https://doi.org/10.1177/0363546520956677

Azizi, E., Brainerd, E. L., & Roberts, T. J. (2008). Variable gearing in pennate muscles. *Proceedings of the National Academy of Sciences*, *105*(5), 1745–1750. https://doi.org/10.1073/pnas.0709212105

Azizi, E., & Roberts, T. J. (2009a). Biaxial strain and variable stiffness in aponeuroses. *The Journal of Physiology*, *587*(17), 4309–4318. https://doi.org/10.1113/jphysiol.2009.173690

Azizi, E., & Roberts, T. J. (2009b). Biaxial strain and variable stiffness in aponeuroses. *The Journal of Physiology*, *587*(Pt 17), 4309–4318. https://doi.org/10.1113/jphysiol.2009.173690

Azizi, E., & Roberts, T. J. (2014). Geared up to stretch: Pennate muscle behavior during active lengthening. *Journal of Experimental Biology*, *217*(3), 376–381. https://doi.org/10.1242/jeb.094383

Baar, K. (2019). Stress Relaxation and Targeted Nutrition to Treat Patellar Tendinopathy. *International Journal of Sport Nutrition and Exercise Metabolism*, *29*(4), 453–457. https://doi.org/10.1123/ijsnem.2018-0231

Barfod, K. W., Riecke, A. F., Boesen, A., Hansen, P., Maier, J. F., Døssing, S., & Troelsen, A. (2015). Validation of a novel ultrasound measurement of Achilles tendon length. *Knee Surgery, Sports Traumatology, Arthroscopy*, *23*(11), 3398–3406.

Barfred, T. (1973). Achilles tendon rupture: Aetiology and pathogenesis of subcutaneous rupture assessed on the basis of the literature and rupture experiments on rats. *Acta Orthopaedica Scandinavica*, *44*(sup152), 1–126.

Baxter, J. R., Farber, D. C., & Hast, M. W. (2019). Plantarflexor fiber and tendon slack length are strong determinates of simulated single-leg heel raise height. *Journal of Biomechanics*, *86*, 27–33. https://doi.org/10.1016/j.jbiomech.2019.01.035

Berg, R. A., & Kerr, J. S. (1992). Nutritional aspects of collagen metabolism. *Annual Review of Nutrition*, *12*(1), 369–390.

Bergkvist, D., Åström, I., Josefsson, P.-O., & Dahlberg, L. E. (2012). Acute Achilles tendon rupture: A questionnaire follow-up of 487 patients. *JBJS*, *94*(13), 1229–1233.

Beyer, R., Agergaard, A.-S., Magnusson, S. P., & Svensson, R. B. (2018). Speckle tracking in healthy and surgically repaired human Achilles tendons at different knee angles—A validation using implanted tantalum beads. *Translational Sports Medicine*, *1*(2), 79–88. https://doi.org/10.1002/tsm2.19

Bhandari, M., Guyatt, G. H., Siddiqui, F., Morrow, F., Busse, J., Leighton, R. K., Sprague, S., & Schemitsch, E. H. (2002). Treatment of acute Achilles tendon ruptures a systematic overview and metaanalysis. *Clinical Orthopaedics and Related Research*, *400*, 190–200.

Biewener, A. A., Konieczynski, D. D., & Baudinette, R. V. (1998). In vivo muscle force-length behavior during steady-speed hopping in tammar wallabies. *The Journal of Experimental Biology*, *201*(11), 1681–1694.

Blix, M. (1894). Die Langrund dei Spennung des Muskels. *Skandinavian Archives in Physiology*, *5*, 149–206.

Bojsen-Møller, J., & Magnusson, S. P. (2015). Heterogeneous Loading of the Human Achilles Tendon In Vivo. *Exercise and Sport Sciences Reviews*, *43*(4), 190–197. https://doi.org/10.1249/JES.0000000000000062

Bojsen-Møller, J., Schwartz, S., Kalliokoski, K. K., Finni, T., & Magnusson, S. P. (2010). Intermuscular force transmission between human plantarflexor muscles in vivo. *Journal of Applied Physiology*, *109*(6), 1608–1618. https://doi.org/10.1152/japplphysiol.01381.2009

Bolsterlee, B., Gandevia, S. C., & Herbert, R. D. (2016). Ultrasound imaging of the human medial gastrocnemius muscle: How to orient the transducer so that muscle fascicles lie in the image plane. *Journal of Biomechanics*, *49*(7), 1002–1008. https://doi.org/10.1016/j.jbiomech.2016.02.014

Bressel, E., & McNair, P. J. (2001). Biomechanical behavior of the plantar flexor muscle-tendon unit after an Achilles tendon rupture. *The American Journal of Sports Medicine*, *29*(3), 321–326.

Bring, D. K.-I., Kreicbergs, A., Renstrom, P. A., & Ackermann, P. W. (2007). Physical activity modulates nerve plasticity and stimulates repair after Achilles tendon rupture. *Journal of Orthopaedic Research*, *25*(2), 164–172.

Brorsson, A., Willy, R. W., Tranberg, R., & Grävare Silbernagel, K. (2017). Heel-Rise Height Deficit 1 Year After Achilles Tendon Rupture Relates to Changes in Ankle Biomechanics 6 Years After Injury. *The American Journal*

of Sports Medicine, *45*(13), 3060–3068. https://doi.org/10.1177/0363546517717698

Brumann, M., Baumbach, S. F., Mutschler, W., & Polzer, H. (2014). Accelerated rehabilitation following Achilles tendon repair after acute rupture–development of an evidence-based treatment protocol. *Injury*, *45*(11), 1782–1790.

Butler, D., Grood, E. S., Noyes, F. R., & Zernicke, R. E. (1978). Biomechanics of ligaments and tendons. *Exercise and Sport Sciences Reviews*, *6*(1), 125. https://journals.lww.com/acsm-essr/Citation/1978/00060/BIOMECHANICS_OF_LIGAMENTS_AND_TENDONS.5.aspx

Carabello, R. J., Reid, K. F., Clark, D. J., Phillips, E. M., & Fielding, R. A. (2010). Lower extremity strength and power asymmetry assessment in healthy and mobility-limited populations: Reliability and association with physical functioning. *Aging Clinical and Experimental Research*, *22*(4), 324–329. https://doi.org/10.3275/6676

Carmont, M. R., Grävare Silbernagel, K., Brorsson, A., Olsson, N., Maffulli, N., & Karlsson, J. (2015). The Achilles tendon resting angle as an indirect measure of Achilles tendon length following rupture, repair, and rehabilitation. *Asia-Pacific Journal of Sports Medicine, Arthroscopy, Rehabilitation and Technology*, *2*(2), 49–55. https://doi.org/10.1016/j.asmart.2014.12.002

Centner, C., Lauber, B., Seynnes, O. R., Jerger, S., Sohnius, T., Gollhofer, A., & König, D. (2019). Low-load blood flow restriction training induces similar morphological and mechanical Achilles tendon adaptations compared with high-load resistance training. *Journal of Applied Physiology*, *127*(6), 1660–1667. https://doi.org/10.1152/japplphysiol.00602.2019

Chen, X.-M., Cui, L.-G., He, P., Shen, W.-W., Qian, Y.-J., & Wang, J.-R. (2013). Shear Wave Elastographic Characterization of Normal and Torn Achilles Tendons. *Journal of Ultrasound in Medicine*, *32*(3), 449–455. https://doi.org/10.7863/jum.2013.32.3.449

Chow, R. S., Medri, M. K., Martin, D. C., Leekam, R. N., Agur, A. M., & McKee, N. H. (2000). Sonographic studies of human soleus and gastrocnemius muscle architecture: Gender variability. *European Journal of Applied Physiology*, *82*(3), 236–244. https://doi.org/10.1007/s004210050677

Christey, G., Amey, J., Campbell, A., & Smith, A. (2020). Variation in volumes and characteristics of trauma patients admitted to a level one trauma centre during national level 4 lockdown for COVID-19 in New Zealand. *The New Zealand Medical Journal (Online)*, *133*(1513), 81–86.

Clark, W. H., & Franz, J. R. (2018). Do triceps surae muscle dynamics govern non-uniform Achilles tendon deformations? *PeerJ*, *6*, e5182. https://doi.org/10.7717/peerj.5182

Clark, W. H., & Franz, J. R. (2021). Age-related changes to triceps surae muscle-subtendon interaction dynamics during walking. *Scientific Reports*, *11*, 21264. https://doi.org/10.1038/s41598-021-00451-y

Čretnik, A., & Frank, A. (2004). Incidence and outcome of rupture of the Achilles tendon. *Wiener Klinische Wochenschrift*, *116*.
Curt, L. (1958). Vascular distribution in the Achilles tendon. *Acta Chir. Scand.*, *116*, 491–495.
Curtis, L. (2016). Nutritional research may be useful in treating tendon injuries. *Nutrition*, *32*(6), 617–619. https://doi.org/10.1016/j.nut.2015.12.039
Cutts, A. (1988). The range of sarcomere lengths in the muscles of the human lower limb. *Journal of Anatomy*, *160*, 79.
Davidsson, L., & Salo, M. (1969). Pathogenesis of subcutaneous tendon ruptures. *Acta Chirurgica Scandinavica*, *135*(3), 209–212.
de Boer, M. D., Seynnes, O. R., di Prampero, P. E., Pišot, R., Mekjavić, I. B., Biolo, G., & Narici, M. V. (2008). Effect of 5 weeks horizontal bed rest on human muscle thickness and architecture of weight bearing and non-weight bearing muscles. *European Journal of Applied Physiology*, *104*(2), 401–407. https://doi.org/10.1007/s00421-008-0703-0
De la Fuente, C. I., Lillo, R. P. y, Ramirez-Campillo, R., Ortega-Auriol, P., Delgado, M., Alvarez-Ruf, J., & Carreño, G. (2016). Medial gastrocnemius myotendinous junction displacement and plantar-flexion strength in patients treated with immediate rehabilitation after Achilles tendon repair. *Journal of Athletic Training*, *51*(12), 1013–1021.
Deng, S., Sun, Z., Zhang, C., Chen, G., & Li, J. (2017). Surgical Treatment Versus Conservative Management for Acute Achilles Tendon Rupture: A Systematic Review and Meta-Analysis of Randomized Controlled Trials. *The Journal of Foot and Ankle Surgery*, *56*(6), 1236–1243. https://doi.org/10.1053/j.jfas.2017.05.036
Depalle, B., Qin, Z., Shefelbine, S. J., & Buehler, M. J. (2015). Influence of cross-link structure, density and mechanical properties in the mesoscale deformation mechanisms of collagen fibrils. *Journal of the Mechanical Behavior of Biomedical Materials*, *52*, 1–13. https://doi.org/10.1016/j.jmbbm.2014.07.008
Devkota, A. C., & Weinhold, P. S. (2003). Mechanical response of tendon subsequent to ramp loading to varying strain limits. *Clinical Biomechanics*, *18*(10), 969–974.
Durgam, S., & Stewart, M. (2017). Cellular and Molecular Factors Influencing Tendon Repair. *Tissue Engineering Part B: Reviews*, *23*(4), 307–317. https://doi.org/10.1089/ten.teb.2016.0445
Edama, M., Kubo, M., Onishi, H., Takabayashi, T., Inai, T., Yokoyama, E., Hiroshi, W., Satoshi, N., & Kageyama, I. (2015). The twisted structure of the human A chilles tendon. *Scandinavian Journal of Medicine & Science in Sports*, *25*(5), e497–e503.
Eliasson, P., Agergaard, A.-S., Couppe, C., Svensson, R., Hoeffner, R., Warming, S., Warming, N., Holm, C., Jensen, M. H., & Krogsgaard, M. (2018). The ruptured Achilles tendon elongates for 6 months after surgical repair regardless of early or late weightbearing in combination with ankle mobilization: A randomized clinical trial. *The American Journal of Sports Medicine*, *46*(10), Article 10.

Eliasson, P., Andersson, T., & Aspenberg, P. (2012). Achilles tendon healing in rats is improved by intermittent mechanical loading during the inflammatory phase. *Journal of Orthopaedic Research*, *30*(2), 274–279. https://doi.org/10.1002/jor.21511

Eliasson, P., Andersson, T., Hammerman, M., & Aspenberg, P. (2013). Primary gene response to mechanical loading in healing rat Achilles tendons. *Journal of Applied Physiology*, *114*(11), 1519–1526.

Ellison, P., Molloy, A., & Mason, L. W. (2017). Early protected Weightbearing for acute ruptures of the Achilles tendon: Do commonly used Orthoses produce the required equinus? *The Journal of Foot and Ankle Surgery*, *56*(5), 960–963.

Epstein, M., Wong, M., & Herzog, W. (2006). Should tendon and aponeurosis be considered in series? *Journal of Biomechanics*, *39*(11), 2020–2025.

Erickson, B. J., Mascarenhas, R., Saltzman, B. M., Walton, D., Lee, S., Cole, B. J., & Bach Jr, B. R. (2015). Is operative treatment of Achilles tendon ruptures superior to nonoperative treatment? A systematic review of overlapping meta-analyses. *Orthopaedic Journal of Sports Medicine*, *3*(4), 2325967115579188.

Finni, T., Bernabei, M., Baan, G. C., Noort, W., Tijs, C., & Maas, H. (2018). Non-uniform displacement and strain between the soleus and gastrocnemius subtendons of rat Achilles tendon. *Scandinavian Journal of Medicine & Science in Sports*, *28*(3), Article 3.

Finni, T., Cronin, N. J., Mayfield, D., Lichtwark, G. A., & Cresswell, A. G. (2017). Effects of muscle activation on shear between human soleus and gastrocnemius muscles. *Scandinavian Journal of Medicine & Science in Sports*, *27*(1), Article 1.

Finni, T., Hodgson, J. A., Lai, A. M., Edgerton, V. R., & Sinha, S. (2003). Nonuniform strain of human soleus aponeurosis-tendon complex during submaximal voluntary contractions in vivo. *Journal of Applied Physiology*, *95*(2), 829–837.

Finni, T., Hodgson, J. A., Lai, A. M., Edgerton, V. R., & Sinha, S. (2006). Muscle synergism during isometric plantarflexion in achilles tendon rupture patients and in normal subjects revealed by velocity-encoded cine phase-contrast MRI. *Clinical Biomechanics*, *21*(1), 67–74.

Finni, T., Peter, A., Khair, R., & Cronin, N. J. (2022). Tendon length estimates are influenced by tracking location. *European Journal of Applied Physiology*. https://doi.org/10.1007/s00421-022-04958-8

Finni, T., & Vanwanseele, B. (2023). Towards modern understanding of the Achilles tendon properties in human movement research. *Journal of Biomechanics*, *152*, 111583. https://doi.org/10.1016/j.jbiomech.2023.111583

Fox, J. M., Blazina, M. E., Jobe, F. W., Kerlan, R. K., Carter, V. S., Shields Jr, C. L., & Carlson, G. J. (1975). Degeneration and rupture of the Achilles tendon. *Clinical Orthopaedics and Related Research®*, *107*, 221–224.

Francis, C. A., Lenz, A. L., Lenhart, R. L., & Thelen, D. G. (2013). The modulation of forward propulsion, vertical support, and center of

pressure by the plantarflexors during human walking. *Gait & Posture*, *38*(4), 993–997. https://doi.org/10.1016/j.gaitpost.2013.05.009
Franz, J. R., & Thelen, D. G. (2015). Depth-dependent variations in Achilles tendon deformations with age are associated with reduced plantarflexor performance during walking. *Journal of Applied Physiology*, *119*(3), 242–249. https://doi.org/10.1152/japplphysiol.00114.2015
Franz, J. R., & Thelen, D. G. (2016). Imaging and simulation of Achilles tendon dynamics: Implications for walking performance in the elderly. *Journal of Biomechanics*, *49*(9), 1403–1410. https://doi.org/10.1016/j.jbiomech.2016.04.032
Freedman, B. R., Gordon, J. A., & Soslowsky, L. J. (2014a). The Achilles tendon: Fundamental properties and mechanisms governing healing. *Muscles, Ligaments and Tendons Journal*, *4*(2), 245–255. https://www.ncbi.nlm.nih.gov/pmc/articles/PMC4187594/
Freedman, B. R., Gordon, J. A., & Soslowsky, L. J. (2014b). The Achilles tendon: Fundamental properties and mechanisms governing healing. *Muscles, Ligaments and Tendons Journal*, *4*(2), 245–255. https://www.ncbi.nlm.nih.gov/pmc/articles/PMC4187594/
Fröberg, Å., Cissé, A.-S., Larsson, M., Mårtensson, M., Peolsson, M., Movin, T., & Arndt, A. (2017). Altered patterns of displacement within the Achilles tendon following surgical repair. *Knee Surgery, Sports Traumatology, Arthroscopy*, *25*(6), 1857–1865.
Fukashiro, S., Rob, M., Ichinose, Y., Kawakami, Y., & Fukunaga, T. (1995). Ultrasonography gives directly but noninvasively elastic characteristic of human tendon in vivo. *European Journal of Applied Physiology and Occupational Physiology*, *71*(6), 555–557. https://doi.org/10.1007/BF00238560
Fukunaga, T., Ichinose, Y., Ito, M., Kawakami, Y., & Fukashiro, S. (1997). Determination of fascicle length and pennation in a contracting human muscle in vivo. *Journal of Applied Physiology*, *82*(1), 354–358. https://doi.org/10.1152/jappl.1997.82.1.354
Fukunaga, T., Ito, M., Ichinose, Y., Kuno, S., Kawakami, Y., & Fukashiro, S. (1996). Tendinous movement of a human muscle during voluntary contractions determined by real-time ultrasonography. *Journal of Applied Physiology*, *81*(3), 1430–1433.
Fukunaga, T., Kubo, K., Kawakami, Y., Fukashiro, S., Kanehisa, H., & Maganaris, C. N. (2001). In vivo behaviour of human muscle tendon during walking. *Proceedings of the Royal Society of London. Series B: Biological Sciences*, *268*(1464), 229–233. https://doi.org/10.1098/rspb.2000.1361
Galloway, M. T., Lalley, A. L., & Shearn, J. T. (2013). The Role of Mechanical Loading in Tendon Development, Maintenance, Injury, and Repair. *The Journal of Bone and Joint Surgery. American Volume*, *95*(17), 1620–1628. https://doi.org/10.2106/JBJS.L.01004
Ganestam, A., Kallemose, T., Troelsen, A., & Barfod, K. W. (2016). Increasing incidence of acute Achilles tendon rupture and a noticeable decline in surgical treatment from 1994 to 2013. A nationwide registry study of

33,160 patients. *Knee Surgery, Sports Traumatology, Arthroscopy*, *24*(12), Article 12.

Geremia, J. M., Bobbert, M. F., Casa Nova, M., Ott, R. D., Lemos, F. de A., Lupion, R. de O., Frasson, V. B., & Vaz, M. A. (2015). The structural and mechanical properties of the Achilles tendon 2 years after surgical repair. *Clinical Biomechanics*, *30*(5), 485–492. https://doi.org/10.1016/j.clinbiomech.2015.03.005

Gollapudi, S. K., & Lin, D. C. (2009). Experimental determination of sarcomere force–length relationship in type-I human skeletal muscle fibers. *Journal of Biomechanics*, *42*(13), 2011–2016.

Gordon, A. M., Huxley, A. F., & Julian, F. J. (1966). The variation in isometric tension with sarcomere length in vertebrate muscle fibres. *The Journal of Physiology*, *184*(1), 170–192. https://doi.org/10.1113/jphysiol.1966.sp007909

Goslow Jr, G. E., Reinking, R. M., & Stuart, D. G. (1973). The cat step cycle: Hind limb joint angles and muscle lengths during unrestrained locomotion. *Journal of Morphology*, *141*(1), 1–41.

Handsfield, G., Slane, L., & Screen, H. (2016). Nomenclature of the tendon hierarchy: An overview of inconsistent terminology and a proposed size-based naming scheme with terminology for multi-muscle tendons. *Journal of Biomechanics*, *49*(13), 3112–3124.

Hansen, W., Shim, V. B., Obst, S., Lloyd, D. G., Newsham-West, R., & Barrett, R. S. (2017). Achilles tendon stress is more sensitive to subject-specific geometry than subject-specific material properties: A finite element analysis. *Journal of Biomechanics*, *56*, 26–31. https://doi.org/10.1016/j.jbiomech.2017.02.031

Haraldsson, B. T., Aagaard, P., Qvortrup, K., Bojsen-Moller, J., Krogsgaard, M., Koskinen, S., Kjaer, M., & Magnusson, S. P. (2008). Lateral force transmission between human tendon fascicles. *Matrix Biology*, *27*(2), 86–95. https://doi.org/10.1016/j.matbio.2007.09.001

Hastad, K., Larsson, L. G., & Lindholm, A. (1959). Clearance of radiosodium after local deposit in the Achilles tendon. *Acta Chirurgica Scandinavica*, *116*(3), 251–255.

Hattrup, S. J., & Johnson, K. A. (1985). A review of ruptures of the Achilles tendon. *Foot & Ankle*, *6*(1), 34–38.

Heikkinen, J., Lantto, I., Piilonen, J., Flinkkilä, T., Ohtonen, P., Siira, P., Laine, V., Niinimäki, J., Pajala, A., & Leppilahti, J. (2017). Tendon length, calf muscle atrophy, and strength deficit after acute Achilles tendon rupture: Long-term follow-up of patients in a previous study. *JBJS*, *99*(18), Article 18.

Heinemeier, K. M., & Kjaer, M. (2011). In vivo investigation of tendon responses to mechanical loading. *J Musculoskelet Neuronal Interact*, *11*(2), 115–123.

Herzog, W., Read, L. J., & ter Keurs, H. E. D. J. (1991). Experimental determination of force—Length relations of intact human gastrocnemius muscles. *Clinical Biomechanics*, *6*(4), 230–238. https://doi.org/10.1016/0268-0033(91)90051-Q

Hess, G. P., Cappiello, W. L., Poole, R. M., & Hunter, S. C. (1989). Prevention and Treatment of Overuse Tendon Injuries. *Sports Medicine*, *8*(6), 371–384. https://doi.org/10.2165/00007256-198908060-00005

Hill, A. V. (1938). The heat of shortening and the dynamic constants of muscle. *Proceedings of the Royal Society of London. Series B-Biological Sciences*, *126*(843), 136–195.

Hill, A. V. (1953). The mechanics of active muscle. *Proceedings of the Royal Society of London. Series B-Biological Sciences*, *141*(902), 104–117.

Hillin, C. D., Fryhofer, G. W., Freedman, B. R., Choi, D. S., Weiss, S. N., Huegel, J., & Soslowsky, L. J. (2019). Effects of immobilization angle on tendon healing after achilles rupture in a rat model. *Journal of Orthopaedic Research*, *37*(3), 562–573. https://doi.org/10.1002/jor.24241

Hirata, K., Kanehisa, H., Miyamoto-Mikami, E., & Miyamoto, N. (2015). Evidence for intermuscle difference in slack angle in human triceps surae. *Journal of Biomechanics*, *48*(6), 1210–1213. https://doi.org/10.1016/j.jbiomech.2015.01.039

Hodgson, J. A., Finni, T., Lai, A. M., Edgerton, V. R., & Sinha, S. (2006). Influence of structure on the tissue dynamics of the human soleus muscle observed in MRI studies during isometric contractions. *Journal of Morphology*, *267*(5), 584–601. https://doi.org/10.1002/jmor.10421

Hodgson, M., Docherty, D., & Robbins, D. (2005). Post-Activation Potentiation. *Sports Medicine*, *35*(7), 585–595. https://doi.org/10.2165/00007256-200535070-00004

Holm, C., Kjaer, M., & Eliasson, P. (2015). A chilles tendon rupture–treatment and complications: A systematic review. *Scandinavian Journal of Medicine & Science in Sports*, *25*(1), e1–e10.

Holzer, D., Paternoster, F. K., Hahn, D., Siebert, T., & Seiberl, W. (2020). Considerations on the human Achilles tendon moment arm for in vivo triceps surae muscle-tendon unit force estimates. *Scientific Reports*, *10*(1), 19559. https://doi.org/10.1038/s41598-020-76625-x

Hope, M., & Saxby, T. S. (2007). Tendon healing. *Foot and Ankle Clinics*, *12*(4), 553–567.

Hopkins, W. G. (2000). Measures of Reliability in Sports Medicine and Science. *Sports Medicine*, *30*(1), 1–15. https://doi.org/10.2165/00007256-200030010-00001

Houshian, S., Tscherning, T., & Riegels-Nielsen, P. (1998). The epidemiology of Achilles tendon rupture in a Danish county. *Injury*, *29*(9), 651–654.

Huang, J., Wang, C., Ma, X., Wang, X., Zhang, C., & Chen, L. (2015). Rehabilitation regimen after surgical treatment of acute Achilles tendon ruptures: A systematic review with meta-analysis. *The American Journal of Sports Medicine*, *43*(4), 1008–1016.

Hullfish, T. J., O'Connor, K. M., & Baxter, J. R. (2019a). Gastrocnemius fascicles are shorter and more pennate throughout the first month following acute Achilles tendon rupture. *PeerJ*, *7*, e6788. https://doi.org/10.7717/peerj.6788

Hullfish, T. J., O'Connor, K. M., & Baxter, J. R. (2019b). Medial gastrocnemius muscle remodeling correlates with reduced plantarflexor kinetics 14 weeks following Achilles tendon rupture. *Journal of Applied Physiology (Bethesda, Md.: 1985)*, *127*(4), 1005–1011. https://doi.org/10.1152/japplphysiol.00255.2019

Huxley, A. F. (1957). Muscle structure and theories of contraction. *Progress in Biophysics and Biophysical Chemistry*, *7*, 255–318.

Inglis, A. E., & Sculco, T. P. (1981). Surgical Repair of Ruptures of the Tendo Achillis. *Clinical Orthopaedics and Related Research (1976-2007)*, *156*, 160. https://journals.lww.com/corr/citation/1981/05000/surgical_repair_of_ruptures_of_the_tendo_achillis.21.aspx

Jerger, S., Centner, C., Lauber, B., Seynnes, O., Sohnius, T., Jendricke, P., Oesser, S., Gollhofer, A., & König, D. (2022). Effects of specific collagen peptide supplementation combined with resistance training on Achilles tendon properties. *Scandinavian Journal of Medicine & Science in Sports*, *32*(7), 1131–1141.

Jones, M. P., Khan, R. J., & Smith, R. L. C. (2012). Surgical interventions for treating acute Achilles tendon rupture: Key findings from a recent Cochrane review. *JBJS*, *94*(12), e88.

Jozsa, L., Kannus, P., Balint, J. B., & Reffy, A. (1991). Three-Dimensional infrastructure of Human Tendons. *Cells Tissues Organs*, *142*(4), 306–312. https://doi.org/10.1159/000147207

Kangas, J., Pajala, A., Ohtonen, P., & Leppilahti, J. (2007). Achilles Tendon Elongation after Rupture Repair: A Randomized Comparison of 2 Postoperative Regimens. *The American Journal of Sports Medicine*, *35*(1), 59–64. https://doi.org/10.1177/0363546506293255

Kannus, P. (2000). Structure of the tendon connective tissue. *Scandinavian Journal of Medicine & Science in Sports*, *10*(6), 312–320. https://doi.org/10.1034/j.1600-0838.2000.010006312.x

Kannus, P., & Józsa, L. (1991). Histopathological changes preceding spontaneous rupture of a tendon. A controlled study of 891 patients. *JBJS*, *73*(10), 1507. https://journals.lww.com/jbjsjournal/Abstract/1991/73100/Histopathological_changes_preceding_spontaneous.9.aspx

Kannus, P., Jozsa, L., Järvinen, T. A. H., Järvinen, T. L. N., Kvist, M., Natri, A., & Järvinen, M. (1998). Location and Distribution of Non-collagenous Matrix Proteins in Musculoskeletal Tissues of Rat. *The Histochemical Journal*, *30*(11), 799–810. https://doi.org/10.1023/A:1003448106673

Karamanidis, K., & Epro, G. (2020). Monitoring Muscle-Tendon Adaptation Over Several Years of Athletic Training and Competition in Elite Track and Field Jumpers. *Frontiers in Physiology*, *11*. https://doi.org/10.3389/fphys.2020.607544

Kastelic, J., Galeski, A., & Baer, E. (1978). The multicomposite structure of tendon. *Connective Tissue Research*, *6*(1), 11–23.

Keating, J. F., & Will, E. M. (2011). Operative versus non-operative treatment of acute rupture of tendo Achillis: A prospective randomised evaluation of

functional outcome. *The Journal of Bone and Joint Surgery. British Volume*, *93*(8), 1071–1078.
Khan, R. J. K., Fick, D., Keogh, A., Crawford, J., Brammar, T., & Parker, M. (2005). Treatment of Acute Achilles Tendon Ruptures: A Meta-Analysis of Randomized, Controlled Trials. *JBJS*, *87*(10), 2202–2210. https://doi.org/10.2106/JBJS.D.03049
Khan, R. J., & Smith, R. L. C. (2010). Surgical interventions for treating acute Achilles tendon ruptures. *Cochrane Database of Systematic Reviews*, *9*.
Kjær, M. (2004). Role of Extracellular Matrix in Adaptation of Tendon and Skeletal Muscle to Mechanical Loading. *Physiological Reviews*, *84*(2), 649–698. https://doi.org/10.1152/physrev.00031.2003
Kjaer, M., Langberg, H., Miller, B. F., Boushel, R., Crameri, R., Koskinen, S., Heinemeier, K., Olesen, J. L., Døssing, S., & Hansen, M. (2005). Metabolic activity and collagen turnover in human tendon in response to physical activity. *J Musculoskelet Neuronal Interact*, *5*(1), 41–52.
Klaiber, L. R., Schlechtweg, S., Wiedemann, R., Alt, W., & Stutzig, N. (2023). Local displacement within the Achilles tendon induced by electrical stimulation of the single gastrocnemius muscles. *Clinical Biomechanics*, *102*, 105901. https://doi.org/10.1016/j.clinbiomech.2023.105901
Komi, P. V., Fukashiro, S., & Järvinen, M. (1992). Biomechanical Loading of Achilles Tendon During Normal Locomotion. *Clinics in Sports Medicine*, *11*(3), 521–531. https://doi.org/10.1016/S0278-5919(20)30506-8
Kongsgaard, M., Nielsen, C. H., Hegnsvad, S., Aagaard, P., & Magnusson, S. P. (2011). Mechanical properties of the human Achilles tendon, in vivo. *Clinical Biomechanics*, *26*(7), 772–777. https://doi.org/10.1016/j.clinbiomech.2011.02.011
Krapf, D., Kaipel, M., & Majewski, M. (2012). Structural and Biomechanical Characteristics After Early Mobilization in an Achilles Tendon Rupture Model: Operative Versus Nonoperative Treatment. *Orthopedics*, *35*(9), e1383–e1388. https://doi.org/10.3928/01477447-20120822-26
Kubo, K., Kanehisa, H., & Fukunaga, T. (2002). Effects of transient muscle contractions and stretching on the tendon structures in vivo. *Acta Physiologica Scandinavica*, *175*(2), 157–164. https://doi.org/10.1046/j.1365-201X.2002.00976.x
Kujala, U. M., Sarna, S., & Kaprio, J. (2005). Cumulative Incidence of Achilles Tendon Rupture and Tendinopathy in Male Former Elite Athletes. *Clinical Journal of Sport Medicine*, *15*(3), 133. https://doi.org/10.1097/01.jsm.0000165347.55638.23
Kurokawa, S., Fukunaga, T., & Fukashiro, S. (2001). Behavior of fascicles and tendinous structures of human gastrocnemius during vertical jumping. *Journal of Applied Physiology*.
Lantto, I., Heikkinen, J., Flinkkila, T., Ohtonen, P., Siira, P., Laine, V., & Leppilahti, J. (2016). A prospective randomized trial comparing surgical and nonsurgical treatments of acute Achilles tendon ruptures. *The American Journal of Sports Medicine*, *44*(9), 2406–2414.

Lehr, N. L., Clark, W. H., Lewek, M. D., & Franz, J. R. (2021). The effects of triceps surae muscle stimulation on localized Achilles subtendon tissue displacements. *Journal of Experimental Biology*, *224*(15). https://doi.org/10.1242/jeb.242135

Lenhart, R. L., Francis, C. A., Lenz, A. L., & Thelen, D. G. (2014). Empirical evaluation of gastrocnemius and soleus function during walking. *Journal of Biomechanics*, *47*(12), 2969–2974. https://doi.org/10.1016/j.jbiomech.2014.07.007

Leppilahti, J., & Orava, S. (1998). Total Achilles Tendon Rupture. *Sports Medicine*, *25*(2), 79–100. https://doi.org/10.2165/00007256-199825020-00002

Lichtwark, G. A., & Barclay, C. J. (2010). The influence of tendon compliance on muscle power output and efficiency during cyclic contractions. *Journal of Experimental Biology*, *213*(5), 707–714.

Lichtwark, G. A., & Wilson, A. M. (2005). Effects of series elasticity and activation conditions on muscle power output and efficiency. *Journal of Experimental Biology*, *208*(15), 2845–2853.

Lichtwark, G. A., & Wilson, A. M. (2007). Is Achilles tendon compliance optimised for maximum muscle efficiency during locomotion? *Journal of Biomechanics*, *40*(8), 1768–1775. https://doi.org/10.1016/j.jbiomech.2006.07.025

Lichtwark, G. A., & Wilson, A. M. (2008). Optimal muscle fascicle length and tendon stiffness for maximising gastrocnemius efficiency during human walking and running. *Journal of Theoretical Biology*, *252*(4), 662–673.

Lieber, R. L., & Bodine-Fowler, S. C. (1993). Skeletal Muscle Mechanics: Implications for Rehabilitation. *Physical Therapy*, *73*(12), 844–856. https://doi.org/10.1093/ptj/73.12.844

Lieber, R. L., Loren, G. J., & Friden, J. (1994). In vivo measurement of human wrist extensor muscle sarcomere length changes. *Journal of Neurophysiology*, *71*(3), 874–881. https://doi.org/10.1152/jn.1994.71.3.874

Llewellyn, M. E., Barretto, R. P. J., Delp, S. L., & Schnitzer, M. J. (2008). Minimally invasive high-speed imaging of sarcomere contractile dynamics in mice and humans. *Nature*, *454*(7205), Article 7205. https://doi.org/10.1038/nature07104

Loram, I. D., Maganaris, C. N., & Lakie, M. (2004). Paradoxical muscle movement in human standing. *The Journal of Physiology*, *556*(3), 683–689. https://doi.org/10.1113/jphysiol.2004.062398

Loram, I. D., Maganaris, C. N., & Lakie, M. (2005). Active, non-spring-like muscle movements in human postural sway: How might paradoxical changes in muscle length be produced? *The Journal of Physiology*, *564*(1), 281–293.

Luke, S. G. (2017). Evaluating significance in linear mixed-effects models in R. *Behavior Research Methods*, *49*(4), 1494–1502. https://doi.org/10.3758/s13428-016-0809-y

Maffulli, N., & Almekinders, L. (Eds.). (2007). *The Achilles tendon*. Springer.

Maffulli, N., Tallon, C., Wong, J., Peng Lim, K., & Bleakney, R. (2003). Early weightbearing and ankle mobilization after open repair of acute

midsubstance tears of the Achilles tendon. *The American Journal of Sports Medicine*, *31*(5), 692–700.
Maganaris, C. N. (2003). Force-length characteristics of the in vivo human gastrocnemius muscle. *Clinical Anatomy*, *16*(3), 215–223. https://doi.org/10.1002/ca.10064
Maganaris, C. N., Baltzopoulos, V., & Sargeant, A. J. (1998). In vivo measurements of the triceps surae complex architecture in man: Implications for muscle function. *The Journal of Physiology*, *512*(2), 603–614. https://doi.org/10.1111/j.1469-7793.1998.603be.x
Maganaris, C. N., Narici, M. V., & Maffulli, N. (2008). Biomechanics of the Achilles tendon. *Disability and Rehabilitation*, *30*(20–22), 1542–1547. https://doi.org/10.1080/09638280701785494
Magnusson, S. P., Aagaard, P., Rosager, S., Dyhre-Poulsen, P., & Kjaer, M. (2001). Load-displacement properties of the human triceps surae aponeurosis in vivo. *The Journal of Physiology*, *531*(1), 277–288. https://doi.org/10.1111/j.1469-7793.2001.0277j.x
Magnusson, S. P., & Kjaer, M. (2019). The impact of loading, unloading, ageing and injury on the human tendon. *The Journal of Physiology*, *597*(5), 1283–1298.
Mahler, F., & Fritschy, D. (1992). Partial and complete ruptures of the Achilles tendon and local corticosteroid injections. *British Journal of Sports Medicine*, *26*(1), 7.
Masood, T., Bojsen-Møller, J., Kalliokoski, K. K., Kirjavainen, A., Äärimaa, V., Peter Magnusson, S., & Finni, T. (2014). Differential contributions of ankle plantarflexors during submaximal isometric muscle action: A PET and EMG study. *Journal of Electromyography and Kinesiology*, *24*(3), 367–374. https://doi.org/10.1016/j.jelekin.2014.03.002
McCormack, R., & Bovard, J. (2015). Early functional rehabilitation or cast immobilisation for the postoperative management of acute Achilles tendon rupture? A systematic review and meta-analysis of randomised controlled trials. *British Journal of Sports Medicine*, *49*(20), 1329–1335.
McHugh, M. P., Orishimo, K. F., Kremenic, I. J., Adelman, J., & Nicholas, S. J. (2019). Electromyographic Evidence of Excessive Achilles Tendon Elongation During Isometric Contractions After Achilles Tendon Repair. *Orthopaedic Journal of Sports Medicine*, *7*(11), 2325967119883357. https://doi.org/10.1177/2325967119883357
McNair, P., Nordez, A., Olds, M., Young, S. W., & Cornu, C. (2013). Biomechanical properties of the plantar flexor muscle–tendon complex 6 months post-rupture of the achilles tendon. *Journal of Orthopaedic Research*, *31*(9), 1469–1474. https://doi.org/10.1002/jor.22381
Miller, K. S., Connizzo, B. K., Feeney, E., & Soslowsky, L. J. (2012). Characterizing local collagen fiber re-alignment and crimp behavior throughout mechanical testing in a mature mouse supraspinatus tendon model. *Journal of Biomechanics*, *45*(12), 2061–2065. https://doi.org/10.1016/j.jbiomech.2012.06.006

Möller, M., Lind, K., Movin, T., & Karlsson, J. (2002). Calf muscle function after Achilles tendon rupture. A prospective, randomised study comparing surgical and non-surgical treatment. *Scandinavian Journal of Medicine & Science in Sports*, *12*(1), 9–16.

Möller, M., Movin, T., Granhed, H., Lind, K., Faxen, E., & Karlsson, J. (2001). Acute rupture of tendo Achillis: A prospective, randomised study of comparison between surgical and non-surgical treatment. *The Journal of Bone and Joint Surgery. British Volume*, *83*(6), 843–848.

Monte, A., & Zignoli, A. (2021). Muscle and tendon stiffness and belly gearing positively correlate with rate of torque development during explosive fixed end contractions. *Journal of Biomechanics*, *114*, 110110. https://doi.org/10.1016/j.jbiomech.2020.110110

Mortensen, N. H. M., Skov, O., & Jensen, P. E. (1999). Early motion of the ankle after operative treatment of a rupture of the Achilles tendon. A prospective, randomized clinical and radiographic study. *JBJS*, *81*(7), 983–990.

Mullaney, M. J., McHugh, M. P., Tyler, T. F., Nicholas, S. J., & Lee, S. J. (2006). Weakness in End-Range Plantar Flexion after Achilles Tendon Repair. *The American Journal of Sports Medicine*, *34*(7), 1120–1125. https://doi.org/10.1177/0363546505284186

Muraoka, T., Muramatsu, T., Fukunaga, T., & Kanehisa, H. (2005). Elastic properties of human Achilles tendon are correlated to muscle strength. *Journal of Applied Physiology*, *99*(2), 665–669. https://doi.org/10.1152/japplphysiol.00624.2004

Myer, G. D., Faigenbaum, A. D., Cherny, C. E., Heidt, R. S., & Hewett, T. E. (2011). Did the NFL Lockout Expose the Achilles Heel of Competitive Sports? *Journal of Orthopaedic & Sports Physical Therapy*, *41*(10), 702–705. https://doi.org/10.2519/jospt.2011.0107

Nagasawa, K., Noguchi, M., Ikoma, K., & Kubo, T. (2008). Static and dynamic biomechanical properties of the regenerating rabbit Achilles tendon. *Clinical Biomechanics*, *23*(6), 832–838.

Newnham, D. M., Douglas, J. G., Legge, J. S., & Friend, J. A. (1991). Achilles tendon rupture: An underrated complication of corticosteroid treatment. *Thorax*, *46*(11), 853–854.

Nicholson, G., Walker, J., Dawson, Z., Bissas, A., & Harris, N. (2020). Morphological and functional outcomes of operatively treated Achilles tendon ruptures. *The Physician and Sportsmedicine*, *48*(3), 290–297. https://doi.org/10.1080/00913847.2019.1685364

Nilsson-Helander, K., Grävare Silbernagel, K., Thomee, R., Faxen, E., Olsson, N., Eriksson, B. I., & Karlsson, J. (2010). Acute Achilles tendon rupture: A randomized, controlled study comparing surgical and nonsurgical treatments using validated outcome measures. *The American Journal of Sports Medicine*, *38*(11), 2186–2193.

Nilsson-Helander, K., Thomeé, R., Grävare-Silbernagel, K., Thomeé, P., Faxén, E., Eriksson, B. I., & Karlsson, J. (2007). The Achilles tendon total rupture

score (ATRS) development and validation. *The American Journal of Sports Medicine*, *35*(3), Article 3.
O'Brien, M. (2005). The Anatomy of the Achilles Tendon. *Foot and Ankle Clinics*, *10*(2), 225–238. https://doi.org/10.1016/j.fcl.2005.01.011
Olsson, N., Nilsson-Helander, K., Karlsson, J., Eriksson, B. I., Thomée, R., Faxén, E., & Silbernagel, K. G. (2011). Major functional deficits persist 2 years after acute Achilles tendon rupture. *Knee Surgery, Sports Traumatology, Arthroscopy*, *19*, 1385–1393.
Olsson, N., Silbernagel, K. G., Eriksson, B. I., Sansone, M., Brorsson, A., Nilsson-Helander, K., & Karlsson, J. (2013). Stable surgical repair with accelerated rehabilitation versus nonsurgical treatment for acute Achilles tendon ruptures: A randomized controlled study. *The American Journal of Sports Medicine*, *41*(12), 2867–2876.
Ömeroğlu, S., Peker, T., Türközkan, N., & Ömeroğlu, H. (2009). High-dose vitamin C supplementation accelerates the Achilles tendon healing in healthy rats. *Archives of Orthopaedic and Trauma Surgery*, *129*(2), 281–286. https://doi.org/10.1007/s00402-008-0603-0
Orselli, M. I. V., Franz, J. R., & Thelen, D. G. (2017). The effects of Achilles tendon compliance on triceps surae mechanics and energetics in walking. *Journal of Biomechanics*, *60*, 227–231. https://doi.org/10.1016/j.jbiomech.2017.06.022
Pajala, A., Kangas, J., Siira, P., Ohtonen, P., & Leppilahti, J. (2009). Augmented Compared with Nonaugmented Surgical Repair of a Fresh Total Achilles Tendon Rupture: A Prospective Randomized Study. *JBJS*, *91*(5), 1092–1100. https://doi.org/10.2106/JBJS.G.01089
Palmes, D., Spiegel, H. U., Schneider, T. O., Langer, M., Stratmann, U., Budny, T., & Probst, A. (2002). Achilles tendon healing: Long-term biomechanical effects of postoperative mobilization and immobilization in a new mouse model. *Journal of Orthopaedic Research*, *20*(5), 939–946. https://doi.org/10.1016/S0736-0266(02)00032-3
Pardes, A. M., Freedman, B. R., Fryhofer, G. W., Salka, N. S., Bhatt, P. R., & Soslowsky, L. J. (2016). Males have Inferior Achilles Tendon Material Properties Compared to Females in a Rodent Model. *Annals of Biomedical Engineering*, *44*(10), 2901–2910. https://doi.org/10.1007/s10439-016-1635-1
Park, C., Sugand, K., Nathwani, D., Bhattacharya, R., & Sarraf, K. M. (2020). Impact of the COVID-19 pandemic on orthopedic trauma workload in a London level 1 trauma center: The "golden month" The COVid Emergency Related Trauma and orthopaedics (COVERT) Collaborative. *Acta Orthopaedica*, *91*(5), 556–561.
Pękala, P. A., Henry, B. M., Ochała, A., Kopacz, P., Tatoń, G., Młyniec, A., Walocha, J. A., & Tomaszewski, K. A. (2017). The twisted structure of the Achilles tendon unraveled: A detailed quantitative and qualitative anatomical investigation. *Scandinavian Journal of Medicine & Science in Sports*, *27*(12), 1705–1715. https://doi.org/10.1111/sms.12835
Peltonen, J., Cronin, N. J., Stenroth, L., Finni, T., & Avela, J. (2013). Viscoelastic properties of the Achilles tendon in vivo. *Springerplus*, *2*(1), 1–8.

Peng, W. C., Chao, Y. H., Fu, A. S. N., Fong, S. S. M., Rolf, C., Chiang, H., Chen, S., & Wang, H. K. (2019). Muscular Morphomechanical Characteristics After an Achilles Repair. *Foot and Ankle International*, *40*(5), 568–577. https://doi.org/10.1177/1071100718822537

Peng, W.-C., Chao, Y.-H., Fu, A. S. N., Fong, S. S. M., Rolf, C., Chiang, H., Chen, S., & Wang, H.-K. (2019). Muscular Morphomechanical Characteristics After an Achilles Repair. *Foot & Ankle International*, *40*(5), 568–577. https://doi.org/10.1177/1071100718822537

Péter, A., Hegyi, A., Stenroth, L., Finni, T., & Cronin, N. J. (2015). EMG and force production of the flexor hallucis longus muscle in isometric plantarflexion and the push-off phase of walking. *Journal of Biomechanics*, *48*(12), 3413–3419. https://doi.org/10.1016/j.jbiomech.2015.05.033

Praet, S. F. E., Purdam, C. R., Welvaert, M., Vlahovich, N., Lovell, G., Burke, L. M., Gaida, J. E., Manzanero, S., Hughes, D., & Waddington, G. (2019). Oral Supplementation of Specific Collagen Peptides Combined with Calf-Strengthening Exercises Enhances Function and Reduces Pain in Achilles Tendinopathy Patients. *Nutrients*, *11*(1), Article 1. https://doi.org/10.3390/nu11010076

Proske, U., & Morgan, D. L. (1987). Tendon stiffness: Methods of measurement and significance for the control of movement. A review. *Journal of Biomechanics*, *20*(1), 75–82. https://doi.org/10.1016/0021-9290(87)90269-7

Randhawa, A., Jackman, M. E., & Wakeling, J. M. (2013). Muscle gearing during isotonic and isokinetic movements in the ankle plantarflexors. *European Journal of Applied Physiology*, *113*(2), 437–447. https://doi.org/10.1007/s00421-012-2448-z

Rassier, D. E., & Herzog, W. (2004). Considerations on the history dependence of muscle contraction. *Journal of Applied Physiology*, *96*(2), 419–427. https://doi.org/10.1152/japplphysiol.00653.2003

Rassier, D. E., MacIntosh, B. R., & Herzog, W. (1999). Length dependence of active force production in skeletal muscle. *Journal of Applied Physiology*, *86*(5), 1445–1457.

Reda, Y., Farouk, A., Abdelmonem, I., & El Shazly, O. A. (2020). Surgical versus non-surgical treatment for acute Achilles' tendon rupture. A systematic review of literature and meta-analysis. *Foot and Ankle Surgery*, *26*(3), 280–288. https://doi.org/10.1016/j.fas.2019.03.010

Reeves, N. D. (2006). Adaptation of the tendon to mechanical usage. *Journal of Musculoskeletal Neuronal Interactions*, *6*(2), 174–180. Scopus.

Reeves, N. D., Narici, M. V., & Maganaris, C. N. (2006). Myotendinous plasticity to ageing and resistance exercise in humans. *Experimental Physiology*, *91*(3), 483–498. https://doi.org/10.1113/expphysiol.2005.032896

Reito, A., Logren, H.-L., Ahonen, K., Nurmi, H., & Paloneva, J. (2018). Risk factors for failed nonoperative treatment and rerupture in acute Achilles tendon rupture. *Foot & Ankle International*, *39*(6), 694–703.

Rendek, Z., Bon Beckman, L., Schepull, T., Dånmark, I., Aspenberg, P., Schilcher, J., & Eliasson, P. (2022). Early Tensile Loading in Nonsurgically Treated Achilles Tendon Ruptures Leads to a Larger Tendon Callus and a Lower

Elastic Modulus: A Randomized Controlled Trial. *The American Journal of Sports Medicine*, 03635465221117780. https://doi.org/10.1177/03635465221117780

Riuttanen, A., Ponkilainen, V., Kuitunen, I., Reito, A., Sirola, J., & Mattila, V. M. (2021). Severely injured patients do not disappear in a pandemic: Incidence and characteristics of severe injuries during COVID-19 lockdown in Finland. *Acta Orthopaedica*, *92*(3), 249–253. https://doi.org/10.1080/17453674.2021.1881241

Roberts, T. J., & Azizi, E. (2010). The series-elastic shock absorber: Tendons attenuate muscle power during eccentric actions. *Journal of Applied Physiology*, *109*(2), 396–404. https://doi.org/10.1152/japplphysiol.01272.2009

Roberts, T. J., & Azizi, E. (2011). Flexible mechanisms: The diverse roles of biological springs in vertebrate movement. *Journal of Experimental Biology*, *214*(3), 353–361.

Roberts, T. J., Marsh, R. L., Weyand, P. G., & Taylor, C. R. (1997). Muscular Force in Running Turkeys: The Economy of Minimizing Work. *Science*, *275*(5303), 1113–1115. https://doi.org/10.1126/science.275.5303.1113

Rosso, C., Vavken, P., Polzer, C., Buckland, D. M., Studler, U., Weisskopf, L., Lottenbach, M., Müller, A. M., & Valderrabano, V. (2013). Long-term outcomes of muscle volume and Achilles tendon length after Achilles tendon ruptures. *Knee Surgery, Sports Traumatology, Arthroscopy*, *21*(6), 1369–1377.

Sandberg, O. H., Dånmark, I., Eliasson, P., & Aspenberg, P. (2015). Influence of a lower leg brace on traction force in healthy and ruptured Achilles tendons. *Muscles, Ligaments and Tendons Journal*, *5*(2), 63.

Sargon, M. F., Ozlu, K., & Oken, F. (2005). Age-related changes in human tendo calcaneus collagen fibrils. *Saudi Medical Journal*, *26*(3), 425–428.

Sawicki, G. S., Robertson, B. D., Azizi, E., & Roberts, T. J. (2015a). Timing matters: Tuning the mechanics of a muscle-tendon unit by adjusting stimulation phase during cyclic contractions. *The Journal of Experimental Biology*, *218*(Pt 19), 3150–3159. https://doi.org/10.1242/jeb.121673

Sawicki, G. S., Sheppard, P., & Roberts, T. J. (2015b). Power amplification in an isolated muscle–tendon unit is load dependent. *Journal of Experimental Biology*, *218*(22), 3700–3709.

Saxena, A., Giai Via, A., Grävare Silbernagel, K., Walther, M., Anderson, R., Gerdesmeyer, L., & Maffulli, N. (2022). Current Consensus for Rehabilitation Protocols of the Surgically Repaired Acute Mid-Substance Achilles Rupture: A Systematic Review and Recommendations From the "GAIT" Study Group. *The Journal of Foot and Ankle Surgery*, *61*(4), 855–861. https://doi.org/10.1053/j.jfas.2021.12.008

Schepull, T., & Aspenberg, P. (2013a). Early Controlled Tension Improves the Material Properties of Healing Human Achilles Tendons After Ruptures: A Randomized Trial. *The American Journal of Sports Medicine*, *41*(11), 2550–2557. https://doi.org/10.1177/0363546513501785

Schepull, T., & Aspenberg, P. (2013b). Early controlled tension improves the material properties of healing human achilles tendons after ruptures: A randomized trial. *The American Journal of Sports Medicine*, *41*(11), Article 11.

Schober, P., Boer, C., & Schwarte, L. A. (2018). Correlation Coefficients: Appropriate Use and Interpretation. *Anesthesia & Analgesia*, *126*(5), 1763–1768. https://doi.org/10.1213/ANE.0000000000002864

Schunck, M., & Oesser, S. (2013). Specific collagen peptides benefit the biosynthesis of matrix molecules of tendons and ligaments. *Journal of the International Society of Sports Nutrition*, *10*(sup1), P23. https://doi.org/10.1186/1550-2783-10-S1-P23

Segal, R. L., Wolf, S. L., DeCamp, M. J., Chopp, M. T., & English, A. W. (1991). Anatomical Partitioning of Three Multiarticular Human Muscles. *Cells Tissues Organs*, *142*(3), 261–266. https://doi.org/10.1159/000147199

Shim, V. B., Fernandez, J. W., Gamage, P. B., Regnery, C., Smith, D. W., Gardiner, B. S., Lloyd, D. G., & Besier, T. F. (2014). Subject-specific finite element analysis to characterize the influence of geometry and material properties in Achilles tendon rupture. *Journal of Biomechanics*, *47*(15), 3598–3604. https://doi.org/10.1016/j.jbiomech.2014.10.001

Shin, D., Finni, T., Ahn, S., Hodgson, J. A., Lee, H.-D., Edgerton, V. R., & Sinha, S. (2008). Effect of chronic unloading and rehabilitation on human Achilles tendon properties: A velocity-encoded phase-contrast MRI study. *Journal of Applied Physiology (Bethesda, Md.: 1985)*, *105*(4), 1179–1186. https://doi.org/10.1152/japplphysiol.90699.2008

Silbernagel, K. G., Nilsson-Helander, K., Thomeé, R., Eriksson, B. I., & Karlsson, J. (2010). A new measurement of heel-rise endurance with the ability to detect functional deficits in patients with Achilles tendon rupture. *Knee Surgery, Sports Traumatology, Arthroscopy*, *18*, 258–264.

Silbernagel, K. G., Steele, R., & Manal, K. (2012a). Deficits in Heel-Rise Height and Achilles Tendon Elongation Occur in Patients Recovering From an Achilles Tendon Rupture. *The American Journal of Sports Medicine*, *40*(7), 1564–1571. https://doi.org/10.1177/0363546512447926

Silbernagel, K. G., Steele, R., & Manal, K. (2012b). Deficits in heel-rise height and achilles tendon elongation occur in patients recovering from an Achilles tendon rupture. *The American Journal of Sports Medicine*, *40*(7), 1564–1571. https://doi.org/10.1177/0363546512447926

Slane, L. C., & Thelen, D. G. (2014a). Non-uniform displacements within the Achilles tendon observed during passive and eccentric loading. *Journal of Biomechanics*, *47*(12), Article 12.

Slane, L. C., & Thelen, D. G. (2014b). Non-uniform displacements within the Achilles tendon observed during passive and eccentric loading. *Journal of Biomechanics*, *47*(12), 2831–2835.

Slane, L. C., & Thelen, D. G. (2014c). The use of 2D ultrasound elastography for measuring tendon motion and strain. *Journal of Biomechanics*, *47*(3), Article 3.

Slane, L. C., & Thelen, D. G. (2015). Achilles tendon displacement patterns during passive stretch and eccentric loading are altered in middle-aged adults. *Medical Engineering & Physics*, *37*(7), Article 7.

Stäudle, B., Seynnes, O., Laps, G., Brüggemann, G.-P., & Albracht, K. (2022). Altered Gastrocnemius Contractile Behavior in Former Achilles Tendon Rupture Patients During Walking. *Frontiers in Physiology*, *13*. https://www.frontiersin.org/articles/10.3389/fphys.2022.792576

Stäudle, B., Seynnes, O., Laps, G., Göll, F., Brüggemann, G.-P., & Albracht, K. (2020). Recovery from Achilles Tendon Repair: A Combination of Postsurgery Outcomes and Insufficient Remodeling of Muscle and Tendon. *Medicine & Science in Sports & Exercise*, *Publish Ahead of Print*. https://doi.org/10.1249/MSS.0000000000002592

Stegeman, D., & Hermens, H. (2007). Standards for surface electromyography: The European project Surface EMG for non-invasive assessment of muscles (SENIAM). *Enschede: Roessingh Research and Development*, *10*, 8–12.

Stenroth, L., Thelen, D., & Franz, J. (2019). Biplanar ultrasound investigation of in vivo Achilles tendon displacement non-uniformity. *Translational Sports Medicine*, *2*(2), 73–81.

Suchak, A. A., Spooner, C., Reid, D. C., & Jomha, N. M. (2006). Postoperative rehabilitation protocols for Achilles tendon ruptures: A meta-analysis. *Clinical Orthopaedics and Related Research®*, *445*, 216–221.

Surgeons, A. A. of O. (2009). The Diagnosis and Treatment of Acute Achilles Tendon Rupture: Guideline and Evidence Report. *Rosemont (IL): American Academy of Orthopaedic Surgeons*.

Suydam, S. M., Buchanan, T. S., Manal, K., & Silbernagel, K. G. (2015). Compensatory muscle activation caused by tendon lengthening post-Achilles tendon rupture. *Knee Surgery, Sports Traumatology, Arthroscopy*, *23*(3), 868–874. https://doi.org/10.1007/s00167-013-2512-1

Svensson, R. B., Couppé, C., Agergaard, A.-S., Ohrhammar Josefsen, C., Jensen, M. H., Barfod, K. W., Nybing, J. D., Hansen, P., Krogsgaard, M., & Magnusson, S. P. (2019). Persistent functional loss following ruptured Achilles tendon is associated with reduced gastrocnemius muscle fascicle length, elongated gastrocnemius and soleus tendon, and reduced muscle cross-sectional area. *Translational Sports Medicine*, *2*(6), 316–324. https://doi.org/10.1002/tsm2.103

Svensson, R. B., Hansen, P., Hassenkam, T., Haraldsson, B. T., Aagaard, P., Kovanen, V., Krogsgaard, M., Kjaer, M., & Magnusson, S. P. (2012). Mechanical properties of human patellar tendon at the hierarchical levels of tendon and fibril. *Journal of Applied Physiology*, *112*(3), 419–426. https://doi.org/10.1152/japplphysiol.01172.2011

Svensson, R. B., Slane, L. C., Magnusson, S. P., & Bogaerts, S. (2021). Ultrasound-based speckle-tracking in tendons: A critical analysis for the technician and the clinician. *Journal of Applied Physiology*, *130*(2), 445–456. https://doi.org/10.1152/japplphysiol.00654.2020

Szaro, P., Witkowski, G., Śmigielski, R., Krajewski, P., & Ciszek, B. (2009). Fascicles of the adult human Achilles tendon–an anatomical study. *Annals of Anatomy-Anatomischer Anzeiger*, *191*(6), Article 6.

Thelen, D. G., Chumanov, E. S., Best, T. M., Swanson, S. C., & Heiderscheit, B. C. (2005). Simulation of Biceps Femoris Musculotendon Mechanics during

the Swing Phase of Sprinting. *Medicine & Science in Sports & Exercise*, *37*(11), 1931–1938. https://doi.org/10.1249/01.mss.0000176674.42929.de
Thorpe, C. T., Birch, H. L., Clegg, P. D., & Screen, H. R. C. (2013). The role of the non-collagenous matrix in tendon function. *International Journal of Experimental Pathology*, *94*(4), 248–259. https://doi.org/10.1111/iep.12027
Thorpe, C. T., & Screen, H. R. C. (2016). Tendon Structure and Composition. In P. W. Ackermann & D. A. Hart (Eds.), *Metabolic Influences on Risk for Tendon Disorders* (pp. 3–10). Springer International Publishing. https://doi.org/10.1007/978-3-319-33943-6_1
Thorpe, C. T., Udeze, C. P., Birch, H. L., Clegg, P. D., & Screen, H. R. (2013). Capacity for sliding between tendon fascicles decreases with ageing in injury prone equine tendons: A possible mechanism for age-related tendinopathy. *Eur Cell Mater*, *25*(4).
Tian, M., Herbert, R. D., Hoang, P., Gandevia, S. C., & Bilston, L. E. (2012). Myofascial force transmission between the human soleus and gastrocnemius muscles during passive knee motion. *Journal of Applied Physiology*, *113*(4), 517–523. https://doi.org/10.1152/japplphysiol.00111.2012
Trofa, D. P., Miller, J. C., Jang, E. S., Woode, D. R., Greisberg, J. K., & Vosseller, J. T. (2017). Professional Athletes' Return to Play and Performance After Operative Repair of an Achilles Tendon Rupture. *The American Journal of Sports Medicine*, *45*(12), 2864–2871. https://doi.org/10.1177/0363546517713001
Tuite, D. J., Renström, P., & O'brien, M. (1997). The aging tendon. *Scandinavian Journal of Medicine & Science in Sports*, *7*(2), 72–77.
Twaddle, B. C., & Poon, P. (2007). Early motion for Achilles tendon ruptures: Is surgery important? A randomized, prospective study. *The American Journal of Sports Medicine*, *35*(12), 2033–2038.
van der Eng, D. M., Schepers, T., Goslings, J. C., & Schep, N. W. L. (2013). Rerupture rate after early weightbearing in operative versus conservative treatment of Achilles tendon ruptures: A meta-analysis. *The Journal of Foot and Ankle Surgery: Official Publication of the American College of Foot and Ankle Surgeons*, *52*(5), 622–628. https://doi.org/10.1053/j.jfas.2013.03.027
Wallace, R. G. H., Heyes, G. J., & Michael, A. L. R. (2011). The non-operative functional management of patients with a rupture of the tendo Achillis leads to low rates of re-rupture. *The Journal of Bone and Joint Surgery. British Volume*, *93*(10), 1362–1366.
Wang, H.-K., Chiang, H., Chen, W.-S., Shih, T. T., Huang, Y.-C., & Jiang, C.-C. (2013). Early neuromechanical outcomes of the triceps surae muscle-tendon after an Achilles' tendon repair. *Archives of Physical Medicine and Rehabilitation*, *94*(8), 1590–1598.
Wang, J. H.-C. (2006). Mechanobiology of tendon. *Journal of Biomechanics*, *39*(9), 1563–1582. https://doi.org/10.1016/j.jbiomech.2005.05.011
Ward, S. R., Eng, C. M., Smallwood, L. H., & Lieber, R. L. (2009). Are Current Measurements of Lower Extremity Muscle Architecture Accurate? *Clinical*

Orthopaedics and Related Research, *467*(4), 1074–1082. https://doi.org/10.1007/s11999-008-0594-8

Waterston, S. W., Maffulli, N., & Ewen, S. W. (1997). Subcutaneous rupture of the Achilles tendon: Basic science and some aspects of clinical practice. *British Journal of Sports Medicine*, *31*(4), 285–298. https://www.ncbi.nlm.nih.gov/pmc/articles/PMC1332561/

Wenning, M., Mauch, M., Heitner, A., Lienhard, J., Ritzmann, R., & Paul, J. (2021). Neuromechanical activation of triceps surae muscle remains altered at 3.5 years following open surgical repair of acute Achilles tendon rupture. *Knee Surgery, Sports Traumatology, Arthroscopy*, *29*(8), 2517–2527. https://doi.org/10.1007/s00167-021-06512-z

Wilkins, R., & Bisson, L. J. (2012). Operative versus nonoperative management of acute Achilles tendon ruptures: A quantitative systematic review of randomized controlled trials. *The American Journal of Sports Medicine*, *40*(9), 2154–2160.

Williams, P. E., & Goldspink, G. (1973). The effect of immobilization on the longitudinal growth of striated muscle fibres. *Journal of Anatomy*, *116*(Pt 1), 45–55. https://www.ncbi.nlm.nih.gov/pmc/articles/PMC1271549/

Wilmink, J., Wilson, A. M., & Goodship, A. E. (1992). Functional significance of the morphology and micromechanics of collagen fibres in relation to partial rupture of the superficial digital flexor tendon in racehorses. *Research in Veterinary Science*, *53*(3), 354–359.

Wilson, A., & Lichtwark, G. (2011). The anatomical arrangement of muscle and tendon enhances limb versatility and locomotor performance. *Philosophical Transactions of the Royal Society B: Biological Sciences*, *366*(1570), 1540–1553. https://doi.org/10.1098/rstb.2010.0361

Wren, T. A. L., Lindsey, D. P., Beaupré, G. S., & Carter, D. R. (2003). Effects of Creep and Cyclic Loading on the Mechanical Properties and Failure of Human Achilles Tendons. *Annals of Biomedical Engineering*, *31*(6), 710–717. https://doi.org/10.1114/1.1569267

Yin, N.-H., Fromme, P., McCarthy, I., & Birch, H. L. (2021). Individual variation in Achilles tendon morphology and geometry changes susceptibility to injury. *ELife*, *10*, e63204. https://doi.org/10.7554/eLife.63204

Zajac, F. E. (1989). Muscle and tendon: Properties, models, scaling, and application to biomechanics and motor control. *Critical Reviews in Biomedical Engineering*, *17*(4), 359–411.

Zatsiorsky, V. M., & Prilutsky, B. I. (2012). *Biomechanics of skeletal muscles*. Human Kinetics.

Zellers, J. A., Cortes, D. H., Corrigan, P., Pontiggia, L., & Silbernagel, K. G. (2018). Side-to-side differences in Achilles tendon geometry and mechanical properties following achilles tendon rupture. *Muscles, Ligaments and Tendons Journal*, *7*(3), 541–547. https://doi.org/10.11138/mltj/2017.7.3.541

Zellers, J. A., Pohlig, R. T., Cortes, D. H., & Grävare Silbernagel, K. (2020). Achilles tendon cross-sectional area at 12 weeks post-rupture relates to 1-year heel-rise height. *Knee Surgery, Sports Traumatology, Arthroscopy*, *28*(1), 245–252. https://doi.org/10.1007/s00167-019-05608-x

ORIGINAL PUBLICATIONS

I

NON-UNIFORM DISPLACEMENT WITHIN RUPTURED ACHILLES TENDON DURING ISO-METRIC CONTRACTION

by

Ra'ad M. Khair, Lauri Stenroth, Annamária Péter, Neil J. Cronin, Aleksi Reito, Juha Paloneva & Taija Finni 2021

Scandinavian Journal of Medicine and Sports 31(5): 1069–1077.

https://doi.org/10.1111/sms.13925

Received: 14 June 2020 | Revised: 8 January 2021 | Accepted: 12 January 2021

DOI: 10.1111/sms.13925

ORIGINAL ARTICLE

WILEY

Non-uniform displacement within ruptured Achilles tendon during isometric contraction

Ra'ad M. Khair[1] | **Lauri Stenroth**[2] | **Annamária Péter**[1] | **Neil J. Cronin**[1,3] | **Aleksi Reito**[4] | **Juha Paloneva**[4] | **Taija Finni**[1]

[1]Faculty of Sport and Health Sciences, Neuromuscular Research Center, University of Jyväskylä, Jyväskylä, Finland

[2]Department of Applied Physics, University of Eastern Finland, Kuopio, Finland

[3]Department for Health, University of Bath, Bath, UK

[4]Central Finland Health Care District, Jyväskylä, Finland

Correspondence
Ra'ad M. Khair, Neuromuscular Research Center, Faculty of Sport and Health Sciences, University of Jyväskylä, PO Box 35, Jyväskylä FI-40014, Finland.
Email: raad.m.khair@jyu.fi

Funding information
Academy of Finland, Grant/Award Number: #323168

The purpose of this study was investigate tendon displacement patterns in non-surgically treated patients 14 months after acute Achilles tendon rupture (ATR) and to classify patients into groups based on their Achilles tendon (AT) displacement patterns. Twenty patients were tested. Sagittal images of AT were acquired using B-mode ultrasonography during ramp contractions at a torque level corresponding to 30% of the maximal isometric plantarflexion torque of the uninjured limb. A speckle tracking algorithm was used to track proximal-distal movement of the tendon tissue at 6 antero-posterior locations. Two-way repeated measures ANOVA for peak tendon displacement was performed. K-means clustering was used to classify patients according to AT displacement patterns. The difference in peak relative displacement across locations was larger in the uninjured (1.29 ± 0.87 mm) than the injured limb (0.69 ± 0.68 mm), with a mean difference (95% CI) of 0.60 mm (0.14-1.05 mm, $P < .001$) between limbs. For the uninjured limb, cluster analysis formed 3 groups, while 2 groups were formed for the injured limb. The three distinct patterns of AT displacement during isometric plantarflexion in the uninjured limb may arise from subject-specific anatomical variations of AT sub-tendons, while the two patterns in the injured limb may reflect differential recovery after ATR with non-surgical treatment. Subject-specific tendon characteristics are a vital determinant of stress distribution across the tendon. Changes in stress distribution may lead to variation in the location and magnitude of peak displacement within the free AT. Quantifying internal tendon displacement patterns after ATR provides new insights into AT recovery.

KEYWORDS
Achilles tendon, clustering, non-surgical treatment, rupture, ultrasound speckle tracking

1 | INTRODUCTION

Achilles tendon rupture (ATR) is a disabling condition with a growing yearly incidence of 20-35 per 100 000 individuals.[1,2] Regardless of the treatment option, ATR leads to long-term deficits in anatomy, function and physical activity that persist several years post-ATR.[3] The factors leading to better ATR recovery are still poorly understood. Thus, although the area is frequently studied, the optimal treatment option is still debatable. Treatment is either surgical or non-surgical, and these modes involve different immobilization periods.[4-6] Early mobilization seems to lead to better functional outcomes, a higher quality of life and a shorter rehabilitation period.[7-10]

The Achilles tendon (AT) is a composite of the three subtendons arising from the triceps surae (TS) muscles: medial gastrocnemius, lateral gastrocnemius, and soleus. The tendon fibers twist so that at the point of insertion, lateral gastrocnemius fibers end up on the ventral side, medial gastrocnemius fibers become dorsal, and soleus fibers become medial. The twisting of the sub-tendons varies among individuals and can be classified into three types depending on the degree of torsion.[11]

The twisting of the subtendons is thought to cause heterogeneity of strain within the tendon. Relative displacement within Achilles tendon has been shown to occur between subtendons[12] and between adjacent tendon fascicles.[13] The fascicles originating from different TS muscles exert differential forces and strains on each sub-tendon[12,14] and are likely to cause non-uniformities between fascicles arising from different muscle heads.[12,14] In several studies, the anterior (deep) tendon has been reported to displace more than the posterior (superficial) tendon.[15-18] Furthermore, the different degrees of torsion among the population would lead to distinct non-uniform displacement patterns within the AT for each group.

The ability of the tendon fascicles and sub-tendons to slide relative to each other is considered a sign of healthy tendon,[16,19] and it is usually overlooked in the management of ATR. Recently, it has been suggested that during muscle contraction, non-uniform displacement within the AT is an indication of healthy AT function,[16] whereas surgically treated injured AT has been found to display more uniform within-tendon displacements 1 year post-ATR.[16,20] In studies to date, participant data have been presented as mean values, but due to individual anatomical variation,[11] it may be expected that AT displacement patterns are also individual-specific.

The aim of the present study was to investigate tendon displacement patterns in non-surgically treated patients 14-months after acute ATR, and to classify patients into groups based on their AT displacement patterns. After identifying groups, the aim was to explore whether individuals in the different groups showed differences in factors previously associated with good recovery from ATR, such as plantarflexion strength, displacement pattern, and preferred gait speed.[16,20,21] We hypothesized that ruptured AT would show a more uniform displacement pattern compared to the contralateral AT and expected different displacement behaviors in different cluster groups.

2 | METHODS

The study is part of a clinical cohort study "Non-operative treatment of Achilles tendon Rupture in Central Finland: a prospective cohort study – NoARC" (trial registration: NCT03704532). The Ethics Committee of the Central Finland Health Care District approved the study (2U/2018).

2.1 | Non-surgical treatment protocol

All participants were treated non-surgically in combination with early mobilization. Immediately after ATR, the ankle was cast in full equinus for two weeks. After two weeks, the foot was allowed to move into plantarflexion using a 20° equinus open sole cast. A custom-made functional walking orthosis with 1 cm thick heel wedge was delivered to the patients at week 4, and patients were encouraged to bear full weight. At 8 weeks, the orthosis was removed, and progressive physiotherapy began. The patients were instructed to use a heel wedge for 4 weeks after returning to daily activities.[22]

2.2 | Participants

Twenty patients (17 males, 3 females) within the Central Finland Health Care District agreed to participate (mean ± SD age: 43.7 ± 9.1 years, height: 1.75 ± 0.08 m, body mass: 81.91 ± 12.68 kg). Acute rupture occurring <14 days before was diagnosed using guidelines by the American Academy of Orthopedic Surgeons. Inclusion criteria were a minimum of 2 of the following 4 criteria: a positive Thompson test, decreased plantarflexion strength, presence of a palpable gap, and increased passive ankle dorsiflexion with gentle manipulation.[23] Other inclusion criteria included clear onset of symptoms, closed rupture, residence in the catchment area of the hospital district, minimum age of 18, ability to understand and speak Finnish, and normal walking ability (>100 m unassisted before rupture). The exclusion criterion included an avulsion fracture of the calcaneus or a re-rupture. Two participants with a re-occurring rupture were admitted for surgical treatment and excluded from the sample. Participants signed an informed consent explaining the details of the study, possible risks, and gave permission to use data for research purposes. Participants were tested 14.1 ± 1.7 months post-ATR.

2.3 | Protocol

Upon arrival to the laboratory, participants sat in a custom-made ankle dynamometer (University of Jyväskylä, Finland) with ankle at 90°, hip at 120° of flexion and the knee fully extended. A 3.6-cm linear ultrasound probe (UST-5411, Aloka alpha10, Japan) was attached over the distal AT (Figure 1). After performing a series of submaximal contractions as a warm-up, data collection started with the uninjured leg. Maximal voluntary isometric contractions (MVCs) were followed by unilateral contractions corresponding to the absolute torque level of 30% MVC of the uninjured limb. Participants were then asked to walk at their preferred speed across a 10-meter walkway, with the instruction "walk at the speed you normally walk when walking freely." Walking speed as an

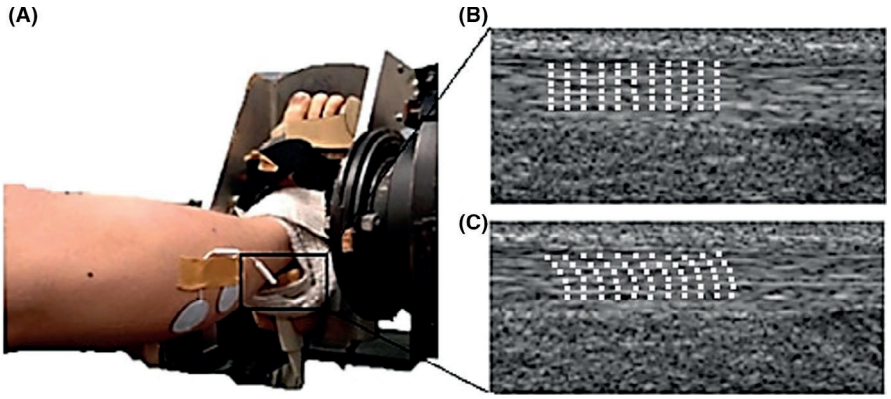

FIGURE 1 An overview of the torque measurement setup (A) and an example of ultrasound image analysis (B, C). The probe was fixed with an elastic bandage over the distal AT. B: The tendon at rest with the grid of 66 nodes generated across the AT (11 across the length and 6 across the width) overlaid on the image. C: The same grid of nodes during 30% MVC ramp contraction

average of 3 trials was determined using photocells placed at the beginning and end of the walkway.

2.4 | Data collection and analysis

For MVCs, the rotation axis of the ankle joint was carefully aligned with the rotation axis of the dynamometer (equipped with Precision TB5-C1, Raute, Nastola, Finland load cell). Torque was sampled with a 16-bit AD-board (Power 1401, CED Limited, Cambridge, England) at a sampling frequency of 1KHz. Following 3-5 familiarization trials, subjects performed 2-3 maximal 3-second plantarflexions with 1 minutes recovery between trials. Cine B-mode ultrasound images were then taken distally from the AT during an isometric ramp contraction up to 30% of the uninjured limb's MVC, at a sampling frequency of 50 Hz and operating frequency of 10 MHz.

Recently, ultrasonic speckle tracking has been validated to allow quantification of AT internal movement.[15,16] In this study, the approach of Slane and Thelen was followed.[16] The speckle tracking algorithm was implemented in MATLAB (R2018a, MathWorks Inc, Natick, MA, USA). The region of interest (ROI) was manually positioned over the distal part of the tendon. The size of the ROI was adjusted individually to ensure that only the tendon tissue was included. Inside the ROI, a grid of six locations across the thickness of the tendon and eleven across the length of the tendon was generated (Figure 1B). All tracking was visually monitored to ensure that the ROI remained within the tendon throughout the movement. Displacements of nodes along each of the six antero-posterior rows were averaged and peak displacements of the average data were extracted for analysis. The 6 locations across the tendon are referred to starting from superficial (location 1), to deep (location 6) respectively. The reliability of tracking was evaluated by analyzing the same video twice. This revealed 0.2% change in mean with a correlation of rp = 0.94, $P < .01$. The values and locations of maximal and minimal displacement across the tendon were extracted. Tendon peak relative displacement was calculated for both limbs (uninjured/injured) as the difference between minimal and maximal displacement in the tendon.

2.5 | Statistical analysis

All statistical analyses (except clustering) were performed using SPSS (IBM SPSS Statistics for Windows, Release 24.0, Chicago, Illinois). The level of significance was set at $P < .05$.

Two-way repeated measures ANOVA was performed for peak tendon displacement (6 locations) and limb condition (uninjured/injured). When the assumption of sphericity determined by Mauchly's test was violated, Greenhouse-Geisser adjustment was applied. Bonferroni-adjusted post hoc test was used to compare displacement values between locations for each group separately.

Two-sided paired *t* tests were used to compare MVC torque values between limbs, and to compare maximal and minimal displacement values at the limb and cluster level. Non-parametric Wilcoxon signed rank test and two-sided paired t tests were used to compare peak relative displacement between limbs due to the skewness of the data. Multiple linear regression analysis was used to examine the relationship between MVC and peak relative displacement while controlling for patient age. Preferred walking speed, submaximal contraction (MVC30%), tendon peak relative displacement, locations of maximum and minimum displacement between uninjured clustered groups, and MVC torque were compared between cluster groups for each limb separately using Independent Samples t test for the injured limb and one-way ANOVA for the uninjured limb. Descriptive data are presented as mean ± standard deviation.

K-means clustering (R clustering package/JASP version 0.11.1, Amsterdam, Netherlands) was used to classify patients according to AT displacement patterns. Cluster numbers (ie, the value of K) were chosen using the elbow method with respect to the Bayesian information criterion (BIC)

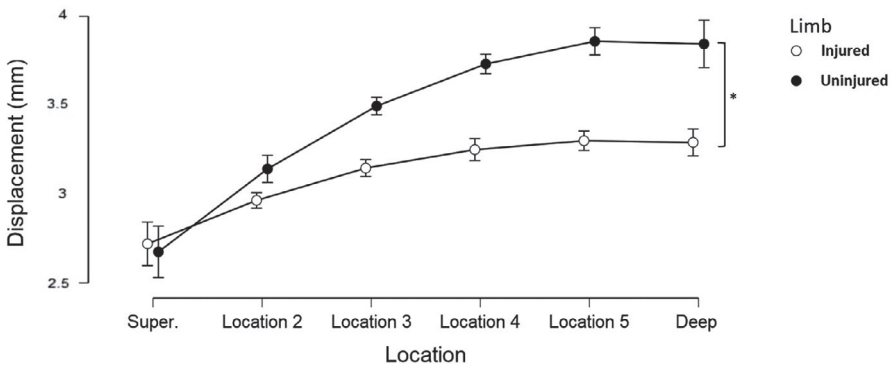

FIGURE 2 Peak displacement (mm) in each of the six locations across the tendon width while performing 30% MVC, starting with superficial and moving deeper in order. *Significant difference between groups ($P = .032$)

TABLE 1 Bonferroni-adjusted post hoc comparisons showing corrected mean differences (95% CI) in peak displacement (mm) between 6 locations across the Achilles tendon

Uninjured Limb	Super.	Location 2	Location 3	Location 4	Location 5	Deep
Superficial	—	0.44 (0.18-0.69)*	0.77 (0.33-1.20)*	0.99 (0.43-1.54)*	1.11 (0.48-1.73)*	1.09 (0.09-1.82)*
Location 2	—	—	0.33 (0.14-0.52)*	0.55 (0.23-0.87)*	0.67 (0.24-1.10)*	0.66 (0.06-1.25)*
Location 3	—	—	—	0.22 (0.07-0.37)*	0.34 (0.05-0.63)*	0.33 (0.17-0.82)
Location 4	—	—	—	—	0.12 (0.05-0.29)	0.11 (0.28-0.49)
Location 5	—	—	—	—	—	0.01 (0.21-0.24)
Injured Limb						
Superficial	—	0.23 (0.05-0.51)	0.40 (0.05-0.84)	0.50 (0.02-1.01)	0.54 (0.04-1.04)*	0.53 (0.09-0.98)*
Location 2	—	—	0.17 (0.03-0.34)	0.27 (0.01-0.52)*	0.31 (0.04-0.59)*	0.30 (0.02-0.63)
Location 3	—	—	—	0.10 (0.01-0.19)*	0.14 (0.02-0.31)	0.13 (0.19-0.46)
Location 4	—	—	—	—	0.05 (0.06-0.16)	0.04 (0.26-0.34)
Location 5	—	—	—	—	—	0.08 (0.20-0.19)

* Significant difference between locations ($P < .05$).

value. Clustering was repeated 5 times for each group and confirmed that each data point was consistently assigned to the same cluster group. Furthermore, to explore the validity of clustering, two-way repeated measures ANOVA for peak tendon displacement (6 locations) and clustered groups as a factor was performed for the injured and uninjured limbs separately.

3 | RESULTS

Torque at 100% MVC was significantly lower in the injured limb (mean ± SD: 136.25 ± 42.49 Nm) compared to the uninjured limb (178.47 ± 39.92 Nm), with a mean difference (95% CI) of 42.2 Nm (26.09-58.37 Nm, $P < .001$). During submaximal contractions, the same torque level was reached: 53.19 ± 11.84 Nm for the uninjured limb and 53.22 ± 12.38 Nm for the injured limb, with a mean difference (95% CI) of 0.04 Nm (−2.26-2.33 Nm, $P = .97$). There were significant differences between maximum and minimum displacement for both limbs, with mean differences (95% CI) of 1.29 mm (0.88-1.7 mm, $P < .001$) and 0.69 mm (0.37-1.00 mm, $P < .001$) in the uninjured and injured limbs, respectively. Peak relative displacement was significantly larger in the uninjured (mean ± SD: 1.29 ± 0.87 mm) than the injured limb (0.69 ± 0.68 mm) according to the Wilcoxon signed rank test ($P < .011$, $z = 2.359$) and paired t test (mean difference (95% CI) of 0.60 mm, 0.14-1.05 mm, $P < .001$). Linear regression analysis was used to test whether peak relative displacement significantly predicted MVC with age as a confounding factor. The model explained 4.6% of the variance ($R2 = 0.046$, $F(2,37) = 0.895$, $P = .417$), and peak relative displacement ($\beta = 0.189$, $P = .251$) did not predict MVC, with age ($\beta = 0.077$, $P = .638$) as a confounding factor. There was a significant interaction of limb*peak tendon displacement ($F(1.63\text{-}61.92) = 3.958$, $P = .032$) (Figure 2). Bonferroni post hoc analysis showed a significant difference between each of the three most superficial locations, but no differences were found between the four deepest locations in the uninjured limb. However, for the injured limb, there were no significant differences between the majority of locations (Table 1), indicating a more uniform displacement pattern across the injured tendon.

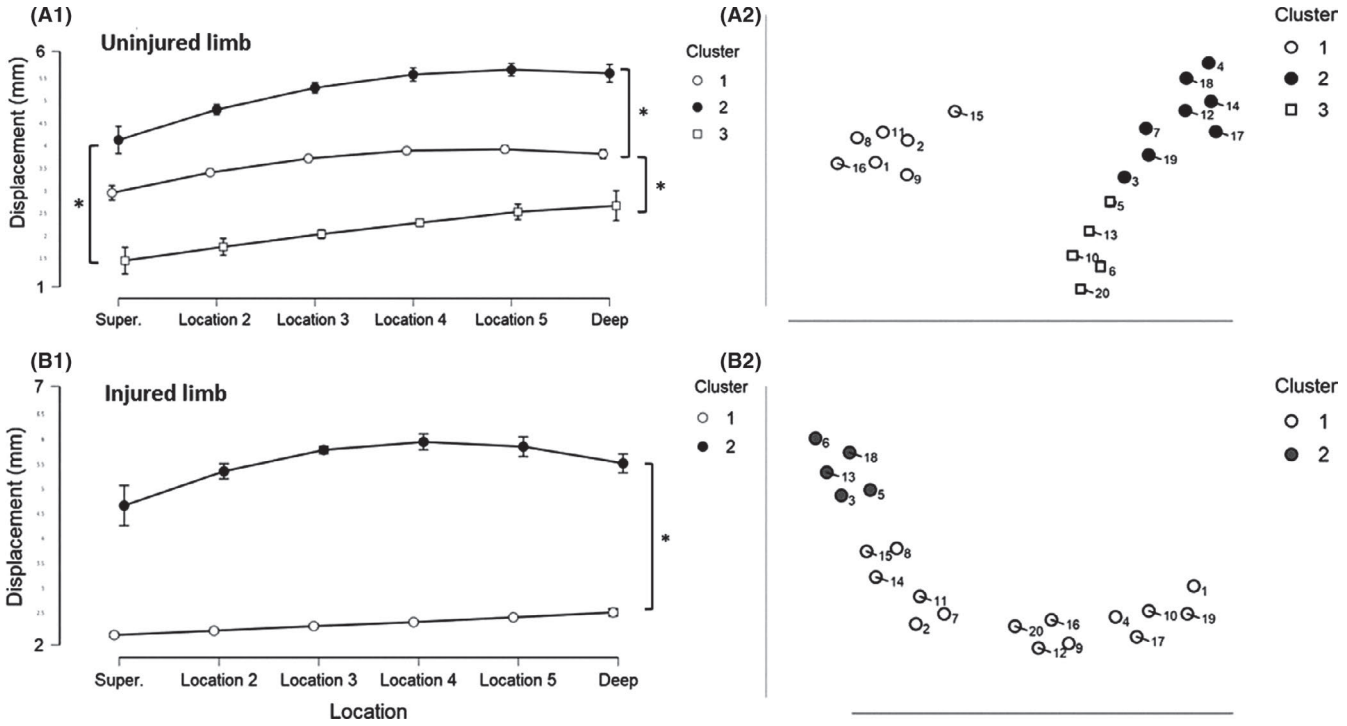

FIGURE 3 Cluster plots based on peak tendon displacements. A-1: mean displacement patterns for the three clusters formed for the healthy limb. A-2: 2D representation of the clusters, whereby each circle represents one patient's data; similar displacement patterns appear close to each other, and dissimilar displacement patterns are further apart in the space. B-1: the displacement patterns for the two clusters found for the injured limb. B-2: Each data point separated into clusters. *Significant difference between groups ($P < .01$)

TABLE 2 Characteristics of the cluster groups (mean ± SD)

Uninjured	Torque at 100% MVC (Nm)	Preferred walking speed (m/s)	Peak relative displacement (mm)	Peak relative displacement (mm) of the other leg
Group 1 (N: 7)	163.9 ± 49.90	1.1 ± 0.25	1.4 ± 1.19	0.5 ± 0.48
Group 2 (N: 8)	185.0 ± 29.12	1.2 ± 0.22	1.0 ± 0.55	0.6 ± 0.64
Group 3 (N: 5)	188.5 ± 44.06	1.1 ± 0.23	1.6 ± 0.78	1.0 ± 0.96
Injured				
Group 1 (N:15)	134.2 ± 39.52	1.2 ± 0.22	0.5 ± 0.34	1.2 ± 0.91
Group 2 (N: 5)	142.4 ± 55.22	1.0 ± 0.30	1.3 ± 1.70	1.4 ± 0.83

3.1 | Clustered groups

For the uninjured limb, the cluster analysis separated subjects into three groups (n = 7, within-cluster sum of squares: 8.40; n = 8, 5.03; n = 5, 5.14; $P < .001$), while only two groups were formed for the injured limb (n = 5, 11.58; n = 15, 25.44; $P < .001$) (Figure 3). There was a significant difference in peak relative displacement ($P = .040$) between injured limb clusters, but not between uninjured limb clusters. There were no significant differences in MVC torque, MVC30% torque, or preferred walking speed in any of the clustered groups for either limb (Table 2). Two-sided paired t test showed significant differences between maximum and minimum displacement for all the uninjured clusters, with mean differences (95% CI) of 1.3 mm (0.29-2.5 mm, $P = .021$) in group 1, 1.1 mm (0.61-1.6 mm, $P < .001$) in group 2, and 1.5 mm (0.18-2.8 mm, $P = .036$) in group 3. For the injured limb clusters, there was a significant difference in group 1, with a mean difference (95% CI) of 0.48 mm (0.29-0.67 mm, $P < .001$), but no significant difference in group 2, mean difference (95% CI) 1.3 mm (0.02-2.6 mm).

3.2 | Maximum and minimum displacement locations

There was no significant difference in maximum mean differences (0.35, 95% CI: 0.38-1.08, $P = .330$) or minimum displacement location (0.10, 0.99-1.19, $P = .850$) between limbs (Figure 4). Uninjured group clusters showed no

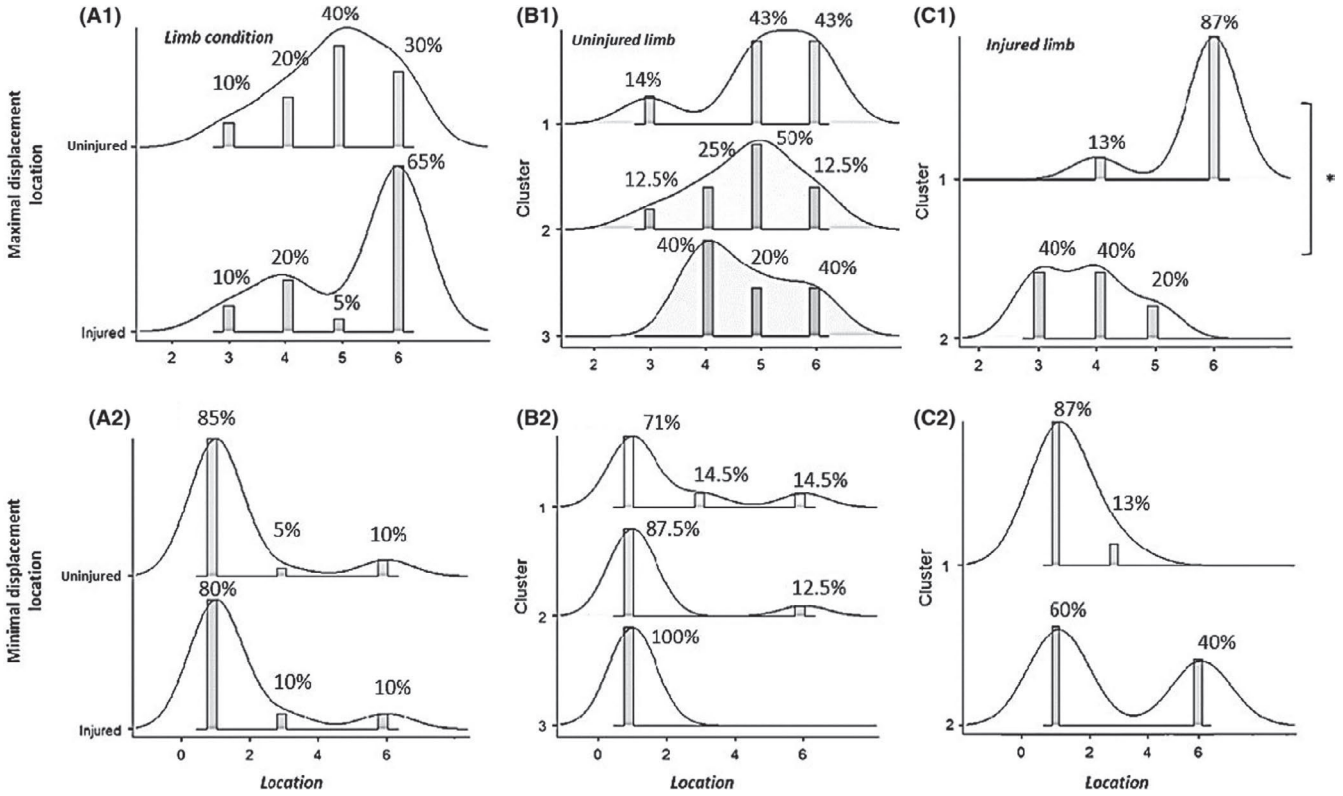

FIGURE 4 Top row: Frequency of maximal displacement location across the tendon for both limbs (A-1), for healthy limb clustered groups (B-1), and for injured limb clustered groups (C-1). Bottom row: Frequency of minimal displacement location across the tendon for both limbs (A-2), for healthy limb clustered groups (B-2), and for injured limb clustered groups (C-2). * Significant difference in maximum displacement location between injured limb clusters ($P < .001$)

statistical differences in maximum or minimum displacement location. In the injured limb clusters, there was a significant difference in maximum displacement location mean difference (1.93, 95% CI: 1.13-2.73, $P < .001$), but no difference in minimum displacement location (1.73, 95% CI: −5.11-1.64, $P = .231$).

4 | DISCUSSION

To our knowledge, this is the first study to investigate within-tendon deformation patterns in non-surgically treated ATR patients, as previous investigations,[20] only included surgically treated patients. We examined patients 14-month post-ATR. As hypothesized, we found evidence of impaired sliding between tendon fascicles originating from different parts of the TS in the injured limb, whereby displacement was more uniform across the width of the injured tendon compared to the uninjured tendon. The impaired tendon internal movement in our non-surgically treated sample has also been observed in surgically treated patients, although it has been suggested that the surgical procedure itself can degrade the gliding properties of the tendon.[20]

At the same absolute plantarflexion torque level, peak relative displacement was ∼32% smaller in the injured limb compared to the uninjured limb. One factor explaining this phenomenon may be a change in the synergistic behavior of plantar flexors in ATR patients. Medial gastrocnemius myotendinous displacement has been reported to decrease post-ATR in multiple studies,[24,25] and deeper flexors such as flexor hallucis longus (FHL) may thus make a bigger contribution to relative plantarflexion force.[26] For example, FHL cross-sectional area has been found to be 5% greater in the injured limb, indicating compensatory hypertrophy.[21] Changes in the motor strategy used to produce plantarflexion torque in the early recovery phase might decrease tensile forces transmitted through the AT, due to a smaller force contribution by the TS. The present results suggest that this compensatory mechanism may be functional for long periods. Although individual motor coordinative strategies vary, the role of FHL in the restoration of function post-ATR should not be neglected.[21]

The impaired displacement observed in the injured limb may have an adverse effect on TS force production and transmission.[20] Our sample showed ~24% plantarflexion strength deficit in the injured limb, highlighting the long-term effects of ATR, which might be a combination of changes in plantar flexor muscle structure,[27,28] and

impaired relative displacement between the different parts of the AT.

4.1 | Clustered groups

A novel finding of the present study was that by using unsupervised cluster analysis, we were able to classify AT displacement behavior into three clusters in the uninjured limb whereas only two were identified in the injured limb, which may arise from subject-specific anatomical variations in AT sub-tendons.[11] Subject-specific tendon characteristics are a vital determinant of stress distribution across the tendon,[29,30] which may lead to variation in the location and magnitude of peak displacement within the free AT. However, in spite of any individual differences, the phenomenon of non-uniform displacement between independent tendon fascicles across the AT was evident in all of the uninjured clusters, further supporting the idea that this is a sign of healthy tendon function.[16,19]

For the injured limb, patients within both clusters showed an impaired displacement pattern. The first group, which included the majority of patients, showed low peak displacement. However, there was a difference between maximum and minimum displacement, indicating some degree of non-uniformity. The second group had similar peak displacement between the injured and uninjured limbs, but there was a more uniform displacement pattern across the injured tendon. Thus, in general, the mechanical sliding of fascicles within the tendon was impaired in our non-surgically treated patients 14-months post-ATR. Interfascicular matrix adhesion might be one reason for the limited inter-fascicle sliding.[19]

Differential displacement in the injured tendon may arise from subject-specific anatomical differences of tendon and its twisting pattern. There was a significant difference in maximal displacement location, whereby group 2 showed a more superficial location compared to a deeper location in group 1 (Figure 4). These differences in behavior may reflect differences in underlying anatomy, although this cannot be confirmed. Alternatively, tendon healing may have caused alterations in normal twisting of the tendon fascicles and consequently affected the displacement pattern.

On average, maximal displacement was observed at location 5 for the uninjured limb and the deepest location for the injured limb. Thus, both limbs showed higher displacement in the deep region of the tendon, whereas minimal displacement occurred at the most superficial part in both limbs, despite the injury. However, patients in different clusters showed different patterns and locations of maximal displacement across the tendon. Such individual differences highlight the importance of personalized diagnostic and treatment approaches.

The present study suggests that non-surgical treatment leads to impairments regarding non-uniform displacement of the tendon. However, some patients in the second cluster group might have regained a normal tendon displacement 14 month post-rupture. Previously, non-uniformity in tendon displacement has been investigated in surgically treated patients. Similarly to the present study, the study of Fröberg et al showed more uniform displacement within the ruptured tendon during active dorsiflexion (0.3 vs 3.3 mm difference between deep and superficial).[20] Future studies are required to investigate whether the treatment or rehabilitation protocol would have an effect on the displacement pattern of the tendon post-rupture.

There are some limitations of this study. One limitation is that only one proximal-distal location of the tendon was investigated. The probe was placed on the most distal portion of the tendon, as tears might have occurred on a more proximal level. However, as established before, fascicles function independently,[13] thus any tear on an upper level would have an adverse effect on the gliding of the fascicles relative to each other. The area investigated is typically the investigated region[16-18,20] where biochemical composition may facilitate greater sliding between fascicles.[31] The small sample size was not enough to identify the factors affecting tendon displacement patterns and AT recovery, or to confirm whether different displacement patterns are associated with functional recovery.

5 | CONCLUSION

We found three distinct patterns of AT displacement during isometric plantarflexion in the uninjured limb and two in the injured limb. These patterns may arise from subject-specific anatomical variations in AT sub-tendons, which may be modified due to the injury. Subject-specific tendon characteristics are a vital determinant of stress distribution across the tendon, which may in turn lead to variations in the location and magnitude of peak displacement within the free AT. Quantifying internal tendon displacement patterns after ATR provides new insights for evaluation of the recovery of Achilles tendon.

6 | PERSPECTIVE

In studies of post-rupture tendon function, group mean values are typically reported, which may ignore patient-specific recovery patterns.[16,20] Here, we examined whether Achilles tendon internal displacement patterns could be classified in order to better understand good recovery. Our results clearly indicate the necessity to consider the variations in

AT sub-tendon anatomy among the population, and hence, the importance of introducing personalized diagnostic and treatment approaches. The results also show that some non-surgically treated patients can recover healthy tendon displacement patterns by 14 months post-rupture, but the majority of patients showed impaired tendon displacement compared to the uninjured limb. Future studies that aim to find optimal treatment approaches post-ATR should consider the possibility that the surgical trauma itself may affects tendon gliding properties and compare between different treatments protocols.[20]

ACKNOWLEDGEMENTS

This study was funded by Academy of Finland grant #323168, UNderstanding REStoration of Achilles Tendon function after rupture (UNRESAT).

CONFLICT OF INTEREST

The authors declare that they have no competing interests.

ORCID

Ra'ad M. Khair https://orcid.org/0000-0002-3226-8840
Lauri Stenroth https://orcid.org/0000-0002-7705-9188
Taija Finni https://orcid.org/0000-0002-7697-2813

REFERENCES

1. Ganestam A, Kallemose T, Troelsen A, Barfod KW. Increasing incidence of acute Achilles tendon rupture and a noticeable decline in surgical treatment from 1994 to 2013. A nationwide registry study of 33,160 patients. *Knee Surg Sports Traumatol Arthrosc*. 2016;24(12):3730-3737.
2. Lantto I, Heikkinen J, Flinkkilä T, Ohtonen P, Leppilahti J. Epidemiology of Achilles tendon ruptures: increasing incidence over a 33-year period. *Scand J Med Sci Sports*. 2015;25(1):e133-e138.
3. Möller M, Kälebo P, Tidebrant G, Movin T, Karlsson J. The ultrasonographic appearance of the ruptured Achilles tendon during healing: a longitudinal evaluation of surgical and nonsurgical treatment, with comparisons to MRI appearance. *Knee Surg Sports Traumatol Arthrosc*. 2002;10(1):49-56.
4. Olsson N, Silbernagel KG, Eriksson BI, et al. Stable surgical repair with accelerated rehabilitation versus nonsurgical treatment for acute Achilles tendon ruptures: a randomized controlled study. *Am J Sports Med*. 2013;41(12):2867-2876.
5. Soroceanu A, Sidhwa F, Aarabi S, Kaufman A, Glazebrook M. Surgical versus nonsurgical treatment of acute Achilles tendon rupture: a meta-analysis of randomized trials. *J Bone Joint Surg Am*. 2012;94(23):2136-2143.
6. van der Eng DM, Schepers T, Goslings JC, Schep NWL. Rerupture rate after early weightbearing in operative versus conservative treatment of Achilles tendon ruptures: a meta-analysis. *J Foot Ankle Surg Off Publ Am Coll Foot Ankle Surg*. 2013;52(5):622-628.
7. Aufwerber S, Heijne A, Edman G, Silbernagel KG, Ackermann PW. Does early functional mobilization affect long-term outcomes after an achilles tendon rupture? A randomized clinical trial. *Orthop J Sports Med*. 2020;8(3):2325967120906522.
8. McCormack R, Bovard J. Early functional rehabilitation or cast immobilisation for the postoperative management of acute Achilles tendon rupture? A systematic review and meta-analysis of randomised controlled trials. *Br J Sports Med*. 2015;49(20):1329-1335.
9. Zhao J-G, Meng X-H, Liu L, Zeng X-T, Kan S-L. Early functional rehabilitation versus traditional immobilization for surgical Achilles tendon repair after acute rupture: a systematic review of overlapping meta-analyses. *Sci Rep*. 2017;7(1):1-7.
10. Barfod KW, Hansen MS, Hölmich P, Kristensen MT, Troelsen A. Efficacy of early controlled motion of the ankle compared with immobilisation in non-operative treatment of patients with an acute Achilles tendon rupture: an assessor-blinded, randomised controlled trial. *Br J Sports Med* 2020;54(12):719-724.
11. Edama M, Kubo M, Onishi H, et al. The twisted structure of the human A chilles tendon. *Scand J Med Sci Sports*. 2015;25(5):e497 -e503.
12. Finni T, Bernabei M, Baan GC, Noort W, Tijs C, Maas H. Non-uniform displacement and strain between the soleus and gastrocnemius subtendons of rat Achilles tendon. *Scand J Med Sci Sports*. 2018;28(3):1009-1017.
13. Haraldsson BT, Aagaard P, Qvortrup K, et al. Lateral force transmission between human tendon fascicles. *Matrix Biol*. 2008;27(2):86-95.
14. Bojsen-Møller J, Hansen P, Aagaard P, Svantesson U, Kjaer M, Magnusson SP. Differential displacement of the human soleus and medial gastrocnemius aponeuroses during isometric plantar flexor contractions in vivo. *J Appl Physiol*. 2004;97(5):1908-1914.
15. Beyer R, Agergaard A-S, Magnusson SP, Svensson RB. Speckle tracking in healthy and surgically repaired human Achilles tendons at different knee angles—A validation using implanted tantalum beads. *Transl Sports Med*. 2018;1(2):79-88.
16. Slane LC, Thelen DG. Non-uniform displacements within the Achilles tendon observed during passive and eccentric loading. *J Biomech*. 2014;47(12):2831-2835.
17. Arndt A, Bengtsson A-S, Peolsson M, Thorstensson A, Movin T. Non-uniform displacement within the Achilles tendon during passive ankle joint motion. *Knee Surg Sports Traumatol Arthrosc*. 2012;20(9):1868-1874.
18. Stenroth L, Thelen D, Franz J. Biplanar ultrasound investigation of in vivo Achilles tendon displacement non-uniformity. *Transl Sports Med*. 2019;2(2):73-81.
19. Thorpe CT, Udeze CP, Birch HL, Clegg PD, Screen HR. Capacity for sliding between tendon fascicles decreases with ageing in injury prone equine tendons: a possible mechanism for age-related tendinopathy. *Eur Cell Mater*. 2013;25(4).
20. Fröberg Å, Cissé A-S, Larsson M, et al. Altered patterns of displacement within the Achilles tendon following surgical repair. *Knee Surg Sports Traumatol Arthrosc*. 2017;25(6):1857-1865.
21. Heikkinen J, Lantto I, Piilonen J, et al. Tendon length, calf muscle atrophy, and strength deficit after acute Achilles tendon rupture: long-term follow-up of patients in a previous study. *JBJS*. 2017;99(18):1509-1515.
22. Reito A, Logren H-L, Ahonen K, Nurmi H, Paloneva J. Risk factors for failed nonoperative treatment and rerupture in acute Achilles tendon rupture. *Foot Ankle Int*. 2018;39(6):694-703.
23. Surgeons AA of O. The diagnosis and treatment of acute Achilles tendon rupture: guideline and evidence report. *Rosemt IL Am Acad Orthop Surg*. 2009.

24. Finni T, Hodgson JA, Lai AM, Edgerton VR, Sinha S. Nonuniform strain of human soleus aponeurosis-tendon complex during submaximal voluntary contractions in vivo. *J Appl Physiol*. 2003;95(2):829-837.
25. De la Fuente CI, Lillo RP, Ramirez-Campillo R, et al. Medial gastrocnemius myotendinous junction displacement and plantar-flexion strength in patients treated with immediate rehabilitation after Achilles tendon repair. *J Athl Train*. 2016;51(12):1013-1021.
26. Finni T, Hodgson JA, Lai AM, Edgerton VR, Sinha S. Muscle synergism during isometric plantarflexion in achilles tendon rupture patients and in normal subjects revealed by velocity-encoded cine phase-contrast MRI. *Clin Biomech*. 2006;21(1):67-74.
27. Baxter JR, Farber DC, Hast MW. Plantarflexor fiber and tendon slack length are strong determinates of simulated single-leg heel raise height. *J Biomech*. 2019;86:27-33.
28. Hullfish TJ, O'Connor KM, Baxter JR. Medial gastrocnemius muscle remodeling correlates with reduced plantarflexor kinetics 14 weeks following Achilles tendon rupture. *J Appl Physiol Bethesda Md 1985*. 2019;127(4):1005-1011.
29. Hansen W, Shim VB, Obst S, Lloyd DG, Newsham-West R, Barrett RS. Achilles tendon stress is more sensitive to subject-specific geometry than subject-specific material properties: A finite element analysis. *J Biomech*. 2017;56:26-31.
30. Shim VB, Fernandez JW, Gamage PB, et al. Subject-specific finite element analysis to characterize the influence of geometry and material properties in Achilles tendon rupture. *J Biomech*. 2014;47(15):3598-3604.
31. Sun Y-L, Wei Z, Zhao C, et al. Lubricin in human achilles tendon: The evidence of intratendinous sliding motion and shear force in achilles tendon. *J Orthop Res*. 2015;33(6):932-937.

How to cite this article: M. Khair R, Stenroth L, Péter A, et al. Non-uniform displacement within ruptured Achilles tendon during isometric contraction. *Scand J Med Sci Sport*. 2021;31:1069–1077. https://doi.org/10.1111/sms.13925

II

MUSCLE-TENDON MORPHOMECHANICAL PROPERTIES OF NON-SURGICALLY TREATED ACHILLES TENDON 1-YEAR POST-RUPTURE

by

Ra'ad M. Khair, Lauri Stenroth, Neil J. Cronin, Aleksi Reito, Juha Paloneva & Taija Finni 2022

Journal of Clinical Biomechanics 92: 105568.

https://doi.org/10.1016/j.clinbiomech.2021.105568

Clinical Biomechanics 92 (2022) 105568

Contents lists available at ScienceDirect

Clinical Biomechanics

journal homepage: www.elsevier.com/locate/clinbiomech

Muscle-tendon morphomechanical properties of non-surgically treated Achilles tendon 1-year post-rupture

Ra'ad M. Khair [a,*], Lauri Stenroth [b], Neil J. Cronin [a,d], Aleksi Reito [c], Juha Paloneva [c,b], Taija Finni [a]

[a] Faculty of Sport and Health Sciences, Neuromuscular Research Center, University of Jyväskylä, Jyväskylä, Finland
[b] Department of Applied Physics, University of Eastern Finland, Kuopio, Finland
[c] Central Finland Health Care District, Finland
[d] School of Sport & Exercise, University of Gloucestershire, UK

ARTICLE INFO

Keywords:
Achilles tendon rupture
Stiffness
Ultrasonography
Patient-reported outcomes

ABSTRACT

Background: Achilles tendon rupture appears to alter stiffness and length of the tendon. These alterations may affect the function of tendon in force transmission and in energy storage and recovery. We studied the mechanical properties of the Achilles' tendon post-rupture and their association with function.
Methods: Twenty-four (20 males, 4 females) participants (mean age: 43 y, 176 cm, 81 kg) were recruited. Ultrasonography and dynamometry were used to assess the muscle-tendon unit morphological and mechanical properties of non-surgically treated patients 1-year post rupture.
Findings: Injured tendons were longer with difference of 1.8 cm (95%CI: 0.5–1.9 cm; $P < 0.001$), and thicker by 0.2 mm (0.2–0.3 mm; $P < 0.01$). Medial gastrocnemius cross-sectional area was 1.0 cm^2 smaller (0.8–1.1 cm^2; $P < 0.001$), fascicles were 0.6 cm shorter (0.5–0.7 cm; $P < 0.001$) and pennation angle was 2.5° higher (1.3–3.6°; $P < 0.001$) when compared to the uninjured limb. We found no differences between injured and uninjured tendon stiffness 1-year post-rupture (mean difference: 29.8 N/mm, −7.7–67.3 N/mm; $P = 0.170$). The injured tendon showed 1.8 mm (1.2–2.4 mm; $P < 0.01$) lower elongation during maximal voluntary isometric contractions. Patient-reported functional outcome was related to the tendon resting length ($\beta = 0.68$, $r(10) = 4.079$, $P = 0.002$). Inter-limb differences in the medial gastrocnemius fascicle length were related to inter-limb differences in maximum contractions ($\beta = 1.17$, $r(14) = 2.808$, $P = 0.014$).
Interpretation: Longer Achilles tendon resting length was associated with poorer self-evaluated functional outcome. Although the stiffness of non-surgically treated and uninjured tendons was similar 1-year post rupture, plantar flexion strength deficit was still present, possibly due to shorter medial gastrocnemius fascicle length.

1. Introduction

The incidence of Achilles tendon rupture (ATR) is rising (Lantto et al., 2015). The recovery of ATR is a long process (Holm et al., 2015), muscle strength decrements persist for several years and seem to be permanent (Heikkinen et al., 2017a). Although non-surgical treatment of ATR is considered safe, assessing biomechanical recovery of the ruptured tendon is important (Deng et al., 2017; Khair et al., 2021; Reda et al., 2020; Reito et al., 2018).

Studies have shown that tendon length increases within the first 4 months post-rupture (Kangas et al., 2007; Silbernagel et al., 2012a) regardless of treatment approach, and that additional tendon slack seems to alter the calf muscles' ability to generate force (Brorsson et al., 2017; Mullaney et al., 2006). Increased AT length and immobilization post-rupture lead to sudden changes in muscle-tendon tension and stimulate changes in plantar flexor muscles (Hullfish et al., 2019). Previous studies found that medial gastrocnemius (MG) fascicles were shorter and more pennate in the first weeks after injury, as well as several months later (Hullfish et al., 2019; Peng et al., 2019).

In vivo human ultrasonography studies performed 2-years post-ATR found lower tendon stiffness in the injured compared to the uninjured tendon (Chen et al., 2013; Geremia et al., 2015; Mcnair et al., 2013; Wang et al., 2013). Conversely, a study performed 2–6 years post-rupture found higher stiffness in the injured tendon (Agres et al.,

* Corresponding author at: PO Box 35, FI-40014 Neuromuscular Research Center, Faculty of Sport and Health Sciences, University of Jyväskylä, Jyväskylä, Finland.
E-mail address: raad.m.khair@jyu.fi (R.M. Khair).

https://doi.org/10.1016/j.clinbiomech.2021.105568
Received 19 March 2021; Accepted 30 December 2021
Available online 5 January 2022

2015). While the majority of long-term follow-ups are done after surgical treatment, understanding how the mechanical properties of the AT change post-rupture is also important after non-surgical treatment.

The purpose of this study was to evaluate alterations in mechanical and structural properties of non-surgically treated muscle-tendon units (MTU) 1-year post-ATR, and to examine their associations with force production capacity and functional outcomes. The following hypotheses were tested: 1) compared to the uninjured limb, the injured AT would be thicker and have a longer resting length, and MG would have smaller cross-sectional area (CSA), and shorter and more pennate fascicles; 2) AT stiffness and maximum elongation would be statistically lower during maximal voluntary isometric contractions (MVC) in the injured limb; 3) inter-limb differences in MTU morphomechanical parameters would be predictive of MVC, walking speed and self-reported clinical outcomes.

2. Methods

2.1. Participants

Twenty-four (20M, 4F) participants (means ± SD age: 43.2 ± 8.9 years, height: 176.1 ± 8.1 cm, mass: 80.9 ± 13.1 kg) in Central Finland were recruited within a clinical cohort study "Non-operative treatment of Achilles tendon Rupture in Central Finland: a prospective cohort study – NoARC" (trial registration: NCT03704532). The Ethics Committee approved the study (2U/2018). Participants were diagnosed within 14 days of the rupture using guidelines by the American Academy of Orthopaedic Surgeons and received non-surgical treatment. Inclusion criteria were a minimum of 2 of the following 4 criteria: a positive Thompson test, decreased plantarflexion strength, presence of a palpable gap, and increased passive ankle dorsiflexion with gentle manipulation (Surgeons AA of O, 2009). The exclusion criteria were avulsion fracture of the calcaneus or a re-rupture. Participants signed an informed consent explaining the details of the study, possible risks, and gave permission to use data for research purposes. Participants were tested 1-year ±3.5 months after rupture.

2.2. Non-surgical treatment protocol

Participants were treated non-surgically in combination with early mobilization. Immediately after ATR, the ankle was cast in full equinus for two weeks. After two weeks, the physician clinically assessed tendon uniformity. If uniformity was confirmed, the foot was moved into plantarflexion using a 20° equinus open sole cast allowing toe movement. Patients were encouraged to bear full weight by treatment week 4 if possible, with a custom-made functional walking orthosis with 1 cm thick heel wedge. At week 8, the orthosis was removed, and progressive physiotherapy began. Walking, swimming, underwater running, and cycling were recommended after 8 weeks. The aim was to gradually increase loading to enable pain-free walking, after which more intense activities could be included. Light jogging was permitted when the patient exhibited ankle mobility close to that of the uninjured limb, was able to walk and could perform heel raises without pain (Reito et al., 2018).

2.3. Laboratory test protocol

Participants were first prepared for the measurements, whereby both malleoli and first and fifth metatarsal heads were marked with a pen, and photos of the foot were taken to approximate the moment arm of the forefoot. AT resting length, MG fascicle length and MG CSA were then assessed using ultrasonography. Participants then sat in a custom-made ankle dynamometer (University of Jyväskylä, Finland) with the hip at 120°, knee at 0° (fully extended), and the ankle and first metatarsophalangeal joints fixed at 90° and 0° respectively. The foot was strapped to the dynamometer pedal and the thigh was strapped to the seat above the knee to minimize alignment changes within and between trials. Data were collected from both legs in one session, starting with the uninjured limb. A series of submaximal voluntary isometric contractions were performed at torque levels ranging from 50% up to maximum. This served as a warm-up and familiarization, and lasted approximately 5 min. Subsequently, MVCs were performed, where participants were asked to reach maximum torque in 2–3 s and decrease torque back to zero in a gradual manner within 2–3 s, resulting in an overall contraction time of 6 s. During these contractions, tendon length changes were quantified using ultrasound imaging. Subjects received verbal encouragement to ensure maximal effort, and visual feedback of the torque trace was also provided. The trial with the highest torque was used for further analysis. Lastly, participants were asked to walk at their preferred speed with the instruction "walk at the speed you normally walk freely down the street" for 6 m with photocells at both ends. Preferred walking speed was defined as the average of three trials.

2.3.1. Force and torque

Force data were collected via a transducer in the foot pedal of the ankle dynamometer. A potentiometer placed under the heel was used to detect heel lift during contractions. Data were sampled at 1KHz via a 16-bit A/D board (Power 1401, Cambridge Electronic Design, Cambridge, UK) connected to the lab computer, and signals were recorded using Spike2 software (Cambridge Electronic Design, Cambridge, UK). To synchronize data, a TTL-pulse was sent manually via Spike2 to trigger the recording of the US device.

AT moment arm length was calculated from photos taken in the sagittal plane from both medial and lateral sides of the foot with a ruler beneath them as a reference and pen marks on the malleoli. The moment arm was measured as the horizontal distance from the estimated centre of rotation (axis through the tip of the medial and lateral malleoli) to the midpoint of the AT (Kongsgaard et al., 2011). First, the horizontal distance from the ankle joint centre to the posterior aspect of the AT skin (M1) was measured with a custom MATLAB (R2018a) script. Then, the distance from the skin to the midpoint of the tendon (M2) was measured from a sagittal plane ultrasound image taken from the AT (see below), and subtracted from the ankle centre of rotation to AT distance, AT moment arm: MA = M1-M2 (Kongsgaard et al., 2011; Zhao et al., 2009).

Plantar flexion torque was calculated by multiplying the dynamometer force by foot moment arm which is the distance between the foot centre of pressure estimated from the pen marks on both 1st and 5th metatarsal, and the strain gauge attachment site on the foot plate (Arampatzis et al., 2005). AT force was calculated as the plantar flexion torque divided by the respective AT moment arm (MA) of each subject. A small joint rotation (heel lift) usually occurs during isometric plantarflexion tasks, resulting in an overestimation of muscle-tendon junction (MTJ) displacement. This displacement was recorded and corrected using the potentiometer under the heel (Ackermans et al., 2016). The mean (SD) magnitude of heel lift during MVCs was 1.4 mm (4.4).

2.3.2. Ultrasonography

AT resting length, MG CSA, and AT thickness were measured using a 3.6-cm linear probe (UST-5411; 7.5 MHz) and an Aloka Alpha-10 device (Aloka, Tokyo, Japan). Images were acquired with subjects in prone position with the feet at the end of the table, with a natural relaxed resting joint angle. Thickness was analysed 1 cm above the calcaneal insertion. Two images per subject and limb were analysed for tendon thickness and the mean values were used for further analysis. Typical repeated measures error for tendon thickness was 4.1%. To measure AT resting length, ultrasound was used to find the most distal point of the MG-MTJ and the tendon insertion on the calcaneus, both of which were marked on the skin. The distance between the points was then measured with a measuring tape (Barfod et al., 2015). MG fascicle length and pennation angle (PA) were acquired in prone position described above using a 6-cm linear probe (UST-5712; 7.5 MHz). Images were taken from the central portion of the muscle belly halfway between the MTJ and the

crease of the knee where the deep and superficial aponeuroses of the muscle were parallel (Bolsterlee et al., 2016). Average values from two images were used for further analysis. Repeated measures typical error was 6.2% for MG fascicle length and 6.5% for pennation angle.

CSA images were taken at 50% of MG muscle length at rest in prone position with the knee flexed to 90°. A guiding frame was attached to the skin to ensure that the image was taken in the transverse plane. The extended field of view function was used to visualize CSA. All structural image analysis was done using ImageJ (1.44b, National Institutes of Health).

During maximal isometric contractions, MG-MTJ displacement was imaged with the 6-cm linear probe in B-mode. The ultrasound probe was strapped over the most distal part of MG, as elongation measured at MTJ represents tendon elongation with the possible heel lift accounted for (Fig. 1). Ultrasound videos were sampled at 70 Hz for 8-s per contraction using the same Aloka device as for the resting measurements. MTJ displacement was tracked manually with Tracker 5.1.3 Software (https://physlets.org/tracker/) using a 4 cm calibration bar and an oval-shaped feature template (length: 0.3–1 cm, height: 0.25–0.50 cm).

2.3.3. AT mechanical properties

Tendon elongation and force recordings were synchronized, allowing AT force-elongation relations to be constructed for each subject and fitted to a second order polynomial forced through zero (Magnusson et al., 2001). In some cases, mostly injured limbs, a second order polynomial fit was applied only up to 80% of MVC or below (Fig. 2). This was done because AT length reached a plateau while plantarflexion force was still increasing, resulting in poorly fitting polynomials when using data up to 100% of MVC (Fig. 2).

The second order polynomial described the force-elongation behaviour of the tendon well as evidenced by R^2 values that always exceeded 0.90. From the polynomial, tendon stiffness was taken as a tangent at 50% MVC of the injured limb (Fig. 2C). In this way, the stiffness of both limbs was calculated at the same absolute force level. We also report normalised stiffness because AT elongation at a given force depends on the resting length of the tendon (Arampatzis et al., 2007). Normalised stiffness was defined as the slope of the tendon force-AT strain relationship.

2.3.4. Patient-reported outcome

Upon 1-year follow up at the hospital, patients filled out Achilles tendon rupture score (ATRS) surveys ($N = 19$, 5 non-responders). The survey consists of 10 questions that assess self-reported limitations in different aspects of AT function with a 0–100 linear score, where 0 indicates no symptoms and a fully functioning AT (Carmont et al., 2013).

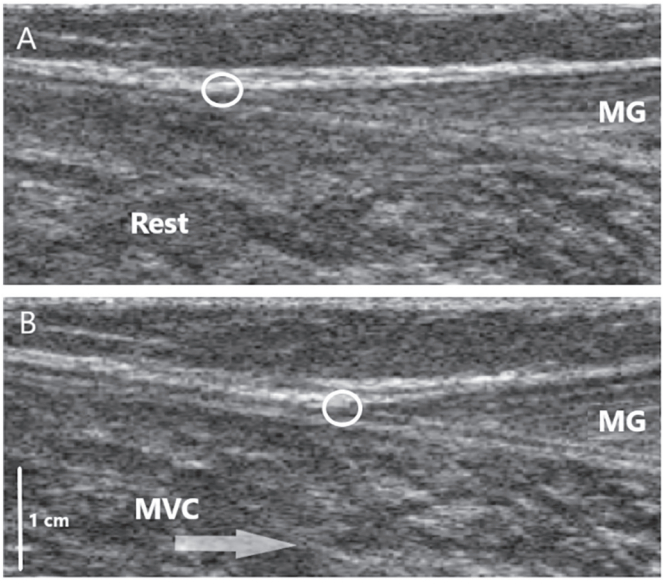

Fig. 1. B-mode ultrasound images of the MG-MTJ (A) at rest and (B) during MVC. Circles indicate the position of the tracked MTJ.

2.4. Statistical analysis

Statistical analysis was performed using JASP (JASP version 0.14.1, Amsterdam, Netherlands). Differences between limbs were compared with adjusted analysis using linear mixed models and unadjusted analysis using pairwise *t*-test. Linear mixed model with random intercepts was built using limb condition (injured vs uninjured) and age as fixed factors, and patient ID as a random factor. Model terms were tested using the Satterthwaite method for each variable independently. Restricted maximum likelihood with Satterthwaite approximation was used since it produces acceptable type 1 error for small sample sizes (Luke, 2017). Descriptive data are presented as fixed effect estimates 95% CI and adjusted *p* values. $P < 0.05$ were considered significant.

Limb asymmetry index (LSI) was calculated for all parameters as percentage (%) difference between limbs: $\frac{Injured-Uninjured}{Un-injured}*100$ (Carabello et al., 2010). Multiple regression was used to predict functional outcomes including walking speed, inter-limb difference in MVC and patient-reported outcomes with age and gender as confounding factors, and mechanical and structural parameters as predictors. All assumptions were found to be met and no outliers were found. Correlations within predictors were examined using Pearson's correlation. If a high correlation (> 0.7) was found, one of the correlated variables was removed to ensure collinearity. Relationships between mechanical and structural parameters were examined using Pearson's correlation. Correlations were interpreted as 0.1 (weak), 0.4 (moderate), and 0.70 (strong) (Schober et al., 2018).

3. Results

3.1. Muscle-tendon structural properties

AT resting length was significantly longer in the injured compared to the uninjured limb with a mean difference (95%CI) of 1.8 cm (0.5–1.9 cm; $P < 0.001$). The injured tendons were also thicker by 0.2 mm (0.2–0.3 mm; $P < 0.001$). In the injured limb at rest, MG had a smaller cross-sectional area (1.0 cm^2, 0.8–1.1 cm^2; $P < 0.001$), as well as shorter fascicles (0.6 cm, 0.5–0.7 cm; $P < 0.001$) that were more pennate (2.5°, 1.3–3.6°; $P < 0.001$). Descriptive data are shown in Table 1.

3.2. AT mechanical properties

We found no statistical difference in AT stiffness between limbs 1-year post-rupture, with a mean difference (95%CI) of 29.8 N/mm (−7.7–67.3 N/mm; $P = 0.170$). Similarly, normalised stiffness did not differ between limbs (1.7 kN/strain, −4.9–8.3 kN/strain; $P = 0.633$). The injured tendons displayed lower AT elongation during MVC with a mean difference (95%CI) of 1.8 mm (1.2–2.4 mm; $P < 0.01$). Plantar flexion MVC torque was lower in the injured limb, with an inter-limb difference of 24.1 Nm (17.5–30.7 Nm; $P < 0.001$; Fig. 3).

3.3. Relationship between functional and morphological outcomes

Multiple regression analysis including all variables except normalised stiffness with age and gender as covariates was used to predict MVC, preferred walking speed (mean (SD) 1.2 (0.1) m/s) and ATRS (mean (SD), median (interquartiles) 14.7 (11.8), 12 (Agres et al., 2015; Arampatzis et al., 2005; Brorsson et al., 2017; Chen et al., 2013; Geremia et al., 2015; Hullfish et al., 2019; Kangas et al., 2007; Khair et al., 2021; Kongsgaard et al., 2011; Mcnair et al., 2013; Mullaney et al., 2006; Peng et al., 2019; Silbernagel et al., 2012a; Surgeons AA of O, 2009; Wang

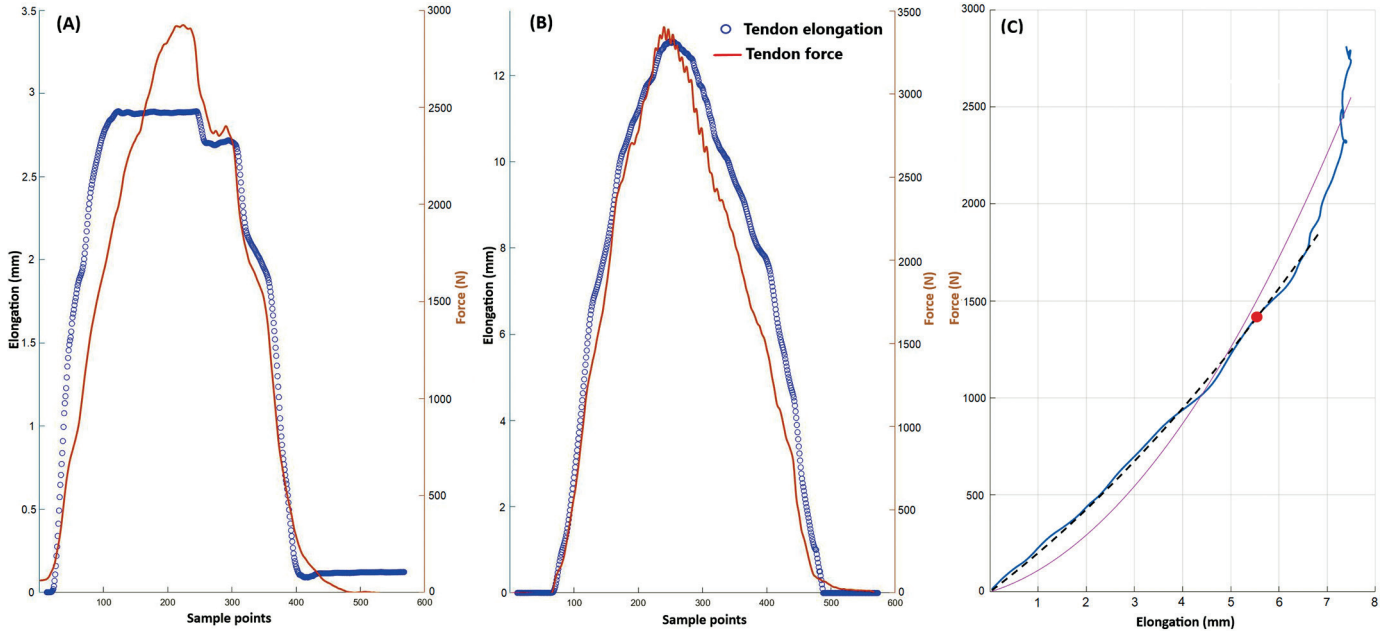

Fig. 2. Example of synchronized raw tendon force and elongation data for both limbs of one subject. (A) Injured limb, where AT elongation reached a plateau while force was still increasing. (B) Data from the same subject's uninjured limb. (C) The elongation plateau in some subjects (as in example in A) causes the force-elongation curve to rise vertically at high forces, resulting in a poor 0–100% polynomial fit (solid pink line). In this case, a polynomial fit to 80% of MVC (black dashed line) yielded a better curve fit. Stiffness was defined as the slope of the fitted curve at 50% MVC of the injured limb (red dot). (For interpretation of the references to colour in this figure legend, the reader is referred to the web version of this article.)

Table 1
Descriptive data and mean differences in muscle-tendon morphomechanical parameters.

	Injured	Uninjured	Mean difference (95%CI)	% difference (LSI)
Thickness mm (SD)	9.3 (2.0)	4.9 (1.1)	4.4 (3.5 to 5.1)	93.2%
AT resting length cm (SD)	21.3 (2.9)	18.8 (1.8)	2.5 (1.5 to 3.5)	13.5%
MG fascicle length cm (SD)	3.6 (0.6)	4.7 (0.6)	1.1 (0.9 to 1.4)	−23.8%
MG pennation angle ° (SD)	26.7 (5.9)	22.1 (4.4)	4.5 (2.6 to 6.4)	21.7%
MG CSA cm^2 (SD)	11.7 (2.6)	13.7 (2.2)	2.0 (1.2 to 2.8)	−14.6%
MVC Nm (SD)	127.4 (38.7)	173.9 (41.1)	45.8 (32.4 to 59.2)	−25.1%
Elongation mm (SD)	7.5 (5.0)	11.0 (5.7)	3.5 (1.9 to 5.1)	−26.7%
Stiffness N/mm (SD)	413.4 (186.6)	486.5 (210.2)	73.1 (−12.2 to 158.4)	−7.2%
Normalised stiffness kN/strain (SD)	89.8 (40.2)	85.1 (35.7)	4.7 (−11.0 to 20.5)	4.3%

Un-adjusted pairwise T-test.

et al., 2013; Zhao et al., 2009)). The ATRS model explained 69% of the variance ($F(8,9) = 2.51$, $P = 0.096$) with a Root mean square error (RMSE) of 9.02. Only resting length was significantly related to ATRS ($\beta = 0.61$ (0.22–1.00), $r(9) = 3.548$, $P = 0.006$). As for MVC LSI, the model explained 46% of the variance ($F(8,13) = 1.38$, $P = 0.292$) with RMSE of 15.83. MG fascicle length LSI positively predicted MVC LSI ($\beta = 1.22$ (0.24–2.20), $r(13) = 2.688$, $P = 0.019$). The preferred walking speed model explained 41% of the variance ($F(8,12) = 1.052$, $P = 0.452$) with RMSE of 0.11. None of the above-mentioned parameters were significantly related to preferred walking speed.

AT resting length LSI was inversely correlated with stiffness LSI (rs = −0.41, 95%CI [−0.7–0.0], $P = 0.045$). MG fascicle length LSI was negatively correlated with AT resting length LSI (rs = −0.43, 95%CI [−0.7–0.0]), $P = 0.037$), and pennation angle LSI (rs = −0.5, 95%CI [−0.8–0.2], $P = 0.04$). MG CSA LSI was positively correlated with normalised stiffness LSI (rs = −0.46, 95%CI [0.1–0.7], $P = 0.26$).

4. Discussion

In the present study we examined the MTU morphomechanical properties of non-surgically treated patients 1-year post rupture. In the injured limb, plantar flexor muscle strength was lower, AT resting length was longer and MG had smaller CSA with shorter and more pennate fascicles. AT stiffness did not differ between limbs. Poor self-evaluated functional outcome was associated with longer AT resting length. MG fascicle length LSI was related to MVC LSI. This study shows that non-surgical treatment may result in restoration of AT mechanical properties, but longer AT resting length was observed and is probably a contributing factor to the observed changes in morphomechanical properties and self-evaluated function.

Tendons in the injured limb were thicker, as reported previously in surgically treated patients (Wang et al., 2013). Animal models have shown that non-surgical treatment leads to higher grade organization of collagen fibres, and a more healthy tendon-like appearance compared with a greater proportion of scar tissue in the operative group (Krapf et al., 2012). Given that non-surgical treatment may be associated with less scar tissue formation than surgical treatment, the increase in tendon thickness in the current study may be a compensation for impaired material properties in the ruptured tendon resulting from compositional changes or changes in the internal organization of the material (Freedman et al., 2014).

In this study, injured AT resting length was on average 13.5% longer than in the contralateral limb, this results are in accordance with Heikkinen et al. 2017 (Heikkinen et al., 2017b). Previously, a longer AT resting length has been reported up to 2 years post-rupture, and has been shown to be associated with impaired walking performance and heel raise performance in the injured limb (Agres et al., 2015; Baxter et al., 2019; Silbernagel et al., 2012b). Since MTU length stays constant, the

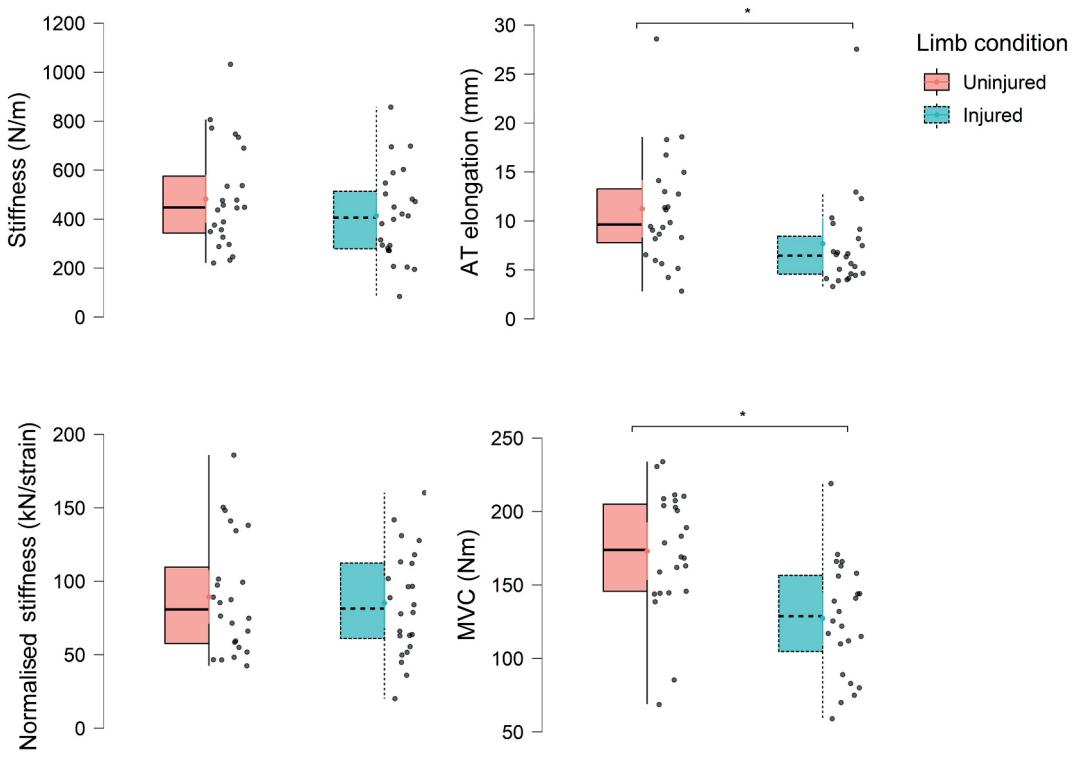

Fig. 3. Box plots illustrating estimated means ± SD for AT mechanical properties during MVC for both limbs. *Significant difference between limbs ($P < 0.001$).

increase in tendon length is presumably associated with decreased MG fascicle length. Indeed, we found an inverse correlation between resting length LSI and MG fascicle length LSI. The functional consequences of tendon elongation and the associated muscle shortening depend on sarcomere level adaptations. If there was no change in serial sarcomere number, the sarcomeres would be shorter for a given joint angle post-rupture, which would negatively affect force production capacity as TS muscles operate mostly on the ascending limb of the force-length relationship (Holzer et al., 2020). On the other hand, reduced sarcomere number can restore the sarcomere operating length at a specific joint angle. However, force production capacity would still be compromised as the sarcomeres would be forced to operate over a larger operating range for a given joint movement.

Our findings demonstrate inter-limb differences in MG morphology at rest. In the injured limb MG had a smaller CSA, with shorter, more pennate fascicles. Muscles are able to sense changes in mechanical tension and regulate their architectural configuration (de Boer et al., 2008) by adding or removing sarcomeres, as shown in animal studies (Williams and Goldspink, 1973). Post-rupture, a sudden loss of muscle-tendon tension due to the increase in AT length probably elicits plantar flexor muscle remodelling and a removal of serial sarcomeres. Hullfish et al. (2019) showed higher pennation angle in the injured limb and

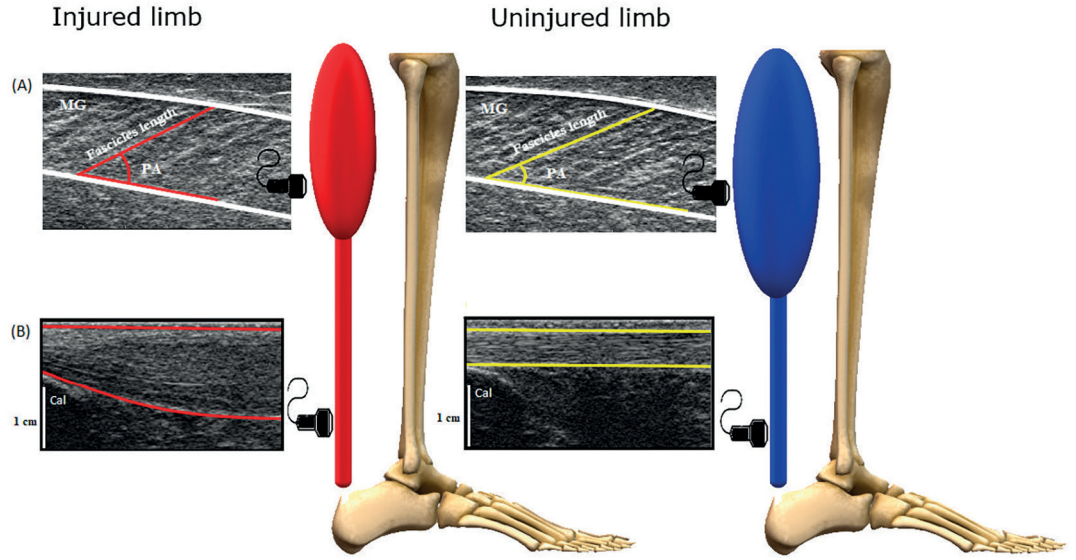

Fig. 4. Ultrasonographic images of muscle-tendon unit structural properties 1-year post-rupture in both limbs. (A) images of MG muscle where pennation angle and fascicle length were analysed. (B) Images where AT thickness was measured 1 cm away from the calcaneal insertion. Injured limb AT was longer and thicker than the uninjured AT. At rest, MG had a smaller CSA with longer and more pennate fascicles.

shorter fascicle length in the first 4 weeks of conservative treatment (Hullfish et al., 2019), but no change in muscle thickness. In the present study performed 1-year post rupture, higher pennation angle and shorter fascicles were accompanied with smaller CSA in the injured versus the contralateral limb (Fig. 4). Therefore, the acute alterations in MG muscle architecture seem to persist after one-year post-rupture, with an additional loss of muscle mass. We also observed that a greater difference in MG CSA between limbs was associated with a greater inter-limb difference in normalised AT stiffness. This may indicate that increased AT length leads to remodelling in MG structure. Change in MG structure change the muscle force production capacity effecting the tendon stiffness and influencing the mechanical loading environment of the tendon.

After rupture, MG muscle probably adapts by resetting fascicle length (dictated by serial sarcomere number) and pennation angle to a new optimum for force production at a joint angle at which the force requirement during normal locomotion is largest. This still leads to reductions in the range of motion at which force can be produced (Stäudle et al., 2020) and the ability of the plantar flexors to perform work (Baxter et al., 2019). We found that the reduction in MG fascicle length was inversely correlated with increased pennation angle, as shown previously (Hullfish et al., 2019). This morphological adaptation has functional consequences, as the increase in pennation angle increases muscle belly gearing (Lichtwark and Wilson, 2007). Muscle belly gearing reduces muscle fiber shortening for a given muscle belly shortening, so the increase in pennation angle helps to preserve force production due to the force-velocity and force-length relationships. The downside of increased pennation angle is that a lower proportion of the fiber force is transmitted in the direction of the tendon and thus to the skeleton. Therefore, the increase in pennation angle likely preserves the muscle's force production and work generation capability in concentric muscle actions but negatively affects force production in isometric conditions.

We found no difference in stiffness between ruptured and contralateral tendons. This contrasts with previous studies where AT stiffness was lower in the injured limb 3–12 months after surgical treatment (Chen et al., 2013; Geremia et al., 2015; Mcnair et al., 2013; Wang et al., 2013), but higher when investigated 2–6 years post-rupture (Agres et al., 2015). Initially, the healing tendon has lower stiffness, which gradually increases towards normal values in the remodelling stage, at least in mice (Palmes et al., 2002). Similarly, in humans, after an initial drop post-rupture, stiffness increases to eventually match or even exceed that of the uninjured tendon (Agres et al., 2015; Karamanidis and Epro, 2020). These changes in tendon stiffness have functional consequences via their effects on the muscle's force-length and force-velocity relationships. As TS muscles operate mostly on the ascending limb of the force-length relationship (Holzer et al., 2020), a higher AT stiffness helps to preserve favourable sarcomere lengths during force generation by reducing muscle shortening. Higher tendon stiffness may also help to minimize the impairments in force production caused by the increased AT resting length, albeit incompletely (Stäudle et al., 2020). AT stiffness is also positively correlated with TS rate of force development (Monte and Zignoli, 2021; Muraoka et al., 2005; Peng et al., 2019). Hence, from the viewpoint of isometric force production, it may be beneficial if the injured tendon remodels to have higher stiffness than the contralateral tendon. However, this may negatively affect locomotion efficiency and performance as there seems to be an optimal stiffness for cyclically generating force and power (Lichtwark and Wilson, 2007; Orselli et al., 2017). In the present study, the observed increase in AT thickness may have contributed to the restoration of AT stiffness. We also observed a negative correlation between stiffness LSI and AT resting length LSI indicating that more AT lengthening is associated with lower stiffness, which negatively affects isometric force production capacity. Thus, minimizing tendon lengthening after rupture may help to restore tendon mechanical properties.

The combination of a ~ 25% plantar flexion strength deficit in the injured limb with no difference in AT stiffness led to the reduction in maximal tendon elongation. Reduced maximal elongation may negatively affect movement economy due to a reduced capacity to store elastic potential energy in the tendon. This may also predispose the muscle to eccentrically-induced muscle damage or strain as the tendon cannot work as efficiently to dissipate energy and reduce the power of the negative work done by the muscle (Roberts and Azizi, 2010). However, there may be benefits associated with the reduced maximal tendon elongation related to tendon injury risk. Lower maximal elongation coupled with an increase in tendon length greatly reduces tendon strain, which has been speculated to be important for reducing the risk of tendon injury (Karamanidis and Epro, 2020) and fatigue damage (Wren et al., 2003).

During stiffness assessments we observed a plateau in MG-MTJ displacement while plantarflexion force continued to increase at the end of an isometric contraction. This phenomenon was more pronounced in the injured limb (Fig. 2) and may have been due to changes in MTU structure post-rupture. The shortened MG fascicles may have led to a relatively quick saturation of MG force generation due to the muscle's force-length properties. Furthermore, deep flexors such as flexor hallucis longus (FHL) may make a larger contribution to plantar flexion torque in the ruptured limb (Finni et al., 2006). Along with the potential contribution of the soleus muscle, these factors may result in increased plantar flexion torque that would not be detectable when tracking the MG-MTJ. This novel observation highlights the role of synergistic muscles in compensating plantarflexion torque after AT rupture (Heikkinen et al., 2017a), and warrants careful examination of data and decision making in relation to stiffness assessments. We decided to compare stiffness at 50% of MVC of the injured limb to get valid data from all participants. Therefore, direct comparisons to previous studies with different methodologies are not advisable.

When examining the significance of morphomechanical variables in relation to the self-reported functional outcomes we found that AT resting length LSI positively predicted ATRS (Kangas et al., 2007; Pajala et al., 2009; Silbernagel et al., 2012b). Our sample had a relatively good ATRS (mean 14.7). The patient with the worst outcome (47/100) also had the most elongated tendon when compared to the contralateral limb. Preferred walking speed was not related to any morphomechanical tendon parameter. The preferred walking speed was close to the values reported for healthy individuals (Stenroth et al., 2017), indicating recovery of daily function in situations where TS muscles operate submaximally. However, during maximal effort tasks (MVC), we observed deficits. The deficits can be long-lasting, even after returning to preinjury activities. Karamanidis & Epro (2020) reported that two elite athletes had significant plantar flexion force deficits in the injured limb 2.5 years post-ATR, despite high training volumes with high loads (Karamanidis and Epro, 2020). Moreover, Trofa et al. (Trofa et al., 2017) reported that for about 30% of professional athletes, ATR is a career ending injury. Thus, although daily function returns after ATR, it may lead to irreversible MTU deficits, preventing participation in some preinjury activities.

One of the study limitations is the assumption that the axes of ankle joint rotation and dynamometer are aligned. This may not be always valid and may have affected the stiffness values. However, the error is likely similar in both limbs within an individual level. During ultrasound imaging, the applied pressure may influence the measures of fascicle length and pennation angle. From the two sequential images, we evaluated that the typical error in these measures was ~6% while the mean value was reported.

5. Conclusion

One-year post-rupture, non-surgically treated tendons seem to heal to an elongated length, accompanied with MG remodelling to shorter, more pennate fascicles along with a decrease in muscle mass. Although the stiffness of non-surgically treated tendons was similar to that of the contralateral limb, plantar flexion strength deficit was still present.

Thus, the observed remodelling of the MG muscle, seems to be one of the main causes of lower force production capacity in the ruptured limb. AT resting length was associated with clinical outcome scores. As the increase in AT length seems to be responsible for the observed objectively measured and self-reported functional deficits.

Funding

This work was funded by the Academy of Finland grant #323168, UNderstanding REStoration of Achilles Tendon function after rupture (UNRESAT).

Declaration of Competing Interest

None.

References

Ackermans, T.M.A., Epro, G., McCrum, C., Oberländer, K.D., Suhr, F., Drost, M.R., et al., 2016. Aging and the effects of a half marathon on Achilles tendon force–elongation relationship. Eur. J. Appl. Physiol. 116 (11–12), 2281–2292.

Agres, A.N., Duda, G.N., Gehlen, T.J., Arampatzis, A., Taylor, W.R., Manegold, S., 2015. Increased unilateral tendon stiffness and its effect on gait 2–6 years after Achilles tendon rupture. Scand J Med Sci Sports [Internet] 25 (6), 860–867 [cited 2020 Oct 20]. Available from: https://onlinelibrary.wiley.com/doi/abs/10.1111/sms.12456.

Arampatzis, A., Morey-Klapsing, G., Karamanidis, K., DeMonte, G., Stafilidis, S., Brüggemann, G.-P., 2005 Apr 1. Differences between measured and resultant joint moments during isometric contractions at the ankle joint. J Biomech [Internet] 38 (4), 885–892 [cited 2020 Oct 2]. Available from: http://www.sciencedirect.com/science/article/pii/S0021929004002349.

Arampatzis, A., Karamanidis, K., Morey-Klapsing, G., De Monte, G., Stafilidis, S., 2007 Jan 1. Mechanical properties of the triceps surae tendon and aponeurosis in relation to intensity of sport activity. J Biomech [Internet] 40 (9), 1946–1952 [cited 2020 Oct 2]. Available from: http://www.sciencedirect.com/science/article/pii/S0021929006003320.

Barfod, K.W., Riecke, A.F., Boesen, A., Hansen, P., Maier, J.F., Døssing, S., et al., 2015. Validation of a novel ultrasound measurement of Achilles tendon length. Knee Surg. Sports Traumatol. Arthrosc. 23 (11), 3398–3406.

Baxter, J.R., Farber, D.C., Hast, M.W., 2019. Plantarflexor fiber and tendon slack length are strong determinates of simulated single-leg heel raise height. J. Biomech. 27 (86), 27–33.

Bolsterlee, B., Gandevia, S.C., Herbert, R.D., 2016 May 3. Ultrasound imaging of the human medial gastrocnemius muscle: how to orient the transducer so that muscle fascicles lie in the image plane. J Biomech [Internet] 49 (7), 1002–1008 [cited 2020 Dec 28]. Available from: http://www.sciencedirect.com/science/article/pii/S0021929016301630149X.

Brorsson, A., Willy, R.W., Tranberg, R., Grävare Silbernagel, K., 2017 Nov 1. Heel-rise height deficit 1 year after achilles tendon rupture relates to changes in ankle biomechanics 6 years after injury. Am J Sports Med [Internet] 45 (13), 3060–3068 [cited 2021 Feb 8]. Available from. https://doi.org/10.1177/0363546517717698.

Carabello, R.J., Reid, K.F., Clark, D.J., Phillips, E.M., Fielding, R.A., 2010 Aug. Lower extremity strength and power asymmetry assessment in healthy and mobility-limited populations: reliability and association with physical functioning. Aging Clin. Exp. Res. 22 (4), 324–329.

Carmont, M.R., Silbernagel, K.G., Nilsson-Helander, K., Mei-Dan, O., Karlsson, J., Maffulli, N., 2013. Cross cultural adaptation of the Achilles tendon Total Rupture Score with reliability, validity and responsiveness evaluation. Knee Surg. Sports Traumatol. Arthrosc. 21 (6), 1356–1360.

Chen, X.-M., Cui, L.-G., He, P., Shen, W.-W., Qian, Y.-J., Wang, J.-R., 2013. Shear wave elastographic characterization of normal and torn achilles tendons. J Ultrasound Med [Internet] 32 (3), 449–455 [cited 2020 Oct 28]. Available from: https://onlinelibrary.wiley.com/doi/abs/10.7863/jum.2013.32.3.449.

de Boer, M.D., Seynnes, O.R., di Prampero, P.E., Pišot, R., Mekjavić, I.B., Biolo, G., et al., 2008 Sep 1. Effect of 5 weeks horizontal bed rest on human muscle thickness and architecture of weight bearing and non-weight bearing muscles. Eur J Appl Physiol [Internet] 104 (2), 401–407 [cited 2021 Jan 28]. Available from. https://doi.org/10.1007/s00421-008-0703-0.

Deng, S., Sun, Z., Zhang, C., Chen, G., Li, J., 2017 Nov 1. Surgical treatment versus conservative management for acute achilles tendon rupture: a systematic review and meta-analysis of randomized controlled trials. J Foot Ankle Surg [Internet] 56 (6), 1236–1243 [cited 2021 Feb 28]. Available from: https://www.sciencedirect.com/science/article/pii/S1067251617303228.

Finni, T., Hodgson, J.A., Lai, A.M., Edgerton, V.R., Sinha, S., 2006. Muscle synergism during isometric plantarflexion in achilles tendon rupture patients and in normal subjects revealed by velocity-encoded cine phase-contrast MRI. Clin. Biomech. 21 (1), 67–74.

Freedman, B.R., Gordon, J.A., Soslowsky, L.J., 2014 Jul 14. The Achilles tendon: fundamental properties and mechanisms governing healing. Muscles Ligaments Tendons J [Internet] 4 (2), 245–255 [cited 2021 Jan 29]. Available from: https://www.ncbi.nlm.nih.gov/pmc/articles/PMC4187594/.

Geremia, J.M., Bobbert, M.F., Casa Nova, M., Ott, R.D., De Lemos, F.A., De Lupion, R.O., et al., 2015 Jun. The structural and mechanical properties of the Achilles tendon 2 years after surgical repair. Clin Biomech Bristol Avon. 30 (5), 485–492.

Heikkinen, J., Lantto, I., Piilonen, J., Flinkkilä, T., Ohtonen, P., Siira, P., et al., 2017a. Tendon length, calf muscle atrophy, and strength deficit after acute Achilles tendon rupture: long-term follow-up of patients in a previous study. JBJS. 99 (18), 1509–1515.

Heikkinen, J., Lantto, I., Flinkkila, T., Ohtonen, P., Niinimaki, J., Siira, P., et al., 2017b. Soleus atrophy is common after the nonsurgical treatment of acute Achilles tendon ruptures: a randomized clinical trial comparing surgical and nonsurgical functional treatments. Am. J. Sports Med. 45 (6), 1395–1404.

Holm, C., Kjaer, M., Eliasson, P., 2015. Achilles tendon rupture - treatment and complications: A systematic review. Scand. J. Med. Sci. Sports 25 (1), e1–e10.

Holzer, D., Paternoster, F.K., Hahn, D., Siebert, T., Seiberl, W., 2020 Nov 11. Considerations on the human Achilles tendon moment arm for in vivo triceps surae muscle-tendon unit force estimates. Sci. Rep. 10 (1), 19559.

Hullfish, T.J., O'Connor, K.M., Baxter, J.R., 2019 Oct 1. Medial gastrocnemius muscle remodeling correlates with reduced plantarflexor kinetics 14 weeks following Achilles tendon rupture. J Appl Physiol Bethesda Md 1985 127 (4), 1005–1011.

Kangas, J., Pajala, A., Ohtonen, P., Leppilahti, J., 2007 Jan 1. Achilles tendon elongation after rupture repair: a randomized comparison of 2 postoperative regimens. Am J Sports Med [Internet] 35 (1), 59–64 [cited 2020 Oct 6]. Available from. https://doi.org/10.1177/0363546506293255.

Karamanidis, K., Epro, G., 2020. Monitoring muscle-tendon adaptation over several years of athletic training and competition in elite track and field jumpers. Front Physiol [Internet]. Dec 16 [cited 2021 Jan 16];11. Available from: https://www.ncbi.nlm.nih.gov/pmc/articles/PMC7772406/.

Khair, M., Stenroth, L., Péter, A., Cronin, N.J., Reito, A., Paloneva, J., et al., 2021. Non-uniform displacement within ruptured Achilles tendon during isometric contraction. Scand. J. Med. Sci. Sports 31 (5), 1069–1077. Jan 19.

Kongsgaard, M., Nielsen, C.H., Hegnsvad, S., Aagaard, P., Magnusson, S.P., 2011 Aug 1. Mechanical properties of the human Achilles tendon, in vivo. Clin Biomech [Internet] 26 (7), 772–777 [cited 2020 Oct 2]. Available from: http://www.sciencedirect.com/science/article/pii/S026800331100060X.

Krapf, D., Kaipel, M., Majewski, M., 2012 Sep 1. Structural and biomechanical characteristics after early mobilization in an achilles tendon rupture model: operative versus nonoperative treatment. Orthopedics [Internet] 35 (9) [cited 2020 Oct 19]. e1383–8. Available from: https://www.healio.com/orthopedics/journals/ortho/2012-9-35-9/{8c4df5b0-f237-446d-a445-e172aadd0ad0}/structural-and-biomechanical-characteristics-after-early-mobilization-in-an-achilles-tendon-rupture-model-operative-versus-nonoperative-treatment.

Lantto, I., Heikkinen, J., Flinkkilä, T., Ohtonen, P., Leppilahti, J., 2015 Feb. Epidemiology of Achilles tendon ruptures: increasing incidence over a 33-year period. Scand. J. Med. Sci. Sports 25 (1), e133–e138.

Lichtwark, G.A., Wilson, A.M., 2007 Jan 1. Is Achilles tendon compliance optimised for maximum muscle efficiency during locomotion? J Biomech [Internet] 40 (8), 1768–1775 [cited 2021 Jan 8]. Available from: http://www.sciencedirect.com/science/article/pii/S0021929006003009.

Luke, S.G., 2017 Aug 1. Evaluating significance in linear mixed-effects models in R. Behav Res Methods [Internet] 49 (4), 1494–1502 [cited 2021 Mar 1]. Available from. https://doi.org/10.3758/s13428-016-0809-y.

Magnusson, S.P., Aagaard, P., Rosager, S., Dyhre-Poulsen, P., Kjaer, M., 2001. Load-displacement properties of the human triceps surae aponeurosis in vivo. J Physiol [Internet] 531 (1), 277–288 [cited 2020 Oct 2]. Available from: https://physoc.onlinelibrary.wiley.com/doi/abs/10.1111/j.1469-7793.2001.0277j.x.

Mcnair, P., Nordez, A., Olds, M., Young, S.W., Cornu, C., 2013. Biomechanical properties of the plantar flexor muscle–tendon complex 6 months post-rupture of the achilles tendon. J Orthop Res [Internet] 31 (9), 1469–1474 [cited 2020 Oct 27]. Available from: https://onlinelibrary.wiley.com/doi/abs/10.1002/jor.22381.

Monte, A., Zignoli, A., 2021 Jan 4. Muscle and tendon stiffness and belly gearing positively correlate with rate of torque development during explosive fixed end contractions. J Biomech [Internet]. 114, 110110 [cited 2021 Jan 8]. Available from. http://www.sciencedirect.com/science/article/pii/S0021929020305340.

Mullaney, M.J., McHugh, M.P., Tyler, T.F., Nicholas, S.J., Lee, S.J., 2006 Jul 1. Weakness in End-Range plantar flexion after achilles tendon repair. Am J Sports Med [Internet] 34 (7), 1120–1125 [cited 2020 Oct 20]. Available from. https://doi.org/10.1177/0363546505284186.

Muraoka, T., Muramatsu, T., Fukunaga, T., Kanehisa, H., 2005 Aug 1. Elastic properties of human Achilles tendon are correlated to muscle strength. J Appl Physiol [Internet] 99 (2), 665–669 [cited 2020 Dec 30]. Available from: https://journals.physiology.org/doi/full/10.1152/japplphysiol.00624.2004.

Orselli, M.I.V., Franz, J.R., Thelen, D.G., 2017 Jul. The effects of Achilles tendon compliance on triceps surae mechanics and energetics in walking. J. Biomech. 26 (60), 227–231.

Pajala, A., Kangas, J., Siira, P., Ohtonen, P., Leppilahti, J., 2009 May 1. Augmented compared with nonaugmented surgical repair of a fresh total achilles tendon rupture: a prospective randomized study. JBJS [Internet] 91 (5), 1092–1100 [cited 2020 Dec 14]. Available from: https://journals.lww.com/jbjsjournal/FullText/2009/05000/Augmented_Compared_with_Nonaugmented_Surgical.8.aspx.

Palmes, D., Spiegel, H.U., Schneider TO, Langer, M., Stratmann, U., Budny, T., et al., 2002. Achilles tendon healing: Long-term biomechanical effects of postoperative mobilization and immobilization in a new mouse model. J Orthop Res [Internet] 20 (5), 939–946 [cited 2020 Oct 19]. Available from: https://onlinelibrary.wiley.com/doi/abs/10.1016/S0736-0266%2802%2900032-3.

Peng, W.C., Chao, Y.H., Fu, A.S.N., Fong, S.S.M., Rolf, C., Chiang, H., et al., 2019 May 1. Muscular morphomechanical characteristics after an achilles repair. Foot Ankle Int. 40 (5), 568–577.

Reda, Y., Farouk, A., Abdelmonem, I., El Shazly, O.A., 2020 Apr 1. Surgical versus non-surgical treatment for acute Achilles' tendon rupture. A systematic review of literature and meta-analysis. Foot Ankle Surg [Internet] 26 (3), 280–288 [cited 2020 Oct 19]. Available from: http://www.sciencedirect.com/science/article/pii/S1268773119300530.

Reito, A., Logren, H.-L., Ahonen, K., Nurmi, H., Paloneva, J., 2018. Risk factors for failed nonoperative treatment and rerupture in acute Achilles tendon rupture. Foot Ankle Int. 39 (6), 694–703.

Roberts, T.J., Azizi, E., 2010 Aug. The series-elastic shock absorber: tendons attenuate muscle power during eccentric actions. J Appl Physiol Bethesda Md1985 109 (2), 396–404.

Schober, P., Boer, C., Schwarte, L.A., 2018. Correlation coefficients: appropriate use and interpretation. Anesth Analg [Internet]. 126 (5), 1763–1768. May [cited 2020 Oct 7. Available from. https://journals.lww.com/anesthesia-analgesia/fulltext/2018/05000/correlation_coefficients_appropriate_use_and.50.aspx.

Silbernagel, K.G., Steele, R., Manal, K., 2012 Jul. Deficits in heel-rise height and achilles tendon elongation occur in patients recovering from an Achilles tendon rupture. Am. J. Sports Med. 40 (7), 1564–1571.

Silbernagel, K.G., Steele, R., Manal, K., 2012 Jul 1. Deficits in heel-rise height and achilles tendon elongation occur in patients recovering from an achilles tendon rupture. Am J Sports Med [Internet] 40 (7), 1564–1571 [cited 2020 Oct 20]. Available from. https://doi.org/10.1177/0363546512447926.

Stäudle, B., Seynnes, O., Laps, G., Göll, F., Brüggemann, G.-P., Albracht, K., 2020 Dec 29. Recovery from achilles tendon repair: a combination of postsurgery outcomes and insufficient remodeling of muscle and tendon. Med Sci Sports Exerc [Internet] 53 (7), 1356–1366 [cited 2021 Jan 12];Publish Ahead of Print. Available from: https://journals.lww.com/acsm-msse/Abstract/9000/Recovery_from_Achilles_Tendon_Repair__A.96127.aspx.

Stenroth, L., Sipilä, S., Finni, T., Cronin, N.J., 2017 Jan. Slower walking speed in older men improves triceps surae force generation ability. Med Sci Sports Exerc [Internet] 49 (1), 158–166 [cited 2021 Feb 5]. Available from: https://journals.lww.com/acsm-msse/Fulltext/2017/01000/Slower_Walking_Speed_in_Older_Men_Improves_Triceps.19.aspx.

Surgeons AA of O, 2009. The diagnosis and treatment of acute achilles tendon rupture: guideline and evidence report. Rosemt IL Am Acad Orthop Surg.

Trofa, D.P., Miller, J.C., Jang, E.S., Woode, D.R., Greisberg, J.K., Vosseller, J.T., 2017 Oct. Professional athletes' return to play and performance after operative repair of an achilles tendon rupture. Am. J. Sports Med. 45 (12), 2864–2871.

Wang, H.-K., Chiang, H., Chen, W.-S., Shih, T.T., Huang, Y.-C., Jiang, C.-C., 2013. Early neuromechanical outcomes of the triceps surae muscle-tendon after an Achilles' tendon repair. Arch. Phys. Med. Rehabil. 94 (8), 1590–1598.

Williams, P.E., Goldspink, G., 1973. The effect of immobilization on the longitudinal growth of striated muscle fibres. J Anat [Internet]. 116 (Pt 1), 45–55. Oct [cited 2021 Jan 28. Available from. https://www.ncbi.nlm.nih.gov/pmc/articles/PMC1271549/.

Wren, T.A.L., Lindsey, D.P., Beaupré, G.S., Carter, D.R., 2003 Jun 1. Effects of creep and cyclic loading on the mechanical properties and failure of human achilles tendons. Ann Biomed Eng [Internet] 31 (6), 710–717 [cited 2021 Feb 5]. Available from. https://doi.org/10.1114/1.1569267.

Zhao, H., Ren, Y., Wu, Y.-N., Liu, S.Q., Zhang, L.-Q., 2009 Mar 1. Ultrasonic evaluations of Achilles tendon mechanical properties poststroke. J Appl Physiol [Internet] 106 (3), 843–849 [cited 2021 Oct 8]. Available from: https://journals.physiology.org/doi/full/10.1152/japplphysiol.91212.2008.

III

IN VIVO LOCALISED GASTROCNEMIUS SUBTENDON REPRESENTATION WITHIN THE HEALTHY AND RUPTURED HUMAN ACHILLES TENDON

by

Ra'ad M. Khair, Lauri Stenroth, Neil J. Cronin, Aleksi Reito,
Juha Paloneva & Taija Finni 2022

Journal of Applied Physiology, 133(1): 11–19.

https://doi.org/10.1152/japplphysiol.00084.2022

In vivo localised gastrocnemius subtendon representation within the healthy and ruptured human Achilles tendon

Ra'ad M. Khair [1*], Lauri Stenroth [2], Neil J. Cronin [1,4], Aleksi Reito [3], Juha Paloneva [3] and Taija Finni [1].

[1] Faculty of Sport and Health Sciences, Neuromuscular Research Center, University of Jyväskylä, Jyväskylä, Finland; [2] Department of Applied Physics, University of Eastern Finland, Kuopio, Finland; [3] Central Finland Health Care District, Finland and University of Eastern Finland, Finland, [4] School of Sport and Exercise, University of Gloucestershire, UK.

*Author for Correspondence

Ra'ad M. Khair

Email: raad.m.khair@jyu.fi

Phone : +358469221362

P.O. Box 35

40014 Jyväskylä, Finland

Author contributions

Conceptualization: T.F., N.J.C., A.R., J.P., R.M.K; Methodology: T.F., N.J.C., A.R., L.S., J.P.; Data acquisition: T.F., R.M.K.; Data curation - analysis: R.M.K.; Writing original draft: R.M.K.; Writing – review & editing: R.M.K., L.S., N.J.C., A.R., J.P., T.F.; Visualization: R.M.K.; Supervision: T.F., N.J.C.; Funding acquisition: T.F; Project administration: T.F.

Abstract

The Achilles tendon (AT) is composed of three distinct in-series elastic subtendons, arising from different muscles in the triceps surae. Independent activation of any of these muscles is thought to induce sliding between the adjacent AT subtendons. We aimed to investigate displacement patterns during voluntary contraction (VOL) and selective transcutaneous stimulation of medial (MG_{stim}) and lateral (LG_{stim}) gastrocnemius between ruptured and healthy tendons, and to examine the representative areas of AT subtendons. Twenty-eight patients with unilateral AT rupture performed bilateral VOL at 30% of the maximal isometric un-injured plantarflexion torque. AT displacement was analysed from sagittal B-mode ultrasonography images during VOL, MG_{stim} and LG_{stim}. Three-way ANOVA revealed a significant two-way interaction of contraction type*location on the tendon displacement ($F(10\text{-}815)=3.72$, $p<0.001$). The subsequent two-way analysis revealed a significant contraction type*location interaction for tendon displacement ($F(10\text{-}410)=3.79$, $p<0.001$) in the un-injured limb only, where LG_{stim} displacement pattern was significantly different from MG_{stim} ($p=0.008$) and VOL ($p=0.005$). When comparing contraction types between limbs the there were no difference in the displacement patterns, but displacement amplitudes differed. There was no significant difference in the location of maximum or minimum displacement between limbs. The displacement pattern was not different in non-surgically treated compared to un-injured tendons one-year post rupture. Our results suggest that near the calcaneus, LG subtendon is located in the most anterior region adjacent to medial gastrocnemius. However, free tendon stiffness seems to be lower in the injured AT, leading to more displacement during electrically-induced contractions compared to the un-injured.

New & Noteworthy

Using selective electrical stimulation, we report the distributions of medial and lateral gastrocnemius subtendon representations within the healthy and ruptured Achilles tendon. In the majority of our sample, lateral gastrocnemius subtendon was found in the most anterior region adjacent to medial gastrocnemius both in the healthy and ruptured, non-surgically treated tendon. The tendon internal displacement pattern does not seem to differ, but displacement amplitude and non-uniformity differed between healthy and ruptured tendons one-year post rupture.

Key words: Achilles tendon, architecture, geometry, anatomy, rupture, human.

Introduction

The Achilles tendon (AT) provides critical series elasticity to the triceps surae, amplifying power for activities such as walking and running (1) and playing a significant role in mechanical energy storage (2). Normal tendon function is disrupted by AT disorders that also cause pain and disability. Achilles tendon rupture (ATR) is prevalent in sport-related activities with an incidence of 31/100,000 individuals per year (3, 4). Understanding the normal and pathological biomechanical function of the AT is crucial to the diagnosis and management of AT-related maladies.

The AT has a complex hierarchical structure and is composed of distinct bundles of fascicles running continuously along the tendon, called subtendons. AT subtendons each arises from a different muscular head of the triceps surae: soleus (SOL), medial gastrocnemius (MG), and lateral gastrocnemius (LG) (5, 6). The tendon twists so that at the calcaneal tuberosity insertion, the MG fibres are located on the lateral surface, LG fibres more deeply, and the SOL fibres on the medial surface (5, 6). The degree of twist varies among individuals and can be classified into three types (5). This variation might lead to interindividual differences in the location of the MG, LG and SOL tendon fascicles along the length of the tendon (5). Due to this structure, AT is subjected to complex non-uniform loading that can cause heterogeneity of strain within the tendon (7).

In vivo studies have exploited advances in ultrasonic imaging and speckle tracking algorithms to reveal non-uniform motion within the AT (8, 9). The ability of subtendons to slide relative to each other is considered to be a function of a healthy tendon (9, 10). Healthy non-uniformity is characterised by smaller displacement of the superficial (posterior) tendon and larger displacement of the deep (anterior) tendon. Assuming that posteriorly the tendon consists of fascicles arising from both gastrocnemius muscles and that the anterior tendon consists of fascicles arising from soleus, researchers have tried to identify structure-function

relationships (11, 12). However, the mechanism of non-uniform displacement and the representation of each subtendon within free AT in different individuals remains elusive due to potential differences in neural control strategies (7), the architecturally complex twisted tendon structure (5, 6), and the difficulty of visualizing individual subtendons using conventional imaging techniques (ultrasound or magnetic resonance imaging).

In recent studies, ruptured ATs have been found to display more uniform within-tendon displacement 1-year post-rupture (13, 14). In addition to an increase in length of the tendon, ATR leads to morphomecahnical changes in the triceps surae muscles and subtendons (15, 16). These changes seem to occur regardless of whether they were treated surgically or conservatively (13, 14), and might alter the force transmission mechanism in the muscle-tendon unit.

Voluntary contraction typically activates all synergistic muscles to a variable degree (17, 18) and leads to disproportionate tissue displacement within the tendon due to mechanical and structural differences between triceps surae muscles (19). During voluntary contractions, complex neuromuscular control of the triceps surae within and across healthy and injured individuals may confound interpretations of tissue displacement in adjacent subtendons. By removing the effects of neural control, one could potentially identify if changes in structure and material properties due to ATR modify the displacement pattern within the AT. Electrical transcutaneous stimulation can be used to stimulate a given muscle selectively (20, 21). Using this method, it can be assumed that selective activation of one of the triceps surae muscles induces serial force transmission that is observed as tendon displacement mainly in the area containing tendon fascicles arising from the activated muscle belly. Therefore, the stimulation method may also help to understand AT subtendon organization in vivo.

By using selective transcutaneous stimulation to medial and lateral gastrocnemius muscles we aimed to find out whether AT tissue displacement pattern differs in voluntary contraction

and electrically evoked contractions between injured (INJ) and un-injured (UNJ) tendons. Examination of the displacement patterns during selective activation was expected to yield information about the representative areas of AT subtendons. We hypothesized that different contraction types would lead to different displacement patterns. Furthermore, it was hypothesized that INJ tendon would show less, and more uniform displacement compared to the UNJ tendon.

Methods

Participants

Twenty-eight ATR patients (24 males, 4 females) treated at the Central Finland Health Care District agreed to participate (Table 1). ATR was diagnosed according to the American Academy of Orthopaedic Surgeons guidelines. Inclusion criteria were a minimum of 2 of the following 4 criteria: a positive Thompson test, decreased plantarflexion strength, presence of a palpable gap, and increased passive ankle dorsiflexion with gentle manipulation. Participants with re-occurring rupture were treated surgically and excluded from the sample, which contains only individuals with non-surgical treatment and early mobilization (22). This study was approved by the Ethics committee of Central Finland health care district (2U/2018). Participants signed an informed consent explaining the details of the study, possible risks, and

gave permission to use data for research purposes. Participants were invited to the laboratory 1-year ± 1.8 months after rupture.

Experimental procedure

B-mode ultrasound was used to examine tendon properties. Scans were done using a 3.6-cm linear probe (UST-5411, Aloka alpha10, Japan). First, the subtendon lengths of MG, LG and SOL were measured from a resting prone position with the subjects' feet over the edge of a table. The limb was scanned to find the most distal point of the muscle-tendon junction of each muscle head and the tendon insertion on the calcaneus, all of which were marked on the skin. The distance between the points was then measured with a measuring tape (23). The reliability of this method was tested, whereby four un-injured limbs was measured on two separate days. The subtendon lengths of the triceps surae muscles were measured and the intraclass correlation coefficient (ICC) was calculated (24). ICC was 0.99 (90% CI 0.97-

0.99) with a coefficient of variation (CV) of 6.6%. Ultrasound imaging was then used to locate the thickest part of both gastrocnemius muscles, where the stimulating electrodes were placed. Participants´ skin was shaved and cleaned with alcohol to ensure good conductivity. A pair of 32 mm diameter electrodes (Niva Medical Oy) was attached over each muscle with ~1 cm inter-electrode distance. During measurements, participants sat in a custom-made ankle dynamometer (University of Jyväskylä, Finland) with the hip at 120°, knee at 0° (fully extended), and the ankle and first metatarsophalangeal joints at 90° and 0° respectively. The foot was strapped to the dynamometer pedal and the thigh secured to the seat above the knee. To image tendon displacement, the ultrasound probe was attached longitudinally with the distal edge ~2 cm above the calcaneus.

A warm-up was done in the form of a series of standardized submaximal contractions. Starting with UNJ, unilateral maximal voluntary isometric contractions (MVCs) were performed followed by contractions corresponding to 30% of UNJ MVC. Then, with the participant relaxed, single stimulation pulses were elicited with increasing intensity using a constant current electrical stimulator (DS7AH; Digitimer, Hertfordshire, UK) until the motor threshold was exceeded, as confirmed by a visible muscle twitch (20, 21). If a corresponding displacement was not observed clearly in the US image of the AT, higher stimulation intensity was used. AT displacement was imaged 1 s before and throughout a tetanic pulse of 1000 μs at 100 Hz at the pre-determined stimulation intensity. MG and LG were stimulated in random order. The entire protocol was then repeated for INJ, starting with voluntary isometric contractions, followed by electrically induced contractions.

Force data were collected via a strain gauge transducer in the foot pedal of the ankle dynamometer. A potentiometer placed under the heel was used to detect heel lift during contractions. Data were sampled at 1 kHz via a 16-bit A/D board (Power 1401, Cambridge Electronic Design, Cambridge, UK) connected to the computer, and signals were recorded

using Spike2 software (Cambridge Electronic Design, Cambridge, UK). To synchronize data, a TTL-pulse was sent manually via Spike2 to first trigger the data acquisition with the US device for 8 seconds and after 1 s to deliver the 0.7 s tetanus to either MG or LG. Ultrasound videos were sampled at 50 HZ and stored for further offline analysis.

Data analysis

Ultrasound B-mode image analysis of tendon displacement was done using a speckle tracking algorithm implemented in Matlab (R2020a, MathWorks Inc, Natick, MA, USA) according to the previously validated and published configuration of Slane and Thelen (9, 25). The region of interest location and size were defined for each subject manually to ensure that only tendon tissue was analysed. A grid of six nodes across the width of the tendon and eleven across the length of the tendon was generated (14). All tracking results were visually inspected to ensure that the nodes remained inside the tendon throughout the movement. Incremental displacements were fitted with a low-order polynomial (25). Displacements of nodes along each of the six antero-posterior rows were averaged and peak displacement of the average data were extracted for analysis. The six locations across the tendon starting from the posterior part to the anterior part are referred to as locations 1-6, respectively. The average peak displacement across the six locations was used to represent mean displacement. Locations of the maximum and minimum displacement were extracted. Tendon non-uniformity was expressed as the difference between minimal and maximal displacement in the tendon. To facilitate the comparison of displacement patterns between electrically induced contractions and volitional activation, the displacement data were normalized to a range between 0-1 where 0 is minimum displacement location and 1 is maximum displacement location. The relative displacement relation between 6 locations across the tendon is hereafter referred to as the displacement pattern. Displacement was normalized since voluntary contraction produced higher torque and overall AT displacement than

electrically induced contractions. Peak torque was calculated for both voluntary and electrically induced contractions.

Statistical analysis

Statistical analysis was performed using JASP (JASP version 0.14.1, Amsterdam, Netherlands). The level of significance was set at $p<0.05$. Three-way repeated-measures ANOVA was performed to investigate the effects of contraction type (VOL, MG, and LG stimulations), limb condition (INJ vs UNJ) and tendon location (across 6 locations) on the normalized displacement of the tendon. The main interest of the analysis is in three- and two-way interaction effects, indicating how the displacements are distributed between the tendon locations (i.e. are affecting the displacement pattern) in the different conditions and limbs. If significant three-way interactions were detected, two-way analysis was performed, followed by simple pairwise comparisons with Bonferroni-adjustment when a significant main effect was found. Greenhouse-Geisser adjustment was applied when the assumption of sphericity was violated. Skewness and kurtosis was checked to insure the normality of the data. If outliers where detected, the test was done with (i.e. the entire sample) and without the outlier. Limb differences (UNJ vs INJ) in AT non-uniformity, displacement amplitude, maximum and minimum displacement locations were compared using two-sided paired t-tests.

209 ## Results

210 Free tendon length below the SOL muscle insertion site was significantly longer in INJ
211 compared to UNJ with a mean difference (95%CI) of 1.6 cm (0.6-2.6 cm; p=0.003). The INJ
212 MG subtendon was also longer by 2.1 cm (1.5–2.7 cm; p<0.01), and LG by 1.9 cm (1.2–2.6
213 cm; p<0.01) than in UNJ. There were no statistically significant differences in stimulation
214 threshold or intensity between limb muscles or between limbs (Table 2).

215

216 Absolute displacement values and torque levels are reported in (Table 3). There was no
217 statistically significant difference in stimulation evoked torque levels between limbs in
218 response to stimulation of either muscle despite the stimulation inducing a significantly
219 higher mean displacement in both INJ in muscles compared to UNJ. The mean (SD)
220 magnitude of heel lift during electrically induced contractions was 0.04 mm (0.5) and 2.5 mm
221 (4.0) during voluntary contractions.

222

223 **Voluntary and stimulation-induced displacement patterns**

224 To explore the differences in displacement patterns, the absolute values of the 6 locations
225 were normalized to enable comparison between VOL and stimulation conditions (Figure 1).
226 Three-way repeated-measures ANOVA was performed to evaluate the effects of contraction
227 type, location and limb condition on tendon displacement. There was a significant two-way
228 interaction of contraction type*location on the tendon displacement (F (10-978) =3.7,
229 p<0.001). Initial three-way analysis was followed by a two-way repeated-measures ANOVA
230 for the effect of contraction type*location on tendon displacement at the two levels of limb
231 condition and the location*limb condition on tendon displacement at each contraction type
232 level.

There was no significant location*limb condition interaction effect on tendon displacement at each contraction type level. There was a significant contraction type*location interaction effect on tendon displacement ($F_{(10\text{-}492)} = 3.8$, $p<0.001$) at the UNJ limb, while the interaction effect was not significant for the INJ limb ($F_{(10\text{-}486)} = 1.11$, $p=0.353$). Simple pairwise comparisons were done between the contraction types for the UNJ with a Bonferroni adjustment applied. The analysis showed that the LG_{stim} displacement pattern was significantly different to MG_{stim} ($p=0.007$), and VOL ($p=0.003$) (Figure 1). Individual displacement patterns are shown in (Figure 2).

In UNJ, maximum displacement during MG_{stim} occurred most frequently in the three most anterior locations, while during $LG_{stim,}$ maximum displacement occurred most often in the most anterior (6^{th}) location (Figure 4). This pattern was also found in INJ, where the most frequent locations of maximum displacement during MG_{stim} were in the anterior half of the tendon (frequency of maximal displacement: 4^{th}: 21.4%, 5^{th}: 32.2% and 6^{th}: 32.7%), while during $LG_{stim,}$ maximum displacement occurred in the 6^{th} location in 48.2% of participants. Minimum displacement was found in the most posterior location for the stimulation of both muscles in both limbs. There was no statistically significant difference in maximum or minimum displacement location between limbs.

Tendon non-uniformity and displacement amplitude during electrical stimulation

Tendon non-uniformity was higher in UNJ compared with INJ with a mean difference (95%CI) of 0.11 mm (0.04 – 0.18mm, $p=0.005$) during MG_{stim}, and 0.09 mm (0.03 – 1.42 mm, $p<0.001$) during LG_{stim} (Figure 3). When non-uniformity was compared between stimulated muscles in the same limb, there was no statistically significant difference in either limb, with a mean difference (95%CI) of 0.016 mm (-0.06 – 0.09 mm) for UNJ and 0.003

257 mm (-0.05 – 0.05 mm) for INJ. One outlier was detected in LG_{stim} mean displacement group
258 (Higher range:1.9mm, outlier:2.7mm), when the whole sample was used there was no
259 significant difference in mean tendon displacement of the INJ between the contractions
260 induced when stimulating different muscles, with a mean difference (95%CI) of 0.28 mm (-
261 0.004 – 0.56 mm, p=0.053), however when the test was done without the outlier there was a
262 significant difference (95%CI) of mean difference of 0.34 mm (0.007 – 0.61 mm, p=0.015).
263 In the UNJ, there was a significant difference in the mean displacement depending on the
264 stimulated muscle, with a greater displacement when MG was stimulated (95%CI) of mean
265 difference of 0.22 mm (0.04 – 0.40 mm, p=0.016).
266

Discussion

In this study, we examined internal AT displacement patterns during voluntary and selective transcutaneous stimulation of medial and lateral gastrocnemius to investigate differences within the AT tissue displacement between INJ and UNJ limbs of patients after AT rupture and to inspect the representative areas of subtendons. The lowest stimulation intensity that induced a visible contraction was used to ensure selective activation of only the targeted muscle. As hypothesized, displacement patterns during voluntary and electrically induced contractions were different; the displacement pattern was significantly different during LG_{stim} compared to VOL and MG_{stim} in both limbs. There was no statistically significant difference when the displacement patterns were compared for each stimulated contraction between limbs. Thus, with the assumption that the stimulation-induced force is primarily serially transmitted to tendon fascicles, the subtendon organization does not seem to be altered in the non-surgically treated limb of ATR patients. In UNJ, peak tendon displacement during MG_{stim} tended to occur more posteriorly compared to VOL. Overall, the anterior half of the AT underwent larger displacement than the superficial posterior part in all contraction conditions.

Despite higher mean displacement in INJ, displacement was more uniform when compared to UNJ during contractions induced by stimulating MG and LG. Tendon stiffness also seemed to be lower in INJ, since ankle joint torque was similar during muscle stimulations in both limbs, but the displacement was larger in INJ than in UNJ. However, this was not observed for voluntary contractions in which tendon mean tendon displacement did not differ between the limbs. Marked inter-individual differences were observed in internal tendon motion. Thus, when investigating AT anatomical organization and internal force sharing, an individualized approach might help to understand AT force sharing mechanisms and tendon recovery from injury.

292 **Voluntary vs. stimulated contractions**

293 Internal tendon displacement patterns were different during LG_{stim} compared to VOL and
294 MG_{tim} in UNJ. In VOL, peak displacement was typically found in the two most anterior
295 locations. Voluntary contraction leads to disparate tissue displacement within the tendon due
296 to disproportionate activation of synergistic muscles and mechanical structural differences
297 between triceps surae muscles (7, 19). On the other hand, the low, stimulation-induced force
298 can be assumed to be mainly transmitted serially to the targeted muscle's subtendon (26).
299 Although lateral force transmission may occur (21), the main pathway of force is the stiffest
300 structure. Hence, the location of peak displacement in response to stimulation can be
301 considered to reveal the location of tendon fascicles within the cross-section of AT.

302 Displacement during LG_{stim} peaked in the anterior tendon, implying that the most anterior area
303 could be occupied by tendon fascicles arising from LG subtendon. In anatomical studies,
304 Pękala et al. (2017) and Edama et al. (2015) found that SOL occupied the anterior portion and
305 LG the lateral portion of the tendon at the level of the SOL muscle-tendon junction.
306 However, due to high torsion within AT, LG tendon fascicles are likely located anteriorly in
307 the more distal tendon (5, 6). Furthermore, in a recent study, three tendons were dissected,
308 and 3D computer aided models were constructed based on these tendons. In the model that
309 twisted the most, LG subtendon was found to completely occupy the anterior portion of the
310 distal AT (27). Therefore, anatomical studies are consistent with the present observations
311 regarding the location of the LG subtendon.

312 There was no difference between VOL and MG_{stim} displacement patterns (Figure 1).
313 However, during MG_{stim} displacement peaked around the 4th and 5th locations in UNJ,
314 indicating that fascicles originating from MG could be present in the mid-to-anterior part of
315 the tendon. Unlike in LG_{stim}, there was more individual variation in the location of peak
316 displacement in MG_{stim}. Due to individual differences in free tendon length, the superior-

inferior field of view may not have been consistent across subjects relative to tendon length. When comparing these observations to the anatomical maps provided by previous cadavers studies, natural anatomical variation may explain the observed heterogeneity in peak displacement in response to MG_{stim} (5, 6, 27).

In addition to the anatomical origin, the observed peak displacement locations may have been affected by lateral force transmission between different subtendons within the AT. Each subtendon transmits the force from a single muscle belly but not fully independently, and force could be laterally transmitted between triceps surae muscle bellies or even subtendons (28, 29). AT force and subsequent displacement might be distributed unevenly with a bias toward the SOL subtendon since SOL subtendon fascicles have been found previously to be compliant in rats (29) and in human cadavers (30) although contradictory results have also been reported (27). This raises questions about the forces transmitted through connective tissue or inter-fascicular matrix, which could be crucial for force transmission mechanisms and inter-fascicular gliding within the tendon (10, 31).

In summary, during VOL and electrically induced contractions of MG and LG, minimum displacement always occurred in the posterior tendon and maximum displacement in the mid-to-anterior tendon. The same observation was made in a recent study where SOL and MG were electrically stimulated (32), and the tendon was split into two halves for analysis purposes; the anterior half always displaced the most in response to MG and SOL stimulations in different ankle positions. This is consistent with the observations made in this study as we found that the mid-to-deep part of the tendon displaced most when MG was stimulated and the deep part when LG was stimulated. The difference between the two studies is in the interpretation of the data in regard to which subtendon are presented in the deep part of the tendon. In Lehr et al. the tendon was split in consideration to the function-structure relationship (11, 12), and the authors interpreted a larger non-uniformity and

displacement in the representative part of the stimulated muscle tendon when SOL was stimulated compared to MG as an evidence of consistency with the anatomical function-structure consideration (32). We relied on the principle that the main pathway of force is the stiffest structure. Thus, when a muscle is selectively stimulated the arising regional tendon displacement can inform us about regions of the tendon corresponding to fascicles arising from different triceps surae muscles. Based on the beforementioned we found that the gastrocnemius subtendons are located in the mid-to-anterior part of the tendon, and that LG is probably located most anteriorly.

Gastrocnemius and soleus have different functional roles, despite having a common distal tendon and working synergistically as ankle plantar flexors (33, 34). It has been suggested that in order to perform their differing functional roles, these muscles rely on the ability of the subtendons to displace relative to each other (35, 36). It is of interest to investigate if normal subtendon organization can be restored after ATR as this most likely is a prerequisite for restoring normal Achilles tendon and triceps surae function including the functional independence of the muscles. If tendon fascicles that were originally part of different subtendons would merge during the healing process this could result in reduced capacity for relative movement between subtendons and disruption of the normal function of the Achilles tendon. In fact, ATR followed by surgical reconstruction has been shown to reduce non-uniform tendon motion observed using speckle tracking (8, 37). Our tendon displacement data (Figure 2) and our previous report (14) suggest that there are considerable individual variations in the subtendon organization in both ruptured and un-injured tendons. This signifies the importance of an individualized assessment and interpretation of the subtendon organization and function after ATR.

Tendon non-uniformity and displacement amplitude during electrical stimulation

Consistent with previous studies, we found a more uniform displacement pattern in INJ compared to the contralateral tendon 1-year post rupture (13, 14), suggesting impaired sliding within the injured tendon. Limited inter-fascicular sliding might be a result of interfascicular matrix adhesions caused by the rupture (10). Mean displacement in INJ was higher than in UNJ. As the same amount of torque was produced during stimulation, this result suggests lower stiffness in INJ. However, this differs from our previous results, where we reported that stiffness of the entire MG tendon during isometric voluntary contraction was similar between injured and un-injured tendons 1-year post rupture (38). This would suggest that in the free distal AT, mechanical properties (stiffness) may be altered locally and manifest themselves at low force levels, while globally stiffness seems to be similar between limbs. This discrepancy between our observations could indicate an extension of the toe region, or slackness of the tendon in the INJ limb while the linear region of the force-displacement curve would be similar between the limbs. A similar phenomenon of an extended range of tendon strain at low stresses has been reported previously after 4 weeks of limb unloading by suspension (39).

We found no differences between limbs (UNJ vs INJ) in the locations of maximum or minimum displacement when stimulating either MG or LG, consistent with our previous findings during voluntary contractions (14). Furthermore, in the three contraction types the displacement patterns were similar when compared between limbs. Thus, the anatomical subtendon organization does not seem to be altered after a rupture in non-surgically treated tendons.

Limitations

There are several limitations of this study. First, the nature of two-dimensional imaging may not fully capture the complex three-dimensional behaviour of the triceps surae subtendons, which could lead to errors when estimating AT tissue displacement. The speckle tracking algorithm uses a low order polynomial fit to regularize displacement (25). This may reduce variation in displacement between the six locations across the tendon. However, filtering has been deemed necessary to reduce noise and erroneous estimates (40), and was applied here in the same manner as in previous studies (32). Furthermore, it should be noted that LG muscle has different compartments that are innervated by two main nerves and numerous sub-branches (41), so stimulation might activate different branches of the muscle causing more variability to the displacement pattern. Furthermore, selective activation of LG might stiffen the connective tissue between SOL and LG, facilitating force transmission (29). Thus, the representation of LG or MG subtendon that we observed within the AT may have been influenced by lateral force transmission at the level of the muscle or tendon. However, this effect was likely minimal since it has been shown that lateral force sharing within the human Achilles tendon is small at low forces (42).

Conclusion

To conclude, Achilles tendon displacement patterns were different in response to selective stimulation of LG compared to MG stimulation or voluntary contraction. Our results suggest that when imaged from a mid-sagittal view, the gastrocnemius subtendons are located in the mid-to-anterior part of the tendon, and that LG is probably located most anteriorly. Previous anatomical studies support these results, but more investigations are needed since results in the literature are inconsistent. The stimulation method could allow for a more individualized approach for investigation of tendon organization, that might help to better understand the complex mechanics and triceps surae subtendon representations within the Achilles tendon.

We found no evidence that non-surgical treatment of ATR alters the displacement pattern within the tendon suggesting that non-surgical treatment may preserve the normal subtendon organization. However, differences in displacement amplitude and non-uniformity of the tendon displacement were present between the limbs in electrically stimulated conditions. These findings suggest an extended toe region of the tendon force-displacement curve after ATR and potential adhesions preventing non-uniform displacements.

Grants

This study was funded by Academy of Finland grant #323168, UNderstanding REStoration of Achilles Tendon function after rupture (UNRESAT), and in part by Academy of Finland grant #332915.

Disclosure

The authors declare that they have no competing interests.

References

1. **Fukashiro S**, **Hay DC**, **Nagano A**. Biomechanical Behavior of Muscle-Tendon Complex during Dynamic Human Movements. *J Appl Biomech* 22: 131–147, 2006. doi: 10.1123/jab.22.2.131.

2. **Roberts TJ**, **Azizi E**. Flexible mechanisms: the diverse roles of biological springs in vertebrate movement. *J Exp Biol* 214: 353–361, 2011.

3. **Ganestam A**, **Kallemose T**, **Troelsen A**, **Barfod KW**. Increasing incidence of acute Achilles tendon rupture and a noticeable decline in surgical treatment from 1994 to 2013. A nationwide registry study of 33,160 patients. *Knee Surg Sports Traumatol Arthrosc* 24: 3730–3737, 2016.

4. **Lantto I**, **Heikkinen J**, **Flinkkilä T**, **Ohtonen P**, **Leppilahti J**. Epidemiology of Achilles tendon ruptures: increasing incidence over a 33-year period. *Scand J Med Sci Sports* 25: e133-138, 2015. doi: 10.1111/sms.12253.

5. **Edama M**, **Kubo M**, **Onishi H**, **Takabayashi T**, **Inai T**, **Yokoyama E**, **Hiroshi W**, **Satoshi N**, **Kageyama I**. The twisted structure of the human A chilles tendon. *Scand J Med Sci Sports* 25: e497–e503, 2015.

6. **Pękala PA**, **Henry BM**, **Ochała A**, **Kopacz P**, **Tatoń G**, **Młyniec A**, **Walocha JA**, **Tomaszewski KA**. The twisted structure of the Achilles tendon unraveled: A detailed quantitative and qualitative anatomical investigation. *Scand J Med Sci Sports* 27: 1705–1715, 2017. doi: 10.1111/sms.12835.

7. **Bojsen-Møller J**, **Magnusson SP**. Heterogeneous Loading of the Human Achilles Tendon In Vivo. *Exerc Sport Sci Rev* 43: 190–197, 2015. doi: 10.1249/JES.0000000000000062.

8. **Beyer R**, **Agergaard A-S**, **Magnusson SP**, **Svensson RB**. Speckle tracking in healthy and surgically repaired human Achilles tendons at different knee angles—A validation using implanted tantalum beads. *Transl Sports Med* 1: 79–88, 2018. doi: 10.1002/tsm2.19.

9. **Slane LC**, **Thelen DG**. Non-uniform displacements within the Achilles tendon observed during passive and eccentric loading. *J Biomech* 47: 2831–2835, 2014.

10. **Thorpe CT**, **Udeze CP**, **Birch HL**, **Clegg PD**, **Screen HR**. Capacity for sliding between tendon fascicles decreases with ageing in injury prone equine tendons: a possible mechanism for age-related tendinopathy. *Eur Cell Mater* 25, 2013.

11. **Clark WH**, **Franz JR**. Do triceps surae muscle dynamics govern non-uniform Achilles tendon deformations? *PeerJ* 6: e5182, 2018. doi: 10.7717/peerj.5182.

12. **Stenroth L**, **Thelen D**, **Franz J**. Biplanar ultrasound investigation of in vivo Achilles tendon displacement non-uniformity. *Transl Sports Med* 2: 73–81, 2019.

13. **Fröberg Å**, **Cissé A-S**, **Larsson M**, **Mårtensson M**, **Peolsson M**, **Movin T**, **Arndt A**. Altered patterns of displacement within the Achilles tendon following surgical repair. *Knee Surg Sports Traumatol Arthrosc* 25: 1857–1865, 2017.

14. **Khair RM**, **Stenroth L**, **Péter A**, **Cronin NJ**, **Reito A**, **Paloneva J**, **Finni T**. Non-uniform displacement within ruptured Achilles tendon during isometric contraction. *Scand J Med Sci Sports* 31: 1069–1077, 2021. doi: https://doi.org/10.1111/sms.13925.

15. **Peng WC**, **Chao YH**, **Fu ASN**, **Fong SSM**, **Rolf C**, **Chiang H**, **Chen S**, **Wang HK**. Muscular Morphomechanical Characteristics After an Achilles Repair. *Foot Ankle Int* 40: 568–577, 2019. doi: 10.1177/1071100718822537.

16. **Svensson RB**, **Couppé C**, **Agergaard A-S**, **Ohrhammar Josefsen C**, **Jensen MH**, **Barfod KW**, **Nybing JD**, **Hansen P**, **Krogsgaard M**, **Magnusson SP**. Persistent functional loss following ruptured Achilles tendon is associated with reduced gastrocnemius muscle fascicle length, elongated gastrocnemius and soleus tendon, and reduced muscle cross-sectional area. *Transl SPORTS Med* 2: 316–324, 2019. doi: 10.1002/tsm2.103.

17. **Hug F**, **Del Vecchio A**, **Avrillon S**, **Farina D**, **Tucker K**. Muscles from the same muscle group do not necessarily share common drive: evidence from the human triceps surae. *J Appl Physiol* 130: 342–354, 2021. doi: 10.1152/japplphysiol.00635.2020.

18. **Masood T**, **Bojsen-Møller J**, **Kalliokoski KK**, **Kirjavainen A**, **Äärimaa V**, **Peter Magnusson S**, **Finni T**. Differential contributions of ankle plantarflexors during submaximal isometric muscle action: A PET and EMG study. *J Electromyogr Kinesiol* 24: 367–374, 2014. doi: 10.1016/j.jelekin.2014.03.002.

19. **Albracht K**, **Arampatzis A**, **Baltzopoulos V**. Assessment of muscle volume and physiological cross-sectional area of the human triceps surae muscle in vivo. *J Biomech* 41: 2211–2218, 2008. doi: 10.1016/j.jbiomech.2008.04.020.

20. **Bojsen-Møller J**, **Schwartz S**, **Kalliokoski KK**, **Finni T**, **Magnusson SP**. Intermuscular force transmission between human plantarflexor muscles in vivo. *J Appl Physiol* 109: 1608–1618, 2010. doi: 10.1152/japplphysiol.01381.2009.

21. **Finni T**, **Cronin NJ**, **Mayfield D**, **Lichtwark GA**, **Cresswell AG**. Effects of muscle activation on shear between human soleus and gastrocnemius muscles. *Scand J Med Sci Sports* 27: 26–34, 2017.

22. **Reito A**, **Logren H-L**, **Ahonen K**, **Nurmi H**, **Paloneva J**. Risk factors for failed nonoperative treatment and rerupture in acute Achilles tendon rupture. *Foot Ankle Int* 39: 694–703, 2018.

23. **Barfod KW**, **Riecke AF**, **Boesen A**, **Hansen P**, **Maier JF**, **Døssing S**, **Troelsen A**. Validation of a novel ultrasound measurement of Achilles tendon length. *Knee Surg Sports Traumatol Arthrosc* 23: 3398–3406, 2015.

24. **Hopkins WG**. Measures of Reliability in Sports Medicine and Science. *Sports Med* 30: 1–15, 2000. doi: 10.2165/00007256-200030010-00001.

25. **Slane LC**, **Thelen DG**. The use of 2D ultrasound elastography for measuring tendon motion and strain. *J Biomech* 47: 750–754, 2014.

26. **Tian M**, **Herbert RD**, **Hoang P**, **Gandevia SC**, **Bilston LE**. Myofascial force transmission between the human soleus and gastrocnemius muscles during passive knee motion. *J Appl Physiol* 113: 517–523, 2012. doi: 10.1152/japplphysiol.00111.2012.

27. **Yin N-H**, **Fromme P**, **McCarthy I**, **Birch HL**. Individual variation in Achilles tendon morphology and geometry changes susceptibility to injury. *eLife* 10: e63204, 2021. doi: 10.7554/eLife.63204.

28. **Bernabei M**, **van Dieën JH**, **Baan GC**, **Maas H**. Significant mechanical interactions at physiological lengths and relative positions of rat plantar flexors. *J Appl Physiol* 118: 427–436, 2015. doi: 10.1152/japplphysiol.00703.2014.

29. **Finni T**, **Bernabei M**, **Baan GC**, **Noort W**, **Tijs C**, **Maas H**. Non-uniform displacement and strain between the soleus and gastrocnemius subtendons of rat Achilles tendon. *Scand J Med Sci Sports* 28: 1009–1017, 2018.

30. **Ekiert M**, **Tomaszewski KA**, **Mlyniec A**. The differences in viscoelastic properties of subtendons result from the anatomical tripartite structure of human Achilles tendon - ex vivo experimental study and modeling. *Acta Biomater* 125: 138–153, 2021. doi: 10.1016/j.actbio.2021.02.041.

31. **Thorpe CT**, **Godinho MS**, **Riley GP**, **Birch HL**, **Clegg PD**, **Screen HR**. The interfascicular matrix enables fascicle sliding and recovery in tendon, and behaves more elastically in energy storing tendons. *J Mech Behav Biomed Mater* 52: 85–94, 2015.

32. **Lehr NL**, **Clark WH**, **Lewek MD**, **Franz JR**. The effects of triceps surae muscle stimulation on localized Achilles subtendon tissue displacements. *J Exp Biol* 224, 2021. doi: 10.1242/jeb.242135.

33. **Francis CA**, **Lenz AL**, **Lenhart RL**, **Thelen DG**. The modulation of forward propulsion, vertical support, and center of pressure by the plantarflexors during human walking. *Gait Posture* 38: 993–997, 2013. doi: 10.1016/j.gaitpost.2013.05.009.

34. **Lenhart RL**, **Francis CA**, **Lenz AL**, **Thelen DG**. Empirical evaluation of gastrocnemius and soleus function during walking. *J Biomech* 47: 2969–2974, 2014. doi: 10.1016/j.jbiomech.2014.07.007.

35. **Clark WH**, **Franz JR**. Age-related changes to triceps surae muscle-subtendon interaction dynamics during walking. *Sci Rep* 11: 21264, 2021. doi: 10.1038/s41598-021-00451-y.

36. **Franz JR**, **Thelen DG**. Imaging and simulation of Achilles tendon dynamics: implications for walking performance in the elderly. *J Biomech* 49: 1403–1410, 2016. doi: 10.1016/j.jbiomech.2016.04.032.

37. **Fröberg Å**, **Cissé A-S**, **Larsson M**, **Mårtensson M**, **Peolsson M**, **Movin T**, **Arndt A**. Altered patterns of displacement within the Achilles tendon following surgical repair. *Knee Surg Sports Traumatol Arthrosc* 25: 1857–1865, 2017. doi: 10.1007/s00167-016-4394-5.

38. **Khair RM**, **Stenroth L**, **Cronin NJ**, **Reito A**, **Paloneva J**, **Finni T**. Muscle-tendon morphomechanical properties of non-surgically treated Achilles tendon 1-year post-rupture. *Clin Biomech* 92: 105568, 2022. doi: 10.1016/j.clinbiomech.2021.105568.

39. **Shin D**, **Finni T**, **Ahn S**, **Hodgson JA**, **Lee H-D**, **Edgerton VR**, **Sinha S**. Effect of chronic unloading and rehabilitation on human Achilles tendon properties: a velocity-encoded phase-contrast MRI study. *J Appl Physiol Bethesda Md 1985* 105: 1179–1186, 2008. doi: 10.1152/japplphysiol.90699.2008.

40. **Svensson RB**, **Slane LC**, **Magnusson SP**, **Bogaerts S**. Ultrasound-based speckle-tracking in tendons: a critical analysis for the technician and the clinician. *J Appl Physiol* 130: 445–456, 2021. doi: 10.1152/japplphysiol.00654.2020.

41. **Segal RL**, **Wolf SL**, **DeCamp MJ**, **Chopp MT**, **English AW**. Anatomical Partitioning of Three Multiarticular Human Muscles. *Cells Tissues Organs* 142: 261–266, 1991. doi: 10.1159/000147199.

42. **Haraldsson BT**, **Aagaard P**, **Qvortrup K**, **Bojsen-Moller J**, **Krogsgaard M**, **Koskinen S**, **Kjaer M**, **Magnusson SP**. Lateral force transmission between human tendon fascicles. *Matrix Biol* 27: 86–95, 2008. doi: 10.1016/j.matbio.2007.09.001.

Figure captions:

Figure 1. Mean normalized displacement patterns ± SD during voluntary and selective electrically induced contractions of the medial (MG) and lateral (LG) gastrocnemius muscles in the un-injured (left) and injured limb (right). Graphs represent group means Individual patterns in the un-injured limb are shown in Figure 2. * Difference between the contraction types ($p < 0.05$).

Figure 2. Normalized displacement patterns in the un-injured limb. Left: Raw data points for each participant during voluntary and selective electrical stimulation across the 6 locations of the Achilles tendon. Right: Box plots of means and SD for each location (1-6 respectively). * Difference between the contraction types ($p < 0.05$).

Figure 3. Tendon displacement (mm) of the whole sample during gastrocnemius muscle stimulation at each of the six locations across the tendon width. The values are expressed as mean ± SD.

Figure 4. Distribution of peak displacement locations across the tendon in the sagittal view when medial gastrocnemius (MG, upper) or lateral gastrocnemius (LG, lower) was selectively stimulated in the un-injured limb.

Table 1. Patient characteristics, free Achilles tendon length, and medial and lateral gastrocnemius subtendon lengths (mean ± SD).

Participants (N=28)		
Age (years)	42.4 ± 9.3	
Height (m)	1.76 ± 0.08	
Body mass (Kg)	82.5 ± 12.2	
Limb condition	**Un-injured**	**Injured**
Free tendon length (cm)	8.79 ± 3.47	10.36 ± 3.71
MG subtendon length (cm)	18.90 ± 1.92	20.99 ±2.20
LG subtendon length (cm)	21.59 ± 1.60	23.51 ± 1.99

Table 2. Descriptive data of motor thresholds, selective electrical stimulation-induced contractions intensities of medial (MG) and lateral (LG) gastrocnemius muscles in the un-injured and injured limbs, and comparisons between limbs and muscles.

	Injured		**Un-injured**		***P*-values comparing stimulations**			
	MG	**LG**	**MG**	**LG**	between limbs		between muscles	
					MG	**LG**	**INJ**	**UNJ**
Stimulation intensity mA (SD)	20.36 (9.26)	18.48 (5.63)	17.75 (9.26)	16.07 (7.37)	0.164	0.155	0.413	0.097
Threshold mA (SD)	15.50 (9.75)	15.25 (4.76)	14.07 (7.98)	19.75 (7.71)	0.513	0.408	0.634	0.210

P-values using un-adjusted pairwise t-test.

Table 3. Descriptive data of mean displacement, non-uniformity, and absolute torque of electrically induced and voluntary contractions.

	Injured			**Un-injured**		
	MG	**LG**	**VOL**	**MG**	**LG**	**VOL**
Mean displacement mm (SD)	0.93 (0.65)	0.65 (0.57)	3.52 (1.71)	0.61 (0.48)	0.39 (0.27)	3.63 (1.18)
Tendon non-uniformity mm (SD)	0.14 (0.11)	0.15 (0.12)	0.85 (0.79)	0.25 (0.23)	0.24 (0.17)	1.48 (1.04)
Torque Nm (SD)	5.18 (2.98)	3.24 (2.72)	57.98 (16.30)	5.56 (4.05)	3.67 (2.53)	57.78 (16.23)

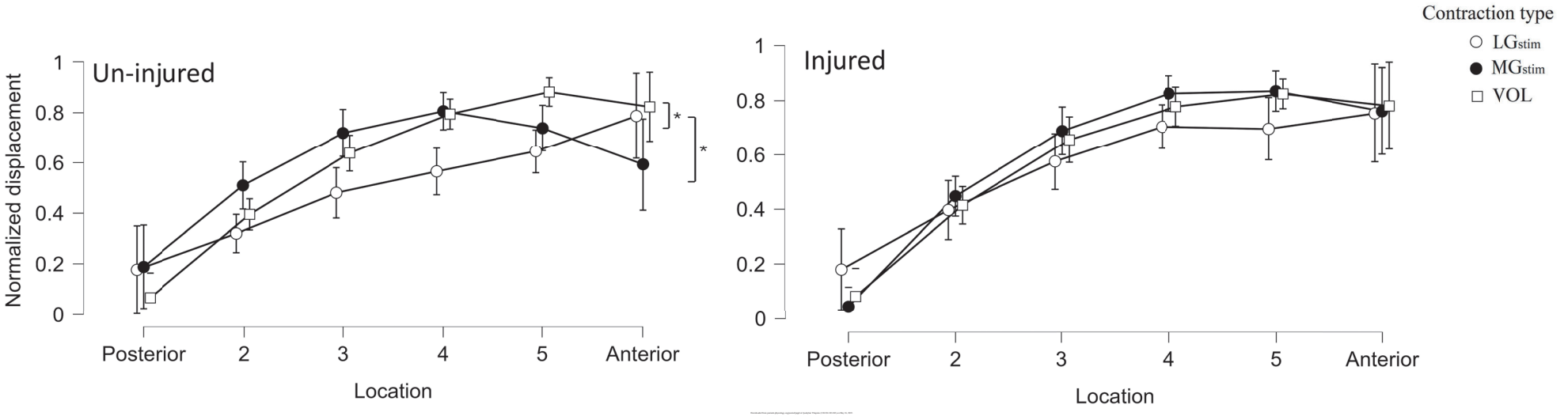
Un-injured
Injured
Normalized displacement
1
0.8
0.6
0.4
0.2
0
Posterior
2
3
4
5
Anterior
Location
*
*
Contraction type
LGstim
MGstim
VOL

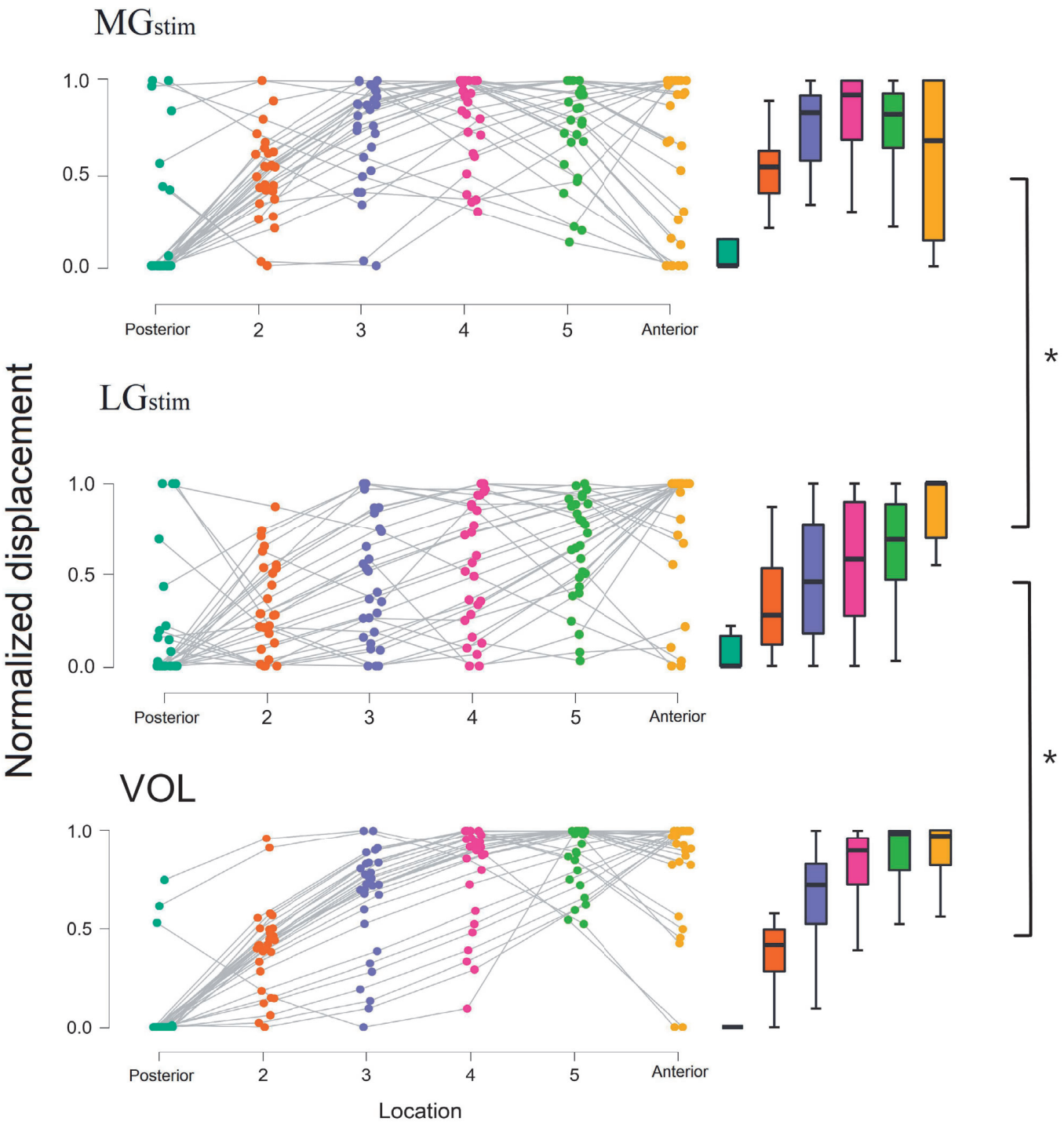

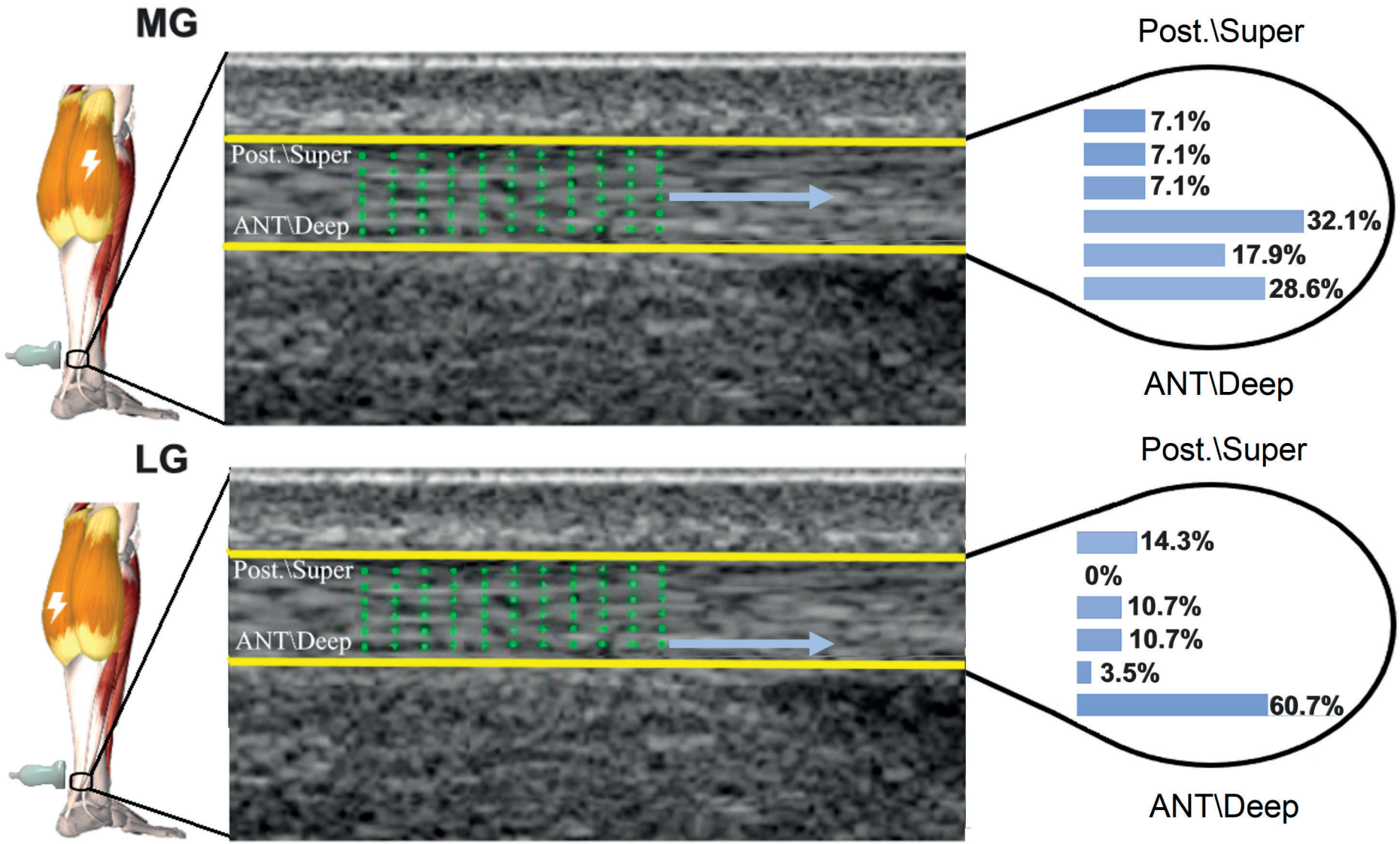

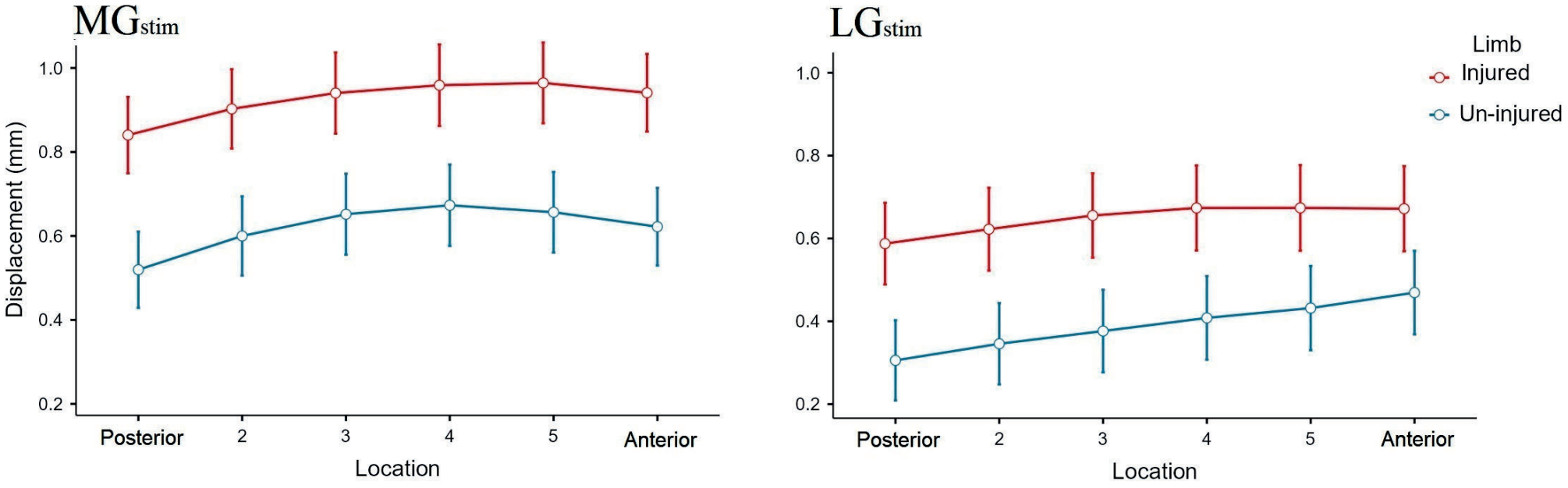

In vivo localised gastrocnemius subtendon representation within the healthy and ruptured human Achilles tendon

N=28

METHODS

Selective electrical stimulation & Voluntary plantarflexion

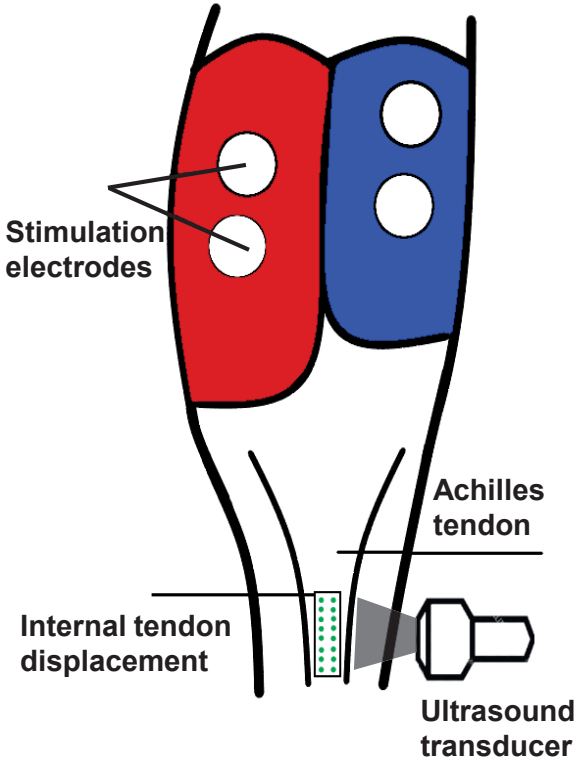

RESULTS

Frequency of maximal displacement locations during selective electrical stimulations

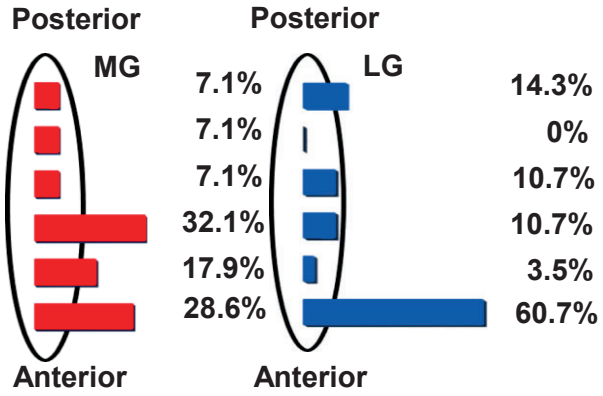

MG subtendon ➡ anterior mid region

LG subtendon ➡ most anterior region

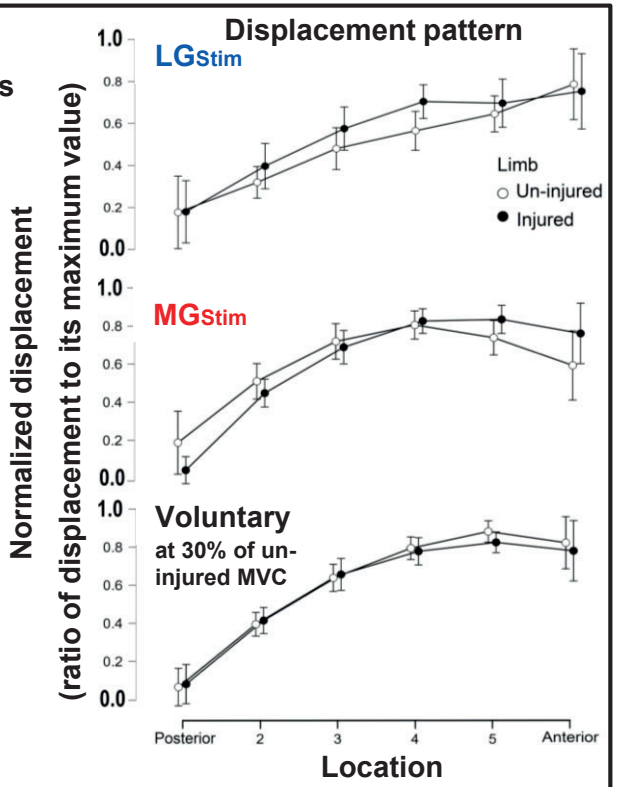

CONCLUSION

When comparing healthy and ruptured tendons one-year post rupture, tendon internal displacement patterns were not different, but absolute displacement amplitude and non-uniformity did differ. **LG** subtendon was found in the most anterior region adjacent to **MG** in both healthy and non-surgically treated tendons.

IV

EXPLORATION OF MUSCLE-TENDON BIOMECHANICS ONE YEAR AFTER ACHILLES TENDON RUPTURE AND THE COMPENSATORY ROLE OF FLEXOR HALLUCIS LONGUS

by

Ra'ad M. Khair, Lauri Stenroth, Neil J. Cronin, Aleksi Reito, Ville Ponkilainen & Taija Finni 2023

Journal of Biomechanics: 111586.

https://doi.org/10.1016/j.jbiomech.2023.111586

Journal of Biomechanics 152 (2023) 111586

Contents lists available at ScienceDirect

Journal of Biomechanics

journal homepage: www.elsevier.com/locate/jbiomech

Exploration of muscle–tendon biomechanics one year after Achilles tendon rupture and the compensatory role of flexor hallucis longus

Ra'ad M. Khair [a,*], Lauri Stenroth [b], Neil J. Cronin [a,d], Ville Ponkilainen [c], Aleksi Reito [c], Taija Finni [a]

[a] Faculty of Sport and Health Sciences, Neuromuscular Research Center, University of Jyväskylä, Jyväskylä, Finland
[b] Department of Applied Physics, University of Eastern Finland, Kuopio, Finland
[c] Central Finland Central Hospital Nova, Jyväskylä, Finland
[d] School of Sport and Exercise, University of Gloucestershire, UK

ARTICLE INFO

Keywords:
Ultrasonography
Flexor hallucis longus muscle
Tendons
Function
Mechanical
Muscle

ABSTRACT

Achilles tendon (AT) rupture leads to long-term structural and functional impairments. Currently, the predictors of good recovery after rupture are poorly known. Thus, we aimed to explore the interconnections between structural, mechanical, and neuromuscular parameters and their associations with factors that could explain good recovery in patients with non-surgically treated AT rupture. A total of 35 patients with unilateral rupture (6 females) participated in this study. Muscle-tendon structural, mechanical, and neuromuscular parameters were measured 1-year after rupture. Interconnections between the inter-limb differences (Δ) were explored using partial correlations, followed by multivariable linear regression to find associations between the measured factors and the following markers that indicate good recovery: 1) tendon length, 2) tendon non-uniform displacement, and 3) flexor hallucis longus (FHL) normalized EMG amplitude difference between limbs. Δmedial gastrocnemius (MG) ($\beta = -0.12$, $p = 0.007$) and Δlateral gastrocnemius ($\beta = -0.086$, $p = 0.030$) subtendon lengths were associated with MG tendon Δstiffness. MG ($\beta = 11.56$, $p = 0.003$) and soleus ($\beta = 2.18$, $p = 0.040$) Δsubtendon lengths explained 48 % of variance in FHL EMG amplitude. Regression models for tendon length and non-uniform displacement were not significant. Smaller inter-limb differences in Achilles subtendon lengths were associated with smaller differences in the AT stiffness between limbs, and a smaller contribution of FHL muscle to the plantarflexion torque. In the injured limb, the increased contribution of FHL appears to partially counteract a smaller contribution from MG due to the elongated tendon, however the role of FHL should not be emphasized during rehabilitation to allow recovery of the TS muscles.

1. Introduction

Tendon rupture leads to long-term structural and mechanical changes in the Achilles tendon (AT) and the triceps surae (TS) muscles (Peng et al., 2019; Svensson et al., 2019). During the first 4 months after rupture, tendon length increases, and the extra length of the tendon alters the operating range of TS muscle sarcomeres, limiting their force generation ability due to the force–length relationship (Stäudle et al., 2020). The increase in tendon length has been found to be associated with inferior clinical and functional outcomes (Khair et al., 2022; Silbernagel et al., 2012a). Along with a change in tendon length, the TS muscles adapt by re-adjusting fascicle length and pennation angle, alleviating the loss of force production capability (Hullfish et al., 2019). Higher AT stiffness could also help to mitigate the impairments caused by tendon lengthening, preserving favourable sarcomere lengths during force generation by allowing the muscle to function within a smaller range (Stäudle et al., 2020).

The AT comprises distinct bundles of fascicles, called subtendons, that arise from the lateral (LG) and medial gastrocnemius (MG), and the soleus (SOL) muscles. Due to the different structure and force generating capacities of the TS muscles (Ward et al., 2009), AT is subjected to complex non-uniform loading that can cause heterogeneity of strain within the tendon (Bojsen-Møller and Magnusson, 2015). Recent in vivo studies have revealed that non-uniform motion within the AT is a function of a healthy tendon (Slane and Thelen, 2014), and might play an important role in the ability of the TS muscles to perform their

* Corresponding author.
E-mail address: raad.m.khair@jyu.fi (R.M. Khair).

https://doi.org/10.1016/j.jbiomech.2023.111586
Accepted 10 April 2023
Available online 13 April 2023

differing functional roles (Clark and Franz, 2021; Franz and Thelen, 2016). Ruptured AT displays more uniform mechanical behaviour after both surgical (Fröberg et al., 2017) and non-surgical treatment (Khair et al., 2021). Non-uniformity within the AT might be associated with TS fascicle length and the maximal amount that fascicles can shorten while exerting force. Thus, more uniform within-tendon displacement after rupture may stem from changes in TS structure and dynamics. Shortening of fascicles in the ruptured limb could result in a smaller operating range, translating to more uniform displacement within the AT. Understanding the associations between TS structural properties and within-AT displacement in patients with ATR could help to inform treatment and rehabilitation choices, leading to better functional outcomes.

Along with the well-documented structural and mechanical changes observed in the tendon after rupture, neuromuscular alterations also contribute to persistent performance deficits after ATR (Wenning et al., 2021). In the injured limb, increased TS muscle activity (Suydam et al., 2015; Wenning et al., 2021) and higher mean frequency of surface electromyography (EMG) (McHugh et al., 2019) have been reported previously in various tasks including eccentric and concentric contractions, indicating alterations in TS motor unit coordination and potentially a preferential activation of fast-twitch muscle fibers. Additionally, flexor hallucis longus (FHL) has been found to have a 5 % bigger cross-sectional area (CSA) in patients with ATR (Heikkinen et al., 2017). Motor control adapts to make greater use of FHL in plantarflexion due to altered force production capabilities in the TS muscles. This leads to a higher relative contribution of FHL to the plantarflexion torque produced in the ruptured limb, as observed in several studies of ATR patients (Finni et al., 2006; Heikkinen et al., 2017), and could be a potential marker of neuromuscular recovery.

Given the force and endurance deficits in plantarflexors after ATR (Khair et al., 2022; Silbernagel et al., 2012b), and the clinical importance of regaining capacity and functionality in the ruptured limb, it would be useful to understand the factors associated with markers of good recovery such as tendon lengthening after rupture, non-uniformity of internal tendon displacements, and neuromuscular alterations.

The aim of this study was to explore interconnections between structural, mechanical and neuromuscular parameters and their associations with markers of good recovery. Interconnections between factors were explored using partial correlations, followed by multivariable linear regression analysis to find associations between measured factors and the following markers of good recovery: 1) tendon length, 2) tendon non-uniform displacement, and 3) FHL normalized EMG amplitude difference between limbs. It was hypothesized that: 1) MG tendon stiffness would be associated with the lengthening of the tendon, 2) MG fascicle length and higher voluntary maximal plantarflexion torque would be related to non-uniformity within the AT, 3) EMG activity of the plantarflexors and the relative contribution of FHL during isometric contraction would be higher in the injured limb to counteract the structural deficits and be proportional to the increased length of the tendon after rupture.

2. Methods

We present data for thirty-five patients (6 females; means ± SD age: 41.1 ± 9.8 years, height: 175.9 ± 7.1 cm, mass: 83.1 ± 13.9 kg) with unilateral non-surgically treated ATR that participated voluntarily (NoARK, trial registration: NCT03704532). This study was approved by the Research Ethics Committee of Central Finland Health Care District (Approval number: 2U/2018). Participants were recruited through Central Finland Hospital (Nova) using the American Academy of Orthopaedic Surgeons guidelines. Inclusion criteria were a minimum of 2 of the following 4 criteria: a positive Thompson test, decreased plantarflexion strength, presence of a palpable gap, and increased passive ankle dorsiflexion with gentle manipulation (Reito et al., 2018). All participants were treated non-surgically with early mobilisation (Reito et al., 2018). Briefly, two weeks after full equinus cast, open cast was used to allow toe movement. At 4 weeks, weight bearing was encouraged with a custom-made special orthosis with 1 cm heel wedge. At week 8, the orthosis was removed and rehabilitation instructions were provided, however participants progressed individually and could consult a private physiotherapist if needed (Khair et al., 2022; Reito et al., 2018). Participants were tested (mean ± SD) 13 ± 1.7 months after rupture.

Upon arrival at the laboratory, both malleoli, heads of the fibula and first and fifth metatarsal heads were marked with a pen, and sagittal plane photos of the foot were taken from the medial and lateral side with a ruler beneath them as a reference to estimate the AT moment arm. AT thickness, TS subtendon length and MG fascicle length were measured from prone position with the foot relaxed over the edge of the bed. Achilles tendon resting angle (ATRA), MG and LG CSA were measured from the same position with the knee flexed to 90° and ankle in neutral position. All structural properties were measured using 3.6 and 6-cm linear probes (Aloka alpha10, Japan), and analysed using Image J. For detailed information on the collection and analysis please refer to (Khair et al., 2022).

For measurement of muscle activity, the skin was shaved and abraded with alcohol pads to reduce skin impedance. Disposable dual surface silver-silver electrode Ambu BlueSensor N electrodes (Ambu A/S, Ballerup, Denmark) were placed on the TS muscles with an interelectrode distance of 22 mm in accordance with SENIAM recommendations (Stegeman and Hermens, 2007). FHL electrodes were placed between the SOL insertion and the FHL muscle–tendon junction (MTJ) where only the FHL muscle belly lies (Péter et al., 2015), with an interelectrode distance of 16 mm. FHL electrode placement was confirmed during isolated big toe plantarflexion using ultrasound imaging. EMG signals were collected at 1500 Hz using a Noraxon wireless EMG system (Noraxon Inc., Scottsdale, AZ, USA). Data were not collected from five participants because of technical difficulties.

EMG data were filtered using a fourth order Butterworth filter between 20 and 450 Hz with a custom-made MATLAB script. Root mean square (RMS) envelopes were then computed using a moving 50 ms window and normalized to the RMS from a 1-*sec* window during MVC. The mean EMG amplitude of each muscle was calculated in a 1-*sec* window around the peak torque of the 30 % MVC contraction condition and used for further analysis. Total EMG activity of all plantarflexor muscles was also computed by summing SOL, MG, LG and FHL activity. This cumulative value denoted 100 % and was used to evaluate the relative contribution of each muscle to total plantarflexion activity (Masood et al., 2014).

After preparation, participants were seated in a custom-made ankle dynamometer (University of Jyväskylä, Finland) with hip, knee, ankle, and first metatarsophalangeal joints fixed at 120°, 0°, 90°, and 0° respectively. The seat was locked in position with the foot and thigh strapped to avoid any heel lift or postural changes during isometric contractions. A monitor was positioned in front of the participant to enable them to follow the torque signal in real time. After a series of submaximal contractions for warm-up, the participants performed unilateral maximal voluntary contractions (MVCs) starting with the non-injured limb. Participants tried to reach maximum torque in 2–3 s and decrease back to zero in 2–3 s, resulting in a 6-second pyramid-shaped torque curve. At least two MVCs were performed and the trial with the highest torque was used for further analysis. During the MVCs, MG-MTJ displacement was imaged at 70 Hz using the 6-cm linear probe.

Force data were collected via a transducer in the foot pedal of the ankle dynamometer, with a potentiometer placed under the heel to detect heel lift during contractions at 1 kHz. AT force was calculated using the individualized AT moment arm acquired from foot pictures. Tendon elongation and force recordings were synchronised to acquire AT force–length relations, and a second-order polynomial fit that was forced through the origin was calculated (Magnusson et al., 2001). For detailed information on the AT force and stiffness calculations please

refer to (Khair et al., 2022). In the text below, the term stiffness refers specifically to MG tendon stiffness.

After performing MVCs, participants were asked to perform ramp contractions corresponding to 30 % of the non-injured MVC, with the 3.6-cm linear probe attached longitudinally ~ 2 cm above the calcaneus to image displacement within the free tendon at 50 Hz. All data were sampled via a 16-bit A/D board (Power 1401, Cambridge Electronic Design, Cambridge, UK) connected to the lab computer, and signals were recorded using Spike2 software. To synchronize data, a TTL pulse was sent manually via Spike2 software (Cambridge Electronic Design, Cambridge, UK), which initiated the recording of the ultrasonography data for 8 s.

A 2D speckle tracking algorithm was used to evaluate AT tissue displacement from B-mode ultrasound videos according to the configuration of Slane and Thelen (Slane and Thelen, 2014). Briefly, superior-inferior displacements of six nodes across the width of the tendon were tracked and peak mean displacement was extracted (Slane and Thelen, 2014). Tendon non-uniformity was calculated as the difference between maximum and minimum displacement across the 6 locations. Lastly, displacement was normalized by dividing non-uniformity by the average peak displacement across all regions. Part of the AT displacement data used in this study was published previously in (Khair et al., 2021).

2.1. Statistical analysis

Statistical analysis was performed using JASP (JASP, Amsterdam, Netherlands). The descriptive data are reported as mean (SD). Pairwise T-tests were used to explore differences between limbs (injured vs non-injured) in structural, neuromechanical and mechanical properties after checking kurtosis and skewness of the data. Inter-limb differences (Δ) were calculated for all variables as percentage (%) difference between limbs: $\frac{Injured-non-njured}{non-injured}*100$ (Khair et al., 2022).

Partial correlations controlled for age and sex were performed to explore the interconnections between the measured biomechanical inter-limb differences. This was followed by multivariable linear regression to investigate variables associated with the following good recovery markers: 1) tendon length, 2) non-uniformity, and 3) FHL normalized EMG% amplitude. Covariates inclusion in models was based on previous knowledge (Clark and Franz, 2018; Hullfish et al., 2019; Stäudle et al., 2020), considering the associations detected in the exploratory correlations. For SOL subtendon model there was scarce previous literature concerning the length of the subtendon after rupture, so general variables that might influence free tendon length were included.

Considering the sample size, only four covariates were included in each model to avoid model overfitting. Age and sex were included in all models and complemented with two other variables. When investigating tendon length, the three AT subtendons had their own covariates: (a) MG model comprised of Δstiffness and ΔMG fascicle length, (b) LG model included Δstiffness and ΔLG CSA, and (c) the SOL model comprised of ΔATRA and Δstiffness. The non-uniformity model consisted of ΔMG fascicle length and ΔMVC. The FHL EMG% model was built with ΔMG subtendon length and ΔSOL subtendon length.

3. Results

Mean values and inter-limb differences are summarized in Table 1. For all measured variables except stiffness and LG-CSA, significant differences between limbs were detected. During submaximal isometric contraction at the same torque level, the combined cumulative RMS of the three TS muscles accounted for 81.9 % of the EMG activity in the non-injured limb compared to 75.8 % in the injured limb with no significant difference between limbs (Fig. 1). The relative MG contribution was lower in the injured limb with a mean difference of 0.061 (95 %CI 0.02–1.0). This was accompanied by an increased FHL contribution to total EMG in the injured limb, with a mean inter-limb difference of −0.061 (95 %CI −1.06 to −0.016).

Table 1
Descriptive data of measured variables and their inter-limb differences.

	Non-injured	Injured	Inter-limb difference (Δ)	p value
Measured at rest				
SOL subtendon length (cm)	8.79 ± 3.47	10.36 ± 3.71	29.1 %	p < 0.001*
MG subtendon length (cm)	18.90 ± 1.92	20.99 ± 2.20	11.4 %	p < 0.001*
LG subtendon length (cm)	21.59 ± 1.60	23.51 ± 1.99	9.1 %	p < 0.001*
AT thickness (cm)	0.48 ± 0.10	0.95 ± 0.22	99.8 %	p < 0.001*
ATRA°	129.34 ± 5.68	123.43 ± 6.88	−4.5 %	p < 0.001*
MG fascicle length (cm)	4.75 ± 0.76	3.75 ± 0.67	− 20.3 %	p < 0.001*
MG CSA (cm^2)	14.64 ± 3.91	12.59 ± 3.61	−13.5 %	p < 0.001*
LG CSA (cm^2)	7.79 ± 2.12	7.19 ± 2.74	−5.9 %	p = 0.091
Measured during MVC				
Stiffness (N/m)	639.23 ± 305.55	594.61 ± 337.51	−2.9 %	p = 0.328
MVC (Nm)	190.03 ± 65.76	158.94 ± 68.03	−19.7 %	p < 0.001*
Measured during 30 % of the non-injured MVC				
Non-uniformity (mm)	1.47 ± 1.02	0.91 ± 0.76	−11.6 %	p = 0.017*
Normalized non-uniformity	0.43 ± 0.29	0.26 ± 0.18	−11.4 %	p = 0.005*
SOL EMG (%)	21.4 ± 7.1	32.8 ± 17.8	67.3 %	p = 0.003*
MG EMG (%)	35.5 ± 11.9	45.0 ± 16.4	35.8 %	p < 0.001*
LG EMG (%)	22.4 ± 12.2	31.7 ± 20.7	65.5 %	p = 0.027*
FHL EMG (%)	19.5 ± 20.0	35.7 ± 21.4	176.3 %	p = 0.005*

Electromyography (EMG) activities are mean values of a 1-second window during the submaximal ramp contraction expressed as % of EMG recorded during maximal voluntary contraction. The submaximal plantarflexion torque level was the same in both limbs (30 % of the maximum of non-injured limbs). P-values refer to pair-wise T-test comparing the limbs with the asterisk indicating a significant difference between limbs ($p < 0.05$).

Inter-limb length differences of MG, SOL and LG subtendons were positively associated with higher ΔFHL normalized EMG% amplitude. Stiffness inter-limb difference was negatively correlated with MG and LG Δsubtendon lengths. All other associations between structural and neuromuscular inter-limb differences are presented in Fig. 2.

The MG subtendon length model explained 26 % of the variance ($F(4,27) = 2.63$, $p = 0.056$) with RMSE of 9.06. ΔStiffness was associated with ΔMG subtendon length ($\beta = -0.12$, [95 %CI −0.20 to −0.03]). In the LG subtendon model, where 19 % of the variance was explained ($F(4,26) = 1.52$, $p = 0.225$) with RMSE of 8.26, Δstiffness was associated with ΔLG subtendon length ($\beta = -0.086$, [95 %CI −0.16 to −0.006]). SOL subtendon length model explained 20 % of the variance ($F(4,31) = 1.72$, $p = 0.174$) with RMSE of 37.09. There were no detectable associations between ΔATRA ($\beta = 0.38$, [95 %CI −2.14 to 2.91]), or Δstiffness ($\beta = 0.05$, [95 %CI −0.30 to 0.40]) and ΔSOL subtendon length.

The non-uniformity model explained 11 % of the variance ($F(4,30) = 0.96$, $p = 0.44$) with RMSE of 149.58. ΔMG fascicle length ($\beta = 5.08$, [95 %CI −0.64 to 10.80]) and ΔMVC ($\beta = -2.49$, [95 %CI −6.36 to 1.40]) were not associated with the inter-limb difference in AT non-uniformity.

The FHL normalized EMG% amplitude model explained 48 % of the variance ($F(5,21) = 3.83$, $p = 0.0127$) with RMSE of 150.5. MG (β =

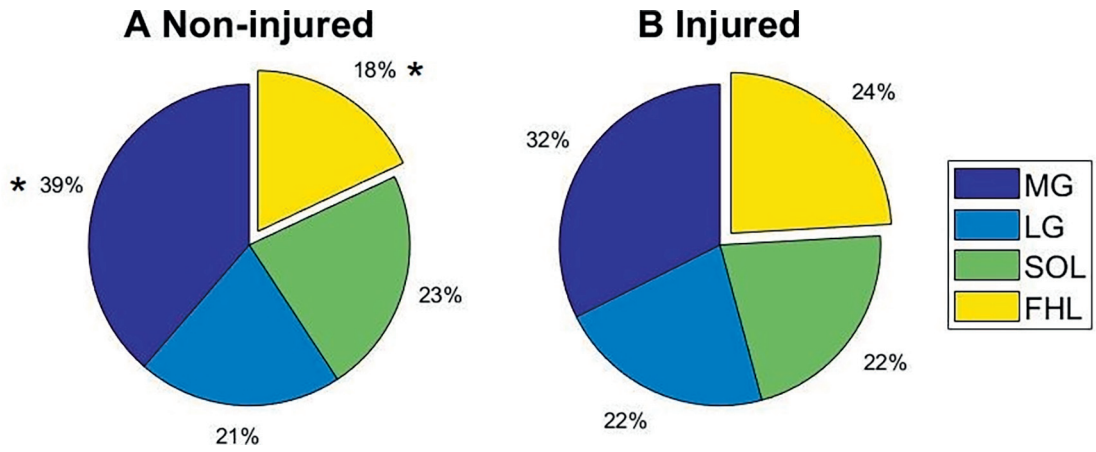

Fig. 1. Relative contribution of medial gastrocnemius (MG), lateral gastrocnemius (LG), soleus (SOL) and flexor hallucis longus (FHL) to total cumulative EMG activity during submaximal ramp isometric contraction in the non-injured (A) and injured limbs (B). * Significant difference between limbs within a given muscle ($p < 0.05$).

11.56, [95 %CI 4.22–18.90]) and SOL Δsubtendon lengths ($\beta = 2.18$, [95 %CI 0.10–4.05]) were both significantly associated with FHL ΔEMG activity.

4. Discussion

The main finding was the higher relative contribution of FHL to the summed normalized EMG activity in the injured compared to the non-injured limb at the same submaximal isometric torque level. The greater relative FHL activity was of similar magnitude to the decrease in MG activity, suggesting a crucial role of FHL in compensating for the reduced force production capacity after ATR. Additionally, differences in tendon length were associated with greater FHL mean amplitude difference between limbs; the more elongated the injured tendon, the greater the relative FHL activity. Lastly, lengthening of the gastrocnemii muscle subtendons after rupture was negatively associated with the difference in stiffness between limbs.

The mean EMG amplitudes of all TS muscles were higher in the injured limb during submaximal isometric contractions. This could be a result of the TS muscle functioning outside the optimum region on the force–length curve, where greater activity is needed to achieve the same absolute torque as the contralateral limb (Suydam et al., 2015). McHugh and colleagues found an increased median frequency of TS EMG in patients with plantarflexion weakness after ATR, and this was more pronounced in patients with excessive tendon lengthening (McHugh et al., 2019). It should be noted that the testing was done in neutral ankle position. Strength deficits after ATR manifest especially when the ankle is in the end-range of plantar flexion. Mullaney and colleagues found an average of 27 % plantar flexion strength deficits when the ankle was in a plantar flexed position but did not observe weakness when the ankle was in dorsi flexion (Mullaney et al., 2006). Thus, it may be that the current sample would show larger neuromuscular and strength impairments in plantar flexed ankle position.

In addition to potential changes in the sarcomere level operating length of the TS muscles, decreased muscle physiological CSA necessitates increased muscle activity to reach a given joint moment in the injured limb. It should be noted that, in accordance with previous studies (Aufwerber et al., 2020; Nicholson et al., 2020), LG was less atrophied and did not demonstrate the same magnitude of difference in CSA as seen in MG, but higher EMG activity was still observed in LG.

In our sample, SOL subtendon length was on average 1.56 cm longer in the injured limb, and although this was less than observed in the gastrocnemii, it resulted in an almost 30 % longer SOL subtendon than on the contralateral side. Furthermore, SOL showed the highest difference in EMG activity among the TS muscles compared to the contralateral limb, suggesting that SOL structure and force production capacity were affected the most by tendon lengthening.

The relative contribution of FHL was 8 % higher in the injured limb, whereas in MG the contribution was 7 % lower compared to the non-injured limb. Compensatory strategies likely start shortly after rupture, where force is averted away from the freshly ruptured AT by increasing the contribution of FHL to plantarflexion torque. This motor strategy may become a persistent feature in ATR patients. Altered motor control may be driven by the potentially disadvantageous position of the TS muscles on the force–length curve. The shift in the TS operating range on the force–length curve (Suydam et al., 2015), and changes in the TS muscles, corresponds to the degree of increase in tendon length after rupture, which seems to be the primary cause of structural and neuromechanical changes. Indeed, we found that patients whose FHL EMG% activity was higher in the injured limb also exhibited greater inter-limb differences in tendon length. It is true that TS muscle weakness is partially compensated by FHL but FHL capacity to compensate for the loss of strength in the injured limb is limited due to relatively short plantarflexion moment arm. Thus, treatments and rehabilitation should not emphasize the role of FHL to allow recovery of the TS, and aim to minimize tendon lengthening after ATR.

As we have shown previously (Khair et al., 2021), our sample showed more uniform displacement within the injured tendon at the same absolute torque, even when non-uniformity was normalized, indicating that mechanical sliding within the tendon fascicles was impaired after ATR. A more uniform displacement within the tendon might limit the ability of the TS muscle to perform their different functional roles in the most optimal way (Clark and Franz, 2021; Franz and Thelen, 2016). Contrary to our initial idea that MG and SOL muscle activity may mirror the differences in non-uniformity (Clark and Franz, 2018), we did not find such associations. However, shorter fascicles likely result in a shorter operating range and quick saturation of TS force production (De la Fuente et al., 2016; Khair et al., 2022), reducing displacement and non-uniformity within the tendon.

Stiffness was negatively associated with the increased length of both gastrocnemii muscle subtendons in agreement with our previous study, where we found that stiffness was associated with MG subtendon length inter-limb difference (Khair et al., 2022). However, in the present study, the interlimb difference in SOL subtendon length was not associated with the stiffness difference between limbs. This is primarily because stiffness was calculated from displacement at the MG-MTJ, and locally the stiffness values might differ at the SOL insertion. Lengthening of the tendon after rupture would result in lower stiffness. For example, if we compare two tendons with the same mechanical properties, a longer tendon would elongate more under the same load, and the change in the

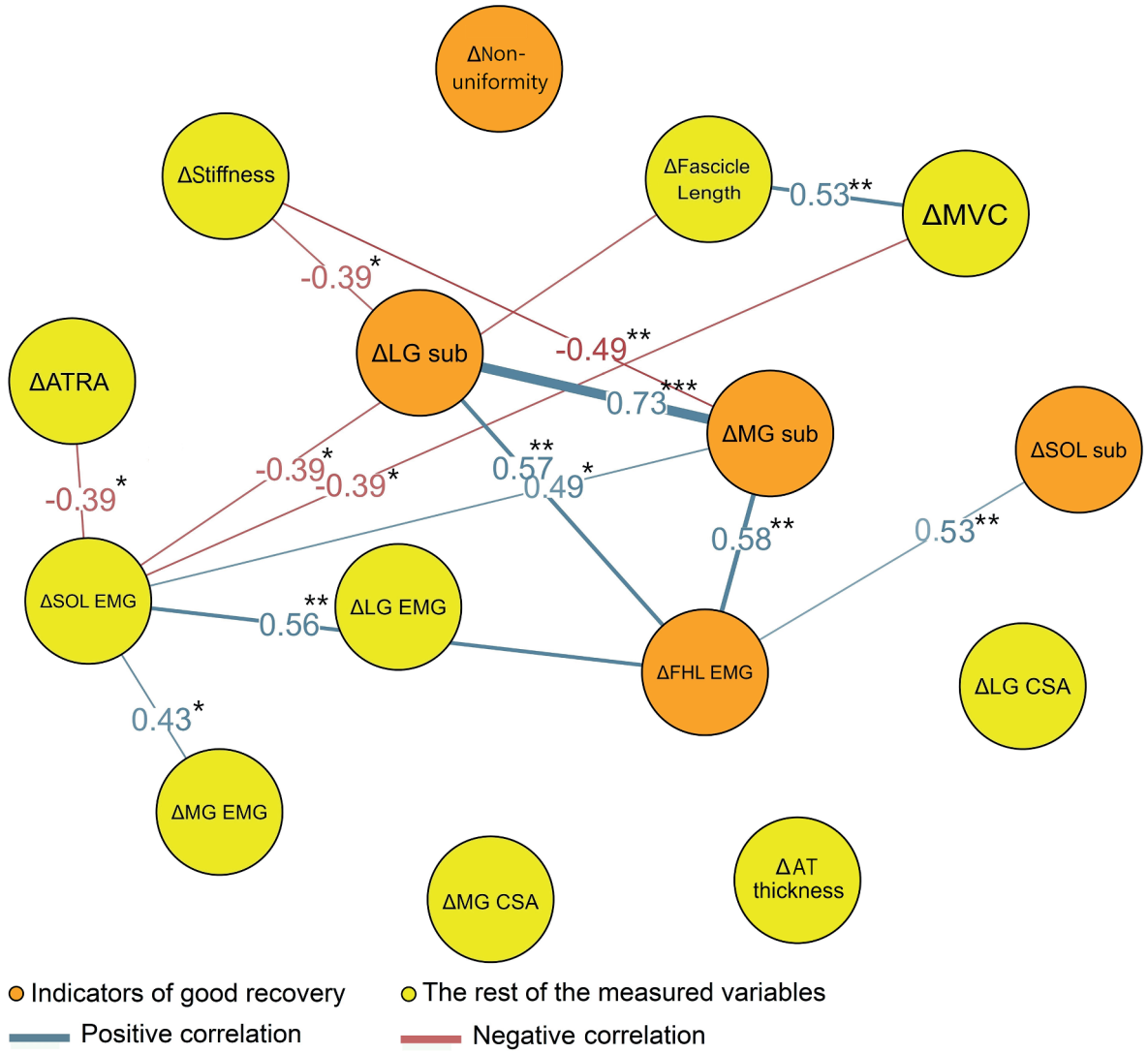

Fig. 2. Network plot exploring the connections between interlimb (Δ) differences in structural and neuromechanical variables. The nodes are positioned using Fruchterman-Reingold algorithm which organizes the network based on the strength of the connections between nodes (Epskamp et al., 2012). Edges between nodes indicate significant interactions with the correlation coefficient outlined on the edge between any two nodes. Blue edges indicate a positive correlation, and red indicates a negative correlation. Orange nodes represent factors that we chose to explore as indicators of good recovery, and yellow nodes represent the other measured variables. *$p < 0.05$, **$p < 0.01$, ***$p < 0.001$. (For interpretation of the references to colour in this figure legend, the reader is referred to the web version of this article.)

force–elongation slope would be directly proportional to the extra length of the tendon (Proske and Morgan, 1987). Considering the previously observed association between muscle strength and tendon stiffness (Arampatzis et al., 2007), it can be speculated that improving muscle strength could help to ameliorate, albeit not completely prevent, the adverse effects of tendon lengthening in patients with ATR. In the early rehabilitation phase, there is a potential risk of excessive tendon lengthening if the tendon is overloaded. Rehabilitative measures, such as blood flow restriction which have been shown to increase tendon stiffness with low mechanical loading (Centner et al., 2019), may be beneficial to induce necessary stimulus especially in the early phase of recovery where loss of muscle strength my prevent proper loading of the tendon.

4.1. Limitations

As commonly recommended, EMG values were normalized to RMS during MVCs. This method may be prone to errors, including the possibility that the ankle flexors were not fully activated during maximal contractions. Thus, caution should be taken when making inferences based on the findings. However, this does not invalidate our results showing that motor control of ankle plantarflexors during submaximal effort differs between limbs in ATR patients, which is consistent with previous studies (McHugh et al., 2019; Wenning et al., 2021).

5. Conclusion

Relative FHL muscle activity was higher in the injured compared to the non-injured limb during submaximal plantarflexion, and this appeared to compensate for decreased MG activity. Despite higher EMG activity in all muscles, plantarflexion maximum torque was still lower in the injured limb. Excessive lengthening of the tendon after ATR is associated with lower stiffness, worsening the ramifications of the rupture.

CRediT authorship contribution statement

Ra'ad M. Khair: Writing – original draft, Writing – review & editing,

Data curation, Visualization, Investigation, Formal analysis, Conceptualization. **Lauri Stenroth:** Methodology, Conceptualization, Writing – review & editing. **Neil J. Cronin:** Supervision, Methodology, Conceptualization, Writing – review & editing. **Ville Ponkilainen:** Writing – review & editing. **Aleksi Reito:** Writing – review & editing, Methodology, Conceptualization. **Taija Finni:** Writing – review & editing, Supervision, Resources, Project administration, Methodology, Funding acquisition, Conceptualization.

Declaration of Competing Interest

The authors declare that they have no known competing financial interests or personal relationships that could have appeared to influence the work reported in this paper.

Data availability

Data used in this manuscript is available for viewing with reasonable request.

Acknowledgments

This work was supported by Academy of Finland (grant #323168), UNderstanding REStoration of Achilles Tendon function after rupture (UNRESAT). The funding organization had no role in collection, analysis and interpretation of the data, or publication.

References

Arampatzis, A., Karamanidis, K., Morey-Klapsing, G., De Monte, G., Stafilidis, S., 2007. Mechanical properties of the triceps surae tendon and aponeurosis in relation to intensity of sport activity. J. Biomech. 40, 1946–1952. https://doi.org/10.1016/j.jbiomech.2006.09.005.

Aufwerber, S., Edman, G., Grävare Silbernagel, K., Ackermann, P.W., 2020. Changes in tendon elongation and muscle atrophy over time after Achilles tendon rupture repair: a prospective cohort study on the effects of early functional mobilization. Am. J. Sports Med. 48, 3296–3305. https://doi.org/10.1177/0363546520956677.

Bojsen-Møller, J., Magnusson, S.P., 2015. Heterogeneous loading of the human Achilles tendon in vivo. Exerc. Sport Sci. Rev. 43, 190–197. https://doi.org/10.1249/JES.0000000000000062.

Centner, C., Lauber, B., Seynnes, O.R., Jerger, S., Sohnius, T., Gollhofer, A., König, D., 2019. Low-load blood flow restriction training induces similar morphological and mechanical Achilles tendon adaptations compared with high-load resistance training. J. Appl. Physiol. 127, 1660–1667. https://doi.org/10.1152/japplphysiol.00602.2019.

Clark, W.H., Franz, J.R., 2018. Do triceps surae muscle dynamics govern non-uniform Achilles tendon deformations? PeerJ 6, e5182.

Clark, W.H., Franz, J.R., 2021. Age-related changes to triceps surae muscle-subtendon interaction dynamics during walking. Sci. Rep. 11, 21264. https://doi.org/10.1038/s41598-021-00451-y.

De la Fuente, C.I., Lillo, R.P., Ramirez-Campillo, R., Ortega-Auriol, P., Delgado, M., Alvarez-Ruf, J., Carreño, G., 2016. Medial gastrocnemius myotendinous junction displacement and plantar-flexion strength in patients treated with immediate rehabilitation after Achilles tendon repair. J. Athl. Train. 51, 1013–1021.

Epskamp, S., Cramer, A.O.J., Waldorp, L.J., Schmittmann, V.D., Borsboom, D., 2012. qgraph: Network visualizations of relationships in psychometric data. J. Stat. Softw. 48, 1–18. https://doi.org/10.18637/jss.v048.i04.

Finni, T., Hodgson, J.A., Lai, A.M., Edgerton, V.R., Sinha, S., 2006. Muscle synergism during isometric plantarflexion in Achilles tendon rupture patients and in normal subjects revealed by velocity-encoded cine phase-contrast MRI. Clin. Biomech. 21, 67–74.

Franz, J.R., Thelen, D.G., 2016. Imaging and simulation of Achilles tendon dynamics: implications for walking performance in the elderly. J. Biomech. 49, 1403–1410. https://doi.org/10.1016/j.jbiomech.2016.04.032.

Fröberg, Å., Cissé, A.-S., Larsson, M., Mårtensson, M., Peolsson, M., Movin, T., Arndt, A., 2017. Altered patterns of displacement within the Achilles tendon following surgical repair. Knee Surg. Sports Traumatol. Arthrosc. 25, 1857–1865.

Heikkinen, J., Lantto, I., Piilonen, J., Flinkkilä, T., Ohtonen, P., Siira, P., Laine, V., Niinimäki, J., Pajala, A., Leppilahti, J., 2017. Tendon length, calf muscle atrophy, and strength deficit after acute Achilles tendon rupture: long-term follow-up of patients in a previous study. JBJS 99, 1509–1515.

Hullfish, T.J., O'Connor, K.M., Baxter, J.R., 2019. Medial gastrocnemius muscle remodeling correlates with reduced plantarflexor kinetics 14 weeks following Achilles tendon rupture. J. Appl. Physiol. Bethesda Md 1985 (127), 1005–1011. https://doi.org/10.1152/japplphysiol.00255.2019.

Khair, R.M., Stenroth, L., Péter, A., Cronin, N.J., Reito, A., Paloneva, J., Finni, T., 2021. Non-uniform displacement within ruptured Achilles tendon during isometric contraction. Scand. J. Med. Sci. Sports 31, 1069–1077. https://doi.org/10.1111/sms.13925.

Khair, R.M., Stenroth, L., Cronin, N.J., Reito, A., Paloneva, J., Finni, T., 2022. Muscle-tendon morphomechanical properties of non-surgically treated Achilles tendon 1-year post-rupture. Clin. Biomech. 92, 105568 https://doi.org/10.1016/j.clinbiomech.2021.105568.

Magnusson, S.P., Aagaard, P., Rosager, S., Dyhre-Poulsen, P., Kjaer, M., 2001. Load-displacement properties of the human triceps surae aponeurosis in vivo. J. Physiol. 531, 277–288. https://doi.org/10.1111/j.1469-7793.2001.0277j.x.

Masood, T., Bojsen-Møller, J., Kalliokoski, K.K., Kirjavainen, A., Äärimaa, V., Peter Magnusson, S., Finni, T., 2014. Differential contributions of ankle plantarflexors during submaximal isometric muscle action: A PET and EMG study. J. Electromyogr. Kinesiol. 24, 367–374. https://doi.org/10.1016/j.jelekin.2014.03.002.

McHugh, M.P., Orishimo, K.F., Kremenic, I.J., Adelman, J., Nicholas, S.J., 2019. Electromyographic evidence of excessive Achilles tendon elongation during isometric contractions after Achilles tendon repair. Orthop. J. Sports Med. 7, 2325967119883357 https://doi.org/10.1177/2325967119883357.

Mullaney, M.J., McHugh, M.P., Tyler, T.F., Nicholas, S.J., Lee, S.J., 2006. Weakness in end-range plantar flexion after Achilles tendon repair. Am. J. Sports Med. 34, 1120–1125. https://doi.org/10.1177/0363546505284186.

Nicholson, G., Walker, J., Dawson, Z., Bissas, A., Harris, N., 2020. Morphological and functional outcomes of operatively treated Achilles tendon ruptures. Phys. Sportsmed. 48, 290–297. https://doi.org/10.1080/00913847.2019.1685364.

Peng, W.C., Chao, Y.H., Fu, A.S.N., Fong, S.S.M., Rolf, C., Chiang, H., Chen, S., Wang, H. K., 2019. Muscular morphomechanical characteristics after an Achilles repair. Foot Ankle Int. 40, 568–577. https://doi.org/10.1177/1071100718822537.

Péter, A., Hegyi, A., Stenroth, L., Finni, T., Cronin, N.J., 2015. EMG and force production of the flexor hallucis longus muscle in isometric plantarflexion and the push-off phase of walking. J. Biomech. 48, 3413–3419. https://doi.org/10.1016/j.jbiomech.2015.05.033.

Proske, U., Morgan, D.L., 1987. Tendon stiffness: methods of measurement and significance for the control of movement: a review. J. Biomech. 20, 75–82. https://doi.org/10.1016/0021-9290(87)90269-7.

Reito, A., Logren, H.-L., Ahonen, K., Nurmi, H., Paloneva, J., 2018. Risk factors for failed nonoperative treatment and rerupture in acute Achilles tendon rupture. Foot Ankle Int. 39, 694–703.

Silbernagel, K.G., Steele, R., Manal, K., 2012. Deficits in heel-rise height and Achilles tendon elongation occur in patients recovering from an Achilles tendon rupture. Am. J. Sports Med. 40, 1564–1571. https://doi.org/10.1177/0363546512447926.

Slane, L.C., Thelen, D.G., 2014. The use of 2D ultrasound elastography for measuring tendon motion and strain. J. Biomech. 47, 750–754.

Stäudle, B., Seynnes, O., Laps, G., Göll, F., Brüggemann, G.-P., Albracht, K., 2020. Recovery from Achilles tendon repair: a combination of postsurgery outcomes and insufficient remodeling of muscle and tendon. Med. Sci. Sports Exerc. Publish Ahead of Print. https://doi.org/10.1249/MSS.0000000000002592.

Stegeman, D., Hermens, H., 2007. Standards for surface electromyography: the European project Surface EMG for non-invasive assessment of muscles (SENIAM). Enschede Roessingh Res. Dev. 10, 8–12.

Suydam, S.M., Buchanan, T.S., Manal, K., Silbernagel, K.G., 2015. Compensatory muscle activation caused by tendon lengthening post-Achilles tendon rupture. Knee Surg. Sports Traumatol. Arthrosc. 23, 868–874. https://doi.org/10.1007/s00167-013-2512-1.

Svensson, R.B., Couppé, C., Agergaard, A.-S., Ohrhammar Josefsen, C., Jensen, M.H., Barfod, K.W., Nybing, J.D., Hansen, P., Krogsgaard, M., Magnusson, S.P., 2019. Persistent functional loss following ruptured Achilles tendon is associated with reduced gastrocnemius muscle fascicle length, elongated gastrocnemius and soleus tendon, and reduced muscle cross-sectional area. Transl. SPORTS Med. 2, 316–324. https://doi.org/10.1002/tsm2.103.

Ward, S.R., Eng, C.M., Smallwood, L.H., Lieber, R.L., 2009. Are current measurements of lower extremity muscle architecture accurate? Clin. Orthop. 467, 1074–1082. https://doi.org/10.1007/s11999-008-0594-8.

Wenning, M., Mauch, M., Heitner, A., Lienhard, J., Ritzmann, R., Paul, J., 2021. Neuromechanical activation of triceps surae muscle remains altered at 3.5 years following open surgical repair of acute Achilles tendon rupture. Knee Surg. Sports Traumatol. Arthrosc. 29, 2517–2527. https://doi.org/10.1007/s00167-021-06512-z.